PB87-124202

REPORT NO.
UCB/EERC-86/04
MARCH 1986

EARTHQUAKE ENGINEERING RESEARCH CENTER

THE USE OF LOAD DEPENDENT VECTORS FOR DYNAMIC AND EARTHQUAKE ANALYSES

by

PIERRE LEGER
EDWARD L. WILSON
RAY W. CLOUGH

Report to the National Science Foundation

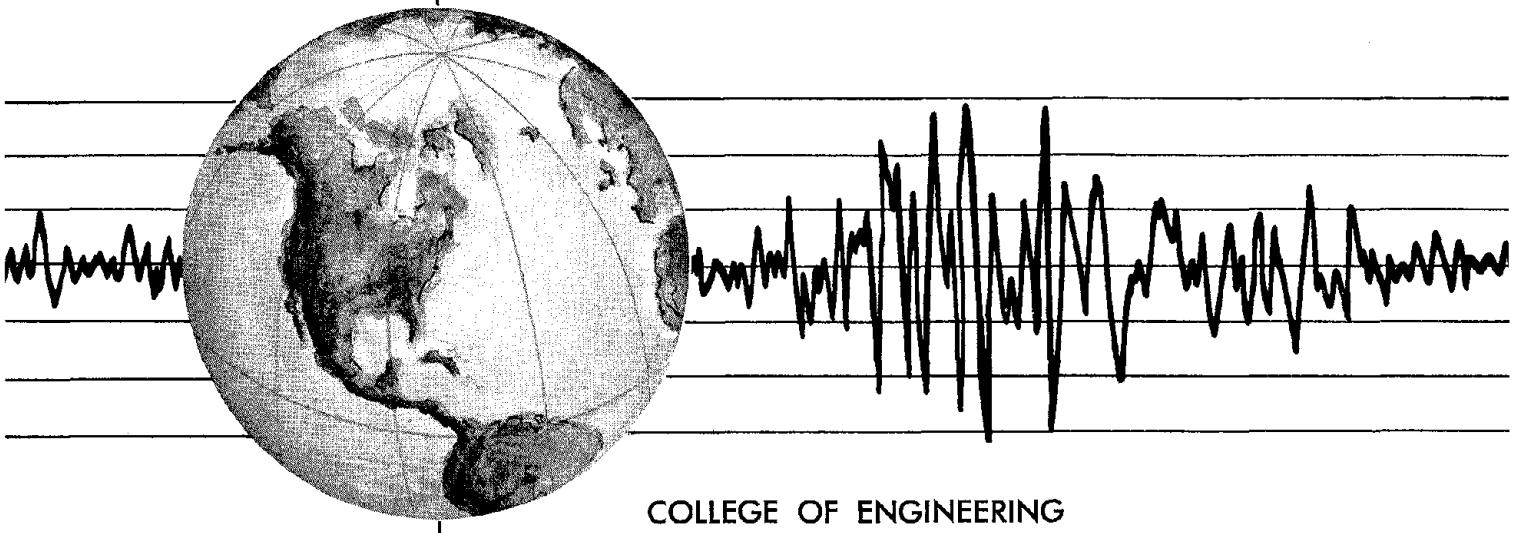

COLLEGE OF ENGINEERING

UNIVERSITY OF CALIFORNIA · Berkeley, California

For sale by the National Technical Information Service, U.S. Department of Commerce, Springfield, Virginia 22161.

See back report for up to date listings of EERC reports.

50272-101

REPORT DOCUMENTATION PAGE	1. REPORT NO. NSF/ENG 86013	2.	3. Recipient's Accession No. PB87 124202/AS
4. Title and Subtitle: The Use of Load Dependent Vectors for Dynamic and Earthquake Analyses			5. Report Date: March, 1986 6.
7. Author(s): Pierre Leger, Edward L. Wilson and Ray W. Clough			8. Performing Organization Rept. No. UCB/EERC-86/04
9. Performing Organization Name and Address: Earthquake Engineering Research Center University of California, Berkeley 1301 South 46th Street Richmond, California 94804			10. Project/Task/Work Unit No. 11. Contract(C) or Grant(G) No. (C) (G) NSF No. ECE-8417857
12. Sponsoring Organization Name and Address: National Science Foundation 1800 G. Street, N.W. Washington, D.C. 20050			13. Type of Report & Period Covered 14.

15. Supplementary Notes

16. Abstract (Limit: 200 words)

A new method of dynamic analysis for systems subjected to fixed spatial distribution of the dynamic load was recently introduced. The WYD Ritz reduction method is based on the direct superposition of a special class of Ritz vectors generated from the spatial distribution of the dynamic load.

The purpose of this report is to investigate practical computer implementation aspects of the WYD Ritz reduction method, its convergence characteristics and its extension to more general forms of loadings and analyses.

17. Document Analysis a. Descriptors

dynamic load
Ritz vectors
computer
load dependent vector bases

b. Identifiers/Open-Ended Terms

c. COSATI Field/Group

18. Availability Statement: Release Unlimited	19. Security Class (This Report): Unclassified	21. No. of Pages: 267
	20. Security Class (This Page): Unclassified	22. Price

(See ANSI-Z39.18) See Instructions on Reverse

OPTIONAL FORM 272 (4-77)
(Formerly NTIS-35)
Department of Commerce

DO NOT PRINT THESE INSTRUCTIONS AS A PAGE IN A REPORT

INSTRUCTIONS

Optional Form 272, Report Documentation Page is based on Guidelines for Format and Production of Scientific and Technical Reports, ANSI Z39.18–1974 available from American National Standards Institute, 1430 Broadway, New York, New York 10018. Each separately bound report—for example, each volume in a multivolume set—shall have its unique Report Documentation Page.

1. Report Number. Each individually bound report shall carry a unique alphanumeric designation assigned by the performing organization or provided by the sponsoring organization in accordance with American National Standard ANSI Z39.23–1974, Technical Report Number (STRN). For registration of report code, contact NTIS Report Number Clearinghouse, Springfield, VA 22161. Use uppercase letters, Arabic numerals, slashes, and hyphens only, as in the following examples: FASEB/NS–75/87 and FAA/RD–75/09.
2. Leave blank.
3. Recipient's Accession Number. Reserved for use by each report recipient.
4. Title and Subtitle. Title should indicate clearly and briefly the subject coverage of the report, subordinate subtitle to the main title. When a report is prepared in more than one volume, repeat the primary title, add volume number and include subtitle for the specific volume.
5. Report Date. Each report shall carry a date indicating at least month and year. Indicate the basis on which it was selected (e.g., date of issue, date of approval, date of preparation, date published).
6. Sponsoring Agency Code. Leave blank.
7. Author(s). Give name(s) in conventional order (e.g., John R. Doe, or J. Robert Doe). List author's affiliation if it differs from the performing organization.
8. Performing Organization Report Number. Insert if performing organization wishes to assign this number.
9. Performing Organization Name and Mailing Address. Give name, street, city, state, and ZIP code. List no more than two levels of an organizational hierarchy. Display the name of the organization exactly as it should appear in Government indexes such as Government Reports Announcements & Index (GRA & I).
10. Project/Task/Work Unit Number. Use the project, task and work unit numbers under which the report was prepared.
11. Contract/Grant Number. Insert contract or grant number under which report was prepared.
12. Sponsoring Agency Name and Mailing Address. Include ZIP code. Cite main sponsors.
13. Type of Report and Period Covered. State interim, final, etc., and, if applicable, inclusive dates.
14. Performing Organization Code. Leave blank.
15. Supplementary Notes. Enter information not included elsewhere but useful, such as: Prepared in cooperation with . . . Translation of . . . Presented at conference of . . . To be published in . . . When a report is revised, include a statement whether the new report supersedes or supplements the older report.
16. Abstract. Include a brief (200 words or less) factual summary of the most significant information contained in the report. If the report contains a significant bibliography or literature survey, mention it here.
17. Document Analysis. (a). Descriptors. Select from the Thesaurus of Engineering and Scientific Terms the proper authorized terms that identify the major concept of the research and are sufficiently specific and precise to be used as index entries for cataloging.

    (b). Identifiers and Open-Ended Terms. Use identifiers for project names, code names, equipment designators, etc. Use open-ended terms written in descriptor form for those subjects for which no descriptor exists.

    (c). COSATI Field/Group. Field and Group assignments are to be taken from the 1964 COSATI Subject Category List. Since the majority of documents are multidisciplinary in nature, the primary Field/Group assignment(s) will be the specific discipline, area of human endeavor, or type of physical object. The application(s) will be cross-referenced with secondary Field/Group assignments that will follow the primary posting(s).
18. Distribution Statement. Denote public releasability, for example "Release unlimited", or limitation for reasons other than security. Cite any availability to the public, with address, order number and price, if known.
19. & 20. Security Classification. Enter U.S. Security Classification in accordance with U.S. Security Regulations (i.e., UNCLASSIFIED).
21. Number of pages. Insert the total number of pages, including introductory pages, but excluding distribution list, if any.
22. Price. Enter price in paper copy (PC) and/or microfiche (MF) if known.

☆U.S. Government Printing Office: 1978—261-647/3308

EARTHQUAKE ENGINEERING RESEARCH CENTER

THE USE OF LOAD DEPENDENT VECTORS FOR DYNAMIC AND EARTHQUAKE ANALYSES

by

Pierre Léger

Edward L. Wilson

and

Ray W. Clough

A Report to the
National Science Foundation
Grant No. ECE-8417857

Report No. UCB/EERC-86/04
College of Engineering
Department of Civil Engineering
University of California
Berkeley, California

March 1986

THE USE OF LOAD DEPENDENT VECTORS FOR DYNAMIC AND EARTHQUAKE ANALYSES

ABSTRACT

A new method of dynamic analysis for systems subjected to fixed spatial distribution of the dynamic load was recently introduced by Wilson, Yuan and Dickens as an economic alternative to classical mode superposition. The WYD Ritz reduction method is based on the direct superposition of a special class of Ritz vectors generated from the spatial distribution of the dynamic load.

The purpose of this report is to investigate practical computer implementation aspects of the WYD Ritz reduction method, its convergence characteristics and its extension to more general forms of loadings and analyses.

First a formal mathematical framework for the WYD Ritz reduction method is established by showing that the algorithm used to produce WYD Ritz vectors is similar to the method used to produce Lanczos vectors. Error norms to measure the representation of the spatial distribution of the dynamic load achieved by truncated WYD Ritz bases and to establish a relationship between WYD Ritz solutions and exact eigensolutions are developed. Computational variants to generate load dependent vector bases for dynamic analyses are then studied. One of the proposed formulations, the LWYD algorithm, is shown to be more stable than the original WYD algorithm and allows a better control of the static correction effects included in the method.

Theoretical developments and computational procedures to apply the proposed Ritz reduction method to three dimensional earthquake response spectra analysis, to analysis of systems subjected to multispatial dynamic load distributions, to multilevel substructure analysis and to nonlinear dynamic problems are presented.

Comparisons between Ritz solutions and traditional eigensolutions are used to show that solution procedures based on the direct superposition of load dependent Ritz vectors can be developed as complete analytical tools being able to improve the convergence characteristics and numerical efficiency of any classical dynamic analysis techniques that are currently using eigenvectors as bases for response computations.

ACKNOWLEDGEMENTS

The research described in this report constitutes the first author's dissertation, submitted in partial satisfaction of the requirements for the degree of Doctor of Philosophy in Engineering at the University of California, Berkeley. The study was carried out under the supervision of Professor Edward L. Wilson with the collaboration of Professor Ray W. Clough.

The research work was sponsored by the National Science Foundation under Grant No. ECE-8417857 titled "A New Method of Seismic Analysis for Linear and Nonlinear Systems". This financial support is gratefully acknowledged.

The Use of Load Dependent Vectors for
Dynamic and Earthquake Analyses

TABLE OF CONTENTS

TABLE OF CONTENTS (CONTINUED)

TABLE OF CONTENTS (CONTINUED)

TABLE OF CONTENTS (CONTINUED)

LIST of FIGURES

LIST of FIGURES (CONTINUED) Page

LIST of FIGURES (CONTINUED) Page

LIST of TABLES

CHAPTER 1

Introduction

During the last twenty years the rapid development of high speed digital computers and of the Finite Element Method (FEM) has greatly increased the range and complexity of structural problems that can be solved. The FEM provided a general method of analysis being able to accommodate arbitrary geometry, boundary conditions, and loading; and applicable to one, two and three dimensional structures. In its application to structural dynamics the dominant characteristic of the FEM is to replace the actual continuous system, which has theoretically an infinite number of degrees of freedom, by an approximate multi-degrees of freedom system. It is not unusual while dealing with engineering structures that the number of degrees of freedom retained in the analysis be very large. Thus, a lot of emphasis in structural dynamics has been put on the development of efficient techniques to evaluate the response of large multi-degrees of freedom systems subjected to various types of dynamic loads.

Although formal solutions in terms of matrix algebra are not affected in principle by the number of degrees of freedom, computational problems, and costs grow rapidly as this number increases. It is very important to maintain reasonable computer costs for any analysis such that inexpensive reanalysis become possible. Low computer costs of a typical analysis cycle will allow some basic assumptions used in selecting models and loads to be varied to study the sensitivity of the results, modify the original design and conduct reliability evaluations. Thus, improvements in numerical techniques and approximations in the methods of solution, which reduce the computation time for large problems, are very useful.

The use of eigenvectors, to reduce the size of structural systems or to represent the stuctural behavior by a small number of generalized coordinates, requires in its traditional formulation, the solution of a large and expensive eigenvalue problem.

A new method of dynamic analysis, which eliminates the requirement for exact evaluation of the free vibration frequencies and mode shapes, has been recently presented by Wilson, Yuan and Dickens (1.17). The WYD Ritz reduction method is based on the direct superposition of Ritz vectors constructed from the spatial distribution of the specified dynamic loads. These vectors are evaluated by a simple recurrence algorithm at a fraction of the computational effort required for the calculation of exact mode shapes. Preliminary evaluation of the algorithm applied to earthquake time history analysis of simple structural systems has shown that the WYD Ritz vectors yield results of comparable accuracy or even better accuracy than those obtain from exact eigensolutions.

The purpose of this report is to investigate practical computer implementation aspects of the WYD Ritz reduction method, its convergence characterisics and its extension to more general forms of loadings. In addition, the development of solution strategies to applied the approach to dynamic analysis of multilevel substructures and to dynamic analysis of nonlinear systems will be presented. Guidelines to develop general purpose FORTRAN subroutine for the generation of Ritz vectors are provided and the various algorithms are evaluated on simple realistic systems to validate the approach for industrial applications.

Chapter 1 describes the basic algorithm as suggested by Wilson et al. and provides some theoretical bases for Ritz analysis in structural dynamics. The influence of the mathematical modelling by the FEM, as defined by the charac-

teristics of the specified mass, stiffness and loading, on the WYD Ritz vectors generation is also presented.

Chapter 2 establishes a relationship between the WYD Ritz algorithm and the Lanczos method. It is shown that the algorithm used to generate the WYD Ritz vectors is similar to the method used to produce Lanczos vectors. However, the use of the resulting basis to solve the dynamic equilibrium problem is different since the objectives of the WYD Ritz method is not to provide an accurate eigensolution but to use the vector basis to transform the equations to a more convenient form for solution by reducing the size and bandwidth of the system matrices. The WYD Ritz approach does not provide a full uncoupling of the equilibrium equations but has proved to be more efficient than the traditional eigensolution approach while maintaining the high expected degree of accuracy of modern computer analysis.

Chapter 3 presents the development of error estimates to indicate how many WYD Ritz vectors should be retained for a satisfactory convergence of the dynamic response and to establish a relationship between the WYD Ritz solution of the reduced system and the eigensolution of the original system. The influence of various vector summation procedures such as modal acceleration and static correction is also compared to the behavior of WYD Ritz solutions.

Chapter 4 presents the development of a new algorithm, the LWYD Ritz algorithm, to generate load dependent vectors to be used in the WYD Ritz reduction method. In the presence of the finite precision arithmetic of the computer, the calculation of transformation vectors by the LWYD Ritz algorithm is shown to be more stable than the application of the original WYD Ritz algorithm for which the basis vectors exhibits a global loss of orthogonality after a few iterations. The LWYD Ritz algorithm also permits a better control of the static correction effects included in

the WYD Ritz reduction method. It is also shown that for algorithms based on the WYD Ritz reduction method, it is possible to form the reduced generalized system directly from the orthonormalization coefficients calculated while generating the vector basis.

Chapter 5 discusses the practical application of the WYD Ritz reduction method in earthquake engineering. The earthquake response spectrum analyses of two structural models of approximately 100 dynamic degrees of freedom are used for that purpose. The computational performances of Ritz solutions and exact eigensolutions are compared and a solution strategy based on transformation vectors obtained from the LWYD Ritz algorithm with minimized static correction is recommended.

Chapter 6 presents a formulation to extend the WYD Ritz reduction method to general multiload pattern analysis where the dynamic loads are a function of space and time. A simultaneous iteration procedure using blocks of vectors in the proposed algorithms is used for that purpose.

Chapter 7 deals with the use of load dependent Ritz vectors in multilevel substructure analysis. Two different approaches are investigated. In a first method, the internal behavior of a substructure is represented by a small number of Ritz coordinates in a component mode synthesis type of formulation where constraint modes are used to interface the components. In the second method, it is shown that it is possible to efficiently generate the load dependent Ritz basis of the complete structure from the structural properties of each substructure by using an iterative version of the familiar static condensation algorithm.

Chapter 8 is concerned by the extension of the WYD Ritz reduction method to nonlinear dynamic systems. Various solution strategies while using the load dependent Ritz

vectors as a coordinate reduction procedure are presented. The emphasis is then put on systems experiencing localized nonlinearities. A solution algorithm using the dynamic substructuring methods of chapter 7 in conjunction with a step - by-step integration procedure for the nonlinear subset of degrees of freedom is recommended.

1.1 Two-Stage Discretization Procedure in Structural Analysis

The first step in a structural analysis using the FEM is to discretize the structure to obtain the stiffness, mass, and damping characteristics needed for the formulation of the equilibrium equations of motion. Then a new discretization can be carried out using the combination of a small number of linearly independent global shape functions, obtained from the previous modelling, to characterize the structural response.

The second reduction technique is not interesting for the solution of linear static analysis because a single step is necessary to get a solution. It is however convenient for nonlinear static and linear and nonlinear dynamics in which several steps must be performed, each one involving the solution of a linear or nonlinear system of equations.

1.1.1 Discretization of Linear Dynamic Problems by Direct Vector Superposition

Study of the static load deflection characteristics and dynamic response time histories of a number of complex structures reveals that the large number of Degrees Of Freedom (DOF) retained in the analysis is often dictated by their topology rather than the expected complexity of behavior. Usually the geometry of the structure does not permit the discretization in a few finite elements but the behavior may be perfectly characterized by a few generalized DOF. This is generally true for structural dynamic problems,

such as earthquake analysis, where typical modal analysis studies on the frequency content and spatial distribution of the excitation have shown that the response is controlled by a relatively small number of low frequency modes. In the case of vibration excitation analysis, only few intermediate frequencies may be excited. However in the case of multishock excited systems, the contribution of intermediate and high frequency structural modes to the response can remain important throughout the time span of interest. The change of basis from the original coordinate system to the generalized modal coordinates, which requires in its traditional formulation the solution of a large eigenvalue problem, is only interesting when the number of contributing modes is relatively small compared to the original number of DOF.

In general, the finite element analysis approximates the lowest exact frequencies best and little or no accuracy can be expected in approximating higher frequencies and mode shapes. This is due to the fact that higher modes have a highly distorted nature that is difficult to accurately represent using a mesh size practical for engineering computations. Therefore there is usually little justification for including the dynamic response in the mode shapes with high frequencies in the analysis. Ideally the FEM mesh should be chosen such that all important frequencies and vibration mode shapes are well approximated, then the solution needs only to be calculated including the response in these modes. This is achieved by vector superposition analysis by considering only the important modes of the FEM system.

The evaluation of the exact natural frequencies and mode shapes of large structural systems requires a significant amount of numerical operations. However, as stated by Wilson et al. (1.17), the direct engineering significance of this information may be of limited value. Frequency values indicate possible resonant conditions and

the mode shapes associated with low frequencies can indicate which regions of the structure are most flexible. In many cases approximate values can provide the same information. For most analyses, the only reason for the evaluation of exact eigenvectors is for their subsequent use to reduce the size of the system in a superposition analysis.

1.2 The Use of Ritz Vectors in Structural Dynamics

1.2.1 Rayleigh's Method for SDOF System

The basic concept in the Rayleigh's method, used to find an approximation to the vibration frequency for a Single Degree of Freedom system (SDOF), is the principle of conservation of energy. The energy in a freely vibrating system must remain constant if no damping acts to absorb it. Therefore, the maximum strain energy in the elastic structure must equal the maximum kinetic energy of the mass. The method can be applied to any Multi-Degrees of Freedom (MDOF) system, which can be represented as a SDOF through the use of an assumed Ritz displacement shape {X} :

$$\bar{w}^2 = \frac{K^*}{M^*} \qquad [1.1]$$

where K^* is the generalized stiffness : $\{X\}^T [K] \{X\}$
M^* is the generalized mass : $\{X\}^T [M] \{X\}$
$\bar{w}$ is the approximate vibration frequency

1.2.2 Rayleigh-Ritz Analysis for MDOF System

The Ritz extension of the Rayleigh's method known as Rayleigh-Ritz analysis has been widely used to find approximation to the lowest eigenvalues and corresponding eigenvectors of the free vibration problem:

$$[K] [\Phi] = [M] [\Phi] [w^2] \qquad [1.2]$$

where [K] and [M] are the stiffness and mass matrix, [Ø] the eigenvectors and w^2_i the eigenvalues or squared frequencies of the system.

The eigenvectors [Ø] can be approximated by a discrete number of trial functions $\{X_i\}$ such that:

$$\{\bar{\emptyset}_i\} = \sum_{i=1}^{r} \{X_i\}\ Y_i \qquad [1.3]$$

$$[\bar{\emptyset}] = [X]\ [Y]$$

The $\{X_i\}$'s are prescribed global shape functions of the original coordinate system called the Ritz vectors and the Y_i's are a set of parameters, the Ritz coordinates, that characterizes the participation of each Ritz vector to the solution.

The Ritz vectors are substituted into the extremum principle form of the Rayleigh's quotient and the set of Y_i's, which gives stationary values, are sought (details of the procedure can be found in ref. 1.2, 1.7).The Rayleigh's quotient can be written as:

$$\frac{[\bar{\emptyset}]^T\ [K]\ [\bar{\emptyset}]}{[\bar{\emptyset}]^T\ [M]\ [\bar{\emptyset}]} = \frac{[Y]^T\ [K]^*\ [Y]}{[Y]^T\ [M]^*\ [Y]} \qquad [1.4]$$

with $[K]^* = [X]^T\ [K]\ [X]$

$[M]^* = [X]^T\ [M]\ [X]$

The stationary condition will lead to the solution of the eigenvalue problem

$$[K]^*\ [Y] = [M]^*\ [Y]\ [\bar{w}^2] \qquad [1.5]$$

The approximation to the eigenvectors [Ø] is then $[\bar{\emptyset}] = [X]\ [Y]$. The reduced eigenvalue problem (eq.[1.5]) leads to a set of r approximate frequencies, $\bar{w}_i$, and corresponding mode

shapes. It can be shown that the r eigenvalues produced by the Rayleigh-Ritz approximation are an upper bound to corresponding exact eigenvalues.

The static condensation procedure, the component mode synthesis, the subspace iteration, and various other methods can be understood as Ritz analyses. The techniques differ only in the choice of the Ritz basis vectors assumed in the analysis.

The Ritz procedure can be applied to reduce the dynamic equilibrium equations of the FEM formulation. The equations of dynamic equilibrium for a finite element model can be written in term of nodal displacements {U} as:

$$[M]\{\ddot{U}\} + [C]\{\dot{U}\} + [K]\{U\} = \{F(s,t)\} \qquad [1.6]$$

where [M], [C], and [K] are respectively the square n x n mass, damping and stiffness matrices and {F(s,t)} the vector of imposed dynamic loading which is a function of space and time. The dots represent derivatives with respect to time.

The vector of nodal displacement {U} can be approximated by a linear combination of r linearly independent Ritz vectors, with r much less than n, as:

$$\{\bar{U}(t)\} = \sum_{i=1}^{r} \{X_i\}\, Y_i(t) \qquad [1.7]$$

where $\{X_i\}$ are the linearly independent basis vectors and $Y_i(t)$ are unknown parameters obtained by solving a reduced system of equations that can be written as:

$$[M]^*\{\ddot{Y}\} + [C]^*\{\dot{Y}\} + [K]^*\{Y\} = \{F(s,t)\}^* \qquad [1.8]$$

where: $[M]^* = [X]^T [M] [X]$

$[C]^* = [X]^T [C] [X]$

$[K]^* = [X]^T [K] [X]$

$$\{F\}^* = [X]^T \{F\}$$

The objective of the transformation is to obtain new system stiffness, mass and damping matrices $[K]^*$, $[M]^*$, $[C]^*$ which are reduced in size (r x r) and have smaller bandwidth than the original system matrices, while maintaining a good accuracy for the response quantities of interest. The transformation matrix [X] should therfore be selected accordingly. The success of the method depends to a great extent on the proper selection of the basis vectors. Various kinds of choices were proposed in the literature for static (nonlinear) and dynamics problems (1.1, 1.5, 1.12, 1.13, 1.14). As noted by Noor (1.12) the ideal set of basis vectors is one which maximizes the quality of the results and minimizes the total effort in obtaining them.

As previously stated, one of the best known reduction method used in linear dynamics problems is the "modal superposition technique". It consists in choosing r free undamped vibration modes, coming from the solution of the eigenvalue problem $[K]\,[\Phi] = [M]\,[\Phi]\,[\omega^2]$, as basis vectors. With this particular choice it is easy to show that the reduced $[K]^*$, $[M]^*$, and $[C]^*$ matrices become diagonal if proportional damping, with a value of ξ_i critical, is assumed;

$$[I]\,\{\ddot{Y}\} + [2\xi\omega]\,\{\dot{Y}\} + [\omega^2]\,\{Y\} = \{F\}^* \qquad [1.9]$$

The reduced system becomes an independent set of r equations which can be integrated one by one. However, it is not a necessary condition for the reduction method that the final system of differential equations be uncoupled.

The lack of generality of Rayleigh-Ritz based code is due to the difficulties in choosing appropriate global functions that will ensure the high expected degree of accuracy of modern computer analysis. This situation has

greatly favored the use of exact eigenvectors as the basis for mode superposition. However, recently Wilson et al. (1.4, 1.17, 1.18) have developed a simple numerical algorithm to automatically generate a special class of Ritz vectors, called WYD Ritz vectors in this report, that produced results of better accuracy with less computer time than the traditional eigenvector approach for a wide variety of studied examples.

1.3 Automatic Generation of WYD Ritz Vectors for Dynamic Analysis

The sequence of WYD Ritz vectors, used to reduce the size of the system, is generated taking into account the spatial distribution of the dynamic loading which is important information that is neglected by direct use of exact mode shapes.

The algorithm, in its actual form, is presented in fig.1.1. It should be noted that the dynamic loading $\{F(s,t)\}$ of equation [1.6], used to initiate the recurrence algorithm, is written as the product of a spatial vector and a time function:

$$\{F(s,t)\} = \{f(s)\}\, g(t) \qquad [1.10]$$

The first WYD Ritz vector is the displacement vector obtained from a static analysis using the spatial distribution of the dynamic load vector, $\{f(s)\}$, as input. The other vectors are generated from a recurrence relationship in which the mass matrix is multiplied by the last WYD Ritz vector; the resulting vector is then used as the load for a static solution. Therefore after the stiffness matrix is triangularized, it is only necessary to solve statically for one load vector for each WYD Ritz vector required. The linear independence of the WYD Ritz vectors is achieved using the Gram-Schmidt orthogonalization process.

Fig. 1.1 Algorithm for Automatic Generation of WYD Ritz Vectors

(Original formulation proposed by Wilson, Yuan, Dickens (1.17))

1. Given Mass, Stiffness Matrices [M], [K], and Load Vector {f}

[M]	n x n system size
[K]	n x n
{f}	n x 1

2. Triangularized Stiffness Matrix:

$[K] = [L]^T [D] [L]$ n x n system

3. Solve for First Vector:

$[K] \{\bar{X}_1\} = \{f\}$ solve for $\{\bar{X}_1\}$

$b = (\{\bar{X}_1\}^T [M] \{\bar{X}_1\})^{1/2}$ M-Normalization

$\{X_1\} = \{X_1\} * 1/b$

4. Solve for Additional Vectors: i=2,...,r

(a) $[K] \{\bar{X}_i\} = [M] \{X_{i-1}\}$ solve for $\{\bar{X}_i\}$

(b) $c_j = \{X_j\}^T [M] \{\bar{X}_i\}$ compute for j=1,...,i-1

(c) $\{\tilde{X}_i\} = \{X_i\} - \sum_{j=1}^{i-1} c_j \{X_j\}$ M-Orthogonalized

(d) $b_i = (\{\tilde{X}_i\}^T [M] \{\tilde{X}_i\})^{1/2}$ M-Normalization

$\{X_i\} = \{\tilde{X}_i\} * 1/b_i$

5. Orthogonalization of WYD Ritz Vectors with Respect to Stiffness Matrix (optional):

$[K]^* [Z] = [M]^* [Z] [\bar{w}^2]$ Solve the r x r eigenvalue problem, where:
$[K]^* = [X]^T [K] [X]$
$[M]^* = [X]^T [M] [X] = [I]$
$\bar{w}$ = approximate frequencies

$[^oX] = [X] [Z]$ Compute final orthogonal WYD Ritz vectors

The technique used to construct WYD Ritz vectors enforces mass orthonormality among the vectors such that the matrix $[M]^*$ of the reduced system (equation [1.8]) will be diagonal and will correspond to the identity matrix, however the matrices $[K]^*$ and $[C]^*$ will in general be full:

$$[I] \{\ddot{Y}\} + [C]^* \{\dot{Y}\} + [K]^* \{Y\} = \{F\}^* \qquad [1.11]$$

Equation [1.11] can thus be solved by a direct step-by-step integration method or by the introduction of an additional transformation in order to reduce the system to a diagonal form.

In the case of proportional damping, the solution of the eigenvalue problem

$$[K]^* [Z] = [M]^* [Z] [\bar{w}^2] \qquad [1.12]$$

will produce a set of modal coordinates [Z] which can be used to diagonalize the system. The values of $\bar{w}^2_i$ are exact eigenvalues of the reduced system and approximate squared frequencies of the complete system. The eigenvectors [Z] can also be used to create a final set of orthogonalized WYD Ritz vectors from:

$$[^oX] = [X] [Z] \qquad [1.13]$$

The set of vectors $[^oX]$, are orthogonal with respect to both the stiffness and mass matrices of the complete system. Some of these vectors may be a good approximation to the exact mode shapes of the structure.

In the case of arbitrary damping, a solution of the complex eigenvalue problem will be required if modal coordinates are to be uncoupled. It should be noted that the numerical effort required for the solution of the reduced system of order r (equation [1.11]) is normally very small compared to the solution of the full original system of order n (equation [1.6]).

Since the WYD Ritz vectors are automatically generated with a fraction of the numerical effort required for the calculation of the exact eigenvectors of the original system, they represent an efficient approach to the reduction of large three dimensional structural systems such as soil/structure, dam/reservoirs, and offshore platforms in which classical solution techniques are found to be costly due to the large numerical effort required to solve the eigenvalue problem. Another important advantage of the WYD Ritz reduction method is the possibility to carry out dynamic analyses of medium size structures on relatively inexpensive micro-computers.

1.4 Influence of the FEM Formulation on WYD Ritz Vectors Generation

The three basic elements of the WYD Ritz vectors generation, as presented in fig. 1.1, are the mass, the stiffness matrices and the spatial load distribution. The mass and stiffness matrices will normally be symmetric positive definite although the following two exceptions can arise:

- if the structure is free to move as a rigid body (for example an aircraft or a ship) then the stiffness matrix is positive semi-definite having rank n-b, where b is the number of independent rigid body motions

- if no mass has been allocated to some nodal displacements then completely null rows and columns occur in the mass matrix which become singular.

To deal with the problem of a rank deficient stiffness matrix a positive definite shifted matrix of the form

$$([K] - w^2_o [M]) \qquad [1.14]$$

can be used instead of the original [K] matrix. The WYD Ritz vectors approach will theoretically generate the same vectors, although not in the same order, for any shifted matrix of the form given by equation [1.14]. The WYD Ritz vectors will be such that eigenvalues of the reduced system matrices, and the corresponding eigenvectors will approximate the roots of the physical model closest to the specified point of interest in the eigenspectrum w^2_o.

The total number of independent WYD Ritz vectors that can be generated, including any existing rigid body modes, is equal to the rank, s of matrix [M]. Thus, the size of the reduced problem, r, can not be greater than s.

Finally it should be noted that for large systems, or for special class of problems, coordinate reduction procedures such as static condensation and substructuring techniques can be used prior to the application of the WYD Ritz algorithm to obtain smaller system matrices ([M], [K] and {f}) to be used in the vector calculation process. The advantages of such solution procedures must be carefully evaluated in order not to increase the total number of operations required for the solution. This topic and the consequences of dealing with a singular mass matrix will be reviewed in Chapter 7.

1.4.1 Mass Matrix

Two possible mass representations in the FEM formulation are possible. First, a consistent mass matrix, based on the same shape functions used to formulate the stiffness matrix, can be used. In terms of energy, this means that the representation of the kinetic energy is consistent with that of the potential energy. The eigenfrequencies obtained by a free vibration analysis using a consistent mass matrix will all lie above the corresponding exact values according to the theory for a true Rayleigh-Ritz analysis.

Since the dynamic behavior of a structure is less sensitive to the mass distribution than its stiffness distribution, it is also possible to replace the distributed mass of the structure and the attached non-structural materials by a set of point masses located at the nodes. If such a lumped mass representation is chosen, as it is generally the case for civil engineering structures, no bound on eigenfrequencies can be stated. The accuracy may be equally good since the use of a lumped matrix tends to increase the value of the denominator of the Rayleigh's quotient, as compared to the consistent formulation, shifting the response toward the beginning of the spectrum.

The computational advantages in using lumped masses are apparent; smaller storage requirements and smaller number of operations in WYD Ritz vectors generation. Furthermore, it could be argued (1.11) that the use of a consistent mass formulation is generally worth while only if the presence of mass coupling coefficients do not substentially increase the amount of computation required for the solution, otherwise the same amount of computation devoted to solving the problem with a larger number of basic variables could be more profitable. Several possibilities using a lumped mass matrix can be used varying the number of lumped masses in combination with the number of WYD Ritz vectors to be taken as basis vectors. For instance by increasing the number of lumped masses, while keeping the number of WYD Ritz vectors fixed, should provide a more accurate solution without increasing the numerical effort significantly.

1.4.2 Loading Vector

The validity of the WYD Ritz basis to be used in coordinate reduction or in direct vector superposition depends on the nature of the loading acting on the vibratory system. In general, the amplitude of each vector component, as given by the corresponding WYD Ritz coordinates, will

depend on both the representation of the spatial distribution of the loading achieved by the truncated vector basis and the frequency content of the loading as compared to the retained structural frequencies.

Frequency content:

The frequency effect can be pictured in fig. 1.2, taken from reference (1.6) showing the relative contribution of the elastic and inertia forces while resisting the load applied to an undamped SDOF system subjected to harmonic loading.

The conclusion drawn from the study of the response of this SDOF also pertains to analyses of MDOF since the complete response is obtained as a superposition of the response measured in each Ritz coordinate treated as a SDOF and that actual loadings can be represented, in a Fourier decomposition, as a superposition of harmonic sine and cosine components.

It is observed that the inertial resistance is significant only for the relatively low frequency modes, while for modes with frequencies greater that about three times the applied loading frequency the resistance is essentially elastic. This suggests that higher modes resistance can be calculated as a static problem.

Spatial Distribution:

While forming the dynamic equilibrium equations of the reduced system, the dynamic loading is calculated as:

$$\{F_i\}^* = \{X_i\}^T \{F(s,t)\} = (\{X_i\}^T \{f(s)\})\, g(t) \qquad [1.15]$$

According to equation [1.15], the force $\{F_i\}^*$ will be insignificant if the spatial distribution of the external load, $\{f(s)\}$, is totally dissimilar to the vector shape $\{X_i\}$ and

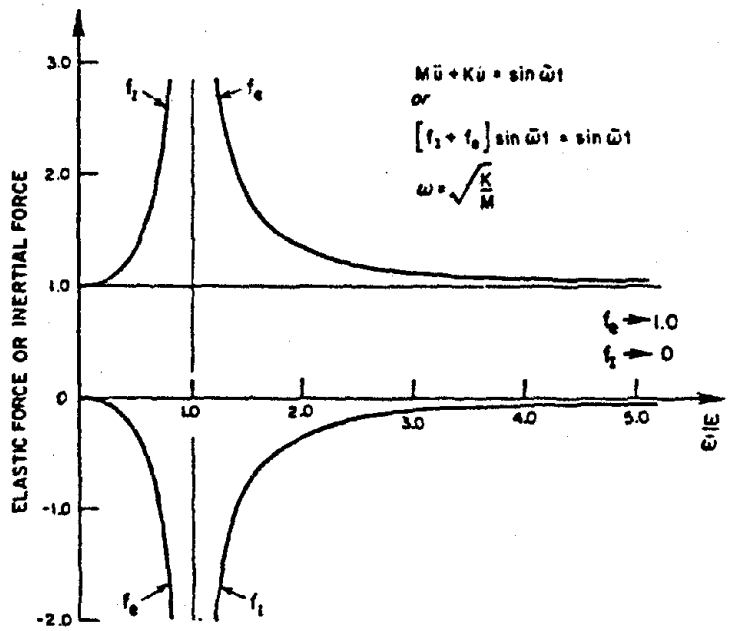

Fig. 1.2 Inertia and Elastic Forces Versus Modal Frequency (after Clough and Wilson, ref. (1.6))

this vector can be omitted from the response without loss of accuracy. An important example of such a behavior is found in earthquake loading where the load is distributed over the entire structure and interacts effectively only with its lower modes.

However, external loads applied at specific points on a structure tend to participate with all modes and none can be omitted arbitrarily from consideration. If the loading is basically of low frequency, the concept of fig. 1.2 is applicable and the higher modes will respond as static loads.

CHAPTER 2

Relationship Between the WYD Ritz Algorithm and the Lanczos Method

The well established transformation methods for small matrix systems (Givens, Householders, LR and QR) are not effective for solving large order eigenvalue problems occuring in the analysis of structural vibration because they can not take advantage of sparsity. Over the last ten years a very significant development effort has been put in vector iteration methods to deal effectively with large sparse eigenproblems. The subspace iteration method has emerged as the standard approach for the eigenvalue analysis of large structural systems and has been implemented in several codes for large main frame computers such as *ADINA* (2.1), *ABAQUS* (2.8) and SAP-IV (2.3). More recently a lot of attention has been devoted to the Lanczos method, which is not in itself an iterative technique, to obtain a practical algorithm that can be used as an alternative for the eigensolution of large sparse matrix systems. In this chapter a formal mathematrical relationship between the WYD Ritz algorithm and the Lanczos method will be established. A lot of basic properties of the WYD Ritz technique can thus be recognized by considering the similarity between the two numerical algorithms.

2.1 The Lanczos Method

The Lanczos method (2.9) was originally proposed as a technique for the tridiagonalization of matrices. A sequence of trial vectors are formed by premultiplication with the matrix to be reduced. Each new vector is orthogonalized with respect to the two previous vectors. This orthogonalization procedure can be shown to be sufficient to obtain orthogonality with all previously calculated vectors. The

coefficients computed from the orthogonalization process then combine to form a tridiagonal matrix which, after n vectors have been calculated, where n is the order of the system, has theoretically the same eigenvalues as the original matrix. It was pointed out later that even if the tridiagonalization is not carried out to completion, good approximations to the extremal eigenvalues can be obtained from the reduced matrices. The Lanczos algorithm applied to the solution of the generalized eigenproblem,

$$[K]\,[\emptyset] = [M]\,[\emptyset]\,[\omega^2] \qquad [2.1]$$

is presented in fig 2.1. In the Lanczos method all the calculated vectors are mutually orthogonal. However the early development of the method was hampered because the implicit orthogonalization tends to break down in practice and formal orthogonalization reduces the computational advantage of the method when it is applied to the complete eigensolution of a matrix system. Various schemes have been proposed to overcome the problem of lack of orthogonality and now reliable Lanczos programs have been developed when the partial eigensolution of a large matrix is sought (2.10 - 2.13).

The traditional use of the Lanczos method for the solution of the dynamic equilibrium equations has been to apply the algorithm to calculate a specified number (m) of exact eigenvalues and corresponding eigenvectors to completely uncouple the equations of motion.

The starting vector is usually chosen at random ignoring important information specific to the dynamic problem. Then the following operations are typically performed:

- Truncated Lanczos tridiagonalization by constructing the $[T_r]$ matrix (r is chosen large enough so that a good approximation to the first m eigenvalues can be obtained (eg. r=2m)).

Fig. 2.1 Lanczos Method for the Solution of the Generalized Eigenproblem $[K][\Phi] = [M][\Phi][\omega^2]$

1. Given Mass and Stiffness Matrices [M] and [K] with :

[M]	n x n system size
[K]	n x n

2. Triangularized Stiffness Matrix:

$[K] = [L]^T [D] [L]$ n x n system

3. Choose an Arbitrary Starting vector {X} :

$b = (\{X\}^T [M] \{X\})^{1/2}$ M-Normalization

$\{X_1\} = \{X\} * 1/b$ Vector one

4. Solve for Additional Vectors with $b_1=0$ and $i=2,\ldots,r$:

(a) $[K] \{\bar{X}_i\} = [M] \{X_{i-1}\}$ Solve for $\{\bar{X}_i\}$

(b) $a_{i-1} = \{\bar{X}_i\}^T [M] \{X_{i-1}\}$

(c) $\{\tilde{X}_i\} = \{\bar{X}_i\} - a_{i-1} \{X_{i-1}\} - b_{i-1} \{X_{i-2}\}$ M-Orthogonalized

(d) $b_i = (\{\tilde{X}_i\}^T [M] \{\tilde{X}_i\})^{1/2}$ M-Normalization

$\{X_i\} = \{\tilde{X}_i\} * 1/b_i$

5. Construct Symmetric Tridiagonal Matrix [T] of order r :

(typically r=2m where m is the number of requested eigenvalues)

$$[T_r] = \begin{bmatrix} a_1 & b_2 & 0 & \cdots & 0 \\ b_2 & a_2 & b_3 & \cdots & \vdots \\ 0 & b_3 & a_3 & \cdots & \vdots \\ 0 & 0 & \cdots & & 0 \\ \vdots & \vdots & \cdots & b_{r-1} & a_{r-1} \; b_r \\ 0 & \cdots & \cdots & b_r & a_r \end{bmatrix}$$

6. Calculate Eigenvalues and Eigenvectors of $[T_r]$:

$$[T_r][Z] = [Z][\lambda]$$

$$[\omega^2] = [1/\lambda]$$

7. Expand Eigenvectors to Full System Size :

$$[\Phi] = [X][Z]$$

- QR eigenvalue extraction of the reduced tridiagonal system.

- Inverse iteration to obtain the eigenvectors of the reduced system.

- Expansion of the eigenvectors to full system size.

The accuracy of the eigensolution and the convergence characteristics of the Lanczos method are considerably influenced by the spectral content of the starting vector $\{X_1\}$, the number r of generated vectors using the method and the spread in the eigenvalues of the eigenproblem. By reviewing the performance of the algorithm (2.15) the following observations can be made on each of the preceeding convergence factors ;

a) <u>The spectral content of the starting vector :</u>

If vector $\{X_1\}$ is orthogonal to a required eigenvector $\{\emptyset_j\}$, the eigenvector $\{\emptyset_j\}$ and the corresponding eigenvalue w^2_j will be missed by the predicted eigensolution. A direct consequence of this property is that if the starting vector $\{X_1\}$ is deficient in some eigenvector components and lies in an i-dimensional sub-space of the n dimensional space formed by the operators [K] and [M], the generated vector $\{X_{i+1}\}$ will theoretically be a null vector.

b) <u>The number r of generated vectors using the method :</u>

The accuracy of the approximation improves as the value of r, the number of vectors generated by the Lanczos method is increased. If $r = n$, the order of the full system, or if the components of eigenvectors $\{\emptyset_{r+1}\}$ to $\{\emptyset_n\}$ are not present in the starting vector then the smallest r eigen-values and associated vectors will be predicted exactly.

c) The spread in the eigenvalues of the eigenproblem :

The accuracy of the eigenpair approximation depends also to some extent on the spreading of the eigenvalues w^2_j of the generalized eigenproblem. The more spreading of the eigenvalues the more accurate will be the prediction obtained from the Lanczos method. The components of eigenvectors corresponding to almost equal eigenvalues undergo very similar magnification hence there will be a poor resolution of the eigenvectors corresponding to very close eigenvalues.

The Lanczos method is not an iterative method so the analyst have little control on the accuracy of the calculated eigensolution other than to choose a large value for r the number of generated vectors. In order to ensure an accurate eigensolution, the Lanczos procedure is usually supplemented by an eigenvalue error bound calculation and a Sturm sequence check to ensure that no eigenvalue has been completely missed by the procedure.

2.2 Basic Properties of WYD Ritz Vectors

Chowdhury (1.5) has proposed that Lanczos vectors could be used in place of normal modes as basic variables in dynamic response calculations but did not carry on the development of the idea. As previously reported, Wilson et al. (1.17) independently developed the idea of generating a set of orthogonal vectors for use in Ritz type of analysis as an alternative to the mode superposition method. By comparing the WYD Ritz vectors algorithm as proposed in fig.1.1 to the Lanczos method shown in fig 2.1 it is recognized that the two basic elements of each technique are:

a) the vector sequence obtained from :

$$(X_1, [K]^{-1}[M]\{X_1\}, ([K]^{-1}[M])^2\{X_1\}, \ldots, ([K]^{-1}[M])^n\{X_1\}) \quad [2.2]$$

known to mathematician as Krylov subspace (2.14),

b) the Rayleigh-Ritz transformation method to obtain an approximation to the eigenvalue problem.

It should be noted that the above vector sequence when obtained without orthogonalization, will converge to the eigenvector corresponding to the lowest eigenvalue of $[K][\Phi] = [M][\Phi][\omega^2]$, this method of solution for the lowest mode is usually called Stodola's iteration by the civil engineering profession.

The Lanczos method and the WYD Ritz approach supplement the Krylov sequence with Gram-Schimdt orthogonalization at each step, the result is a set of [M] orthonormal vectors used to reduce the size of the system of dynamic equilibrium equations to a small number of generalized coordinates. A parallel will be established between the two methods showing that the WYD Ritz algorithm is similar to the method used to produce Lanczos vectors. It should however be recognized that the philosophy behind the choice of the starting vector used to initiate the recurrence algorithm and the subsequent use of the vector basis in the reduction of dynamic equilibrium equations, as proposed in the WYD Ritz reduction method, is new and requires further research and development to become fully operational.

The basic algorithm to generate the WYD Ritz vectors, as presented in fig 1.1, will next be reviewed to show its equivalence to the Lanczos method presented in fig 2.1;

A) Generate and mass normalize the first vector :

$$\{\bar{X}_1\} = [K]^{-1}\,[M]\,\{f\} \qquad [2.3]$$

$$b = (\{\bar{X}_1\}^T\,[M]\,\{\bar{X}_1\})^{1/2}$$

$$\{X_1\} = \{\bar{X}_1\} * 1/b \qquad [2.4]$$

B) Generate a typical additional vector : i = 2,...,r

$$\{\bar{X}_i\} = [K]^{-1}\,[M]\,\{X_{i-1}\} \qquad [2.5]$$

C) Orthogonalize $\{\bar{X}_i\}$ against all previously obtained vectors, assuming that $\{\bar{X}_i\}$ has components common to each vector of the basis :

$$\{\tilde{X}_i\} = \{\bar{X}_i\} - a_{i,i-1}\{X_{i-1}\} - a_{i,i-2}\{X_{i-2}\} - \ldots - a_{i,1}\{X_1\} \qquad [2.6]$$

$$a_{i,j} = \{X_j\}^T\,[M]\,\{\bar{X}_i\} \quad \text{for } j=1,\ldots,i-1 \qquad [2.7]$$

D) Mass normalize $\{\tilde{X}_i\}$ to obtain orthonormal $\{X_i\}$,

$$\{X_i\} = \{\tilde{X}_i\} * 1/b_i \qquad [2.8]$$

$$b_i = (\{\tilde{X}_i\}^T\,[M]\,\{\tilde{X}_i\})^{1/2} \qquad [2.9]$$

E) Equation [2.6] can be written as

$$\{\bar{X}_i\} = b_i\{X_i\} + a_{i,i-1}\{X_{i-1}\} + a_{i,i-2}\{X_{i-2}\} + \ldots + a_{i,1}\{X_1\}$$
$$= [K]^{-1}\,[M]\,\{X_{i-1}\} \qquad [2.10]$$

writing [2.10] in matrix form we get :

$$[K]^{-1}\,[M]\,[X] = [X]\,[H] \qquad [2.11]$$

with

$$[H] = \begin{bmatrix} a_{2,1} & a_{3,1} & a_{4,1} & \cdot & \cdot & \cdot & \cdot & a_{r,1} \\ b_2 & a_{3,2} & a_{4,2} & \cdot & \cdot & \cdot & \cdot & \cdot \\ 0 & b_3 & a_{4,3} & \cdot & \cdot & \cdot & \cdot & \cdot \\ 0 & 0 & b_4 & \cdot & \cdot & \cdot & \cdot & \cdot \\ \cdot & 0 & 0 & \cdot & \cdot & \cdot & \cdot & \cdot \\ \cdot & \cdot & \cdot & \cdot & \cdot & \cdot & \cdot & \cdot \\ \cdot & \cdot & \cdot & \cdot & \cdot & \cdot & \cdot & \cdot \\ 0 & 0 & 0 & 0 & . & 0 & b_r & a_{r,r} \end{bmatrix} \qquad [2.12]$$

[H] is a matrix of upper Hessenberg form, that is an upper triangular matrix with nonzero entries on first line below the main diagonal ($h_{i,j}=0$ for $i>j+1$).

Premultiplying equation [2.11] by $[X]^T [M]$, we get:

$$[X]^T [M] [K]^{-1} [M] [X] = [X]^T [M] [X] [H] \qquad [2.13]$$

The right hand side of equation [2.13] must be symmetric since [K] and [M] are symmetric, and that the inverse of a symmetric matrix must be symmetric;

$$([X]^T [M] [K]^{-1} [M] [X])^T = [X]^T [M]^T [K]^{-T} [M]^T [X] = [X]^T [M] [K]^{-1} [M] [X] \qquad [2.14]$$

using the fact that $[X]^T [M] [X] = [I]$ in equation [2.13], we get

$$\underbrace{[X]^T [M] [K]^{-1} [M] [X]}_{\text{symmetric}} = \underbrace{[H]}_{\text{upper Hessenberg}} \qquad [2.15]$$

The only way that equation [2.15] can be satisfied is if [H] is tridiagonal that is (using only the first subscript of the a coefficients);

$$[H] = [T_r] = \begin{bmatrix} a_1 & b_2 & 0 & . & . & 0 \\ b_2 & a_2 & b_3 & . & . & . \\ 0 & b_3 & a_3 & . & . & . \\ 0 & 0 & . & . & . & 0 \\ . & . & . & . & . & b_r \\ 0 & . & . & 0 & b_r & a_r \end{bmatrix} \qquad [2.16]$$

Equation [2.16] shows that while calculating vector $\{X_i\}$ orthogonality with only two of the preceeding vectors $\{X_{i-1}\}$, $\{X_{i-2}\}$ is sufficient to obtain orthogonality with all previously calculated vectors. Equation [2.16] is also identical to the tridiagonal matrix $[T_r]$ generated from the Lanczos algorithm.

2.3 Note on Orthogonality of the WYD Ritz Vector Basis

In practice, it is found that in the solution of large systems, the vector $\{X_i\}$ may not be [M] orthogonal due

to round off error and cancellation in the Gram-Schmidt process. Orthogonalization procedure using iterative improvements on a local scale with vectors $\{X_{i-1}\}$, $\{X_{i-2}\}$ and whenever necessary on a global scale with all previously formed vectors have been sucessfully implemented to overcome the numerical instability of the Gram-Schmidt method.

The algorithm used to produce WYD Ritz vectors thus corresponds to the method used to obtain Lanczos vectors for which the starting vector used to initiate the recurrence relationship is given by the spatial distribution of the dynamic loading. Furthermore, in the WYD Ritz approach a full reorthogonalization against all previously calculated vectors is used for each new vector added to the basis to maintain global orthogonality among the basis vectors as the algorithm proceeds. It will however be shown that this is generally not sufficient to ensure that the required [M]-orthogonality condition has been satisfied. A complete discussion with numerical applications will be presented in chapter 4.

2.4 Solution of Undamped Dynamic Equilibrium Equations in Generalized Coordinates

Consider the undamped equilibrium equation given by:

$$[M]\{\ddot{U}\} + [K]\{U\} = \{F(s,t)\} = \{f(s)\} * g(t) \qquad [2.17]$$

2.4.1 Solution in WYD Ritz Coordinates

Using the substitution $\{\bar{U}\} = [X]\{Y\}$ directly in equation [2.17] and premultiplying by $[X]^T$ to complete the transformation we get,

$$[X]^T[M][X]\{\ddot{Y}\} + [X]^T[K][X]\{Y\} = [X]^T\{F\} \qquad [2.18]$$

$$[I]\{\ddot{Y}\} + [K]^*\{Y\} = [X]^T\{F\} \qquad [2.19]$$

Equation [2.19] can theoretically be solved by any standard numerical technique used in structural dynamics, it can notably be uncoupled by solving the reduced eigenvalue problem in WYD Ritz coordinates as explained in section 1.3 .

2.4.2 Solution in Lanczos Coordinates

The reduced structural system expressed in generalized Lanczos coordinates (see ref. 1.14) is obtained by premultiplying equation [2.17] by $[M]\,[K]^{-1}$ and using the substitution $\{\bar{U}\} = [X]\,\{Y\}$. The transformation is then completed by premultiplying by $[X]^T$ to obtain,

$$[X]^T[M][K]^{-1}[M][X]\{\ddot{Y}\}+[X]^T[M][K]^{-1}[K][X]\{Y\}=[X]^T[M][K]^{-1}\{F\} \qquad [2.20]$$

Assumming that the dynamic loading distribution {f} is used to initiate the vector sequence we get,

$$[T_r]\,\{\ddot{Y}\} + [I]\,\{Y\} = [X]^T\,[M]\,[K]^{-1}\,\{f\} * g(t) = [X]^T\,[M]\,\{\bar{X}_1\} * g(t) \qquad [2.21]$$

$$[T_r]\,\{\ddot{Y}\} + [I]\,\{Y\} = \{e_1\}\,(\{\bar{X}_1\}^T\,[M]\,\{\bar{X}_1\})^{1/2} * g(t)$$

where $\{e_1\}$ is the first column of the identity matrix.

The reduced Lanczos system, as expressed by equation [2.21], can be uncoupled by the solution of the eigenproblem in Lanczos coordinates. Recalling that,

$$[X]^T\,[M]\,[K]^{-1}\,[M]\,[X] = [T_r] \qquad [2.22]$$

where $[T_r]$ is tridiagonal of order r, we can now relate the eigenvalues $[\lambda]$ and eigenvectors $[Z]$ of $[T_r]$ when r=n, the order of the unreduced system, to those of the original system:

$$[K]\,[\Phi] = [M]\,[\Phi]\,[\omega^2] \qquad [2.23]$$

$$[M]\,[\Phi]\,[\omega^2]^{-1} = [M]\,[K]^{-1}\,[M]\,[\Phi] \qquad [2.24]$$

using the transformation $[\Phi] = [X][Z]$ and premultiplying by $[X]^T$,

$$[X]^T[M][X][Z][\omega^2]^{-1} = [X]^T[M][K]^{-1}[M][X][Z] \qquad [2.25]$$

$$[Z]\,[\omega^2]^{-1} = [T_n]\,[Z] \qquad [2.26]$$

Hence the eigenvalues of $[T_n]$ are reciprocal of the eigenvalues of $[K][\Phi] = [M][\Phi][\omega^2]$ and the eigenvectors of the two problems are related by the equation $[\Phi] = [X]\,[Z]$.

If r is smaller than n the eigenvalues of $[T_r]$ can give good approximations to the smallest eigenvalues of $[K][\Phi] = [M][\Phi][\omega^2]$.

It can be shown that equation [2.21] in Lanczos coordinates and [2.19] in WYD Ritz coordinates are entirely equivalent;

$$([K]^*)^{-1} = ([X]^T\,[K]\,[X])^{-1} = [X]^{-1}\,[K]^{-1}\,[X]^{-T} \qquad [2.27]$$

Since $[X]^T\,[M]\,[X] = [I]$ we get,

$$[M]\,[X] = [X]^{-T} \qquad [2.28]$$

$$[X]^T\,[M] = [X]^{-1} \qquad [2.29]$$

Substituting [2.28] and [2.29] in [2.27] we get,

$$([K]^*)^{-1} = [X]^T\,[M]\,[K]^{-1}\,[M]\,[X] = [T_r] \qquad [2.30]$$

Premultiplying [2.19] by [2.27], we thus get:

$$([K]^*)^{-1}[I]\{\ddot{Y}\}+([K]^*)^{-1}[K]^*\{Y\} = [X]^{-1}[K]^{-1}[X]^{-T}[X]^T\{F\} \qquad [2.31]$$

$$[T_r]\,\{\ddot{Y}\} + [I]\,\{Y\} = [X]^T\,[M]\,[K]^{-1}\,\{f\} * g(t) \qquad [2.32]$$

The equilibrium equation [2.32] derived from equation

[2.19], the equilibrium equation in WYD Ritz coordinates, is identical to the Lanczos equilibrium equation (eq. [2.21]), thus showing that the solution in WYD Ritz coordinates is equivalent to the solution in Lanczos coordinates, one approach being the inverse of the other. It should be noted that the topologies of the reduced systems are different since in Lanczos coordinates the structure of the $[T_r]$ matrix is tridiagonal and in WYD Ritz coordinates the structure of the $[K]^*$ matrix is full. The solution in Lanczos coordinates will thus potentially be more efficient than the solution in WYD Ritz coordinates. It should also be noted that in practical applications, the reduced systems are generally small, of the order of 10 to 50 generalized DOF, such that the difference between the actual efficiency of the two solutions might not be of major significance.

The methods used to obtain the reduced systems are also different. In the Lanczos approach the $[T_r]$ matrix is constructed directly using the information generated during the orthonormalization of the vector sequence, while in the WYD Ritz algorithm this information is not retained. The WYD Ritz approach uses the formal transformation $[X]^T[K][X]$ (that can be imbeded in the vector generation algorithm for greater efficiency) to obtain the reduced systems.

2.5 Analysis of Damped Systems

While using the FEM the generation of the damping matrix [C] usually presents special difficulties due to the lack of information regarding damping mechanisms and damping levels in structures. If the damping mechanisms are limited to internal, or material damping and the structure is made from one homogeneous material the damping matrix will be proportional to the stiffness matrix. For structures build from two or more homogeneous materials or in interaction problems such as soil-structure or fluid-structure systems each component damping matrix may be proportional to the

corresponding stiffness matrix but as the constants of proportionality differ, the system damping matrix will not be proportional to the system stiffness matrix. Non-proprotionally damped systems require special considerations if a dynamic solution using direct vector superposition is to be used.

2.5.1 Solution Procedures for Proportional Damping

Consider the basic equilibrium equation obtained from the FEM for the free damped vibration problem;

$$[M]\{\ddot{U}\} + [C]\{\dot{U}\} + [K]\{U\} = \{0\}$$
$$\{U\} + [M]^{-1}[C]\{U\} + [M]^{-1}[K]\{U\} = \{0\} \qquad [2.33]$$

if the normal mode method is used, the exact eigenvectors of the free undamped vibration problem will be used to diagonalized the system stiffness and mass matrices according to;

$$[K][\emptyset] = [M][\emptyset][w^2]$$
$$[M]^{-1}[K][\emptyset] = [\emptyset][w^2] \qquad [2.34]$$

with $[\emptyset]^T[K][\emptyset] = [w^2]$ and $[\emptyset]^T[M][\emptyset] = [I]$ [2.35]

the damping terms are uncoupled if $[C]^* = [\emptyset]^T[C][\emptyset]$ is a diagonal matrix. In order to achieve damping uncoupling the matrix $([M]^{-1}[C])$ and matrix $([M]^{-1}[K])$ of equation [2.33] should share the same eigenspace. From mathematical analysis it is well known that two matrices [A] and [B] share the same eigenspace if they commute, that is [A][B] = [B][A]. The necessary and sufficient condition for damping uncoupling thus become;

$$([M]^{-1}[C])([M]^{-1}[K]) = ([M]^{-1}[K])([M]^{-1}[C])$$
or
$$([C][M]^{-1}[K]) = ([K][M]^{-1}[C]) \qquad [2.36]$$

In general this condition is not satisfied but

Caughey (2.4,2.5) has shown that by expressing the damping matrix [C] in terms of [M] and [K] according to

$$[C] = [M] \sum_i a_i ([M]^{-1}[K])^i \qquad [2.37]$$

the reduced damping matrix $[C]^*$ will be diagonal. In most analyses using the normal mode method the damping matrix [C] is not formed explicitly, it is rather assumed that damping is proportional to [M] and [K] matrices such that;

$$\{\emptyset_i\}^T [C] \{\emptyset_j\} = 2 w_i \xi_i \delta_{ij} \qquad [2.38]$$

where ξ_i is a modal damping parameter and δ_{ij} is the Kronecker delta ($\delta_{ij} = 1$ for $i=j$, $\delta_{ij} = 0$ for $i \neq j$).

If the damping matrix [C] needs to be formed explicitly it is important to consider a special case of equation [2.37], using i=0,1 we get;

$$[C] = a_0[M] + a_1[K] \qquad [2.39]$$

which is known as Rayleigh damping. The constants a_0, a_1 are arbitrary proportionality constants applied to the [M] and [K] matrices of the complete system. The modal damping ratio ξ_i for any mode can be defined as,

$$\xi_i = 1/2 \left(a_0/w_i + a_1 w_i \right) \qquad [2.40]$$

it is observed from equation [2.40] that the lower modes are primarily damped by the mass proportional damping and the higher modes by the stiffness proportional part. The constants a_0, a_1 are selected to obtain, as closely as possible, the desired level of damping for the modes covering the frequency range considered important to the dynamic response. Rayleigh damping represents a convenient way of introducing the damping concept as no extra storage is needed since the matrices [M] and [K] already exist. The damping

matrix [C] get the same orthogonality properties as [M] and [K].

An important observation from a numerical stand point, is that if more than two proportionality constants (a_o,a_1 plus others) are used the matrix [C] will in general be full, that is the banded form of [M] and [K] matrices will be lost. This will require more storage if [C] is explicitly formed and significantly more numerical operations if a step-by-step solution on the full unreduced system is performed. In most analyses by direct integration Rayleigh damping is therefore assumed.

The reduced Rayleigh damped FEM equilibrium equations using the WYD Ritz vectors [X] as coordinate transformation vectors will give the following reduced damping matrix ;

$$[C] = a_o[M] + a_1[K]$$
$$[X]^T [C] [X] = a_o [X]^T [M] [X] + a_1 [X]^T [K] [X]$$
$$[C]^* = a_o[I] + a_1[K]^* \qquad [2.41]$$

the matrix $[K]^*$ will in general be full and the matrix $[C]^*$ will have the same topology as $[K]^*$. The introduction of the additional transformation matrix [Z] to orthogonalize the WYD Ritz vectors with respect to the stiffness matrix, as explained in section 1.3 will diagonalized the reduced system

$$[K]^* [Z] = [M]^* [Z] [\bar{w}^2]$$
$$[Z]^T [C]^* [Z] = [2\xi\bar{w}] \qquad [2.42]$$

If the solution is carried out in Lanczos coordinates with a Rayleigh damped system we get;

$$[C] = a_o[M] + a_1[K]$$
$$[X]^T([M][K]^{-1}[C])[X]=a_o[X]^T([M][K]^{-1}[M])[X]+a_1[X]^T([M][K]^{-1}[K])[X]$$
$$[C]^* = a_o[T_r] + a_1[I] \qquad [2.43]$$

the reduced damping matrix [C]* will thus be tridiagonal. If more than two terms are included in the Caughey serie (eq. [2.37]) the reduced damping matrix [C]* will lose its tridiagonal characteristic and will in general be full.

2.5.2 Solution Procedures for Non-Proportional Damping

Once the non-proportional damping matrix has been determined from damping properties of the various components of the structure, an appropriate numerical technique for the solution of the equilibrium equation

$$[M]\{\ddot{U}\} + [C]\{\dot{U}\} + [K]\{U\} = \{F\} \qquad [2.44]$$

must be found under the restriction that the normal undamped modes, or the mass and stiffness orthogonal WYD Ritz vectors, will not diagonalize the system. The most frequently used solution procedures are :

- the direct integration method using either the original geometric coordinates or a reduced set of generalized Ritz coordinates,

- the vector superposition approach using either complex shape vectors or real vectors along with weighted damping ratios.

An obvious method for analyzing a structure with non-proportional damping is to integrate directly the coupled equations of motion expressed in original discrete coordinates. The important disadvantage of this procedure is that all the equations of motion must be included in the analysis requiring a large computational effort.

In order to obtain a more efficient solution a direct integration procedure on a reduced system expressed in generalized Ritz coordinates was recommended by Clough and Mojtahedi (2.6). In their presentation Clough and Mojtahedi

used a set of the lowest exact mode shapes of the undamped free vibration problem as transformation vectors to obtain a reduced coupled system of equations that will be integrated directly. The reduced coupled system will be of much smaller order than the original system so an economic solution is still possible even if a small time step increment is used over a long loading record. In fact, the same procedure using the WYD Ritz algorithm presented in fig. 1.1 to generate the transformation vectors will lead to an even more efficient solution technique since these vectors are more economical to generate than the exact eigenvectors of the structure. This numerical technique was tested on the earthquake analysis of a small shear beam model and proved to be very effective.

The equations of motion of a structure with non-proportional damping may also be uncoupled by the solution of the complex eigenproblem

$$- [w^2] [M] [\emptyset] + i [w] [C] [\emptyset] + [K] [\emptyset] = \{0\} \qquad [2.45]$$

in such a case the complex mode shapes and frequencies will contain in phase and out of phase components such that the eigenproblem is essentially of order 2n. The same approach can be used to diagonalize the reduced system expressed in WYD Ritz coordinates by the matrices $[M]^*$, $[C]^*$ and $[K]^*$, the order of the complex eigenproblem will then be 2r where r is the number of vectors retained in the transformation.

A major advantage of this uncoupling procedure over the direct integration method of the coupled system is that an exact mathematical solution is possible if an approximate description of the forcing function is used. The solution for integration of the uncoupled differential equations subjected to dynamic loads represented by a series of straight line between equal or unequal intervals of time can be formulated in closed form. This approximate loading description is

generally used for any digitized transient record. The disadvantage of the direct integration method of the coupled system is that the dynamic response will generally exhibit period elongation and amplitude decay with increasing time.

The major drawbacks of the complex eigenmethod is the larger size of the eigenproblem that must be considered and the necessity of dealing with complex numbers in the dynamic response.

2.6 Basic Philosophy Behind the WYD Ritz Algorithm

If the objective of the calculation is an accurate eigensolution we note, from the Lanczos method, that the number of generalized coordinates in the reduced system, r, must be much greater than the number of modes, m, retained in the modal superposition summation. In view of the uncertainty in the loading, especially for earthquake analysis, it appears that the extra cost of extracting higher and more accurate modes is not really worth while. A numerical method devised to correctly represent the specified loading and associated response with a minimum number of numerical operations, even if not producing an accurate eigensolution, should be considered acceptable for design applications.

The objective of the WYD Ritz vectors procedure is not to obtain an accurate solution of the free vibration eigenproblem but to from an accurate load dependent vector basis to transform the dynamic equilibrium equations to a more suitable form for solution. The solution of the transformed set of equations to a specified number of WYD Ritz coordinates can then be carried out by any standard numerical method used in structural dynamics, such as direct step-by-step integration, frequency domain analysis or the response spectra technique. If a vector superposition solution is chosen, the number of WYD Ritz coordinates used

in the transformation will thus typically be the same as the number of vectors retained in the summation leading to an optimal solution technique.

In theory while using the WYD Ritz method only vectors which are excited by the spatial load pattern are generated whereas some of the exact eigenvectors may be nearly orthogonal to the spatial load pattern and therefore do not significantly participate in the response. The numerical results presented in Chapter 4 and 5 indicates clearly that a dynamic solution working directly in WYD Ritz coordinates, or in Lanczos coordinates obtained from load dependent Ritz vectors, is much more efficient than an exact eigensolution for the particular type of problems under consideration.

CHAPTER 3

Development of Error Estimates for the WYD Ritz Reduction Method

Reduction methods become unreliable without efficient error estimates. In classical direct vector superposition methods for linear systems, only approximations to the lower modes of the structure are used. Even if interest is centered around frequencies closed to a specified value to discover possible resonant conditions from oscillatory disturbing forces, the specified frequencies should be in the lower end of the spectrum since approximations involved in the physical idealization by the FEM cause higher frequencies of the mathematical model to be inacurate. Higher modes are thus discarded from the analysis and it should be verified that the retained vectors will adequately represent the spatial distribution and sufficiently span the frequency range of the applied loading.

In this chapter error estimates to ensure that the specified loading is correctly represented by the WYD Ritz basis and to measure the relationship between the WYD Ritz solution of the reduced system and the exact eigensolution of the original system will be presented. A parallel will be established between the WYD Ritz reduction method and the familiar static correction and modal acceleration procedures used to improve the traditional modal superposition summation while dealing with a truncated vector set. Finally, some frequency considerations in the error estimation process will also be discussed.

3.1 Spatial Error Estimates for Loading Representation

One of the important aspect of direct vector superposition techniques for the solution of the dynamic equilibrium

equations pertains to the number of vectors that must be retained in the analysis. As the number of required vectors for a satisfactory solution increases, the cost of the analysis grows rapidly. The simplest way to know how many vectors, or generalized coordinates, to retain in the FEM analysis for a given mesh, is to use an iterative solution procedure adding new vectors until convergence of two successive solutions is achieved. It is obvious that this method is uneconomical even for small systems. A better approach would be to develop an error norm, at the level of the vectors generation algorithm, to indicate when to stop generating new vectors while ensuring a satisfactory convergence for the response quantities of interest.

3.1.1 Representation of the Loading by the WYD Ritz Basis

Hansteen and Bell (3.4) demonstrated that the inaccuracies of modal truncation are caused by the omission of load components that are orthogonal to the modes included in the solution. The basic idea to measure the part of the external load vector that has not been included in the vector superposition summation, will be to expand the load vector in terms of the truncated vectors basis and define error norms that are functions of the residual.

A complete set of mass orthogonal Ritz vectors constitutes a basis for an n-dimensional linear space so that an arbitrary vector such as the spatial loading distribution, $\{f(s)\}$, can be expressed as

$$\{f(s)\} = [M]\{X_1\}\, p_1 + [M]\{X_2\}\, p_2 + \ldots + [M]\{X_n\}\, p_n$$
$$\{f(s)\} = [M][X]\,\{p\} \qquad [3.1]$$

Premultiplying equation [3.1] by $[X]^T$ and using the M-orthonormality condition $[X]^T[M][X] = [I]$ we get,

$$[X]^T\{f(s)\} = \{p\} \qquad [3.2]$$

substituting [3.2] in [3.1] we get,

$$\{f(s)\} = [M]\,[X]\,[X]^T\,\{f(s)\} \qquad [3.3]$$

The spatial loading distribution can thus be expressed by the following finite serie,

$$\{f(s)\} = \sum_{j=1}^{n} p_j\,[M]\{X_j\} \qquad [3.4]$$

where the vector participation factor, p_j, is defined as,

$$p_j = \{X_j\}^T\,\{f(s)\} \qquad [3.5]$$

In the use of exact eigenvectors or WYD Ritz vectors in a direct superposition analysis, the participation factor is a direct indication if the shape vector, $\{X_j\}$, will participate in the dynamic solution. The participation factor, p_j, can thus be viewed as the coordinate of the load vector expressed in term of the vector $[M]\{X_j\}$. Therefore, the error in the representation of the load by a reduced number of retained vectors, r, can be defined as,

$$\{E_r(s)\} = \{f(s)\} - \sum_{j=1}^{r} p_j\,[M]\{X_j\} = \{f(s)\} - \{f_r(s)\} \qquad [3.6]$$

It should be noted that the validity of equations [3.3] to [3.6] is ensured by using shape vectors, $\{X_j\}$ that are only [M] orthonormal. If we substitute [K] and [M] orthogonal WYD Ritz vectors, $\{^oX_j\}$, for the vector matrix [X] into equation [3.3] we get,

$$\{f(s)\} = [M]\,[^oX]\,[^oX]^T\,\{f(s)\} \qquad [3.7]$$

Using $[^oX] = [X][Z]$, where [X] are WYD Ritz vectors that are mass orthogonal only, we get,

$$\{f(s)\} = [M]\,[X]\,[Z]\,[Z]^T\,[X]^T\,\{f(s)\} \qquad [3.8]$$

$$\{f(s)\} = \sum_{j=1}^{n} {}^{o}p_j \, [M]\{{}^{o}X_j\} \qquad [3.9]$$

where $$ {}^{o}p_j = \{Z_j\}^T \, [X]^T \, \{f(s)\} \qquad [3.10]$$

is the participation factor for [M] and [K] orthogonal vectors. The matrix [Z] of equation [3.8] represents the eigenvectors of the reduced system, $[K]^*[Z] = [M]^*[Z][\bar{w}^2]$, normalized such that,

$$[Z]^T \, [Z] = [I]$$

or $$ [Z]^T = [Z]^{-1} \qquad [3.11]$$

Substituting equation [3.11] into [3.8] we get,

$$\{f(s)\} = [M] \, [X] \, [X]^T \, \{f(s)\} \qquad [3.12]$$

Equation [3.12] is exactly the same as equation [3.3] developed previously. Using a reduced vector set we can therefore write,

$$\{f_r(s)\} = \sum_{j=1}^{r} p_j \, [M]\{X_j\} = \sum_{j=1}^{r} {}^{o}p_j \, [M]\{{}^{o}X_j\} \qquad [3.13]$$

The important fact about equation [3.13] is that for a fixed number of retained vectors, r, we obtain exactly the same value for $\{f_r(s)\}$ using either mass only orthogonal vectors, $\{X_j\}$, or the [M] and [K] orthogonal vectors $\{{}^{o}X_j\}$. For a practical implementation of the WYD Ritz algorithm this is very significant since if the reduced system is to be diagonalized, it is possible to know prior to the solution of the reduced eigenproblem what will be the error in the loading representation obtained from the final vector basis $[{}^{o}X]$.

An extension of the loading representation is necessary to deal with more general three dimensional analyses. In such a case the loading can be written as,

$$\{F(s,t)\} = \sum_{j=1}^{3} \{f_j(s)\}\, g_j(t) \qquad [3.14]$$

where $\{f_j(s)\}$ is the spatial distribution in the jth direction (x,y or z) and $g_j(t)$ is the corresponding time variation function.

A first analytical approach might consists in applying the summation sign of equation [3.14] at the response calculation level. The WYD Ritz algorithm will thus be run for each axis separately using $\{f_x(s)\}$, $\{f_y(s)\}$ and $\{f_z(s)\}$ as initial loading distributions to form three directional vector bases that will be superimposed to obtain the total response. This procedure will be most efficient if the loading axes correspond to the principal axes of the structure such that there is no coupling of the response when the stucture is subjected to independent excitations.

Actual numerical experimentation on the seismic response of a three dimensional structure (see chapter 5) has shown that the summation sign can advantageously be applied at the initial loading distribution level to form a single WYD Ritz basis constructed from the starting vector given by

$$\{f(s)\} = \{f_x(s)\} + \{f_y(s)\} + \{f_z(s)\} \qquad [3.15]$$

It should be noted that even though a single vector basis can be used in all calculations, it is very important for consistency that the error calculations consider the directionality of the loading. An independent evaluation of the representation of the dynamic loads achieved by the truncated basis should be done for the "X", "Y" and "Z" directions. For example, if directionality is ignored in a three dimensional analysis, the participation factor, p_j, obtained from $\{X_j\}^T\{f(s)\}$, with $\{f(s)\}$ given by the sum of the directional loading distributions as described by equation [3.15], will be equal to

$$p_j = p_{x,j} + p_{y,j} + p_{z,j} \qquad [3.16]$$

Substituting equation [3.16] into [3.13] we get,

$$\{f_r(s)\} = \sum_{j=1}^{r} (p_{x,j} + p_{y,j} + p_{z,j})\ [M]\{X_j\} \qquad [3.17]$$

It is obvious that this equation will produce inconsistent results with respect to a particular loading direction since the participation factors applied to individual vector components of $[M]\{X_j\}$ in the x,y and z directions should be the participation factor of the corresponding direction and not the sum of all directions.

The vector $\{E_r(s)\}$ defined by equation [3.6] is the spatial error in the loading representation due to truncation of the vector basis. Since $\{E_r(s)\}$ is a vector with many individual components it is difficult to develop a direct appreciation for the total amount of the force vector that has been omitted in the calculations.

Two different suggestions, taking directionality of the loading into account, will next be presented to measure the error in the loading representation due to truncation of the vector basis.

3.1.2 Error Estimates Using Summation of Represented Forces

For earthquake analysis, an effective mass corresponding to the part of the total mass responding to the earthquake in each mode is commonly used as a good indication to the relative contribution of a particular mode to the global structural response. A typical development in the "X" direction, while using the exact mass orthonormal eigenvectors of the structure as basis vectors, is presented below.

The loading $\{f_x(s)\}$, acting in the "X" direction, is defined as

$$\{f_x(s)\} = [M]\ \{r_x\} \qquad [3.18]$$

where [M] is the mass matrix and $\{r_x\}$ is the influence vector corresponding to the displacement obtained at each DOF of the structure from a unit base input displacement in the "X" direction. The modal participation factor is defined for mode j as

$$*p_{x,j} = \{\emptyset_j\}^T\ [M]\ \{r_x\} \qquad [3.19]$$

The total mass in the "X" direction is given by

$$m_{xx} = \{r_x\}^T\ [M]\ \{r_x\} \qquad [3.20]$$

For a truncated vector basis containing r modes a comparaison of m_{xx} to

$$m_{r,xx} = \sum_{j=1}^{r} *p^2_{x,j} \qquad [3.21]$$

is made. The value of $*p^2_{x,j}$ corresponds to the fraction of the total mass, in the "X" direction, represented by the modal contribution of vector $\{\emptyset_j\}$, a complete development of equation [3.21] can be found in Clough and Penzien (3.2). The value of $m_{r,xx}$ is thus the spatial summation in the "X" direction of the loading represented by the mode set $[\emptyset_r]$. The percentage of the total mass, m_{xx}, that should be retained in $m_{r,xx}$ for satisfactory convergence is somewhat open to discussion but for example the API-RP2A (3.1) code suggests that a value of at least 90% should be used.

A generalization of this measure to arbitrary spatial loading is natural. Using equation [3.3] with a truncated WYD vector set $[X_r]$ to write an expression similar to $m_{r,xx}$ in its full form and summing in the "X" direction by premultiplying by $\{r_x\}^T$ we get,

$$f_{r,xx} = \{r_x\}^T\ [M]\ [X_r]\ [X_r]^T\ \{f_x(s)\} \qquad [3.22]$$

It is important to note that while using the WYD Ritz method

equation [3.22] should be used instead of equation [3.21] since the participation factors $p_{x,j}$ and ${}^{e}p_{x,j}$ obtained from [M] orthonormal vectors, $\{X_j\}$, or [M] and [K] orthogonal vectors, $\{{}^{e}X_j\}$, are different, it is only the final total sum as given by equation [3.22] that is identical. Thus if the sum of the participation factors squared is used to calcualte the portion of the total load represented by the basis, different results will be obtained from individual vectors of the $[X_r]$ and $[{}^{e}X_r]$ bases. Considering a general three dimensional analysis, the error estimates using summation of the represented forces becomes,

$$e_x = (\{r_x\}^T [M][X_r] ([X_r]^T\{f_x(s)\})) / (\{r_x\}^T\{f(s)\} * 100 \quad [3.23]$$

$$e_y = (\{r_y\}^T [M][X_r] ([X_r]^T\{f_y(s)\})) / (\{r_y\}^T\{f(s)\} * 100 \quad [3.24]$$

$$e_z = (\{r_z\}^T [M][X_r] ([X_r]^T\{f_z(s)\})) / (\{r_z\}^T\{f(s)\} * 100 \quad [3.25]$$

This measure could also be generalized to consider moments applied to some DOF. Numerical experimentation on small structural systems has shown that for earthquake loading, the error norm based on the summation of represented forces will exhibit a monotonically increasing type of convergence. The value of e_x,e_y or e_z will vary between 0 and 100 indicating the relative percentage of the total load represented in the solution by the vector set $[X_r]$. For more general type of dynamic loads, the error norm based on summation of represented forces will not necessarily exhibit a monotonic convergence and negative values as well as intermediate values in excess of 100 are possible.

3.1.3 Error Estimate Using the Euclidean Norm of Error Force Vector

Alternative formulations to measure the relative amount of dynamic load represented by the vector basis were studied in order to obtain an error estimate that will exhibit more similar convergence characteristics for any spatial distribution of the dynamic load. This new error

estimate should also avoid a potential problem of the first error estimate which is that there might be cancellation in the summation such that local fluctuations, with change in sign in the represented forces, might not be fully accounted for by the indexes e_x, e_y or e_z.

After numerical experimentation with various implementation strategies it was found that a measure of the error force vector based on the Euclidean norm ($|X|_2 = (\{X\}^T\{X\})^{1/2}$) and written as

$$e^*_x = 1 - \frac{|\{f_x(s)\} - \{f_{r,x}(s)\}|_2}{|f_x(s)|_2} * 100 \qquad [3.26]$$

$$e^*_x = 1 - \frac{(\{E_{x,r}\}^T\{E_{x,r}\})^{1/2}}{(\{f_x(s)\}^T\{f_x(s)\})^{1/2}} * 100 \qquad [3.27]$$

exhibited convergence characteristics that are similar to the error norm based on the summation of the represented forces for earthquake loading with individual values being generally sligthly more conservative. For more general spatial distribution of the dynamic load it was found from numerical experimentation that,

- the error norm based on equation [3.26] was more conservative and more reliable than the simpler form given by $|\{f_{r,x}(s)|_2 / |\{f_x(s)\}|_2 * 100$,

- that although some fluctuations are possible when the first few vectors are added to the solution, the error norm e^*_x had a better tendency than the error norm e_x to exhibit monotonic convergence.

A sample of these calculations is given in fig. 3.1 where a single concentrated load was applied at the top of a 7 DOF shear beam model and the proposed error estimates were plotted as a function of the number of vectors retained in the analysis.

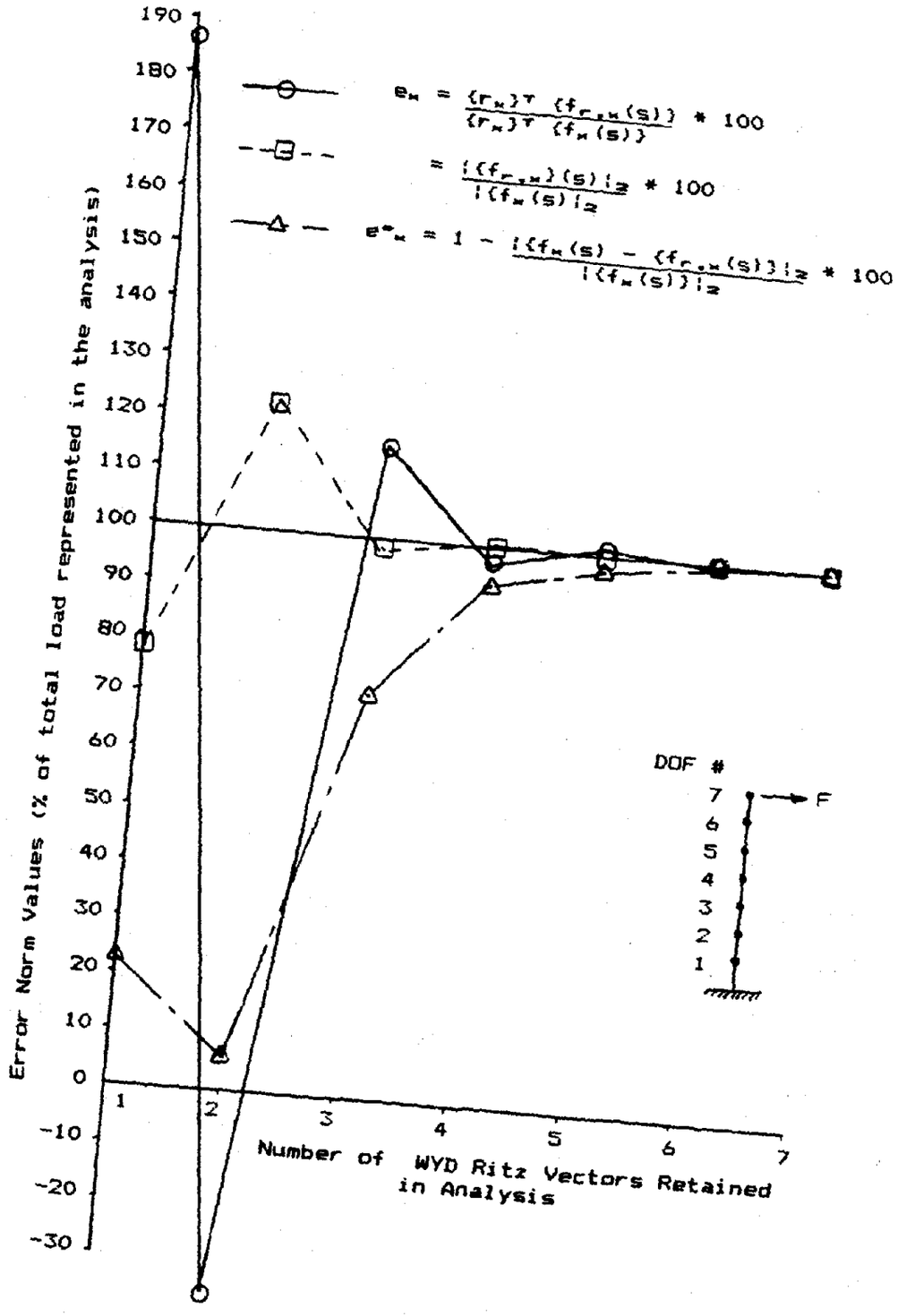

Fig. 3.1 Convergence Characteristics of Various Error Norms

Equation [3.26] is developed for typical "X" direction, similar calculations must be performed to obtain the value of e^*_y and e^*_z. It is also possible to combine the error indexes to obtain a single index reflecting the overall representation of the loading by the basis;

$$e^* = 1 - \frac{(|\{f_x\}-\{f_{x,r}\}|_2+|\{f_y\}-\{f_{y,r}\}|_2+|\{f_z\}-\{f_{z,r}\}|_2)^{1/2}}{|\{f\}|_2} * 100 \qquad [3.28]$$

In equation [3.28] it is implicitly assumed that all loading vectors are a function of space only. The single index e^* is thus based on a comparaison of the length of the loading vector not represented in the analysis to the length of the total load vector.

The key element of the two norms that have been presented is the vector $\{f_r(s)\}$ equal to the fraction of the total load that can be obtained from the truncated basis as given by equation [3.13]. The directional monitoring of the values of e or e^* during the WYD Ritz vectors generation can thus be implemented at the cost of a few extra numerical operations since the product $[M]\{X_j\}$, required to obtain $\{f_r(s)\}$, has to be formed as part of the vector calculation process anyway.

An appropriate value for e or e^* can then be selected to set a cut-off criterion to stop generating new vectors when a good representation of the loading vector by the WYD Ritz basis is ensured. It should be kept in mind that although reliable estimate of gross system behavior, expressed in term of global horizontal displacements, can be achieved with a small number of WYD Ritz coordinates, in practical design application forces and stresses rather than global displacements are of primary interest. Member end rotations, axial forces and bending moments which are dependent upon small differential deformations may be in error leading to poor stress recovery. Performance evaluation

of the numerical scheme should thus be judged on both displacement and stress convergence.

The two error norms, as presented in section 3.1.2 and 3.1.3, were implemented in the computer program used to study the WYD Ritz algorithm and numerical experimentation was used to establish a correlation between the values of e or e^* and the displacement and stress convergence for some studied examples. A complete description of the models used for these analyses and the relevant numerical results are presented in chapters 4 and 5.

3.2 Summation Methods for Direct Vector Superposition Analysis

For most dynamic analyses the higher modes are generally of local character and have a negligible contribution to the overall or global structural response. However, they can be quite important for accurate stress recovery if the load vector has significant components in its expension into modal coordinates. The exact response to the residual force vector $\{E_r(s)\}$ of equation [3.6] while using a truncated vector set can be written as

$$[M]\{\ddot{U}_E\} + [C]\{\dot{U}_E\} + [K]\{U_E\} = \{E_r(s)\}\, g(t) \qquad [3.29]$$
$$(\{f(s)\} - \{f_r(s)\})\, g(t)$$

where $\{U_E\}$ represents the response of the system to the force component neglected by the vector basis representation of the loading. This displacement should be added to the response obtained from the truncated vector superposition to obtain exact results.

3.2.1 Static Correction Method

By assuming that the modes with frequencies substentially greater than the frequencies of the applied loading will respond in a static manner, it is possible to

use a pseudo-static solution to account for the flexiblity of modes which were not retained in the mode displacement summation. The acceleration and velocity in equation [3.29] are set to zero for all time to obtain

$$\{U_E(t)\} = [K]^{-1} (\{f(s)\} - \{f_r(s)\}) g(t) \qquad [3.30]$$

The total response of the system using a static correction for higher modes thus becomes

$$\{U(t)\} = \sum_{i=1}^{r} \{\emptyset_i\} y_i(t) + [K]^{-1} (\{f(s)\} - \{f_r(s)\}) g(t) \qquad [3.31]$$

The natural frequencies of the structure to be analyzed, w_i, compared to the frequency content of the loading, w_L, plays a key role on the effectiveness of the static correction method. As noted in fig. 1.2, the assumption that the static part of higher modal response is a good approximation to the dynamic response is very good only for large frequency ratios w_i/w_L. As the frequency ratios approach unity the approximation becomes doubtfull and for w_i/w_L smaller than 0.6 the static correction based upon equation [3.31] is less satisfactory than neglecting the correction altogether. It is for this reason that the static correction method is always very effective for loading whose frequency content is well below the sructural frequencies such as ocean waves on offshore structures but not always as effective for earthquake loading whose frequency content is wide band and can extend in regions of high structural frequencies.

3.2.2 Modal Acceleration Method

A variation of the static correction method known as modal acceleration has also been widely used to include higher mode effects in vector superposition solution. The formulation of modal acceleration derived here is a computational variant that can be shown equivalent to the classical formulation which deals explicitly with generalized

acceleration and velocity components (see ref. 3.3, 5.1). Consider modes $\{\phi_i\}$, $i=r+1,\ldots,n$ not retained in the summation, by using a pseudo-static solution of the uncoupled modal equation

$$\ddot{y}_i + 2\,w_i\,\xi_i\,\dot{y}_i + w^2_i\,y_i = \{\phi_i\}^T\,\{f(s)\}\,g(t) \qquad [3.32]$$

we get, $y^*_i = (\{\phi_i\}^T\,\{f(s)\})\,/\,w^2_i \quad i=r+1,\ldots,n \qquad [3.33]$

Going back to geometric coordinates, we have

$$\{U(t)\} = \sum_{i=1}^{r} \{\phi_i\}\,y_i(t) + \sum_{i=r+1}^{n} \{\phi_i\}\,y^*_i\,g(t) \qquad [3.34]$$

where the first term of the summation corresponds to the usual modal displacement solution and the second term represents the additional static correction. Substituting equation [3.33] into [3.34] we get,

$$\{U(t)\} = \sum_{i=1}^{r} \{\phi_i\}\,y_i(t) + \sum_{i=r+1}^{n} \frac{\{\phi_i\}\,\{\phi_i\}^T\{f(s)\}}{w^2_i}\,g(t) \qquad [3.35]$$

This may be written as,

$$\{U\} = \sum_{i=1}^{r} \{\phi_i\}\,y_i + \sum_{i=1}^{n} \frac{\{\phi_i\}\,\{\phi_i\}^T\{f\}}{w^2_i}\,g - \sum_{i=1}^{r} \frac{\{\phi_i\}\,\{\phi_i\}^T\{f\}}{w^2_i}\,g \qquad [3.36]$$

where $\{f\}$ is a function of space and $\{U\}$, y_i and g are function of time. By using the stiffness orthogonality properties of the transformation vectors, $[\phi]^T[K][\phi] = [w^2]$, written as

$$[K]^{-1} = [\phi]\,[w^2]^{-1}\,[\phi]^T \qquad [3.37]$$

the second term of the summation in equation [3.36] is thus equal to $[K]^{-1}\,\{f(s)\}$ since

$$\sum_{i=1}^{n} \frac{\{\phi_i\}\,\{\phi_i\}^T}{w^2_i} = [\phi]\,[w^2]^{-1}\,[\phi]^T \qquad [3.38]$$

Equation [3.36] can therefore be written as

$$\{U\} = \sum_{i=1}^{r} \{\phi_i\}\, y_i + [K]^{-1}\,\{f\}\, g - \sum_{i=1}^{r} \frac{\{\phi_i\}\,\{\phi_i\}^T\,\{f\}}{\omega^2_i}\, g \qquad [3.39]$$

$$\{U\} = [\phi_r]\,\{Y_r\} + ([K]^{-1} - [\phi_r]\,[\omega^2_r]^{-1}\,[\phi_r]^T)\,\{f\}\, g \qquad [3.40]$$

$$\{U\} = [\phi_r]\,\{Y_r\} + ([K]^{-1} - [K_r]^{-1})\,\{f\}\, g \qquad [3.41]$$

where $[K_r]$ is a symbolic representation for the truncated expansion of the inverted stiffness matrix using a reduced set of r vectors.

3.2.3 Static Correction Vs Modal Acceleration Vs WYD Ritz Vectors

The analogy between the static correction method, the modal acceleration method and the WYD Ritz approach can easily be established by looking at the vector summation technique used to obtain the total response;

- Static Correction

$$\{U(t)\} = \sum_{i=1}^{r} \{\phi_i\}\, y_i(t) + [K]^{-1}\,(\{f(s)\} - \{f_r(s)\})\, g(t) \qquad [3.42]$$

- Modal Acceleration

$$\{U(t)\} = \sum_{i=1}^{r} \{\phi_i\}\, y_i(t) + ([K]^{-1} - [K_r]^{-1})\,\{f(s)\}\, g(t) \qquad [3.43]$$

- WYD Ritz Vectors approach

$$\{U(t)\} = \sum_{i=2}^{r} \{X_i\}\, y^*_i(t) + [K]^{-1}\,\{f(s)\}\, y^{**}_1(t) \qquad [3.44]$$

$$\text{where } y^{**}_1(t) = \frac{y^*_1(t)}{(([K]^{-1}\{f(s)\})^T\,[M]\,([K]^{-1}\{f(s)\}))^{1/2}} \qquad [3.45]$$

In each of the first two summation methods the full loading vector $\{f(s)\}$ has been accounted for either in a dynamic manner by the first term of the summation or in a static manner by the second term. By looking at equation

[3.44] it should be noted that when mass orthogonal only WYD Ritz vectors, $\{X_i\}$, are used in a direct vector superposition analysis, the first vector corresponds to the static solution, $[K]^{-1}\{f(s)\}$ to which an appropriate scaling factor has been applied, while the additional vectors represent the dynamic contribution neglected by the static solution. The mechanics of WYD Ritz vector generation spread the spectral content of the starting vector among all the basis vectors such that the static correction for higher modes effects is automatically included in the formulation with the most significant term coming from the first vector. Since the WYD Ritz basis is able to achieve a good representation of the loading with very few vectors it will be more reliable, if the benefit of static correction can not be ascertained, to use the error norm concept to include dynamically, in the usual modal superposition summation procedure, enough vectors to obtain a good loading representation. This argument is applicable also to WYD Ritz vectors, $\{^eX_i\}$, that are both mass and stiffness orthogonal since it was shown that the residual error force vector will be the same if the truncated basis is formed from vectors $\{X_i\}$ or vectors $\{^eX_i\}$.

After ensuring that the vector basis is able to provide an adequate representation to the loading spatial distribution, it might be of interest to check if the corresponding approximate structural frequencies, calculated from the reduced eigenproblem, will sufficiently span the frequency range of the applied loading to produce an efficient solution procedure. For loadings with a frequency content contained in a narrow band at the beginning of the structural eigenspectrum, the static correction effects included in the Ritz technique will be very efficient and it is possible to obtain very good result even if the representation of the loading by the truncated basis is poor. It becomes however more difficult for the analyst to get some appreciation of the accuracy achieved by the summation procedure.

3.3 Relationship Between WYD Ritz Solution and Exact Eigensolution

Even though the basic objective of the WYD Ritz approach is not to provide an accurate solution of the free vibration eigenproblem, it might be of interest to establish error bounds on the approximate structural frequencies obtained by the WYD Ritz method from the solution of the reduced eigenproblem.

A first approach consists in evaluating the final approximate eigenpair $(\bar{w}^2_j, \{^oX_j\})$ and then back substituting in the original eigenproblem. An error norm given by

$$^oe_j = \frac{|[K]\{^oX_j\} - \bar{w}^2_j [M]\{^oX_j\}|_2}{|[K]\{^oX_j\}|_2} \qquad [3.46]$$

can be used for this purpose. Physically $[K]\{^oX_j\}$ represents the elastic nodal point forces and $\bar{w}^2_j [M]\{^oX_j\}$ represents the inertia nodal point forces when the FEM model is vibrating in mode $\{^oX_j\}$. Equation [3.46] is thus the norm of out-of-balance nodal forces divided by the norm of the elastic forces. The quantity ^oe_j should be small if $\bar{w}^2_j$ and $\{^oX_j\}$ are an accurate solution of an eigenpair.

In principle it is possible to compute the approximate eigenpairs $(\bar{w}^2_j, \{^oX_j\})$ from the solution of the reduced matrix system at any step of the algorithm and use equation [3.46] to assess the accuracy of the eigensolution achieved by the WYD Ritz basis at that step. However if the WYD Ritz algorithm is implemented by calculating the tridiagonal form of the reduced system $[T_r][Z] = [Z][\lambda]$ directly as explained in the next chapter, a simpler approach is possible. It was shown by Paige, in the context of the Lanczos method, (3.7) that it is possible to monitor the eigenconvergence of the algorithm at step r by computing the residual norm of a Ritz pair, $(\bar{w}^2_j, \{^oX_j\})$, associated with a back substitution in the original free vibration problem,

without computing the Ritz vector $\{^{p}X_j\}$ at all.

The off-diagonal elements of $[T_r]$ automatically provide an error bound parameter for the extracted eigenvalues. In particular for the generalized eigenproblem of structural dynamics, the absolute error bound for each approximate root $\bar{w}^2_j$ can be found from the inequality

$$| (\bar{w}^2_j)/(w^2_j) - 1 | \leq | b_{r+1} * z_{r,j} | / \lambda_j = \epsilon_j \quad [3.47]$$

where b_{r+1} is the next off-diagonal element of $[T_r]$ computed from vector $\{X_r\}$ and $z_{r,j}$ is the last element of the eigenvector, normalized such that $\{Z_j\}^T\{Z_j\} = 1$, corresponding to λ_j, the root obtained from the solution of the reduced tridiagonal system.

Numerical applications dealing with equations [3.46] and [3.47] as eigenvalue error bounds for the WYD Ritz method will be presented in chapter 5.

It should be noted that if a more accurate eigensolution of the modes represented in the spectral content of the starting vector is sought, a combination of the WYD Ritz reduction method and of the subspace iteration (1.2) may provide a very efficient algorithm. In the subspace iteration the eigenpairs are calculated to an accuracy specified by the analyst therefore an iterative procedure is required. For a rapid convergence in the subspace iteration the starting vectors need only to span a subspace that is close to the subspace spanned by the required eigenvectors. The individual iteration vectors need not to be good approximations to the required eigenvectors. The subspace spanned by the sequence of vectors generated using the WYD Ritz method tend to be close to the least dominant subspace of [K] and [M]. Therefore the vectors generated by the WYD Ritz algorithm can be use effectively as the starting vectors for the subspace iteration. The details

of the algorithm are presented in fig 3.2.

The stiffness orthogonalization of the WYD Ritz vectors, through the solution of the reduced eigenproblem (see section 1.3 and fig 1.1), corresponds in fact to one cycle of the subspace iteration procedure. Putting k equal to zero, the algorithm of fig 3.2 combining the WYD Ritz method and the subspace iteration is started at step 4.b), the projection of matrices [K] and [M] on subspace E_1, using the WYD Ritz vectors generated by the standard algorithm (fig 1.1) as transformation vectors [X]. No check on convergence is performed since the reduced problem is only solved once. If a closer approximation to the exact eigenspectrum is required it is possible to continue the iterative process by performing more cycles of subspace iterations.

Fig. 3.2- Algorithm combining the WYD Ritz Method and the Subspace Iteration for the Solution of the Generalized Eigenproblem $[K]\,[\Phi] = [M]\,[\Phi]\,[\omega^2]$

1. Given Mass, Stiffness Matrices [M], [K] and Load Vector {f} :

[M]	n x n system size
[K]	n x n
{f}	n x 1

2. Triangularized Stiffness Matrix:

$[K] = [L]^T [D] [L]$ n x n system

3. Use WYD Ritz Method to Initiate Subspace Iteration :

Establish r starting vectors in matrix $[X]_1$ of size n x r from the WYD Ritz method. The number of iteration vectors r is chosen greater than the number of requested eigenvalues.

4. Perform Subspace Iteration calculations :

for k=1,2,... iterate from subspace E_k to E_{k+1}

a) calculate inertia contribution

$[K]\,[\bar{X}]_{k+1} = [M]\,[X]_k$ solve for $[\bar{X}]_{k+1}$

b) project matrices [K] and [M] on subspace E_{k+1}

$[K]^*_{k+1} = [\bar{X}]^T_{k+1}\,[K]\,[\bar{X}]_{k+1}$

$[M]^*_{k+1} = [\bar{X}]^T_{k+1}\,[M]\,[\bar{X}]_{k+1}$

c) solve reduced eigensystem

$[K]^*_{k+1}\,[Z]_{k+1} = [M]^*_{k+1}\,[Z]_{k+1}\,[\omega^2]_{k+1}$

d) calculate an improved approximation to the eigenvectors [Φ]

$[X]_{k+1} = [\bar{X}]_{k+1}\,[Z]_{k+1}$

e) check for convergence

$tolc = | \omega^2_1{}^{(k+1)} - \omega^2_1{}^{(k)} | \,/\, \omega^2_1{}^{(k+1)}$

if $tolc \leq 10^{-4}$ stop
if $tolc > 10^{-4}$ set k = k+1 go to step 4.a

CHAPTER 4

A New Algorithm for Ritz Vectors Generation

In this chapter the behavior of the WYD Ritz reduction method in the presence of the finite precision arithmetic of the computer will be first investigated. It will be shown that if the algorithm is directly implemented from the original version presented in chapter 1, the actual behavior of the method can be quite different than the expected theoretical behavior since the resulting vector set is usually not linearly independent as implied by the algorithm. The consequences of this deficiency will be reviewed and an effective remedy to obtain an orthogonal set of transformation vectors will be proposed. Then a new algorithm to generate load dependent Ritz vectors will be intoduced. The LWYD Ritz algorithm will be shown to be more stable than the original WYD Ritz algorithm and allows a better control of the static correction effects included in the method. It will also be shown that for algorithms based on the WYD Ritz method, it is possible to form the reduced tridiagonal matrix $[T_r]$, which was shown to be equal to $([K]^*)^{-1}$, from the orthonormalization coefficients calculated while generating the vector basis. Finally numerical results obtained from a simple structural system will be used to illustrate the performance of the proposed variations of the basic method.

4.1 Linear Independence of WYD Ritz Vectors

It was shown in chapter 2 that the algorithm used to generate the WYD Ritz vectors is similar to the method used to produce Lanczos vectors. The WYD Ritz approach will thus be suceptible to exhibit the same problem of loss of orthogonality that affected the early computer implementation of the Lanczos method. To be more specific we are concerned

by the actual computer implementation, using finite arithmetic, of step 4.(b) and 4.(c) of the algorithm presented in fig.1.1, corresponding to the Gram-Schmidt orthogonalization procedure, used to get a basis of linearly independent vectors that will span the subspace defined by the WYD Ritz vectors. The numerical stability of the Gram-Schmidt process has received a lot of attention in the development of a stable Lanczos method to solve for the first eigenvalues of large matrix systems and much can be learned from the actual computer implementation of these algorithms.

4.1.1 The Lanczos Method and the Loss of Orthogonality Problem

The problem of loss of orthogonality of the Lanczos method was always tackled by mathematicians bearing in mind the ultimate objective of the method which is to obtain an accurate solution of the eigenproblem. If the Lanczos method is directly implemented from the algorithm given in fig. 2.1, orthogonalizing the current vector against only the two preceeding ones, it is found in practice that the Lanczos vectors basis [X] will not be globally orthogonal. The loss of orthogonality implies that the generated vectors $\{X_i\}$ do not satisfy the mass orthogonality, that is ;

$$\{X_j\}^T [M] \{X_i\} \neq 0 \quad \text{for } i \neq j \qquad [4.1]$$

also, the matrix $[T_r]$ of fig. 2.1, consisting of the elements a_i and b_i, does not satisfy the relation given by equation [2.20],

$$[T_r] \neq [X]^T[M][K]^{-1}[M][X] \qquad [4.2]$$

In such a case even when r is equal to n, the order of the original system, the one to one correspondance between the computed eigenvalues of $[T_r]$ and the eigenvalues of $[K][\Phi] = [M][\Phi][\omega^2]$ no longer exists and the recurrence algorithm does not terminate for r equal to n.

Paige (3.7) demonstrated that the losses of orthogonality in the Lanczos vectors were caused primarily by the convergence of eigenvalues of $[T_r]$ to eigenvalues of $[K][\Phi] = [M][\Phi][\omega^2]$ and not simply by cancellation errors as it was previously thought. Paige also demonstrated that although global orthogonality was lost a localized near orthogonality of the Lanczos vectors persisted as long as the off-diagonal entries, b_s of $[T_r]$, were not too small.

What goes wrong in practice is that after an eigenvector has been predicted accurately rounding errors, rapidly amplified by repeated multiplication with the unreduced mass matrix, start to create another copy of the same eigenvector. So it is possible to have two, three or more approximate Ritz pairs which will accurately estimate the same exact eigenpair of the generalized eigenproblem. These Ritz vectors will be parallel which manifest the loss of linear independence among the Lanczos vectors.

As pointed out in chapter 2, the Lanczos method or the WYD Ritz algorithm is theoretically unable to detect any eigenvectors that are orthogonal to the starting vector. That is why a random starting vector is usually chosen hoping that all required eigenvectors will be represented and thus obtained from the algorithm. It should be noted that in theory the Lanczos method without modification is thus unable of finding more than one eigenvector for any eigenvalue, namely the projection of the starting vector on the eigenspace, and so is unable to determine the multiplicity of any eigenvalues it finds since the eigenvectors of reapeated eigenvalues are chosen to be orthogonal. In practice rounding errors are magnified in the matrix multiplication and in the orthogonalization process so that the computed vectors will also partially originate from this source. This property is important since in practice Lanczos programs find multiple eigenvalues quite naturally. Rounding errors introduce components in all directions. After one

eigendirection of a multiple eigenvalue has been found the components in the orthogonal directions will persist after purification. These components will grow as the algorithm continues until a second eigenvector, orthogonal to the first, has been found.

If we insist that every eigenvalue of $[T_r]$ must approximate an eigenvalue of $[K][\emptyset] = [M][\emptyset][\omega^2]$ then the near global orthogonality is essential. Near global orthogonality cannot be maintained without reorthogonalization with respect to converged eigenvectors. Subsequent algorithm to the basic method presented by Lanczos maintain the global orthogonality of the vector basis by continuously reorthogonalizing the Lanczos vectors, as they are generated, against all previously calculated vectors, see for example Paige (4.12), Newman and Pipano (2.11), Ojlavo and Newman (4.11).

The advantage of carrying out reorthogonalization with respect to earlier vectors is that multiple copies of the same eigenvectors are avoided without endangering the late development of eigenvectors of multiple eigenvalues.

4.1.2 The WYD Ritz Reduction Method and the Loss of Orthogonality Problem

Even if the objective of the WYD Ritz approach is not to obtain an accurate solution of the eigenvalue problem the near global orthogonality of the WYD Ritz basis is mandatory for the success of the method. If a linearly dependent basis is used directly as transformation vectors, the reduced FEM system will be rank deficient and will yield completely erronous results. Moreover if the reduced system is diagonalized, as required by the response spectrum method for earthquake analysis, it is important that the approximate eigenvalues corresponding to the low frequency modes of the reduced system be close to exact eigenvalues of the original system. If an approximate eigenvalue of the reduced system,

$\bar{w}^2_i$, is close to a number of exact eigenvalues $w^2_p,\ldots,w^2_q$ of the original system, the corresponding WYD Ritz vector $\{^oX_i\}$ will be close to a vector that lies in the subspace corresponding to $\{\emptyset_p\},\ldots,\{\emptyset_q\}$. In a practical analysis using vector superpositon and the response spectrum for dynamic response calculation, this is most likely all that is required because close eigenvalues may almost be dealt with as equal eigenvalues in which case the calculated eigenvector would also not be unique but lie in the subspace corresponding to equal eigenvalues.

Another advantage of maintaining the global orthogonality of the WYD Ritz basis is that the reduced mass matrix can directly be assumed to be equal to the identity matrix avoiding to actually perform the transformation $[X]^T[M][X]$ to obtain $[M]^*$. The mass orthonormality of the vector basis was also shown to be essential to develop error norms to provide a criteria to know when to stop generating new vectors while ensuring a satisfactory convergence for the response quantities of interest.

The generation of a null vector by the WYD Ritz approach will indicate that the subspace obtained from the method will completely span the spectral content of the starting vector which is precisely one of the objective of the method. If additional vectors are required to extend the frequency span of the basis, the algorithm can be restarted by orthogonalizing a random vector with the previously calculated vectors and use this to initiate the calculation of additional vectors. This solution strategy will thus become a combination of the WYD Ritz reduction method and the pure Lanczos technique.

Since the objective of the WYD Ritz approach is not to obtain an accurate eigensolution but to form an accurate load dependent vector basis a reorthogonalization strategy that monitors the loss of orthogonality of the vectors as

they are generated will be most appropriate to obtain the global orthogonality of the vector basis.

4.1.3 Corrective Measures by Selective Reorthogonalization

To maintain the global orthogonality of the Lanczos vectors Gregory (4.7) experimented with the use of higher precision computer operations but found only marginal improvements. Later, Ojalvo and Newman (4.11) found that the introduction of an iterative reorthogonalization loop can make the trial vectors as orthogonal as necessary for large systems. This procedure, adapted to the generation of the WYD Ritz vectors, will be as follows:

1. The vector $\{\tilde{X}_i\}$ is obtained after a first orthogonalization from the recurrence algorithm presented in fig. 1.1 and denoted $\{\tilde{X}_i^{(1)}\}$, a check is performed to verify if the vector $\{\tilde{X}_i^{(1)}\}$ satisfy the orthogonality criterion described by equation [4.7]. If this criterion is met, the algorithm proceeds to step 5. If the criterion is not met, the algorithm proceeds to steps 2 to 4.

2. The vector $\{\tilde{X}_i^{(1)}\}$ is reorthogonalized with respect to all previously calculated vectors according to:

$$\{\tilde{X}_i^{(2)}\} = \{\tilde{X}_i^{(1)}\} - \sum_{j=1}^{i-1}(\{X_j\}^T [M] \{\tilde{X}_i^{(1)}\}) \{X_j\} \qquad [4.6]$$

$$\vdots$$

$$\{\tilde{X}_i^{(m+1)}\} = \{\tilde{X}_i^{(m)}\} - \sum_{j=1}^{i-1}(\{X_j\}^T [M] \{\tilde{X}_i^{(m)}\}) \{X_j\}$$

3. The iterations are carried out until the acceptable vector $\{\tilde{X}_i^{(m+1)}\}$ will satisfy the orthogonality criterion:

$$\text{Max} \quad | \{X_j\}^T [M] \{\tilde{X}_i^{(m+1)}\} | < TOL \qquad \text{for } 1<j<i-1 \qquad [4.7]$$

where TOL is a function of the number of significant digits carried by the computer. A matrix form of the check performed by equation [4.7] can be defined by using the vector

$$\{V_i^{(m+1)}\} = [X_{j-1}]^T [M] \{\tilde{X}_i^{(m+1)}\} \qquad [4.8]$$

where $[X_{j-1}]$ is a matrix of size n x (j-1). The orthogonality criterion is verified by ensuring that the infinite norm ($\{V\}_\infty = \max_k |\{V(k)\}|$) of $\{V_i^{(m+1)}\}$ is less than the TOL parameter. For greater numerical efficiency the components of vector $\{V_i^{(m+1)}\}$ can be saved since they correspond to the coefficients required by the Gram-Schmidt process if another orthogonalization cycle, to form vector $\{\tilde{X}_i^{(m+2)}\}$, is requested.

4. If for some vectors the above criterion is not satified after a set number of iterations, NOG, a warning is issued specifying the maximum value of the orthogonality coefficient:

$$c_j = \max | \{X_j\}^T [M] \{\tilde{X}_i^{(m+1)}\} | \qquad 1<j<i-1 \qquad [4.9]$$

The user has then two options:

(a) It can be assumed that a new WYD Ritz vector $\{X_i\}$ can not be generated within the maximum number of iterations and tolerance specified and a reduced problem of order i-1 will be solved

(b) Calculation can be pursued with reduced accuracy.

5. If the orthogonality criterion is met, the resulting vector is mass normalized and calculations will proceed to the generation of the next vector:

$$b_i = (\{\tilde{X}_i^{(m+1)}\}^T [M] \{\tilde{X}_i^{(m+1)}\})^{1/2}$$
$$\{X_i\} = \{\tilde{X}_i^{(m+1)}\} * 1/b_i \qquad [4.10]$$

It should be noted that in the case where no iterative orthogonalization improvements are allowed the algorithm corresponds exactly to the original version presented in fig. 1.1.

4.1.4 Computer Implementation of Selective Reorthogonalization

Numerical experimentations were conducted on a simple structural system to study the performance of the proposed orthogonalization procedure and to verify the relative efficiency of various implementation strategies. The following variations were studied :

1. Basic Gram-Schmidt orthogonalization algorithm in single and double precision.

2. Modified Gram-Schmidt orthogonalization in single precision.

3. Partial higher precision arithmetic where all inner product summations are accumulated in double precision.

The difference between the regular Gram-Schmidt and the modified Gram-Schmidt procedure is that in the modified scheme the improved version of the trial vector is always used in the c_j calculation according to:

$$
\begin{aligned}
&\text{compute for } j=1,\ldots,i-1\\
&\quad c_j = \{X_j\}^T\,[M]\,\{\bar{X}_i\}\\
&\quad \{\tilde{X}_i\} = \{\bar{X}_i\} - c_j\,\{X_j\}\\
&\quad \{\bar{X}_i\} = \{\tilde{X}_i\}\\
&\text{continue}
\end{aligned}
\qquad [4.11]
$$

Typical operation counts are presented in table 4.1. From the results of numerical experimentation it can be observed that:

TABLE 4.1

Typical Operation Counts for Various Orthogonalization Procedures

n: order of unreduced mass matrix [M]
r: number of WYD Ritz vectors to be calculated

	Lumped mass matrix	Full mass matrix
Regular G.S.	$n\ (r^2 + r - 1)$	$n\ [r^2 + n\ (r - 1)]$
Modified G.S.	$n\ (3/2\ r^2)$	$nr^2\ [1 + n/2]$

Note that if one iterative improvement is allowed, it has been observed that approximately 50% of the vectors to be calculated will require it and that these vectors are evenly distributed among the total set to be generated.

Example: n = 100 r = 25

	Lumped mass matrix	Full mass matrix
Regular G.S.	64 900	302 500
Regular G.S. one iterative improvement	97 350	453 750
Modified G.S.	93 750	3 187 500
Modified G.S. one iterative improvement	140 625	4 781 250

- The matrix product $\{X_j\}^T$ [M] $\{X_j\}$ which will be repeated many times should be coded in a special subroutine that should exploit any known special properties of [M].

- If a "large" system is analysed by the original WYD formulation and no control is done on orthogonalization, the vectors will in fact be far from orthogonal.

- The selective reorthogonalization procedure used with regular Gram-Schmidt is sensitive to the specified TOL parameter.

- To get optimum results, a maximum of only one iterative improvement after a full initial orthogonalization cycle is usually sufficient to bring all vectors within the specified tolerance. It has been observed that approximately 50% of the vectors to be calculated will actually require this iteration and that these vectors are evenly distributed among the total set of vectors to be calculated.

- The optimum TOL value to be used with regular Gram-Schmidt with one iterative improvement allowed will be approximately 10^{-7} for single precision arithmetic carrying 7 significant digits (10^{-14} for double precision carrying 16 significant digits) . It should be noted that the allowance of a larger tolerance value (eg. TOL=10^{-5}) reduced dramatically the number of vectors that can be obtained within the specified tolerance, with one iteration allowed, by the regular Gram-Schmidt procedure. This is because the large tolerance will permit the first generated vectors to have large errors in orthogonality that are very difficult to annihilate while orthogonalization with new vectors is done.

- The modified Gram-Schmidt procedure is not as sensitive to large tolerance allowed for orthogonality between vectors.

It is more stable than the regular Gram-Schmidt process.

- Selective or complete higher precision arithmetic brings only marginal improvements.

- The modified Gram-Schmidt procedure requires a significant amount of extra operations over the regular Gram-Schmidt algorithm especially if a non diagonal mass matrix is used. This is due to the fact that orthogonality with respect to the mass matrix, forcing a multiplication with the matrix [M] in the most inner loop, and not orthonormality is sought for the basis.

- An alternative implementation that was found sligthly more efficient was to orthogonalize the current vector $\{\bar{X}_i\}$ against only the two previous vectors $\{X_{i-1}\}$, $\{X_{i-2}\}$ twice and then enter the selective reorthogonalization procedure at the level of the orthogonality check.

It is thus recommended that the original WYD Ritz formulation be supplemented by the selective reorthogonalization procedure presented in section 4.1.3 in order to obtain a stable solution when the method is applied to a large structural system. Typical results to illustrate the performance of the proposed variations will be presented in section 4.3 dealing with numerical applications.

Finally it should be remembered that in vibration analysis of large structures discretized by the FEM, the forward and backward reduction of the inertia loads is usually more expensive than reorthogonalization. For example it happens very often that the same model is used for static and dynamic analysis to avoid the cost of generating two different models and maintain compatibility for subsequent loading combinations. In such case a condensed mass matrix is usually selected to obtain the global response of the system but the stiffness matrix will retain a very large

bandwidth, the relative cost of vector - mass multiplication will then become very small. The modified Gram-Schmidt and selective reothogonalization procedure can then be introduced without a significant increase in total computer execution time.

4.2 Computational Variants of the WYD Ritz Algorithm

4.2.1 The LWYD Ritz Algorithm

A new algorithm formulation to produce load dependent Ritz vectors was studied to evaluate the possibility of obtaining a more stable vector generation scheme. This algorithm, called the LWYD Ritz algorithm, is shown in fig 4.1. An initial vector, $\{U_o\}$, corresponding to the static deflection of the structure subjected to the spatial distribution of the dynamic loads is first generated. As new vectors are calculated this initial static vector is updated using Gram-Schmidt orthogonalization to remove components common to the vector basis. The updated static vector is then used in the usual recurrence relationship to generate additional vectors. A physical interpretation of the algorithm suggests that the basic solution is obtained from a static analysis, the static response is then modified by removing "dynamic" contribution components and this is used as the mechanism to calculate new vectors. It is anticipated that by always returning to the initial static deflected shape rounding errors that are accumulated in the original WYD Ritz algorithm will be partially eliminated. Furthermore this formulation allows a better control of the static correction effects included included in the solution procedure. The first group of generated vectors, which capture the inertia effects by multiplication with the mass matrix, will represent the dynamic contribution to the modal summation. The residual of the static solution can then be added optionally to the basis as a static correction term.

Fig. 4.1 The LWYD Ritz Algorithm

1. Given Mass, Stiffness Matrices [M], [K], load vector {f}

[M]	n x n
[K]	n x n
{f}	n x 1

2. Triangularized Stiffness Matrix:

$[K] = [L]^T [D] [L]$ n x n system

3. Solve for initial static deflected shape $\{U_o\}$

$[K] \{U_o\} = \{f\}$

4. Solve for First vector

(a) solve for vectors $\{X^*_1\}$

$[K] \{X^*_1\} = [M] \{U_o\}$

(b) [M]-normalize $\{X^*_1\}$

$b_1 = (\{X^*_1\}^T [M] \{X^*_1\})^{1/2}$
$\{X_1\} = \{X^*_1\} * 1/b_1$

(c) Update Static Vector $\{U_o\}$

$c_{u1} = \{U_o\}^T [M] \{X_1\}$
$\{U_1\} = \{U_o\} - c_{u1} \{X_1\}$

5. Solve for Additional Vectors: i=2,...,r-1

(a) solve for new vectors $\{X^*_i\}$

$[K] \{X^*_i\} = [M] \{U_{i-1}\}$

(b) [M]-orthogonalize $\{X^*_i\}$ against previous vectors $\{X_j\}$

$c_j = \{X_j\}^T [M] \{X^*_i\}$ compute for j=1,...,i-1

$$\{X^{**}_i\} = \{X^*_i\} - \sum_{j=1}^{i-1} c_j \{X_j\}$$

(c) [M]-normalize $\{X^{**}_i\}$

$v = (\{X^{**}_i\}^T [M] \{X^{**}_i\})^{1/2}$
$\{X_i\} = \{X^{**}_i\} * 1/v$

(d) Update Static Vector $\{U_{i-1}\}$

$c_{ui} = \{U_{i-1}\}^T [M] \{X_i\}$
$\{U_i\} = \{U_{i-1}\} - c_{ui} * \{X_i\}$

6. Add Static Residual $\{U_{r-1}\}$ as Static Correction $\{X_r\}$ (optional)

(a) [M] orthogonalize $\{U_{r-1}\}$ (by precaution)

$$\{\tilde{U}_{r-1}\} = \{U_{r-1}\} - \sum_{j=1}^{i-1} (\{X_j\}^T [M] \{U_{r-1}\}) \{X_j\}$$

(b) [M]-normalize $\{U_{r-1}\}$

$$b_r = (\{\tilde{U}_{r-1}\}^T [M] \{\tilde{U}_{r-1}\})^{1/2}$$
$$\{X_r\} = \{\tilde{U}_{r-1}\} * 1/b_r$$

7. Orthogonalization of Ritz Vectors with Respect to Stiffness Matrix (optional):

(a) Solve the r x r eigenvalue problem ,

$$[K]^* [Z] = [M]^* [Z] [\bar{w}^2]$$

where
$$[K]^* = [X]^T [K] [X]$$
$$[M]^* = [X]^T [M] [X] = [I]$$
$\bar{w}$ = approximate frequencies

(b) Compute final orthogonal Ritz vectors

$$[^o X] = [X] [Z]$$

By using this formulation it is possible to define an alternative error estimate that can be used to indicate when the spectral content of the starting vector will be exhausted. At any step of the calculation the norm of the static residual $|\{U_i\}|_2$ can be checked against the norm of the initial static solution $|\{U_o\}|_2$ for that purpose. When the ratio of $|\{U_i\}|_2$ / $|\{U_o\}|_2$ will drop below a certain value the algorithm will potentially become able to generate null vectors. From numerical experimentations it was found that this error estimate will exhibit a logarithmic type of decrement until its value reaches the order of the numerical roundoff of the computer.

It is recommended however that the loading error estimates developed previously also be used along with the LWYD Ritz algorithm since their values have a physical interpretation closely realted to the analytical procedure of vector superposition, indicating the fraction of the total load that will participate in the calculation of the structural response and are also able to indicate when the spectral content of the starting vector will be completely spanned by the vector basis.

Finally, it is interesting to note that the LWYD Ritz algorithm, without the addition of the static residual, can be shown to be numerically equivalent to the original WYD algorithm if the vector $\{X_1\}$ used to initiate the recurrence relationship is given by the [M]-normalization of $\{([K]^{-1}[M])*([K]^{-1}\{f(s)\})\}$ instead of $\{[K]^{-1}\{f(s)\}\}$. From the description of the LWYD Ritz algorithm it can be deducted that its basic recurrence relationship is given by

$$\{X^*_i\} = \{X^*_{i-1}\} - c_{ui-1}\,([K]^{-1}[M])\,\{X_{i-1}\} \qquad [4.12]$$

with $$c_{ui-1} = \{U_{i-2}\}^T\,[M]\,\{X_{i-1}\} \qquad [4.13]$$

as compared to $$\{X_i\} = ([K]^{-1}[M])\,\{X_{i-1}\} \qquad [4.14]$$

in the original WYD formulation. From the orthogonality properties of the Ritz vectors it can be shown that

$$\{X^*_{i-1}\} = (\{X_{i-1}\}^T[M]\{X^*_{i-1}\})\{X_{i-1}\} + (\{X_{i-2}\}^T[M]\{X^*_{i-1}\})\{X_{i-2}\} \quad [4.15]$$

Therefore the orthogonalization of the current vector $\{X^*_i\}$ against the two previously formed vectors $\{X_{i-1}\}$ and $\{X_{i-2}\}$ included in step 5 b) of the LWYD Ritz algorithm will produce a purified vector $\{X^{**}_i\}$ that is theoretically equal to the purified vector of the original WYD algorithm scaled by a factor of c_{ui-1}, that is

$$\{X^{**}_i\}_{LWYD} = c_{ui-1}\ \{X_i\}_{WYD} \quad [4.16]$$

The mass normalization of the purified vectors will then produce theoretically identical vectors $\{X_i\}$.

4.2.2 Computer Implementation Using the Tridiagonal Form of the Reduced System

By exploiting the similarity between the vector generation algorithms used in the WYD Ritz reduction method and the Lanczos method it becomes possible to form the reduced tridiagonal matrix $[T_r] = ([K]^*)^{-1}$, directly from orthonormalization coefficients calculated while generating the vector basis. This variation applied to the original WYD formulation is presented in fig 4.2. The main advantages of this strategy are to avoid the explicit calculation of the transformation $[X]^T[K][X]$ and to further minimize the bandwidth and storage requirements of the generalized coordinate system.

If a full uncoupling of the reduced system is required the solution of the eigenproblem in generalized coordinates can then potentially take a full advantage of the symmetric tridiagonal topology of the reduced matrix system. The QR algorithm using Wilkinson's shifts (4.1) will be very

Fig. 4.2 Algorithm for Generation of WYD Ritz Vectors Taking Advantage of the Tridiagonal Form of the Reduced System (Extension of Original Formulation)

1. Given Mass, Stiffness Matrices [M], [K], and Load Vector {f}

[M]	n x n system size
[K]	n x n
{f}	n x 1

2. Triangularized Stiffness Matrix:

$[K] = [L]^T [D] [L]$ n x n system

3. Solve for First Vector:

$[K] \{\bar{X}_1\} = \{f\}$ solve for $\{\bar{X}_1\}$

$b_1 = (\{\bar{X}_1\}^T [M] \{\bar{X}_1\})^{1/2}$ M-Normalization

$\{X_1\} = \{\bar{X}_1\} * 1/b_1$

4. Solve for Additional Vectors: i=2,...,r

(a) $[K] \{\bar{X}_i\} = [M] \{X_{i-1}\}$ solve for $\{X_i\}$

(b) $a_{i-1} = \{\bar{X}_i\}^T [M] \{X_{i-1}\}$ diagonal of $[T_r]$

(c) $c_j = \{X_j\}^T [M] \{\bar{X}_i\}$ compute for j=1,...,i-1

(d) $\{\tilde{X}_i\} = \{\bar{X}_i\} - \sum_{j=1}^{i-1} c_j \{X_j\}$ M-Orthogonalized

(e) $b_i = (\{\tilde{X}_i\}^T [M] \{\tilde{X}_i\})^{1/2}$ off-diagonal of $[T_r]$

(f) $\{X_i\} = \{\tilde{X}_i\} * 1/b_i$ M-normalize

5. Orthogonalization of WYD Ritz Vectors with Respect to Stiffness Matrix (optional)

(a) Construct symmetric tridiagonal matrix [T] of order r :

$$[T_r] = \begin{bmatrix} a_1 & b_2 & 0 & \cdots & 0 \\ b_2 & a_2 & b_3 & \cdots & \vdots \\ 0 & b_3 & a_3 & \cdots & \vdots \\ 0 & 0 & \cdots & & 0 \\ \vdots & \vdots & \cdots & b_{r-1} & a_{r-1} \; b_r \\ 0 & \cdots & \cdots & b_r & a_r \end{bmatrix}$$

(b) Calculate eigenvalues and eigenvectors of $[T_r]$:

$$[T_r] [Z] = [Z] [\lambda]$$

$$[\bar{W}^2] = [1/\lambda]$$

(c) Compute final orthogonal WYD Ritz vectors :

$$[^oX] = [X] [Z]$$

efficient to calculated the eigenvalues, λ . By experience approximately $9r^2$ operations are required for the solution of all eigenvalues. The calculation of the eigenvectors however requires special consideration. If shifted inverse iteration is used to take advantage of the tridiagonal form of $[T_r]$, two problems may occur;

- the shifted matrix $([T_r] - \lambda[I])$ used in the inverse iteration procedure is not generally positive definite so there is a possibility that normal symmetric factorization will fail due to the presence of a zero pivot and a more general matrix factorization algorithm may be required,

- while using inverse iteration the computed eigenvectors of two close eigenvalues may be acceptable and yet not be mutually orthogonal.

After proper numerical variations have been included to overcome these problems the simplicity of inverse iteration is lost and rival techniques that do not exploit the tridiagonal topology of the reduced matrix become competitive. The convergence of the WYD Ritz reduction method is fairly rapid such that the task of computing the eigenvalues and eigenvectors of the reduced system represents a small fraction of the total exececution time. Therefore the optimization of that final step does not appear to be critical for the success of the method.

Actual numerical experimentations that will be presented in chapter 5 have also shown that working directly with $[T_r]$ is sometimes less stable than working with $[X]^T[K][X]$ especially if the eigenspectrum has close eigenvalues regardless of the numerical technique used to solve the reduced eigenproblem. Convergence of displacements and stresses can be obtained with approximately the same number of vectors but intermediate results are more likely to exhibit larger fluctuations, particularly for stresses,

showing that the resolution of eigenvectors calculated from $[T_r]$ was not always as sharp as the resolution obtained from $[X]^T[K][X]$.

By studying the basic recurrence relationship of the LWYD Ritz algorithm it can be shown that it is also possible to form the corresponding reduced tridiagonal system directly from the orthonormalization of the calculated vectors. The details of this implementation strategy are presented in fig. 4.3.

4.3 Numerical Application on Simple Structural Systems

4.3.1 The CALSAP Computer Program Development System

The basic tool to carry out the development, implementation, and preliminary evaluation of load dependent Ritz vectors generation algorithms, is a modern version of the computer program CAL (4.16) a Computer Assisted Learning language adapted to the micro-computer. All computer operations are conducted in FORTRAN 77 and use the CALSAP development system (4.8, 4.17) in order to obtain program modularity and portability. Therefore, the new program modules will operate efficiently on both micro and mainframe computer systems.

4.3.2 Description of Mathematical Model for Numerical Applications

In order to evaluate the proposed variations of the WYD Ritz reduction method, numerical experimentations were carried out on a simple structural system. A fictitious offshore platform was modeled as a 40 DOF shear beam structure as shown in fig. 4.4 . The material properties were selected such that the fundamental period of vibration is close to 6 sec (5.93 sec). The steady state dynamic responses to two type of loadings were then examined. The

Fig. 4.3 Implementation of the LWYD Ritz Algorithm Taking Advantage of the Tridiagonal Form of the Reduced System

1. Given Mass, Stiffness Matrices [M], [K], load vector {f}

[M]	n x n
[K]	n x n
{f}	n x 1

2. Triangularized Stiffness Matrix:

$[K] = [L]^T [D] [L]$ n x n system

3. Solve for Initial Static Deflected Shape $\{U_o\}$

$[K] \{U_o\} = \{f\}$

4. Solve for First vector

(a) solve for vectors $\{X^*_1\}$

$[K] \{X^*_1\} = [M] \{U_o\}$

(b) [M]-normalize $\{X^*_1\}$

$b_1 = (\{X^*_1\}^T [M] \{X^*_1\})^{1/2}$
$\{X_1\} = \{X^*_1\} * 1/b_1$

(c) Update Static Vector $\{U_o\}$

$c_{u1} = \{U_o\}^T [M] \{X_1\}$
$\{U_1\} = \{U_o\} - c_{u1} \{X_1\}$

5. Solve for Additional Vectors: i=2,...,r-1

(a) solve for new vectors $\{X^*_i\}$

$[K] \{X^*_i\} = [M] \{U_{i-1}\}$

(b) calculate diagonal element of [T]

$a_{i-1} = ((\{X^*_i\} - \{X^*_{i-1}\})^T [M] \{X_{i-1}\}) * (-1/c_{ui-1})$

(c) [M]-orthogonalize $\{X^*_i\}$ against previous vectors $\{X_j\}$

$c_j = \{X_j\}^T [M] \{X^*_i\}$ compute for j=1,...,i-1

$$\{X^{**}_i\} = \{X^*_i\} - \sum_{j=1}^{i-1} c_j \{X_j\}$$

(d) [M]-normalize $\{X^{**}_i\}$

$v = (\{X^{**}_i\}^T [M] \{X^{**}_i\})^{1/2}$
$\{X_i\} = \{X^{**}_i\} * 1/v$

(e) calculate off-diagonal element of [T]

$$b_i = -v/c_{ui-1}$$

(f) Update Static Vector $\{U_{i-1}\}$

$$c_{ui} = \{U_{i-1}\}^T [M] \{X_i\}$$
$$\{U_i\} = \{U_{i-1}\} - c_{ui} * \{X_i\}$$

6. Add Static Residual $\{U_{r-1}\}$ as Static Correction $\{X_r\}$ (optional)

(a) [M] orthogonalize $\{U_{r-1}\}$ (by precaution)

$$\{\tilde{U}_{r-1}\} = \{U_{r-1}\} - \sum_{j=1}^{i-1} (\{X_j\}^T [M] \{U_{r-1}\}) \{X_j\}$$

(b) [M]-normalize $\{\tilde{U}_{r-1}\}$

$$b_r = (\{\tilde{U}_{r-1}\}^T [M] \{\tilde{U}_{r-1}\})^{1/2}$$
$$\{X_r\} = \{\tilde{U}_{r-1}\} * 1/b_r$$

(c) complete diagonal of [T]

$$[K] \{X_{r+1}\} = [M] \{X_r\} \qquad \text{solve for } \{X_{r+1}\}$$
$$a_r = \{X_{r+1}\}^T [M] \{X_r\}$$

(d) complete off-diagonal of [T]

$$b_r = \{X_{r-1}\}^T [M] \{X_{r+1}\}$$

7. Orthogonalization of Ritz Vectors with Respect to Stiffness Matrix (optional)

(a) Construct symmetric tridiagonal matrix [T] of order r :

$$[T_r] = \begin{bmatrix} a_1 & b_2 & 0 & \cdots & 0 \\ b_2 & a_2 & b_3 & \cdots & \vdots \\ 0 & b_3 & a_3 & \cdots & \vdots \\ 0 & 0 & \cdots & & 0 \\ \vdots & \vdots & \cdots & b_{r-1} & a_{r-1} \; b_r \\ 0 & \cdots & \cdots & b_r & a_r \end{bmatrix}$$

(b) Calculate eigenvalues and eigenvectors of $[T_r]$:

$$[T_r] [Z] = [Z] [\lambda]$$

$$[\bar{w}^2] = [1/\lambda]$$

(c) Compute final orthogonal Ritz vectors :

$$[^oX] = [X] [Z]$$

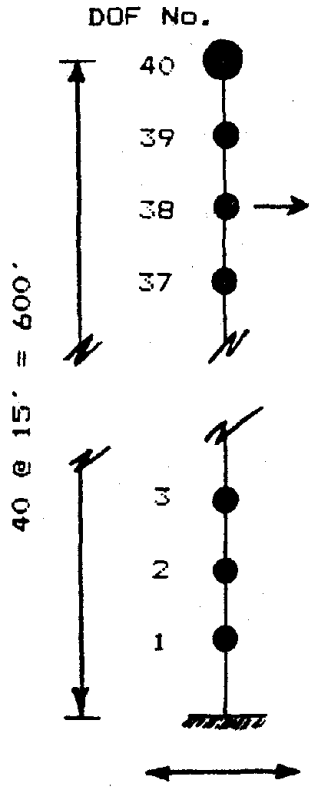

Wave Loading
1000^{K} Sin(0.78 t)

W_L = 0.78 rad/sec
T_L = 8.0 sec

Structural Properties

$$[k]_{beam} = \begin{bmatrix} 1 & -1 \\ -1 & 1 \end{bmatrix} * 6854 \text{ kips/ft}$$

$$[M]_{diag} = \{7, 7, 7, \ldots, 7, 7, 49\}$$
(kips - sec²) / ft

Earthquake Loading
$\{F(s,t)\} = [M]\{r\}$ (0.2g Sin(8.5 t)

W_L = 8.5 rad/sec
T_L = 0.74 sec

$\{r\} = \{1, 1, 1, \ldots, 1, 1, 1,\}^T$

"Exact" Eigensolution $[K][\emptyset] = [M][\emptyset][w^2]$

Mode no.	Freq. (rad/sec)	Period (sec)
1	1.06	5.93
2	3.22	1.95
3	5.47	1.15
4	7.78	0.81
5	10.13	0.62
6	12.49	0.50
7	14.84	0.42
8	17.19	0.36
9	19.51	0.32
10	21.81	0.29

Fig. 4.4 Fictitious Offshore Platform Modelled as a 40 DOF Shear Beam Structure

first case represented wave loading idealized as a sinusoidal forcing function with a maximum amplitude of 1000 Kips and a period of 8 sec. This example is specifically designed such that

- the participation of higher modes is important to the structural response since a single concentrated load and no damping were being used,

- the static correction or modal acceleration summation methods should be very effective.

The second case represented earthquake loading. The ground acceleration was idealized as a sinusoidal motion with a period of 0.74 sec and a maximum amplitude of 0.2g. The static correction or modal acceleration summation methods will not be as effective for this loading since the forcing frequency, w_L, is in the range of important structural frequencies (between the 4th and 5th modes).

In both cases an exact mathematical solution corresponding to the spatial distribution of the steady state response, {U(s)}, of the proposed discrete structural model can easily be computed from

$$([K] - w^2_L [M])^{-1} \{f(s)\} = \{U(s)\} \qquad [4.17]$$

the exact displacements will be given by

$$\{U(s,t)\} = \{U(s)\} * \sin (w_L t) \qquad [4.18]$$

The exact shear force in each beam can then be calculated from the differential displacements of the nodes.

4.3.3 Evaluation of Computational Variants of the WYD Ritz Algorithm

The overall quality of an algorithm should be judged

by the numerical effort and storage requirements necessary to achieve displacement and stress convergence. More specifically the following aspects of the WYD Ritz reduction method should be considered;

- computational efficiency monitoring computer execution time for vector calculation,

- the number of required vectors to be considered in the superposition summation,

- the representation of the spatial distribution of the dynamic load achieved by the truncated vector basis,

- the degree of global orthogonality achieved by the vector basis,

- the spectral content of the starting vector,

- the frequency content of the dynamic loads as compared to the structural frequencies represented in the reduced Ritz system,

- the spread in the eigenvalues of the free vibration problem,

- the formulation of the reduced Ritz system using either $[K]^*$ or $[T_r]$.

The computational efficiency study and an assessment of the influence of the form of the reduced Ritz system and of the spread in the eigenvalues of the free vibration problem will be postponed to the next chapter where the response of a fully coupled 3D model of approximately 100 dynamic DOF will be investigated.

The representation of the spatial distribution of the

dynamic load, as given by the Euclidean norm of the error force vector, e^*, for various number of vectors included in the calculations is shown in fig. 4.5 and 4.6. The superiority of the WYD Ritz reduction method over the exact eigensolution is clearly evident. Load dependent Ritz bases are able to obtain a good reresentation of dynamic load, say from 90% to 100%, with a fraction of the number of vectors required from the eigensolution.

To monitor the degree of orthogonality achieved by the vector bases a global orthogonality index, OI, was defined using the ratio of the lowest to the largest eigenvalue of the matrix $[V] = [X]^T[M][X]$. For a perfectly orthogonal set of vectors this index, corresponding to the inverse of the condition number of [V], should be equal to 1. For a linearly dependent set OI should be equal to zero, intermediate values will show the relative degree of orthogonality achieved by the bases.

The results comparing the performance of the LWYD Ritz algorithm without selective reorthogonalization and the original WYD Ritz algorithm for the case of wave loading are presented in fig 4.7 . It is shown that the orthogonality of the basis generated from the original WYD algorithm decays rapidly after the first 12 vectors were calculated the vector basis becoming linearly dependent at the inclusion of the 18th vector. The LWYD Ritz algorithm maintained a high level of orthogonality until the spectral content of the starting vector was exhausted. The orthogonality index (without reorthogonalization) was obtained as .9999936 after 20 vectors, the loading error norm e^* indicating a value of 99.9964. The orthogonality characteristics of the LWYD Ritz algorithm are so good that the algorithm started to generate null vectors after the calculation of the 20th vector. The error estimate monitoring the norm of the static residual $\|\{U_1\}\|_2$ against the norm of the initial static solution $\|\{U_0\}\|_2$ was found to exhibit a logarithmic type of decrement

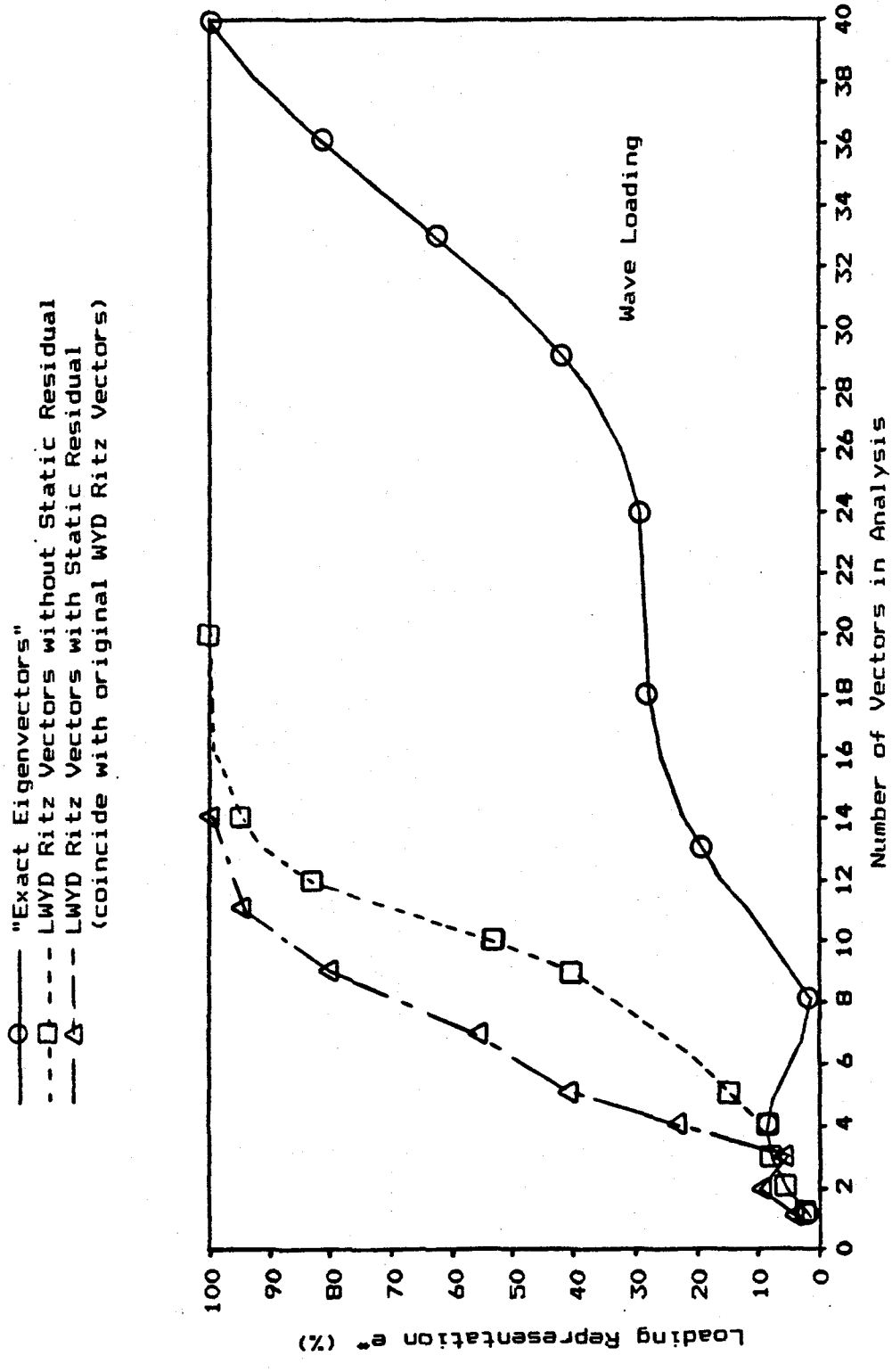

Fig. 4.5 Wave Loading Representation, (%), from Euclidean Norm of Error Force Vector for Truncated Vector Bases

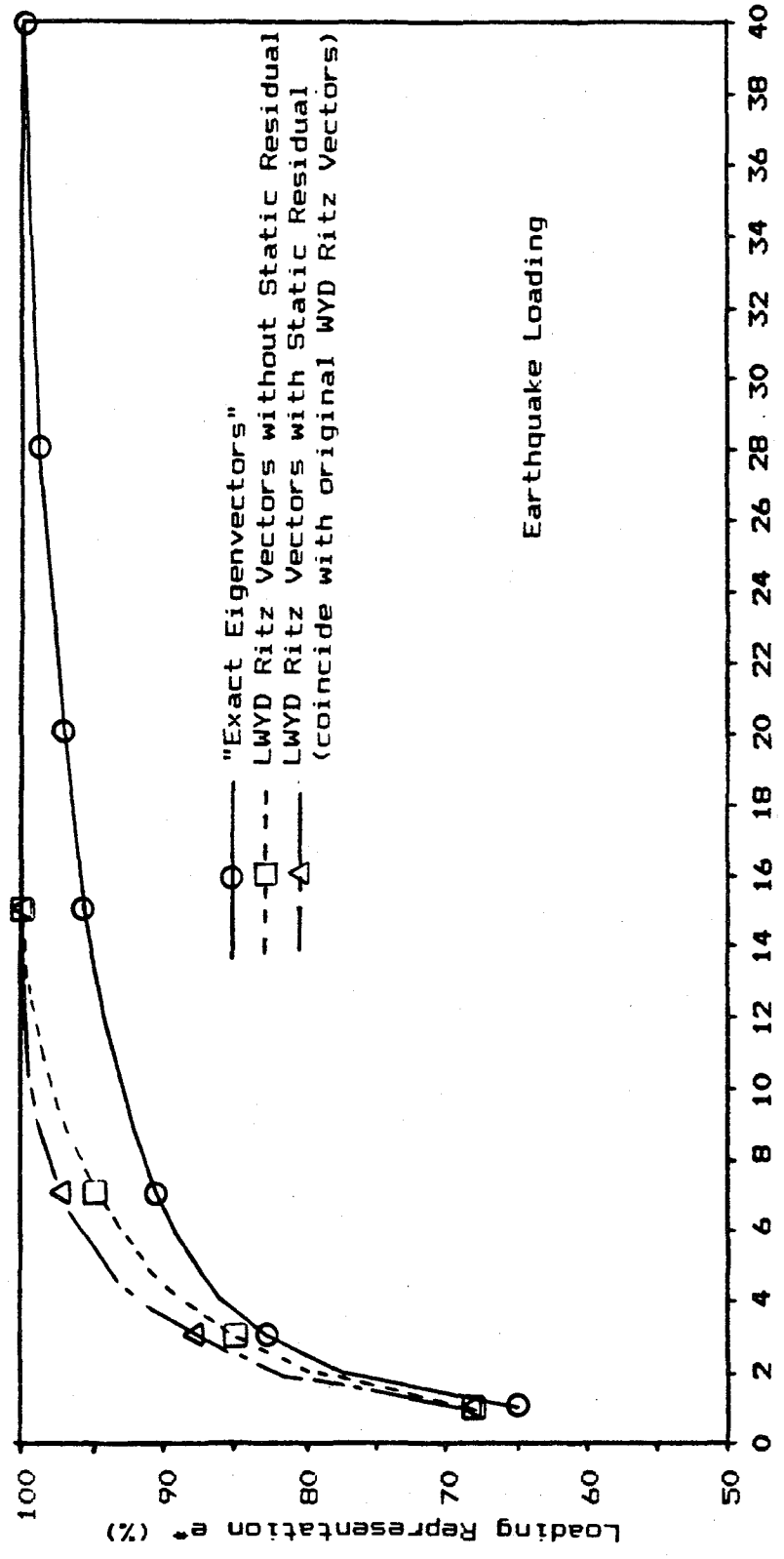

Fig. 4.6 Earthquake Loading Representation, (%), from Euclidean Norm of Error Force Vector for Truncated Vector Bases

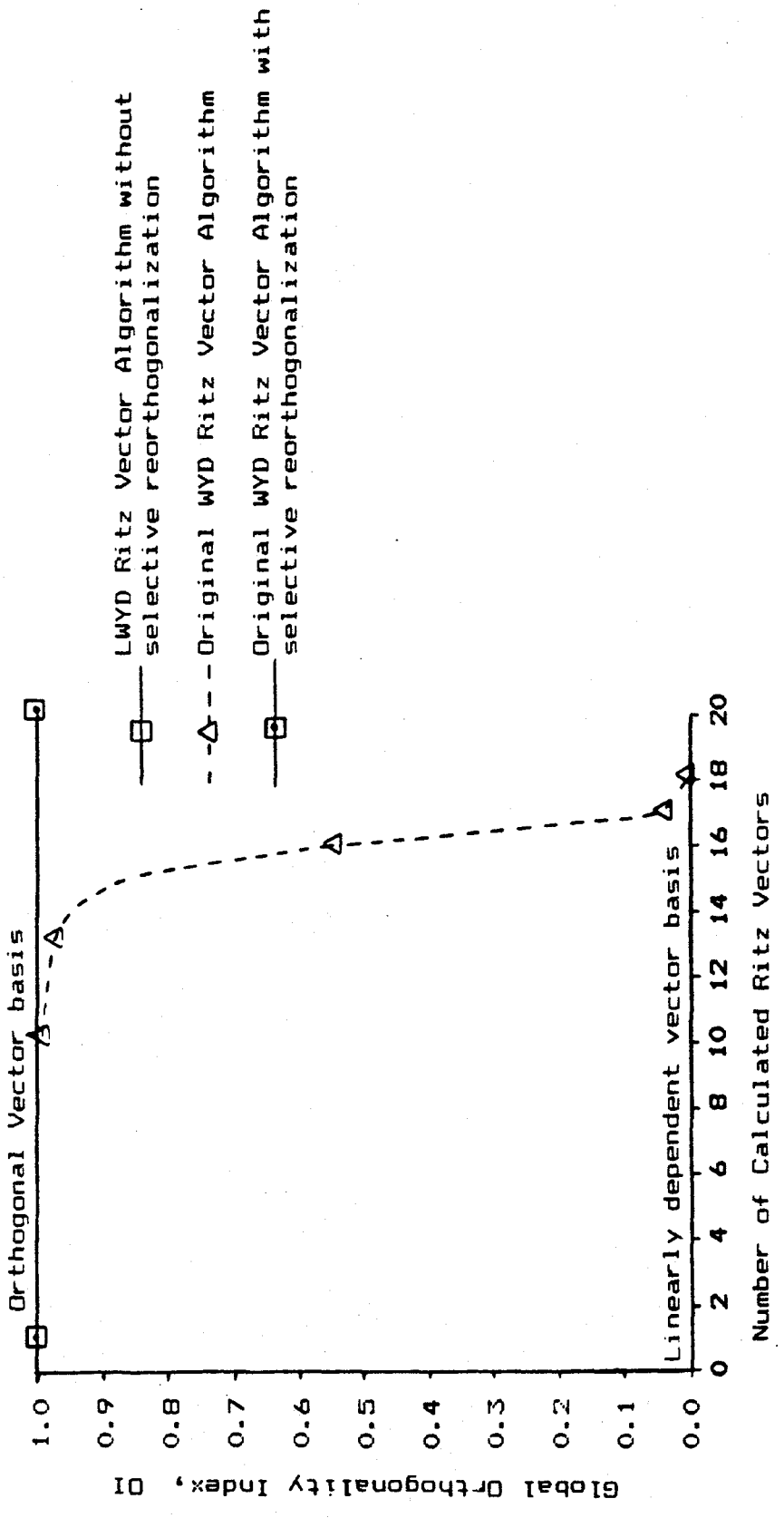

Fig. 4.7 Global Orthogonality Level Maintained by Different Algorithms

reaching a value of 10^{-7}, the order of the roundoff, used in these calculations at the 20th vector.

The original WYD Ritz algorithm with one selective reorthogonalization loop permitted was able to obtain an orthogonality index of .9981955 after 20 vectors were calculated for a loading error norm, e*, of 99.9932. The behavior of the two algorithms being now very similar.

A significant difference then happened after the calculation of the 20th vector. The original WYD Ritz formulation (with selective reorthogonalization) kept on generating new vectors reaching an orthogonality index of .9906620 after the calculation of the 40th vector, while the loading error norm oscillated between 99.9932 and 99.9944. What was happening is that the first orthogonalization pass produced an almost random starting vector containing numerical noise and the reorthogonalization pass was then restarting the method in a stable fashion. On the other hand the superior orthogonality characteristics of the LWYD Ritz algorithm terminated the vector generation in accordance with the basic philosophy of the WYD Ritz reduction method, when a complete representation of the spatial distribution of the dynamic load was obtained from the basis and this without the requirement for any iterative reorthogonalization.

The convergence characteristics of the structural responses are shown in fig 4.8 and 4.9. The maximum error in beam shear forces were calculated for various number of vectors considered by different algorithms. The error was obtained as

$$\left| \frac{S_{k,i} - S_{k,exact}}{S_{k,exact}} \right|_{\text{max over } k} * 100 \qquad [4.19]$$

where $S_{k,i}$ is the shear force in beam "k" considering "i" modes in the summation. This error evaluation will not necessarily exhibit a monotonically decreasing type of

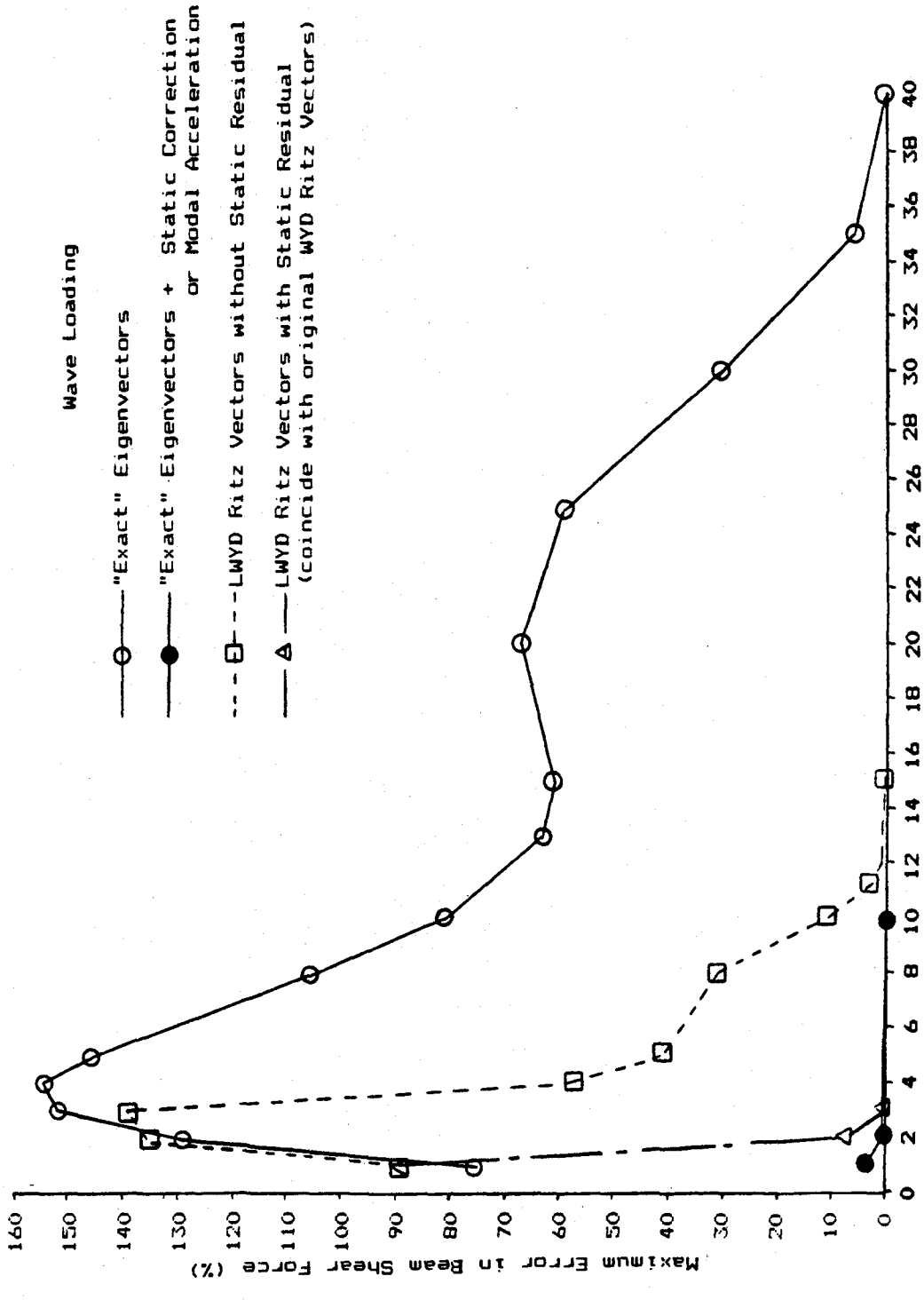

Fig. 4.8 Maximum Error in Beam Shear Force Vs Number of Vectors in Analysis (Wave Loading)

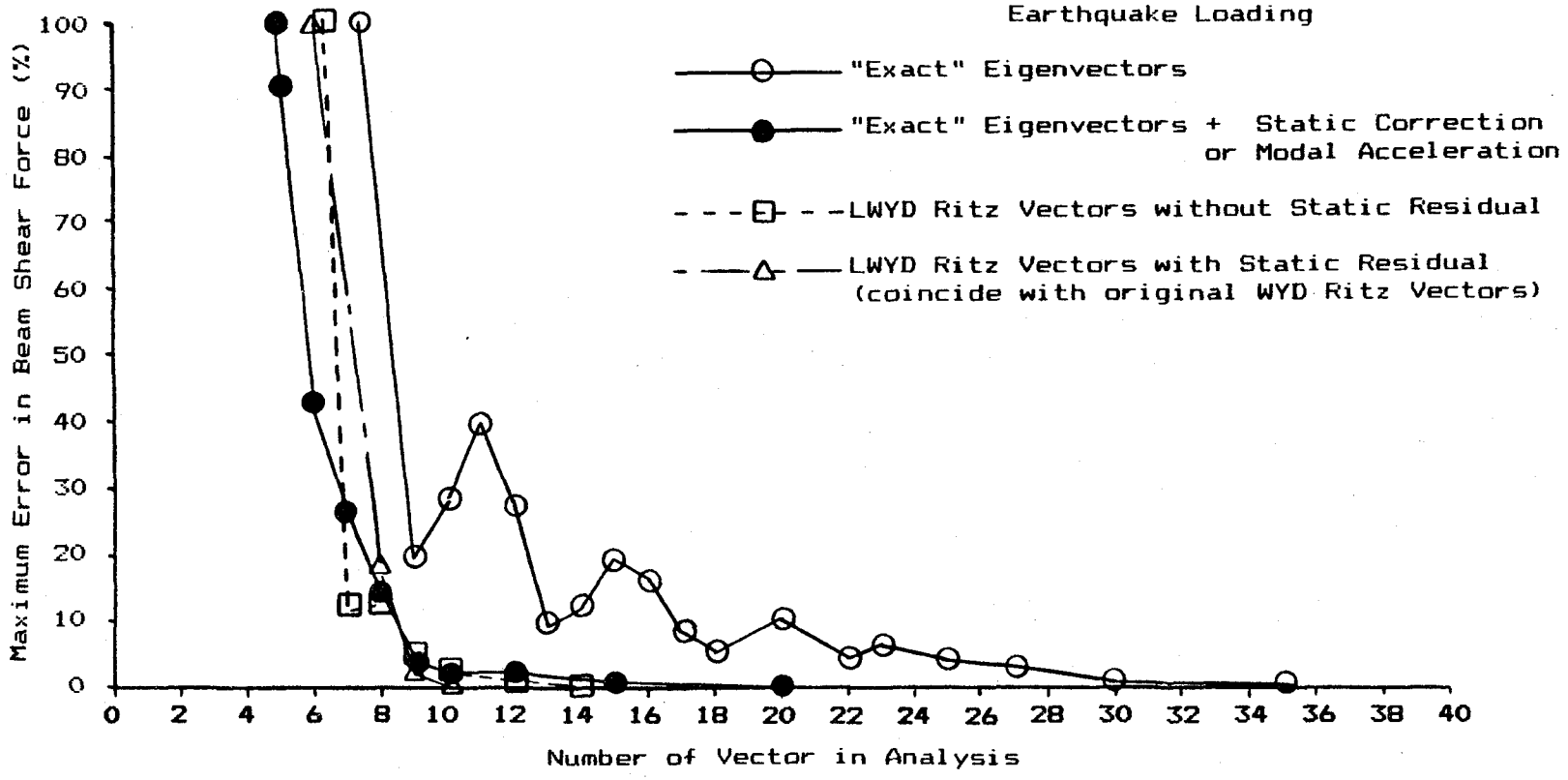

Fig. 4.9 Maximum Error in Beam Shear Force Vs Number of Vectors in Analysis (Earthquake Loading)

convergence since the maximum value can occur from a different beam for a different number of modes retained in the summation. The error in displacements were generally small and were not worth tabulating.

A fully converged solution was defined when the maximum error in beam shear forces was found to be less than 1%. For the case of wave loading convergence was obtained from 3 LWYD Ritz vectors with static residual or from 3 vectors calculated from the original WYD formulation. The exact eigensolution required a complete basis of 40 vectors for convergence while 2 eigenvectors supplemented by static correction or modal acceleration were able to achieve convergence. This example emphasized the benefit of the static correction effect included in the WYD Ritz reduction method to obtain rapid convergence of the stuctural response when the ratio of loading frequency to structural frequencies suggest that higher modes are responding in a static manner.

The LWYD Ritz algorithm without static residual converged with 12 vectors. It can be further observed that the convergence characteristics of the LWYD Ritz algorithm without static residual is somewhat similar to the exact eigensolution but shifted to the left suggesting that vectors of similar contribution occur much earlier in the Ritz mode basis than exact eigenbasis.

A graphical representation of the vector shapes that were calculated for convergence under wave loading is presented in fig 4.10 and 4.11. The original WYD Ritz algorithm or the LWYD Ritz algorithm with static residual generated [M] orthonormal vectors $\{X_i\}$ or [M] and [K] orthogonal vectors $\{^eX_i\}$, that were very close to the vectors obtained from the exact eigensolution supplemented by static correction.

The LWYD Ritz algorithm without static residual

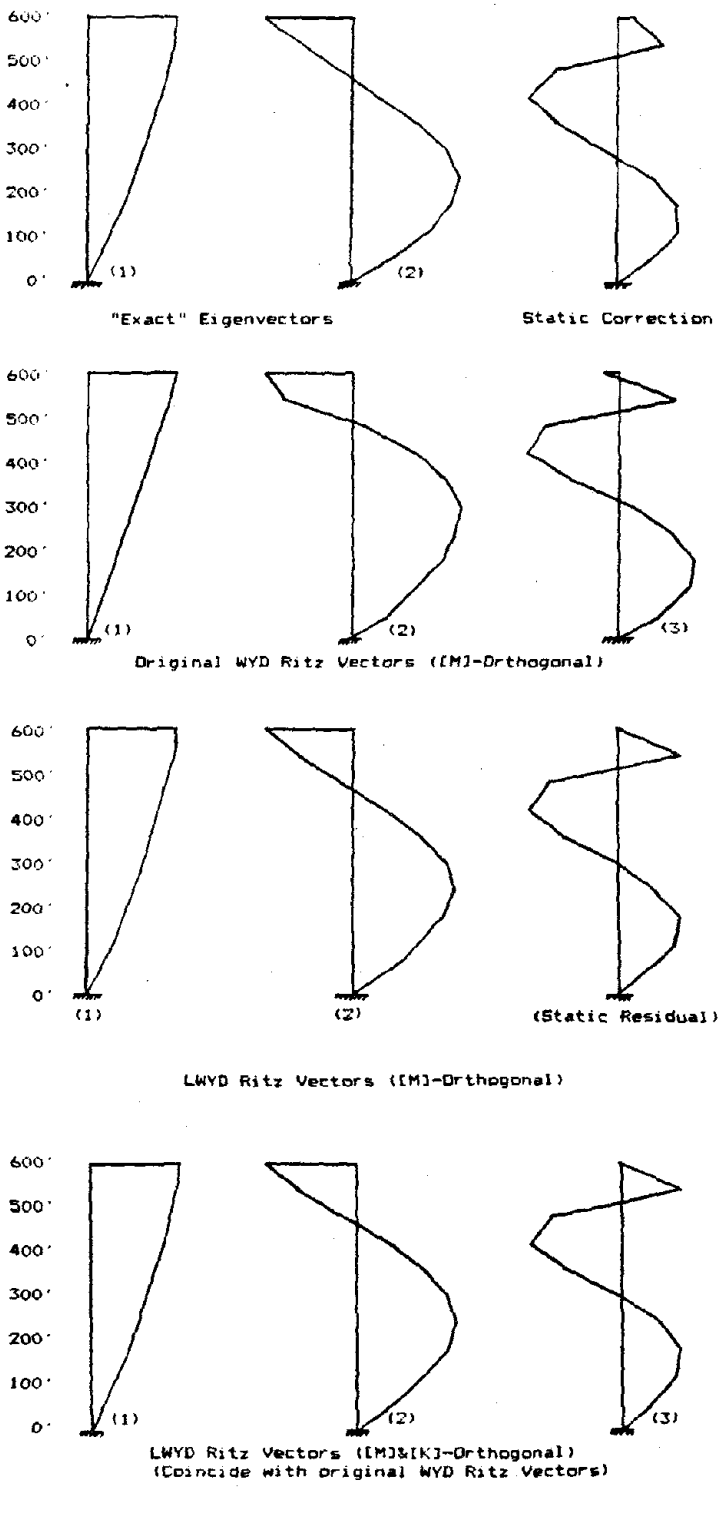

Note : All shapes of different algorithms are normalized such that the same DOF is unity

Fig 4.10 Vector Shapes Calculated for Convergence under Wave Loading when a Static Correction or a Static Residual is Included in the Basis

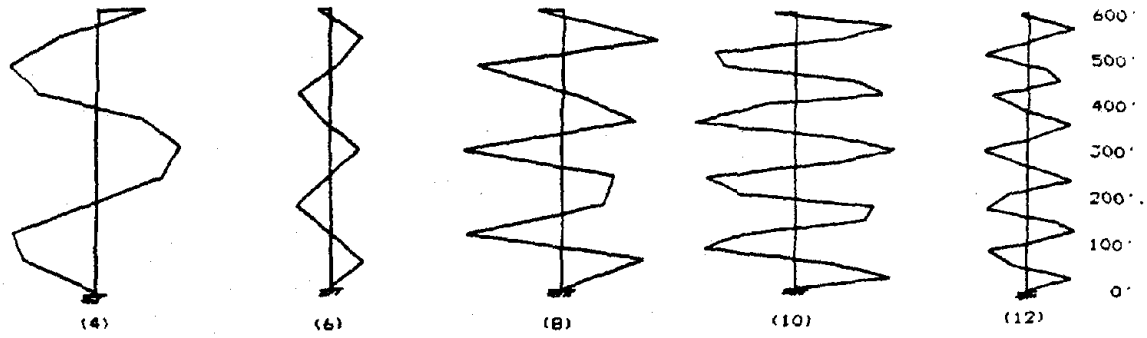

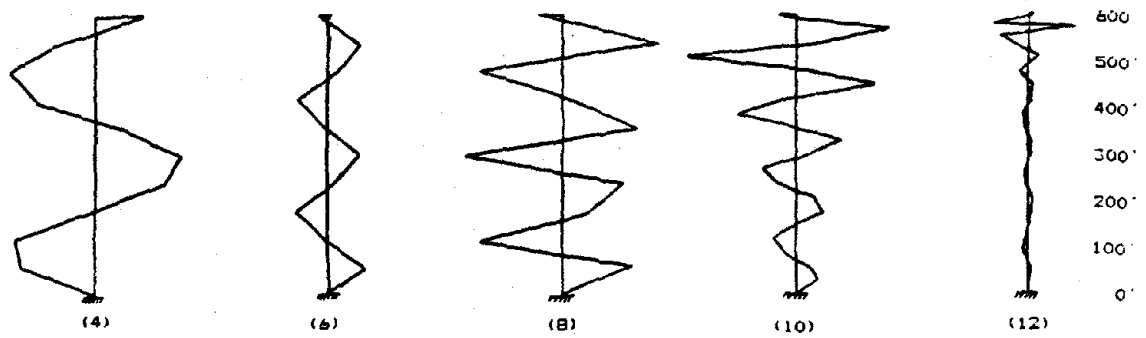

LWYD Ritz Vectors ([M]&[K]-Orthogonal, without Static Residual)

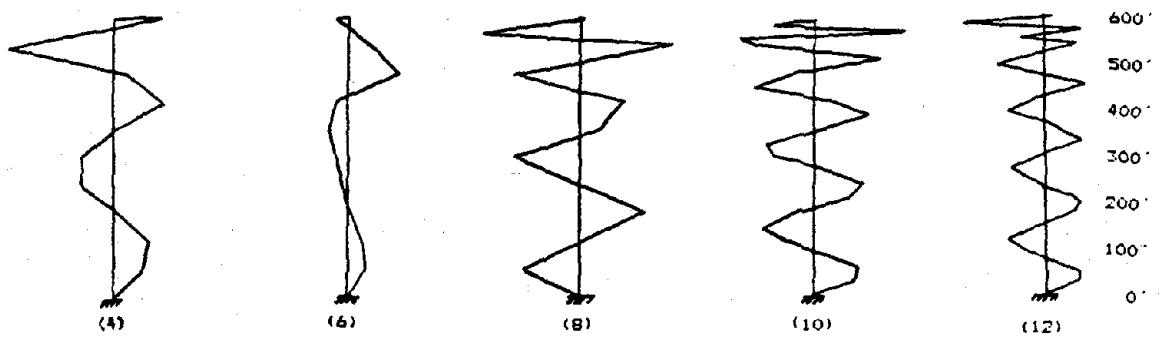

LWYD Ritz Vectors ([M]-Orthogonal, without Static Residual)

Note : All shapes of different algorithms are normalized such that the same DOF is unity

Fig 4.11 Vector Shapes Calculated for Convergence under Wave Loading when there is no Static Correction or Static Residual Included in the Basis

generated [M] orthonormal vectors $\{X_i\}$ that had much more oscillations in amplitude near the applied loading than the corresponding exact eigenvectors. The first [M] and [K] orthogonal vectors $\{^pX_i\}$, obtained from $\{X_i\}$, had shapes that were very similar to the corresponding exact eigenshapes. Then "specialized" vectors that had high amplitude components in the vicinity of the loading were obtained. These vectors will be very efficient to modify locally the solution capturing the effect of the concentrated load. Vectors of high oscillatory nature are obtained last from exact eigensolutions such that a linear combination of all the eigenvectors is required to reproduce the localized effects of the Ritz modes, this is why a complete eigenbasis was necessary for convergence.

For earthquake loading, applied with a forcing frequency between the 4th and the 5th mode, convergence was obtained from 10 vectors for the LWYD Ritz algorithm with static residual or the original WYD formulation (with reorthogonalization), while 12 vectors were required from the LWYD Ritz algorithm without static residual. The eigensolution converged with 30 vectors while the eigensolution supplemented by static correction or modal acceleration required 15 vectors. For this example where the effects of static correction can not be expected to be very effective the LWYD Ritz algorithm with or without static residual produced results of comparable accuracy for modal summation including 7 vectors or more. When the first few vectors were considered in the summation wide fluctuations in the response were observed as reported in table 4.2. However, the solution using the LWYD Ritz algorithm without static residual did stablize more rapidly.

It should also be noted that as Ritz vectors are added to the solution, the first structural frequencies of the reduced system are converging toward values of the exact eigensolution. It is thus possible for the reduced Ritz

TABLE 4.2

Maximum Error in Beam Shear Force (%)

Earthquake Loading

vector no.	Eigenvectors	Eigenvectors +Static corr.	LWYD vectors+ Static resid.	LWYD vectors no Static residual
1	331	2066	333	333
2	494	982	415	486
3	453	884	523	401
4	714	510	1435[2]	14592[1]
5	170	91	3516	646
6	117	43	348	147
7	118	26	100	12

note 1- Ritz mode # 4 has a period of 0.75 sec which is close to resonance with applied loading

2- Ritz mode # 4 has a period of 0.77 sec which is close to resonance with applied loading

system to enter in a state of resonance at an intermediate stage of calculation. If the eigenvalues of the reduced system are not yet stabilized the inclusion of additional vectors in the solution will correct the situation; if the eigenvalues are stabilized then a true resonance condition is to be expected and appropriate design modifications must be considered. The calculation of the eigenvalues from the reduced tridiagonal matrix offers a very economical way of checking the ratios of retained structural frequencies to loading frequency at any stage of the calculation.

In summary, for both analyses it is obvious that an exact eigensolution is not very effective to obtain the structural response. The eigensolution supplemented by static correction or modal acceleration is able to compete with the WYD Ritz reduction method in terms of the number of vectors to be considered in the superposition summation but as it will be shown in the next chapter the load dependent Ritz vectors are approximately 7 times cheaper to generate than eigenvectors such that the WYD Ritz reduction method is clearly superior.

4.3.4 Influence of Starting Vector on Convergence Characteristics of Ritz Solutions

To demonstrate the influence of the choice of the starting vector on the convergence characteristics of the solution a vector basis generated from the LWYD Ritz algorithm without static residual and using a random vector as initial loading distribution was used to calculate the structural response of the system to wave loading in a Lanczos type of analysis. The spectral content of the starting vector was exhausted after the calculation of 19 vectors with a corresponding maximum shear force error term of 63%. To obtain convergence the procedure will thus require a restart to add new vectors to the basis in order to force convergence of the eigensolution of the reduced system

to the exact eigensolution of the original structure. The original WYD formulation with selective reorthogonalization, which was shown to automatically restart itself from numerical roundoffs was used to pursue the analysis. The convergence of the solution was found to follow closely that of the exact eigensolution requiring a full basis of 40 vectors to achieve convergence.

This analysis illustrate that the fast convergence rate obtained from the WYD Ritz reduction method is mainly due to the inclusion of the spatial distribution of the dynamic load in the vector generation process. To obtain convergence the Lanczos method was forced to extract higher modes accurately, in such situation the Lanczos method is not very effective.

4.4 Recommendations

From the analysis of the numerical results it can be concluded that if the benefit of static correction can not be ascertained, the most reliable solution strategy while using the WYD Ritz method will be to assume that the static correction effects obtained from the addition of the static residual to the basis will have a small contribution to the rate of convergence of the solution. The loading error norms should then be used to ensure that a "good" loading representation, say from 90% to 100%, is obtained from the modal summation of "dynamic" vectors, the static residual being then optionally added to the solution.

The frequencies spanned by the Ritz solution should also be compared, whenever possible, with the frequency range of the applied loadings. If there is an insufficient number of vectors after the spectral content of the starting vector has been exhausted a random vector can be used to restart the algorithm. It should however be recognized that any vector superposition technique is generally not very effective to

evaluate the structural response of systems subjected to high frequency loading nor is the structural (FEM) model likely to be very good for such loading condition.

CHAPTER 5

Application of the WYD Ritz Reduction Method in Earthquake Engineering

This chapter presents numerical results obtained from the seismic analysis of a structural system using approximately 100 dynamic DOF in its idealization. The earthquake response spectra technique was used in the analysis to validate the WYD Ritz reduction method for this particular solution procedure. The analysis tries to answer, from a practical standpoint, two important questions; (1) how many load dependent Ritz vectors should be retained in the reduction process and (2) how accurate are the ensuing results. For that purpose comparisons were established between analytical results obtained from exact eigensolutions and Ritz solutions. It is shown that the WYD Ritz reduction method used along with response spectra type of calculations, has definite advantages over the traditional eigensolution in terms of a much reduced numerical effort to generate the transformation vectors and improved convergence rate of the resulting basis. Finally, specific numerical criteria, established in terms of the error norms presented in chapter 3 are suggested to serve as guidelines for an efficient use of the WYD Ritz reduction method in actual engineering applications.

5.1 SAP-80 Program Module for Ritz Vectors Calculations

In order to gain experience with a larger and more complex structural system than the shear beam model used for preliminary algorithms development by the CAL program, computational variants to generate load dependent Ritz vectors, with the addition of error norms calculations, were coded as a new modules of the SAP-80 computer program (4.18), a general purpose structural analysis package developed for micro and mainframe computers.

5.2 Description of Mathematical Models for Numerical Applications

A fixed offshore platform was selected for this study since it represents a complete dynamic problem where multiload patterns, dynamic substructuring and local nonlinearities have found many applications. An idealized version of a three dimensional steel jacket platform described in some details by Ferrante et al. (5.6) was scaled up from a 150 ft high tower to a 300 ft structure. The mathematical model, a space frame composed of three dimensional linear beam elements of tubular section, is shown in fig 5.1. The platform has a total of 192 static DOF. The 96 dynamic DOF retained in the analysis were taken as the 3 translational components at each node. The mass matrix, obtained from a special computer program, was thus generated ignoring rotatory inertia at all nodes.

Two different models having the same stiffness characteristics but using different mass distribution at the deck level were studied using the response spectra technique for three component earthquake design. The first model uses a symmetrical mass distribution and the second model an asymmetrical mass distribution. The inertial characteristics of the two models are presented in table 5.1. The purpose of the symmetric model is to study the behavior of WYD Ritz solutions for systems that do not have a simple eigen-spectrum; that is, repeated eigenvalues can be expected from the mathematical model. The asymmetric model will be more likely to possess a simple eigenspectrum and will also be useful to examine the behavior of structures where the torsional response can become significant.

5.2.1 Mass Matrix

The structural mass matrix was formed by lumping at the nodes the member masses in air including deck loads and

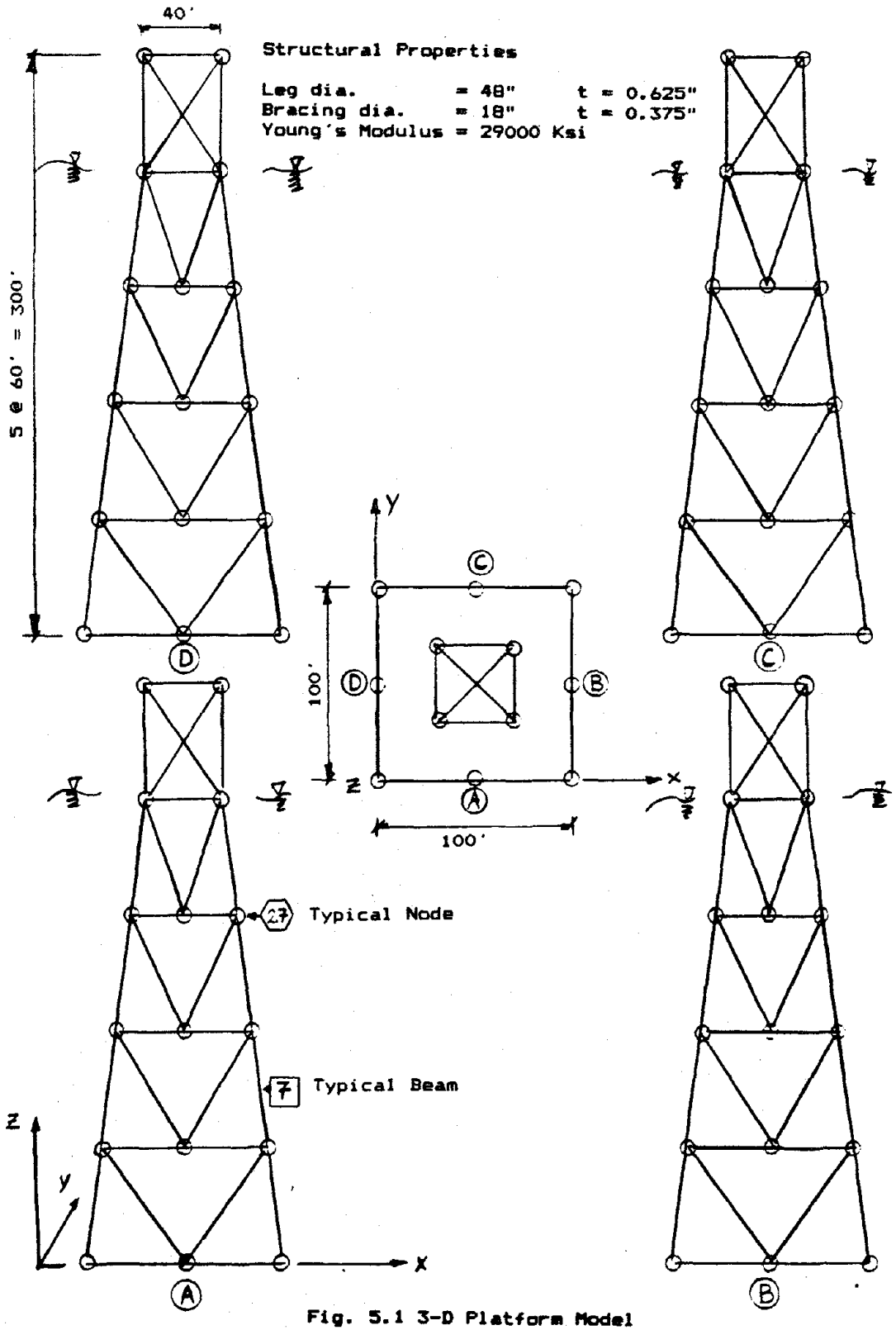

Fig. 5.1 3-D Platform Model

TABLE 5.1

Inertial Characteristics of the Two Studied Models

The mass matrices were formed considering contributions from the mass of the material of structural elements including contained fluid, the added mass at submerged nodes and the mass of the deck.

	Symmetric Mass Model		Asymmetric Mass Model	
Center of Gravity				
(ft)	CGX:	50.00	CGX:	44.89
	CGY:	50.00	CGY:	52.84
	CGZ:	273.09	CGZ:	273.09
Total Mass (Including non active DOF)				
$\left[\frac{\text{Kip-sec}^2}{\text{ft}}\right]$	MX:	492.8	MX:	492.8
	MY:	492.8	MY:	492.8
	MZ:	471.7	MZ:	471.7
Moment of Inertia				
$\left[\frac{\text{Kip-sec}^2}{\text{ft}} * \text{ft}^2\right]$	IXX:	270,044	IXX:	257,158
	IYY:	270,044	IYY:	266,066
	IZZ:	2,397,463	IZZ:	2,397,463

water (up to still water level) contained in the members. The hydrodynamic forces coming from motions in the water were accounted for by using an added mass, corresponding to the mass of fluid accelerated by the structure, for each node below still water level. The total added mass at a node was obtained by summing the volumetric contributions of members contained in the nodal tributary zone which was calculated using the specified diameter, D, and projected length, L, of the elements onto the structural coordinate axes. For a typical node the added mass in the "X" direction was thus given by

$$m^a_{i,x} = (C_x - 1)\,\rho \sum_{j=1}^{m} V_{i,j,x} \qquad [5.1]$$

where $m^a_{i,x}$ = total added mass at node "i" in "X" direction

C_x = inertia coefficient taken as 2 (see ref. 3.1)

ρ = fluid density (64 #/ft^3 for sea water)

$V_{i,j,x}$ = tributary volumetric contribution of element "j" in direction "X"; $(\pi D^2_j/4) * L_{i,j,x}$ for nodal zone "i"

m = number of elements in nodal zone "i"

Similar calculations were performed to obtain $m^a_{i,y}$ and $m^a_{i,z}$. This lumping procedure will result in a diagonal mass matrix, which is in accordance to the usual practice in the dynamic analysis of fixed jacket platforms (see ref. 5.1, 5.5).

5.2.2 Stiffness Matrix

The stiffness matrix was obtained by using static condensation on the massless DOF. The main advantages of using static condensation are to get a reduced matrix size for storage requirements in further manipulations (such as eigenvalue extraction) and to reduce the number of numerical operations required for successive matrix decomposition used in the subspace iteration with shifting to extract exact

eigenvalues. The characteristics of the stiffness matrix used for this analysis are presented in table 5.2.

It is noted that a saving of approximately 4% in the operations count and 30% in storage requirements is achieved by using a reduced system. For micro-computer applications this was advantageous since the initial static condensation was done using a block-out-of-core solver and the smaller storage requirements of the reduced system allowed the use of an incore solver for subsequent calculations. The incore solver is much more efficient since I/O transmissions to and from low speed storage are eliminated.

5.2.3 Dynamic Loading Characteristics

Time history analysis may be attractive to some analysts because it provides completely deterministic results for a particular ground motion. However, any two motions may produce quite different peak responses, even though they have the same intensity and statistical properties. Thus, for design it is necessary to analyze for several ground motions and use an average or envelope of the results. The quantity of computations becomes rapidly excessive and in practice it is much more convenient to introduce the averaging process in the construction of a smoothed response spectrum. Moreover, certifying agencies and national or regional building codes usually provide response spectra specifications to help the engineers to comply with the requirements of the seismic analysis. It is therefore very important, from a practical standpoint, to assess the performance of the WYD Ritz reduction method for the earthquake response spectra analysis technique. For that purpose a comparaison between the convergence characteristics obtained from exact eigen-solutions and load dependent Ritz solutions will be presented.

The response spectra used in the calculations follows

TABLE 5.2

Characteristics of the Stiffness Matrices used in the Numerical Example

	Original [K] Matrix	Reduced [K] Matrix
Number of equations (n) :	192	96
Semi bandwidth (b) :	40	96
Number of mass points :	96	96
Number of operations for matrix factorization :	153 600*	147 456**
Storage requirements (real values) :	7 052	4 656

* $1/2\ nb^2$ for $(n << b)$

** $n^3/6$ for $(n = b)$

the earthquake design recommendations for offshore platforms (API-RP2A, ref.3.1) and is shown in fig. 5.2. An effective horizontal ground acceleration of 0.2g with 5% damping was used. The resulting spectrum was applied along the horizontal "X" axis of the structure. An acceleration spectrum of 2/3 the acceleration used in the principal "X" direction was applied in the orthogonal "Y" direction and an acceleration spectrum of 1/2 the principal "X" acceleration was applied in the vertical "Z" direction. The three spectra were applied simultaneously.

The spatial distribution of the dynamic load $\{f(s)\}$ used to initiate the calculation of load dependent Ritz vectors was taken as

$$\{f(s)\} = [M]\{r_x\} + [M]\{r_y\} + [M]\{r_z\} \qquad [5.2]$$

where $[M]$ is the mass matrix and $\{r_j\}$ is the influence vector representing the displacements of each DOF of the model from unit directional displacement of base input.

5.3 Earthquake Analysis by the Response Spectrum Technique

A response spectrum is an envelope of maximum response of a SDOF subjected to a particular disturbance and plotted as a function of the natural period of the oscillator. Different spectrum curves are obtained for different damping ratios. For earthquake analysis typical response spectra are obtained from the average maximum response of SDOF systems subjected to a serie of earthquake accelerograms scaled to the same intensity.

The traditional approach of response spectra analysis for MDOF systems is to use a truncated set of the lowest eigenvectors, $\{\emptyset_i\}$, corresponding to the displacement solution of the free vibration equilibrium equations with damping neglected, to transform the original system expressed

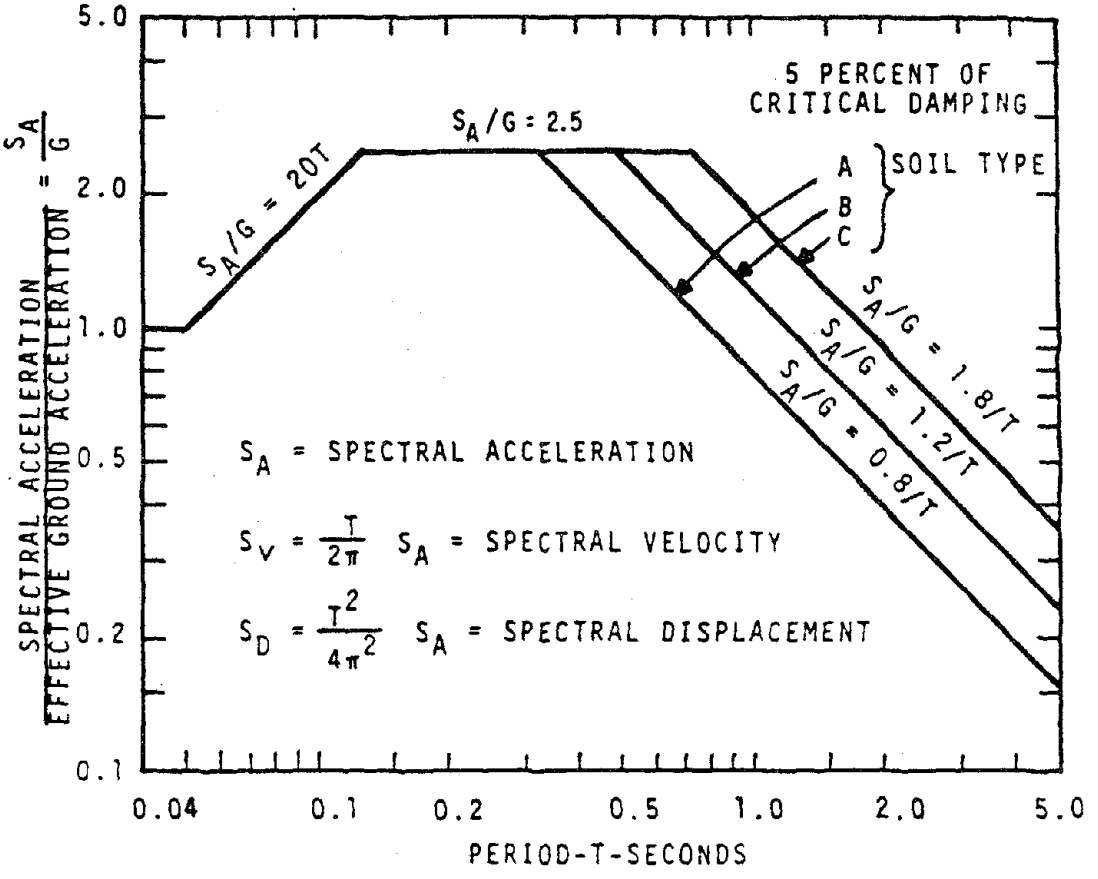

SOIL TYPE

A ROCK — CRYSTALLINE, CONGLOMERATE, OR SHALE-LIKE MATERIAL GENERALLY HAVING SHEAR WAVE VELOCITIES IN EXCESS OF 3000 FT/SEC (914 M/SEC)

B SHALLOW STRONG ALLUVIUM — COMPETENT SANDS, SILTS AND STIFF CLAYS WITH SHEAR STRENGTHS IN EXCESS OF ABOUT 1500 PSF (72 kPa) LIMITED TO DEPTHS OF LESS THAN ABOUT 200 FEET (61 M) AND OVERLYING ROCK-LIKE MATERIALS

C DEEP STRONG ALLUVIUM – COMPETENT SANDS, SILTS AND STIFF CLAYS WITH THICKNESSES IN EXCESS OF ABOUT 200 FEET (61 M) AND OVERLYING ROCK-LIKE MATERIALS

Fig. 5.2 Response Spectra Used in Calculation

in geometric coordinates to a serie of uncoupled generalized SDOF expressed in modal coordinates. The damping matrix is not formed explicitly, it is rather assumed that damping is proportional to [M] and [K] such that a modal damping parameter, ξ_i, can be assigned to each generalized coordinate. A typical equation of motions in modal coordinate is thus given by

$$\ddot{y}_i + 2\xi_i w_i \dot{y}_i + w^2_i y_i = \frac{\{\emptyset_i\}^T [M] \{r\}}{\{\emptyset_i\}^T [M] \{\emptyset_i\}} g(t) \qquad [5.3]$$

The typical maximum contribution of mode "i", taken as a generalized SDOF, to the total displacement response of the structure, is obtained as:

$$\{U_{i,max}\} = \{\emptyset_i\} * p_i * S_{d,i} \qquad [5.4]$$

where $S_{d,i}$ is the spectral displacement at the period of mode "i" and p_i is the modal participation factor given by:

$$p_i = \frac{\{\emptyset_i\}^T [M] \{r\}}{\{\emptyset_i\}^T [M] \{\emptyset_i\}} \qquad [5.5]$$

the vector {r} being defined from the usual directional coefficients resulting from unit support displacements. The maximum value of the generalized coordinate $y_i(t)$ is thus equal to $p_i * S_{d,i}$.

The uncoupled form of equation [5.3] can also be obtain from the load dependent Ritz pair $\{^oX_i\}$. The resulting equation of motion in generalized Ritz coordinate is given by

$$\ddot{^oy}_i + 2\xi_i \bar{w}^2_i \dot{^oy}_i + \bar{w}^2_i {}^oy_i = \frac{\{^oX_i\}^T [M] \{r\}}{\{^oX_i\}^T [M] \{^oX_i\}} g(t) \qquad [5.6]$$

The maximum value of $^oy_i(t)$ will also be derived from the specified spectral displacement.

For an arbitrary orientation of a three dimensional input acceleration vector, the modal responses associated with a particular direction of excitation are first evaluated. An approximation to the maximum response is then obtained by combining modal maximum of individual response quantities (modal combinations) using a specified combination rule. The total response is obtained by summing the response from the three directions by the Square Root of the Sum of the Square (SRSS) method (spatial combination).

As previously stated, the use of response spectra for the design of earthquake resistant structures has been established as an inexpensive and reliable alternative to multiple time history analyses. The main drawbacks of the method are pertaining to the number of modes that should be retained in the analysis and the choice of an appropriate combination rule for the superposition of modal maxima, not all of which occur at the same time.

For this study, the modal response were combined using the Complete Quadratic Combination method (CQC). The CQC method requires that all modal response terms be combined by the application of the following equations:

for typical displacement components u(k):

$$u(k) = \left(\sum_i \sum_j u(k)_i \; \rho_{ij} \; u(k)_j\right)^{1/2} \qquad [5.7]$$

for typical force component f(k):

$$f(k) = \left(\sum_i \sum_j f(k)_i \; \rho_{ij} \; f(k)_j\right)^{1/2} \qquad [5.8]$$

where $u(k)_i$ is a typical component of the modal displacement response vector $\{U_{i,max}\}$ and $f(k)_i$ is a typical force component which is produced by the modal displacement vector $\{U_{i,max}\}$. The CQC method considers a cross modal correlation factor, ρ_{ij}, which is a function of the modal frequencies and

damping ratios of the structure. The method has proved to be more accurate, when compared to actual time history analyses, than the traditional SRSS method (for modal combinations) specially for asymmetric models or models having closely spaced modes. A complete description of the method has been given by Wilson, Der Kiureghian and Bayo in reference 5.8.

Finally it should be noted that while working with the response spectra method, the basic static correction procedure can not be applied directly to supplement the modal summation since a special combination rule to approximate the expected value of the added effects of individual maximum response must be used. The LWYD Ritz algorithm without static residual would therefore appear to be more consistent with the response spectra method.

5.4 Computational Efficiency Study

Typical operation counts required by the subspace iteration technique, the Lanczos method and the WYD Ritz reduction method to obtain a fixed number of transformation vectors, r, to expressed the original structural system in generalized coordinates are presented in table 5.3. The purpose of this comparison is to provide an indication of the potential efficiency of each method assuming that all techniques have been implemented with the same programming skills. Each operation is assumed to consist of a multiplication followed by an addition, the value of n denotes the order of the stiffness matrix in the analysis and b its average semi bandwidth. It is assumed that the mass matrix is diagonal. The average bandwidth parameter is used primarily to provide a measure of the number of nonzero matrix elements, since in actual implementation a profile solver which does not require a uniform band structure is used for efficient computational operations. It should also be noted that each method has the same order of storage requirements O(nb).

TABLE 5.3

Operation Counts for Alternate Methods of Transformation Vectors Calculation

Method	Approximate Operation Count for r vectors[1] (significant terms)
Subspace Iteration[2] Method	
(assuming ten iterations on a subspace of r+8 vectors to obtain r eigenvectors $\{\emptyset_j\}$)	$nb^{2\bullet} + 20\ nbr + 18\ nr^2 + 147\ nb \ldots + 1368\ n + 162\ r^3 + 324\ r^2$
Lanczos Method	
(assuming 2r vectors required for r eigenvectors $\{\emptyset_j\}$)	$1/2\ nb^2 + 4\ nbr + 10.5\ nr^2 + \ldots 16\ nr + 24\ r^3 + 80\ r^2$
WYD Ritz Vectors Method	
(original algorithm using $[K]^*$, r vectors $\{^oX_j\}$)	$1/2\ nb^2 + 3\ nbr + 3.7\ nr^2 + \ldots 9.5\ nr + 9\ r^3 + 18\ r^2$
LWYD Vector Algorithm	
(algorithm using $[K]^*$, r vectors $\{^oX_j\}$)	$1/2\ nb^2 + 3\ nbr + 3.5\ nr^2 + \ldots 15\ nr + 9\ r^3 + 18\ r^2$
LWYD Vector Algorithm	
(algorithm using $[T_r]$, r vectors $\{^oX_j\}$)	$1/2\ nb^2 + 2\ nbr + 2.5\ nr^2 + \ldots 15\ nr + 3\ r^3 + 20\ r^2$

where n = order of stiffness matrix
b = average semi bandwidth
r = number of transformation vectors to calculate

note 1 - The mass matrix is assumed to be diagonal
2 - Adapted from Bathe and Wilson (ref. 5.4)
• - Includes a Sturm sequence check

From table 5.3 it can be seen that the major computational effort of the WYD Ritz reduction technique involves the decomposition of the stiffness matrix and provides the leading term of 1/2 nb^2 in the total operation count. In the subspace iteration method, the leading term of the count, nb^2, is twice as large as in the WYD Ritz approach and all other terms involving the same functional of the parameters n,b,r are also much larger.

To get an appreciation of the performance of each technique on a real problem, the parameters of the original offshore system were substituted in the equations and it was assumed that 25 transformation vectors were to be calculated. According to these calculations, the original WYD Ritz algorithm and the LWYD Ritz algorithm will present an operation count that is approximately one half of the Lanczos method and one seventh of the subspace iteration if $[K]^*$ is used as the reduced Ritz system, if the reduced [T] matrix is formed directly this value will drop to one ninth.

To confirm this theoretical analysis, the total computer execution time of the standard SAP-80 subspace iteration module (using the incore solver) and of the new Ritz modules were monitored as a function of the number of requested vectors. The calculations were performed in single precision arithmetic carrying 7 significant digits on a micro-computer working with a Z80 eight bits micro-processor. The results are presented in fig 5.3. It is shown that after the overhead of initial matrix factorization was overcome, the load dependent Ritz technique using $[K]^*$ was approximately 7 times more efficient than the subspace iteration technique requiring only 33 minutes of execution time as compared to nearly 4 hours by the subspace iteration for the generation of 25 transformation vectors. The implementation using the tridiagonal form of the reduced system decreased the execution time for Ritz vectors calculation by approximately 20 %. The computational

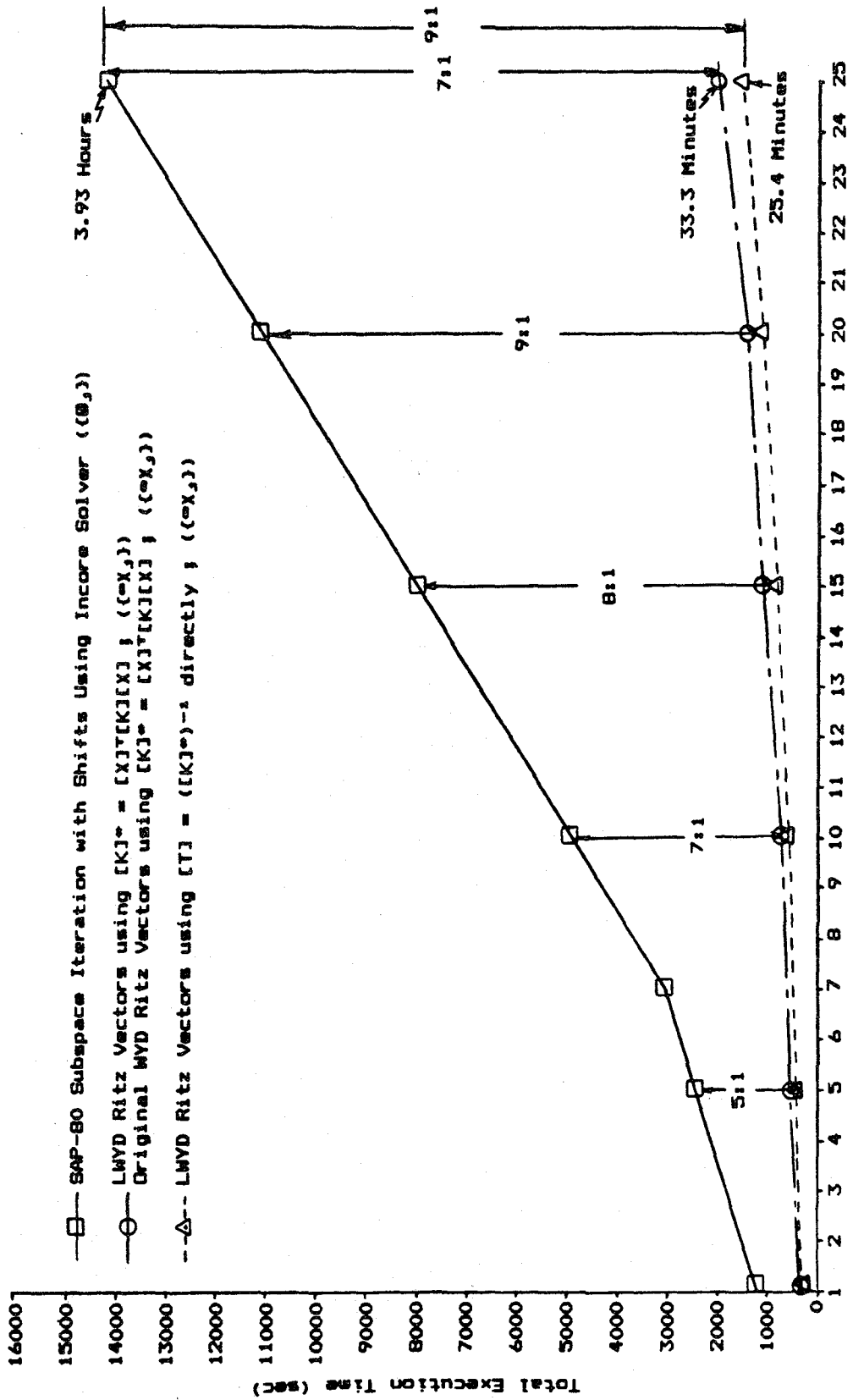

Fig. 5.3 Computer Execution Time for Transformation Vectors Calculations

advantage of the WYD Ritz reduction method over the subspace iteration technique, using either [K]* or [T] as generalized system, is thus very significant and the method is well suited for micro-computer applications.

The transformation vectors, $\{\emptyset_i\}$, obtained from subspace iteration are an "accurate" eigensolution of the free vibration problem while some vectors, $\{^{e}X_j\}$, obtained from the load dependent Ritz approach are only approximate eigenvectors of the original structural system. Traditionally the accuracy of the eigensolution, obtained at high computational costs, has been a primary criterion for the analyst to accept a vector basis for coordinate transformation. It will however be shown that a criterion based on the representation of the dynamic load by the vector basis is actually sufficient to ensure a satisfactory solution for the seismic analysis and that the accuracy of the eigensolution might be considered of secondary importance. The long execution time of the subspace iteration are thus hardly justifiable for this type of analysis where a fixed load distribution has been specified.

5.5 Computer Results

Computational variants of the algorithms used to generate load dependent Ritz vectors were evaluated in preliminary calculations to select the best algorithm to be used along with the response spectra method. It was found that the more stable solution in terms of moderate stress and displacements fluctuations calculated during convergence can be obtained from the LWYD Ritz algorithm without static residual using [K]* as reduced structural system. The addition of the static residual to the solution resulted in larger displacements and stress fluctuations when the first few vectors were added to the basis.

The computer results reported in the next sections

were thus obtained from Ritz vectors calculated by the LWYD Ritz algorithm without static residual unless otherwise specified.

5.5.1 Representation of the Dynamic Load Using Spatial Error Estimates

Figures 5.4 (a) and (b) present the percent of overall loading representation, as expressed by the Euclidean norm of the error force vector, e^* (see equation [3.28]), achieved by the vector bases using exact eigenvectors, $\{\emptyset_j\}$, and LWYD Ritz modes $\{^{\circ}X_j\}$. It is shown that the representation of the loading is much smoother while using LWYD Ritz modes than eigenvectors and that a good representation, given by an e^* value of 90% to 100%, is obtained with much fewer LWYD Ritz vectors than exact eigenvectors. For example, in the asymmetrical model a value of e^* equal to 90% is obtained from 5 LWYD Ritz vectors while 14 eigenvectors are required to get the same e^* value.

To get a better understanding of this phenomenon it is useful to consider the directional values of the error norms. For that purpose the directional components of the error estimate based on the Euclidean norm of the error force vector and the error norm based on the summation of represented forces, measuring directional effective modal masses in this application, were evaluated for both models as shown in fig. 5.5 and 5.6 Only the values related to the "X" and "Z" directions are reported since the "Y" values are very similar to the "X" results.

The most obvious difference in the convergence characteristics of the LWYD Ritz and eigensolutions is the way in which the vertical "Z" contribution is included in the analysis. The first vertical mode of deformation in the "Z" direction is occuring much earlier in the LWYD Ritz expansion than in exact eigenvectors analysis. This is due to the fact

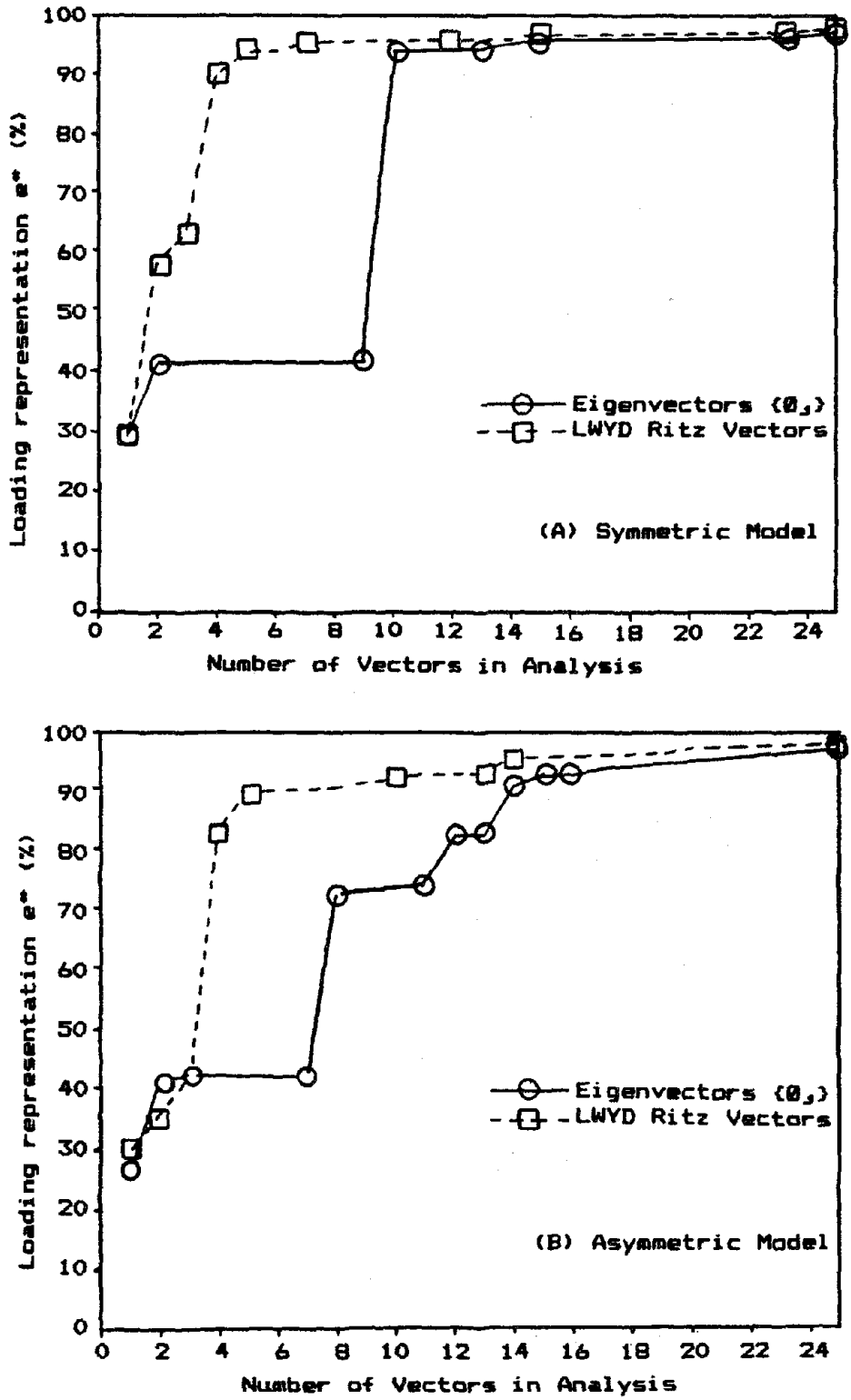

Fig. 5.4 Overall Loading Representation using Error Estimate Based on the Euclidean Norm of Error Force Vector

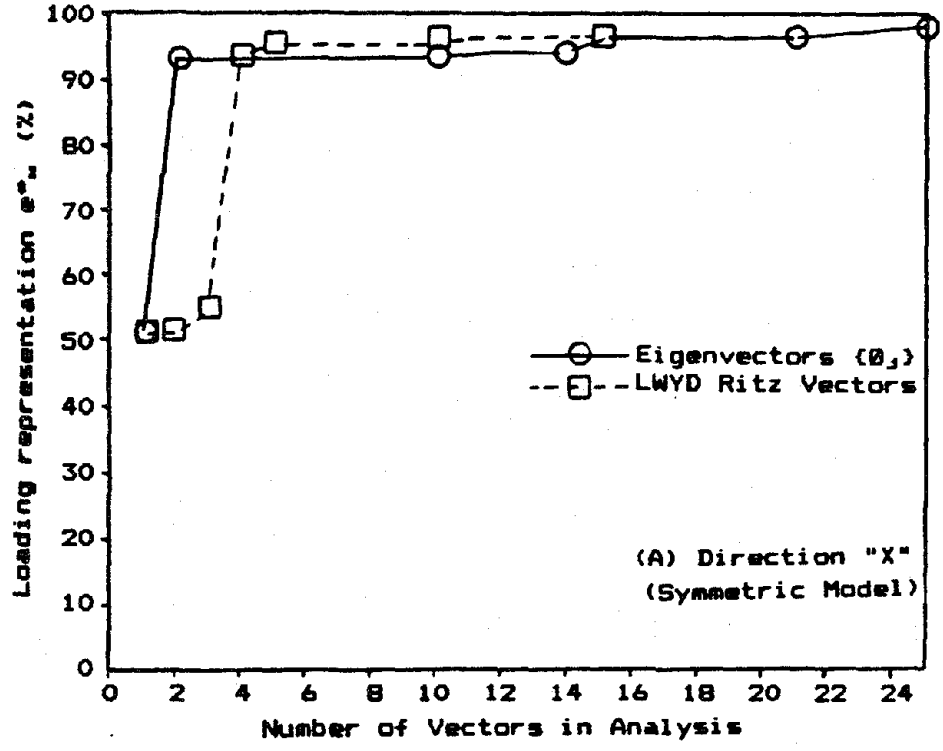

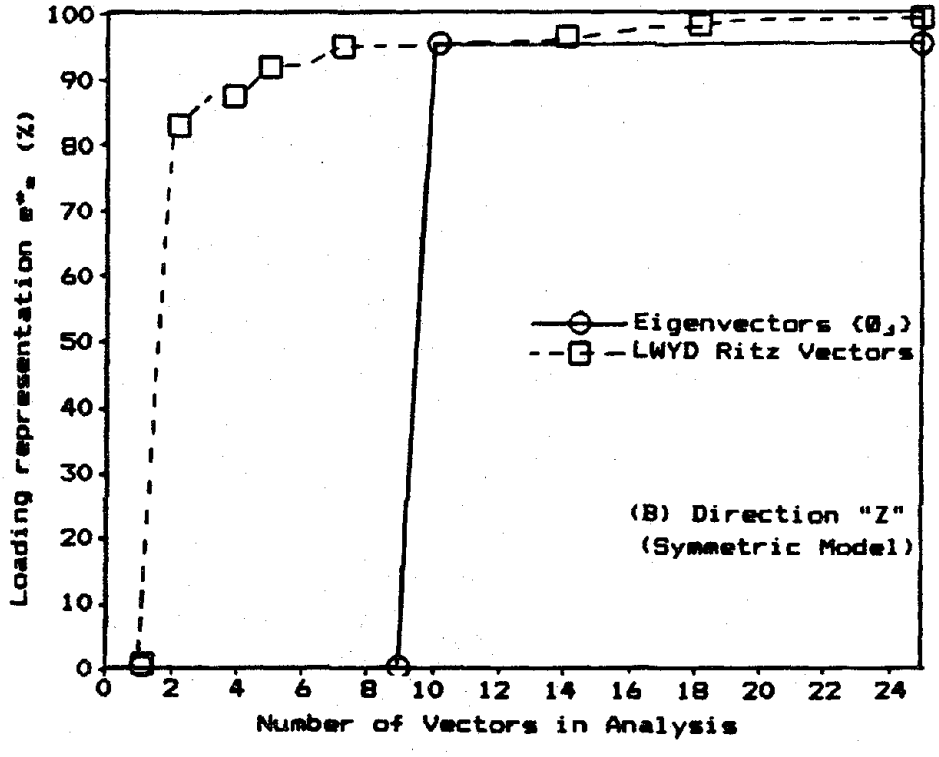

Fig. 5.5 Loading Representation using Euclidean Norm of Error Force Vector (Directional Calculations)

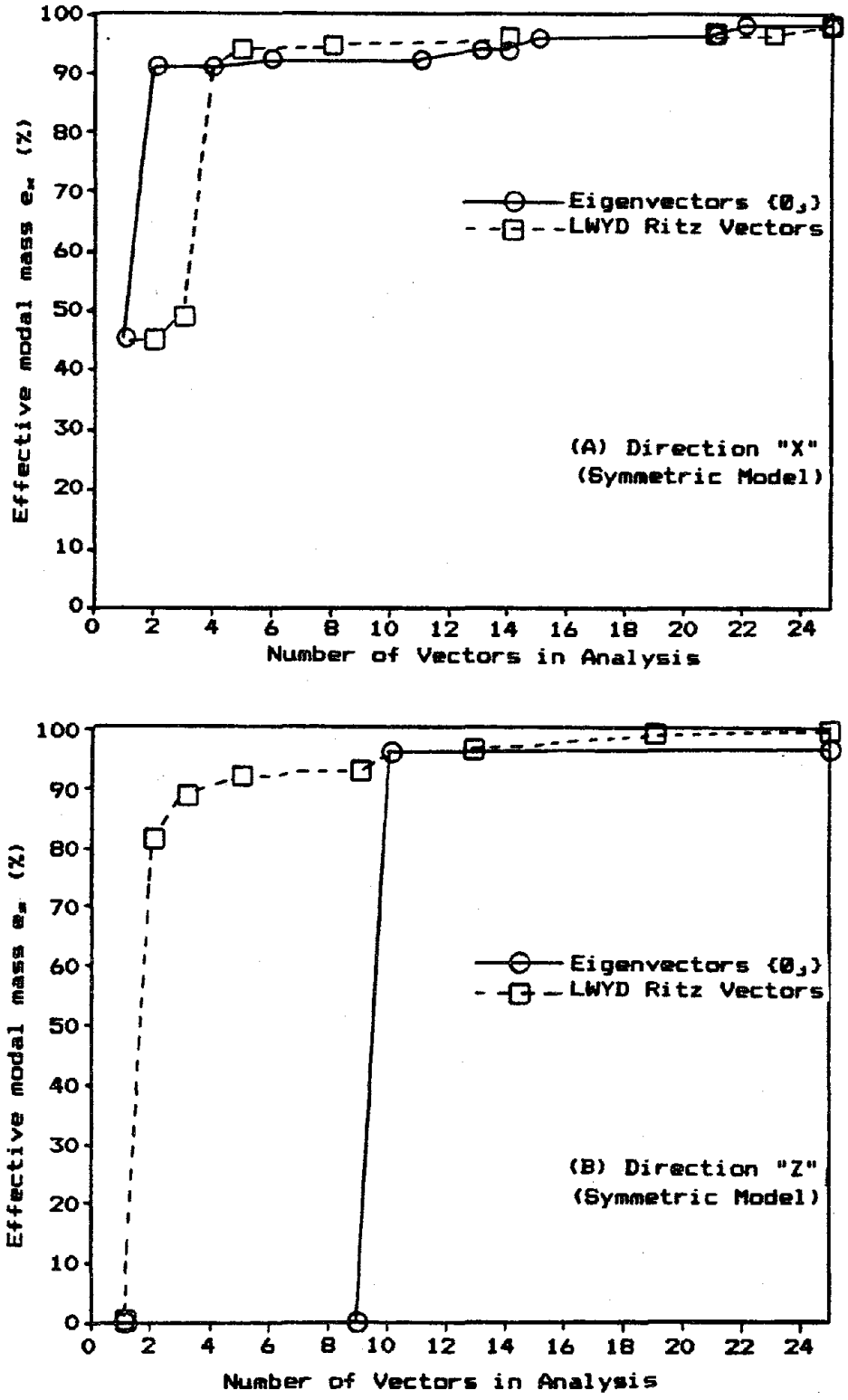

Fig. 5.6 Effective Modal Mass as a Function of the Number of Vectors Retained in the Analysis

that the initial spatial distribution of the loading to generate LWYD Ritz vectors is causing significant deformations in the "Z" direction favoring early appearance of relatively stiff axial deformation modes. This is a major advantage of LWYD Ritz solutions over exact eigensolutions if vertical excitation is to be included in the analysis. This is also why a better overall loading representation can be achieved with less vectors considering the LWYD Ritz solution.

Table 5.4 presents the number of vectors required from the two solution methods to obtain a good representation of the dynamic load. If a satisfactory convergence in the loading representation is considered to be obtained with at least 90% of the total dynamic load included in the analysis, as suggested by the API-RP2A specifications, the eigensolution for the symmetric model will achieve convergence with the contribution of only 2 modes in the "X" and "Y" directions while 10 modes are required in the "Z" direction. The LWYD Ritz solution achieved convergence with 4 vectors for any direction "X", "Y" or "Z". For the asymmetric model the eigensolution requires 2 modes in the "X" direction, 3 modes in the "Y" direction and 14 modes in the "Z" direction while the LWYD Ritz solution converged with 3 vectors in the "X" and "Y" directions and 10 vectors in the "Z" direction.

If vertical excitation is considered, the LWYD Ritz solution achieved loading convergence with fewer vectors than the eigensolution for both models. If one disregard convergence in the "Z" direction and a 90% dynamic load representation is required then the eigenvectors are sligthly more efficient , in term of the number of required vectors, than the LWYD Ritz approach for the horizontal loading representation. However, if a higher precision in the loading representation is required, say 95% of the total load is to be included in the analysis, then the LWYD Ritz

TABLE 5.4

Number of Required Vectors for Adequate Loading Representation Using Spatial Error Estimates

1- Error norm based on summation of represented forces

Model	direction	# of vectors for effective modal mass of			
		90%		95%	
		Ritz	Eigen	Ritz	Eigen
Symmetric	e_x	4	2	10	15
	e_y	4	2	10	14
	e_z	4	10	10	10

Model	direction	# of vectors for effective modal mass of			
		90%		95%	
		Ritz	Eigen	Ritz	Eigen
Asymmetric	e_x	3	2	10	15
	e_y	3	3	12	14
	e_z	10	14	15	18

2- Error norm based on Euclidean norm of error force vector

Model	direction	# of vectors for error norm value of			
		90%		95%	
		Ritz	Eigen	Ritz	Eigen
Symmetric	e^*_x	4	2	5	15
	e^*_y	4	2	5	14
	e^*_z	5	10	7	10
	e^*	4	10	7	14

Model	direction	# of vectors for error norm value of			
		90%		95%	
		Ritz	Eigen	Ritz	Eigen
Asymmetric	e^*_x	3	2	6	15
	e^*_y	3	3	8	14
	e^*_z	13	17	19	23
	e^*	5	14	14	22

solution is equally or more effective, in terms of the number of required vectors, than the eigensolution for both models and in all directions.

It should be noted that in all cases the LWYD Ritz solutions proved to be numerically more efficient since the Ritz vectors were obtained at a fraction of the cost (1/7) of exact eigenvectors clearly demonstrating the advantage of the LWYD Ritz solutions over the eigensolutions.

5.5.2 Relationship Between Ritz Solutions and Eigensolutions

Natural periods of vibration are important information to the analyst to identify possible resonant conditions and to indicate how changes in the mass and stiffness matrices will affect the dynamic response. Even in the case of a direct step-by-step solution on coupled systems a limited approximate eigenvalue analysis is highly desirable to provide this type of informations or to construct an explicit damping matrix from specified modal damping ratios.

Tables 5.5 and 5.6 list natural periods of vibration of the platform models using exact eigensolutions of the original systems calculated by the subspace iteration module of the SAP-80 computer program and the approximate eigenvalues obtained from reduced systems using [K] and [M] orthogonal LWYD Ritz vectors $\{^{o}X_{j}\}$. The results are reported in terms of periods instead of frequencies to be compatible with the specified earthquake response spectra. The fundamental periods were obtained as 3.690 sec for the symmetric model and 3.758 sec of the asymmetric model indicating a relatively flexible structure for which the response is controlled by the displacement bound region of the earthquake spectra, that is the maximum spectral displacement approaches the maximum ground displacement. The LWYD Ritz solutions spanned a larger period range than the exact eigensolutions, for example according to table 5.5, 25

TABLE 5.5

Natural Periods (sec) of Symmetric Mass Model

Mode	Exact Eigensolution on Original System	LWYD Ritz Analysis on Reduced System			
		r[1]=25	r=15	r=10	r=5
1	3.690	3.690	3.690	3.690	3.690
2	3.690	3.690	3.690	3.690	3.690
3	2.309	2.309	2.309	2.309	0.873
4	0.930	0.930	0.926	0.873	0.662
5	0.873	0.873	0.873	0.826	0.488
6	0.873	0.873	0.827	0.663	
7	0.827	0.827	0.663	0.562	
8	0.692	0.692	0.661	0.547	
9	0.673	0.673	0.596	0.361	
10	0.663	0.663	0.560	0.217	
11	0.661	0.661	0.425		
12	0.661	0.598	0.362		
13	0.598	0.561	0.290		
14	0.560	0.560	0.222		
15	0.560	0.430	0.128		
16	0.470	0.401			
17	0.430	0.363			
18	0.430	0.344			
19	0.427	0.270			
20	0.407	0.226			
21	0.400	0.165			
22	0.363	0.149			
23	0.363	0.107			
24	0.358	0.084			
25	0.346	0.051			

note 1 - r is the number of generalized coordinates retained in the reduced eigenproblem

TABLE 5.6

Natural Periods (sec) of Asymmetric Mass Model

Mode	Exact Eigensolution on Original System	LWYD Ritz Analysis on Reduced System			
		r[1]=25	r=15	r=10	r=5
1	3.758	3.758	3.758	3.758	3.758
2	3.696	3.696	3.696	3.696	3.696
3	2.200	2.200	2.200	2.200	2.200
4	0.930	0.930	0.929	0.873	0.775
5	0.873	0.873	0.873	0.754	0.623
6	0.873	0.873	0.828	0.702	
7	0.827	0.827	0.754	0.631	
8	0.754	0.754	0.664	0.536	
9	0.692	0.692	0.631	0.398	
10	0.659	0.659	0.577	0.253	
11	0.657	0.657	0.536		
12	0.630	0.630	0.427		
13	0.598	0.597	0.360		
14	0.554	0.554	0.244		
15	0.533	0.533	0.169		
16	0.470	0.434			
17	0.434	0.422			
18	0.430	0.375			
19	0.422	0.340			
20	0.408	0.321			
21	0.401	0.271			
22	0.375	0.223			
23	0.364	0.159			
24	0.344	0.115			
25	0.328	0.083			

note 1- r is the number of generalized coordinates retained in the reduced eigenproblem

exact mode shapes of the symmetrical model stop at a period of 0.346 sec, while 25 LWYD Ritz modes extended to 0.051 sec. It is also observed that for the symmetric model, modes tend to occur in pairs with the same period of vibration indicating the presence of reapeated eigenvalues in the eigenspectrum as expected from the mathematical modelling.

The first two modes of each model were dominated by global flexural behavior acting simultaneously in the "X" and "Y" directions while the third mode was characterized by torsional behavior. Higher modes had generally small participation factors and included local deformations as well as "breathing" type of behavior. There was however one important exception related to the relatively stiff global vertical deformation mode. A graphical representation of the first few modes of each model is given in fig. 5.7.

The natural period of vibration of a specific mode of the reduced dynamic system as expressed by the free vibration problem is not a function of the number of vectors retained in the analysis if exact eigenvectors are used. However if [K] and [M] orthogonal LWYD Ritz vectors are used the period of vibration associated with a specific vector becomes a function of the number of Ritz coordinates retained in the solution.

Figures 5.8 (a) and 5.8 (b) illustrate the change in natural periods of vibration as a function of the number of LWYD Ritz vectors retained in the reduced systems. As the number of generalized Ritz coordinates increases the first few [K] and [M] orthogonal LWYD Ritz vectors becomes closer and closer approximations to the exact eigenvectors at the beginning of the spectrum as expected from the similarity between the LWYD Ritz algorithm and the Lanczos method.

To get a better appreciation of the relationship between the LWYD Ritz solution and the eigensolution in terms

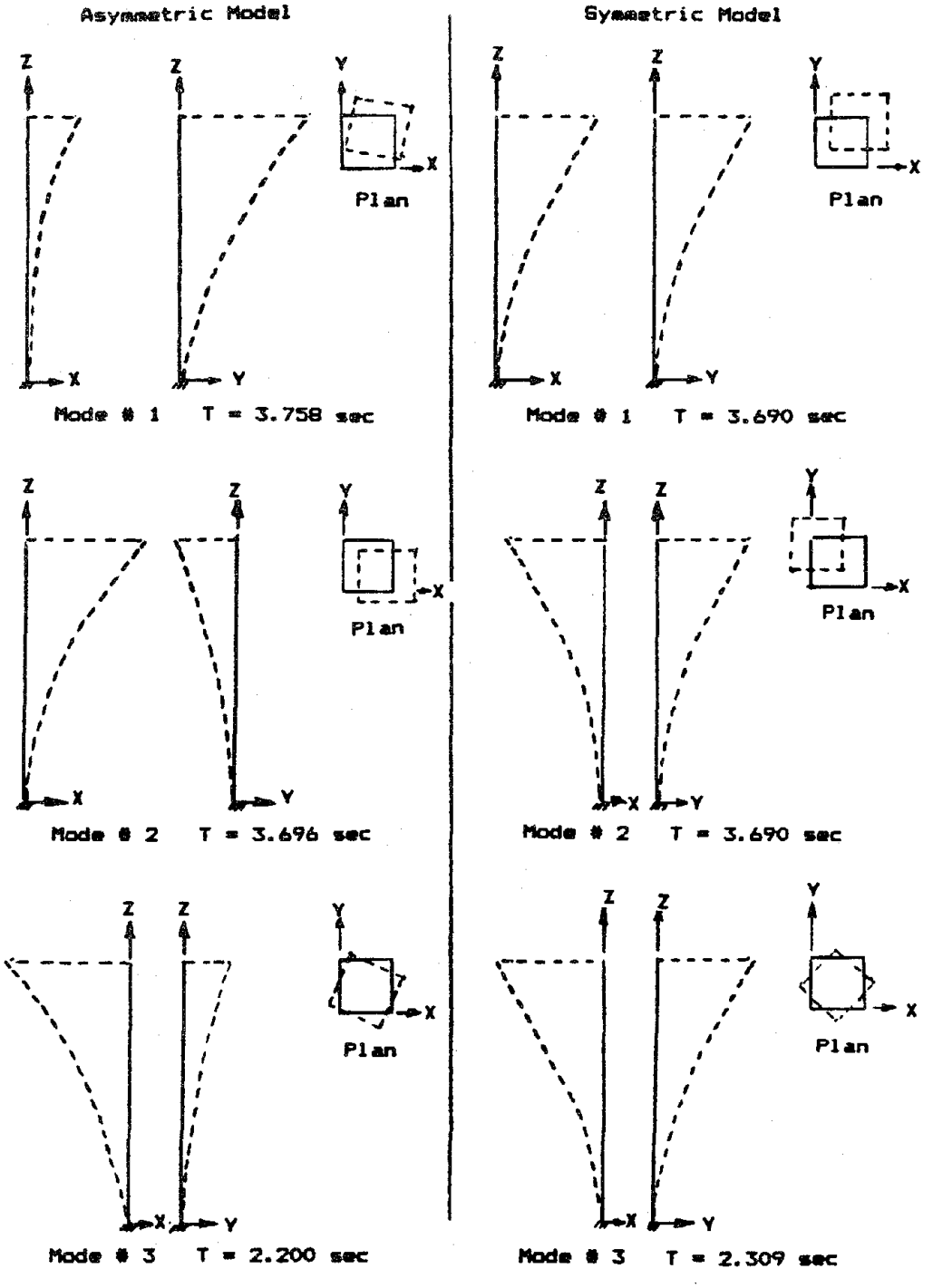

Fig. 5.7 Graphical Representation of Mode Shapes Using Average Centerline Deformation of X-Z and Y-Z Frames

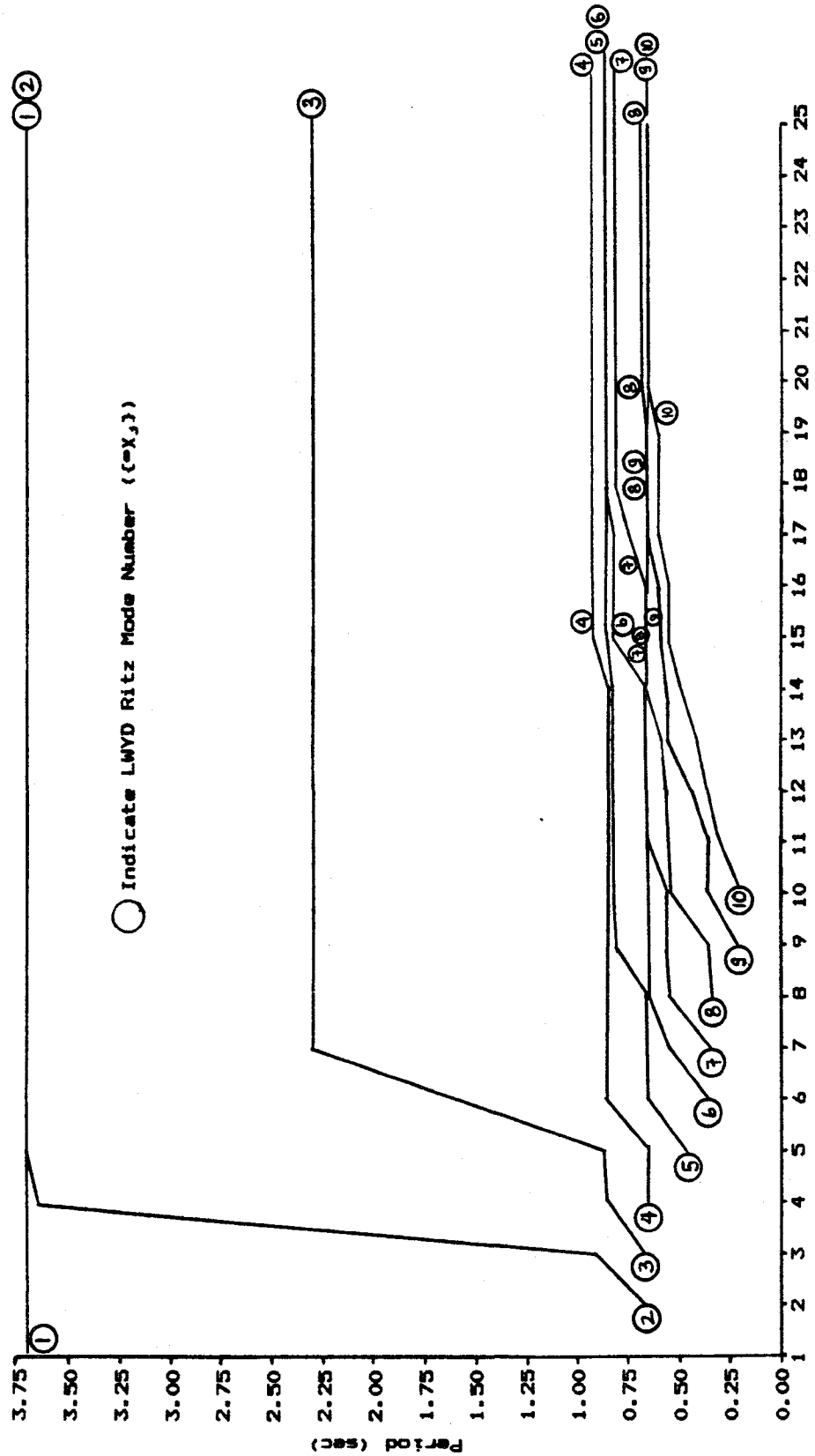

Fig. 5.8 (a) Change in Natural Periods of Vibration as a Function of the number of Ritz Coordinates Retained in the Solution of the Reduced Eigenproblem (Symmetric Model)

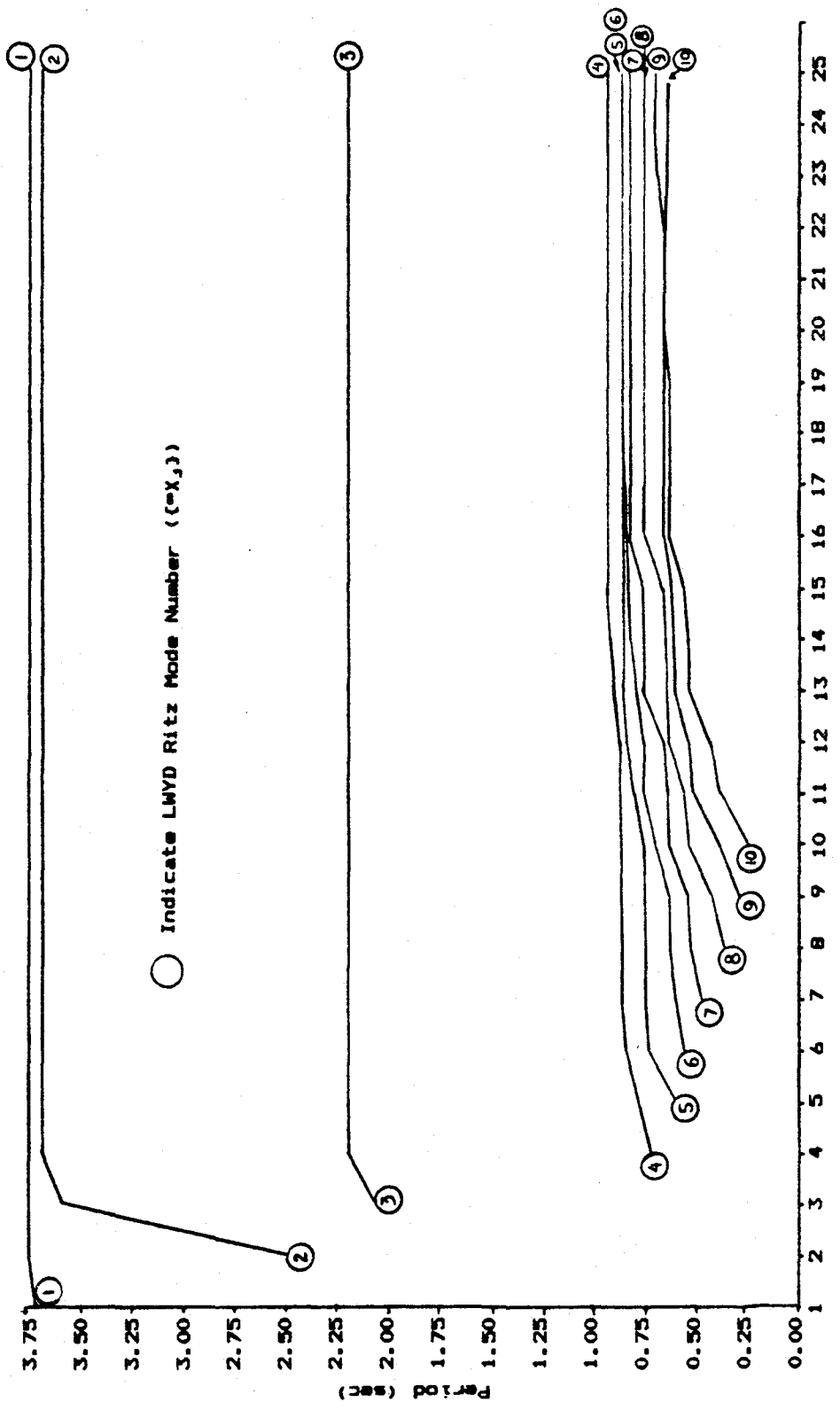

Fig. 5.8 (b) Change in Natural Periods of Vibration as a Function of the number of Ritz Coordinates Retained in the Solution of the Reduced Eigenproblem (Asymmetric Model)

of the accuracy of the Ritz pair ($\bar{w}^2_j$, $\{^eX_j\}$) as a solution of the free vibration problem [K][Ø] = [M][Ø][w^2], the error norms, ^ee_j, described by equation [3.46] were calculated for various number of generalized coordinates retained in the reduced systems for both models. A comparison was also established with the exact eigenvectors obtained from subspace iteration.

The first step in the interpretation of these results was to define what might be considered an "accurate" eigensolution while using the error bounds. Result obtained from the subspace iteration module for which a tolerance of 10^{-6} was requested for the eigenvalues, yielded a maximum value of ^ee_j equal to 8×10^{-3} (symmetric model), moreover it was shown by Bathe (1.2) that a value of ^ee_j equal to 10^{-2} is able to ensure a precision of 4 significant digits in the related eigenvectors. A maximum values of 10^{-2} for ^ee_j was thus considered acceptable to qualified a given LWYD Ritz pair as an accurate eigensolution.

The number of LWYD Ritz pairs that can be considered exact eigenpairs (based on the value ^ee_j) as a function of the number of Ritz coordinates retained in the reduced system is shown in fig. 5.9 (a) and 5.9 (b). These plots illustrate the number of LWYD Ritz pairs located at the beginning of the eigenspectrum that were classified as exact eigenpairs which is consistent with a Lanczos interpretation of the LWYD Ritz algorithm to seek an exact eigensolution. The total number of LWYD Ritz pairs satisfying the eigenconvergence error norms but located anywhere along the eigenspectrum was also reported.

For example the total number of LWYD Ritz pairs, with a reduced system of 25 Ritz coordinates, that can be classified as eigenpairs was 12 for the asymmetric model and 18 for the symmetric model. The first 8 LWYD Ritz pairs of the asymmetric model and the first 12 LWYD Ritz pairs of the

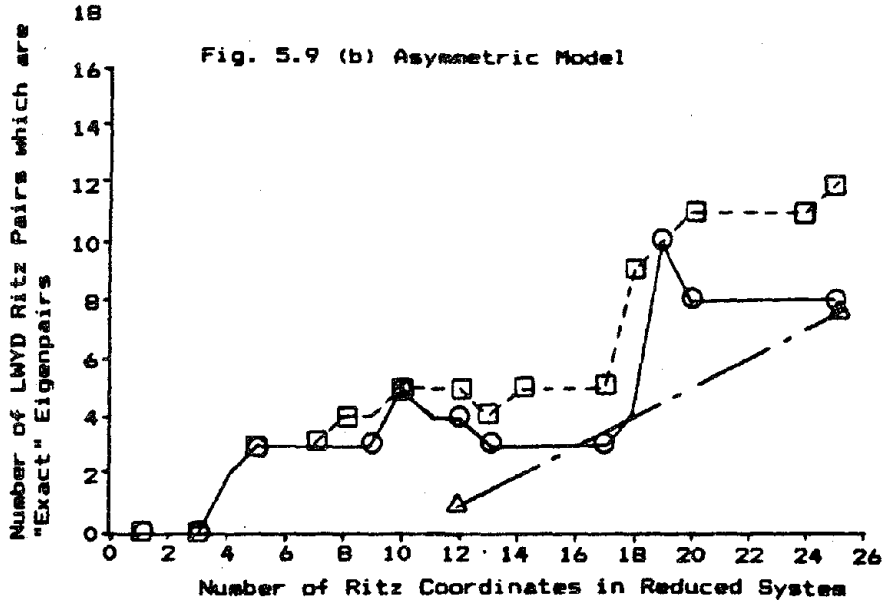

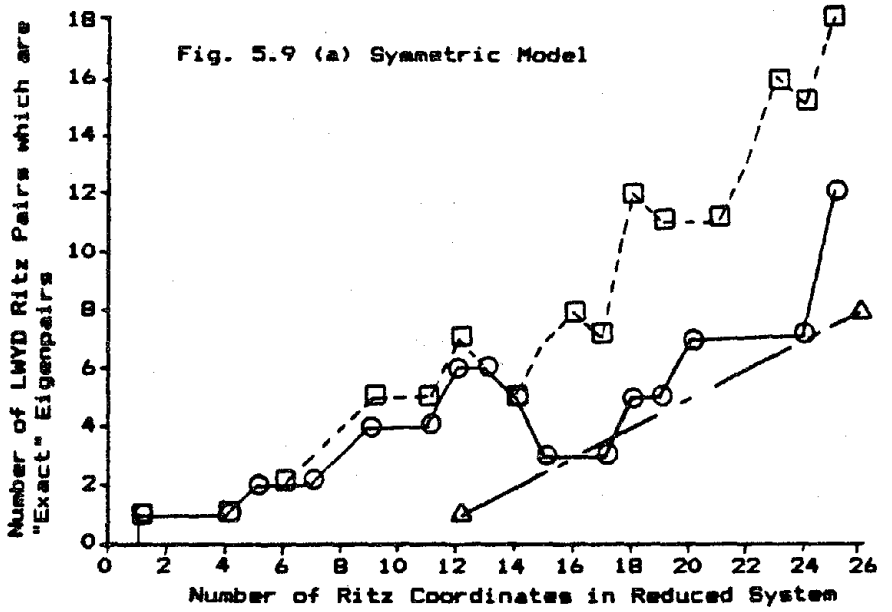

—○— Number of consecutive LWYD Ritz pairs at the beginning of the eigenspectrum that are "exact" eigenpairs (m)

- □ - Total number of LWYD Ritz pairs that are "exact" eigenpairs

- △ — Rule of thumb for (m) (equation [5.11])

Fig. 5.9 Relationship Between LWYD Ritz Solutions of Reduced System and "Exact" Eigensolutions of Original System

symmetric model were considered "exact" eigensolutions. Even though some of the remaining LWYD Ritz pairs were not classified as "exact" eigensolutions they nevertheless provide a good indication of the content of the rest of the eigenspectrum for which confidence intervals can be established from the error bounds calculations.

The following guideline can be used to get an accurate agreement between the lower frequencies of the reduced system and exact frequencies of the original system :

$$r = \min (2m + 10, n) \qquad [5.11]$$

where

r is the order of the reduced eigenvalue problem
m is the number of requested exact eigenvalues
n is the order of the original system

It was observed in the context of the Lanczos method (2.11, 2.12), that in the case where $r<<n$, a first grouping of more than $r/2$ eigenvalues of the reduced system are in good agreement with the corresponding number of exact eigenvalues. The remaining reduced system roots are spread across the remaining exact eigenspectrum.

To evaluate the influence of the form of the reduced Ritz system on the convergence characteristics of the LWYD Ritz solution the accuracy of the Ritz pairs ($\bar{w}^2_j$, $\{^e X_j\}$) as a solution of the free vibration problem were calculated. The error norm $^e e_j$ was applied to Ritz pairs obtained from the LWYD Ritz algorithm without static residual using $[K]^*$ and $[T_r]$ as reduced Ritz system.

The eigensolution of the reduced Ritz system was first obtained from the threshold Jacobi method applied to $[K]^*[Z] = [M]^*[Z][\bar{w}^2]$ and $[T_r][Z] = [Z][\lambda]$ such that the numerical method used for the reduced eigensolution was identical in both cases and therefore did not contribute to

discrepency in the results.

The results are shown in fig. 5.10 for the case where 25 Ritz coordinates were included in the analysis. It is shown that for the symmetric model having closely spaced eigenvalues, the results using $[T_r]$ are not as accurate as the results using $[K]^*$. For the asymmetric model where the eigenvalues are generally more distinct the results using either $[K]^*$ or $[T_r]$ followed closely each other. It can thus be concluded that the reduced system using $[K]^*$ is able to provide a higher resolution in the solution especially for systems that do not have a single eigenspectrum.

In terms of displacements and stresses it was found that the asymmetric model exhibited convergence characteristics that were almost identical using either $[K]^*$ or $[T_r]$. For the symmetric model, convergence was obtained from approximately the same number of vectors but larger stress and displacement fluctuations were observed in intermediate calculations if $[T_r]$ was used instead of $[K]^*$.

The eigensolution of the reduced tridiagonal system was also obtained from the QR algorithm followed by inverse iteration. The trial vectors were continuously reorthogonalized with all previously calculated eigenvectors to obtain orthogonality in eigenvectors of closely spaced eigenvalues. The results essentially followed those obtain from the Jacobi method except for few eigenpairs where the resolution was sligthly better or worse.

The error norm ϵ_j used to provide error bounds on the eigenvalues of the tridiagonal matrix was also evaluated and a comparison with error norm ${}^e e_j$ was established. It was found that a value of ϵ_j equal to 10^{-4} was sufficient to qualify a given LWYD Ritz pair as an accurate eigensolution by this approach. A sample of these calculations is presented in fig. 5.11 for models considering 25

Fig. 5.10 (a) Symmetric Model

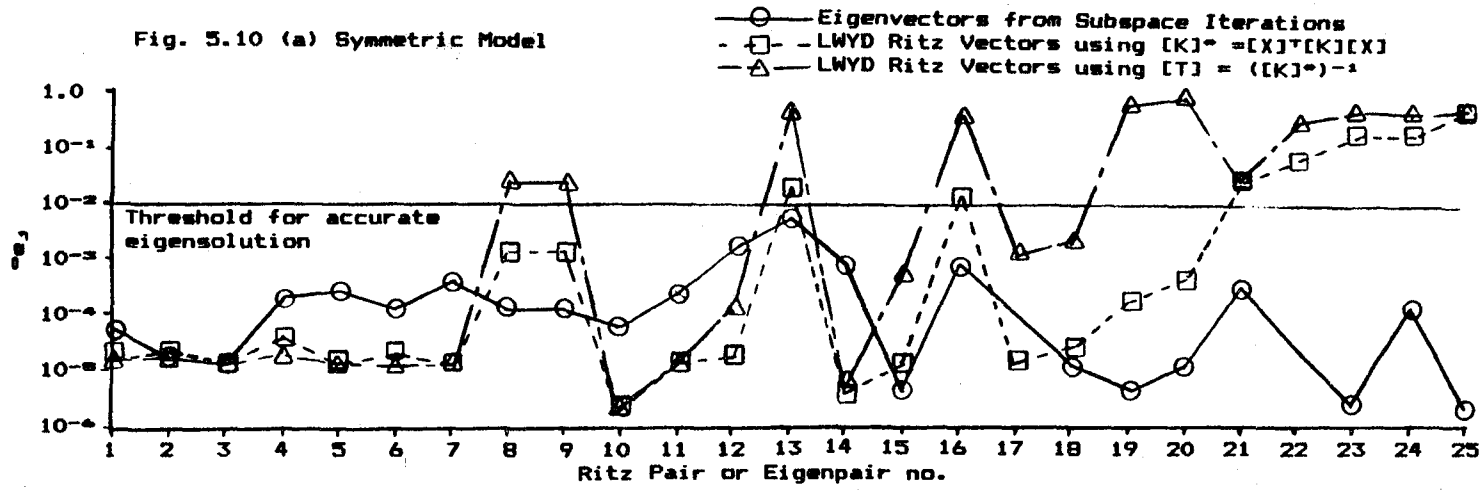

Fig. 5.10 (b) Asymmetric Model

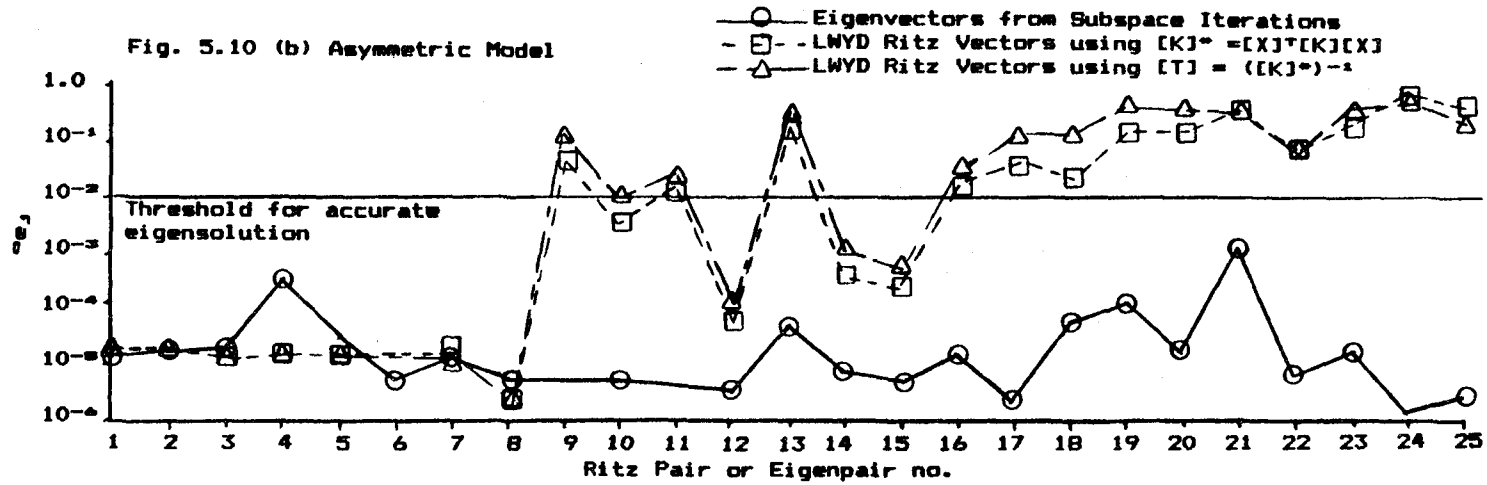

Fig. 5.10 Accuracy of LWYD Ritz Pairs or "Exact" Eigenpairs as the solution of the free vibration problem

$$ {}^{*}e_j = \frac{\|[K]\{{}^{*}X_j\} - \bar{w}^2_j [M]\{{}^{*}X_j\}\|_2}{\|[K]\{{}^{*}X_j\}\|_2} $$

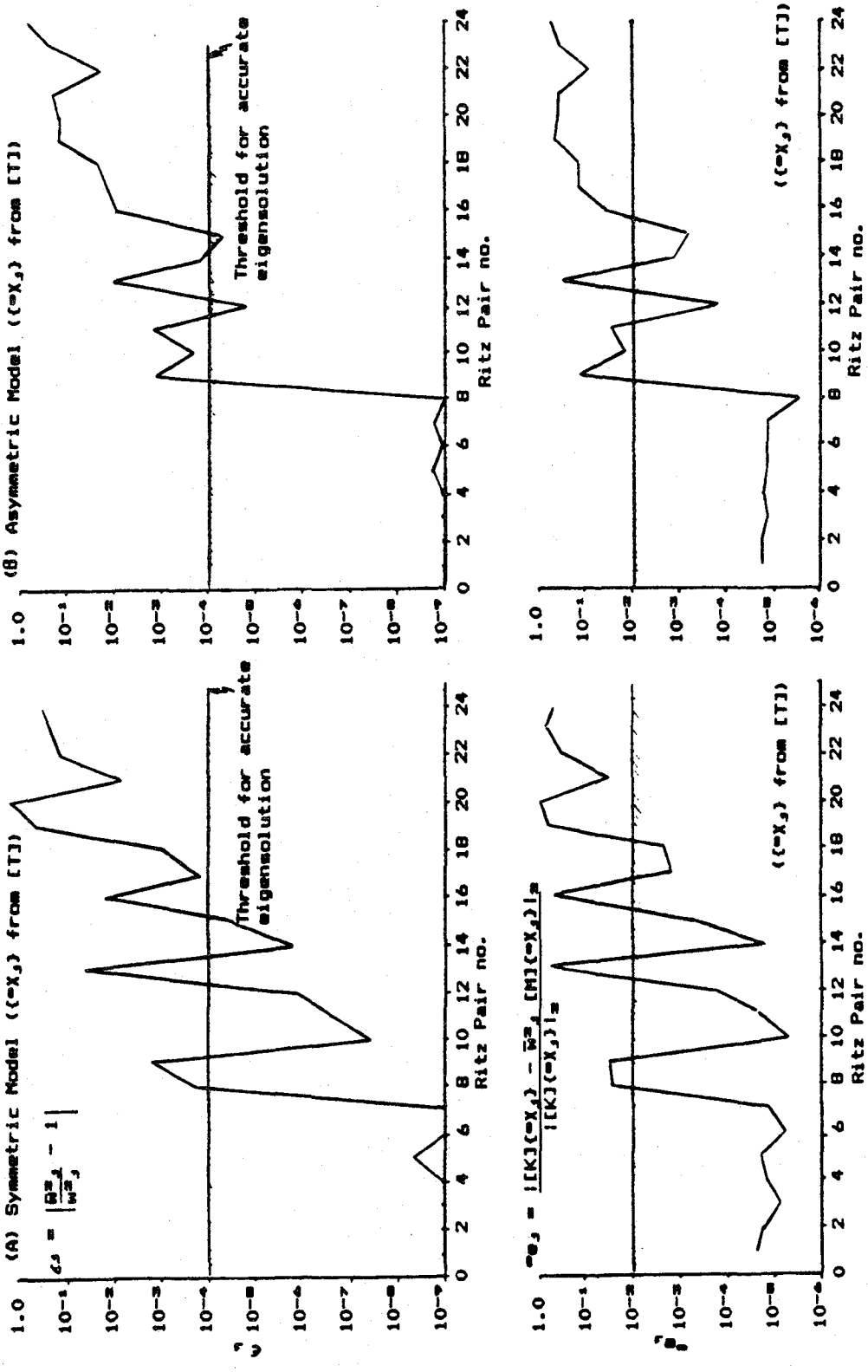

Fig. 5.11 Accuracy of LWYD Ritz pairs ($\bar{w}^2_j$, (*X_j)) as a solution of the Free Vibration Problem using Reduced System in Tridiagonal form , [T]

transformation vectors. It is interesting to note that the pattern exhibited by the error norm ${}^{n}e_j$ and ϵ_j calculated from the same LWYD Ritz pair ($\bar{w}^2_j$, $\{{}^{n}X_j\}$ were very similar, apart from a scaling factor, illustrating that it is sufficient to monitor ϵ_j to evaluate the relative accuracy achieved by a given LWYD Ritz pair obtained from the reduced tridiagonal system.

5.5.3 Convergence of Diplacements and Stresses

The behavior of the structural seismic responses using the exact eigenvectors and LWYD Ritz vectors (obtained from the LWYD Ritz algorithm without static residual and using $[K]^*$ as reduced system) were calculated for each model to study the performance of the WYD Ritz reduction technique when used along with the response spectra method. The dynamic responses were compared in terms of the convergence of nodal displacements and axial stresses. In the elastic regime the total stresses used for the design of the leg and bracing members are largely dominated by the contribution of the axial force components. The contributions of local bending moments to the total stresses are generally small and were not considered for these analyses. It should be noted that the axial forces in a member depend primarily on small differential displacements of the nodes and can thus exhibit different convergence characteristics than the global nodal displacement behavior.

The "X" and "Z" components of translational displacements at node 27 (see fig. 5.1) were selected to illustrate the convergence characteristics of typical nodal displacements. The "Y" displacement component had a behavior very similar to the "X" component and is not reported. Figure 5.12 shows the calculated displacements as a function of the number of vectors retained in the solution. Typical results of axial stress responses obtained from beam no. 7 (see fig. 5.1) are also shown in fig. 5.12.

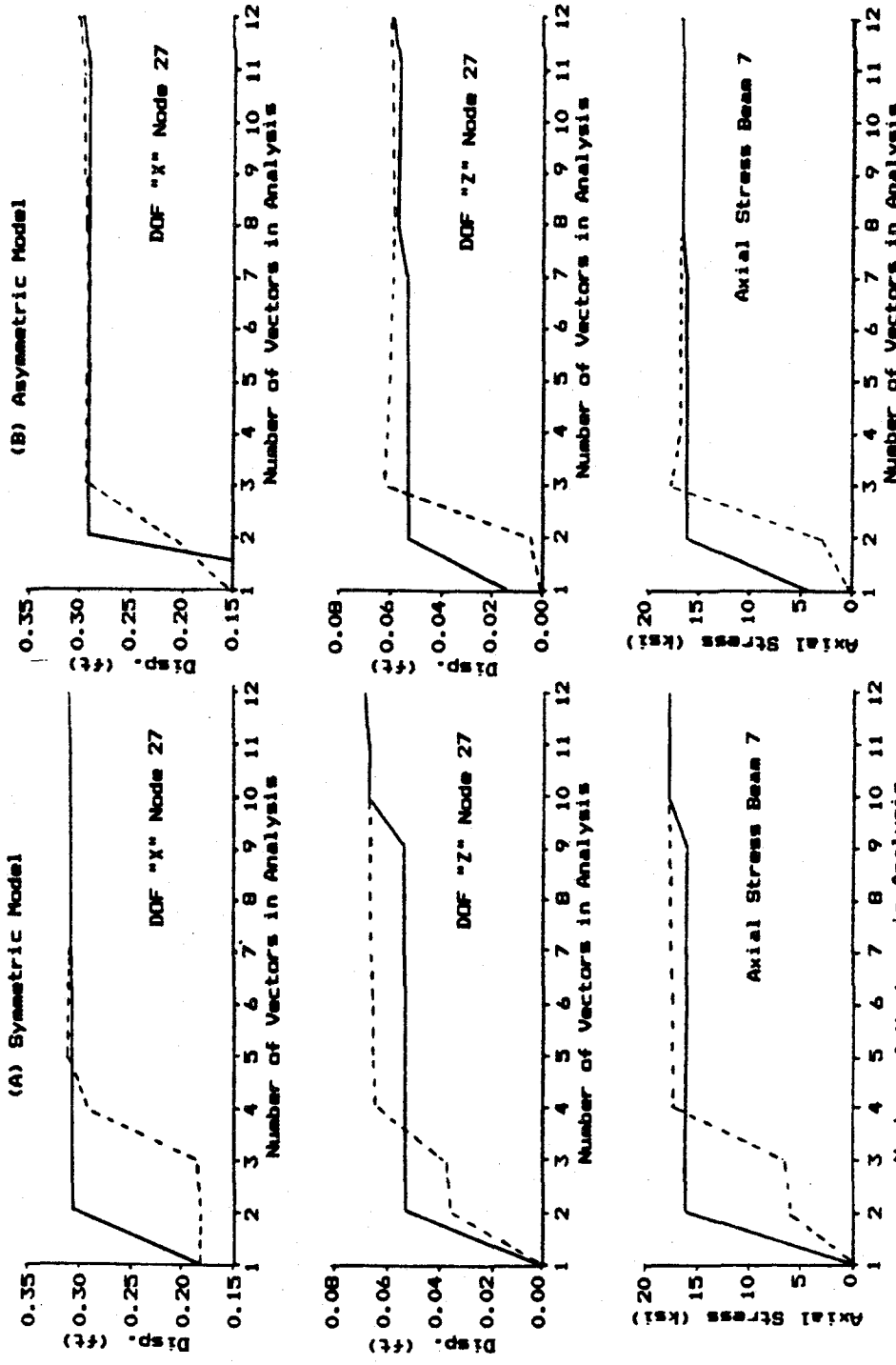

Fig. 5.12 Typical Convergence Characteristics of Spectral Analysis

To obtain a better appreciation of the convergence characteristics of the two solution procedures, "exact" solutions were defined from the responses obtained after an overall loading representation of at least 98%, as defined by e*, has been included in the CQC summations. It was found that for these master solutions the WYD Ritz reduction method and the eigenvector technique yielded results that were on the average, after considering all DOF and all beams, within 1% of each other for both models with the most significant error terms arising from the stress responses. The eigen-solutions and the Ritz solutions will thus virtually be forced to converge to the same results.

Calculations were then performed to study how each solution procedure will reach its corresponding master solution by adding one vector at a time in the analyses. The following error estimates were used for that purpose;

- absolute maximum error of a response quantity:

$$\text{Max. \% error} = \left| \frac{(S_{k,i} - S_{k,25})}{S_{k,25}} \right|_{\text{Max over k}} * 100 \qquad [5.12]$$

- average error of a response quantity:

$$\text{Avge \% error} = \frac{1}{m} \sum_{k=1}^{m} \left| \frac{(S_{k,i} - S_{k,25})}{S_{k,25}} \right| * 100 \qquad [5.13]$$

where $S_{k,i}$ = response quantity S (displacement "X" or "Z" or axial stress) for component k (DOF or beam no.) in mode "i"

m = total number of components in model

The results are shown in fig. 5.13, 5.14 and 5.15 for the asymmetric model and fig. 5.16, 5.17 and 5.18 for the symmetric model.

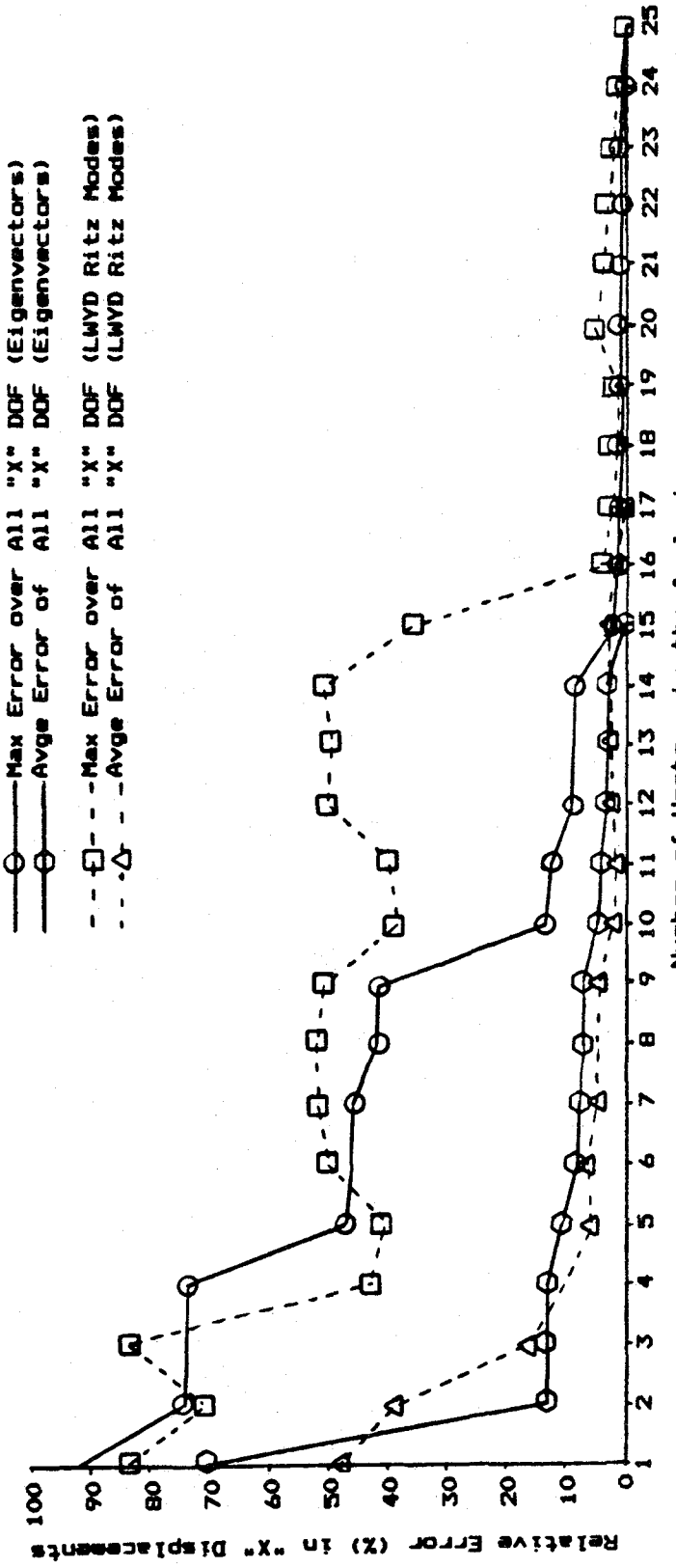

Fig. 5.13 Displacement Convergence in "X" Direction (Asymmetric Model)

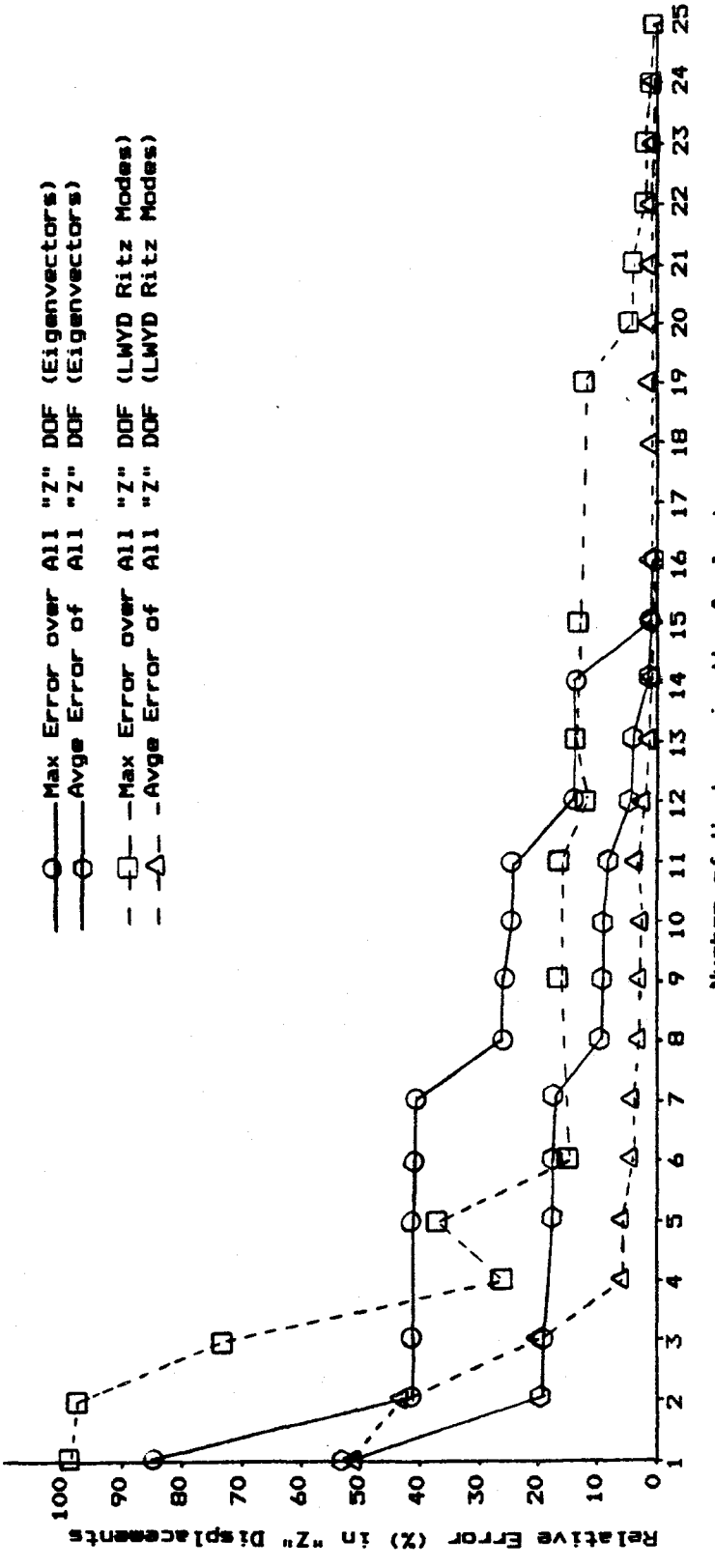

Fig. 5.14 Displacement Convergence in "Z" Direction (Asymmetric Model)

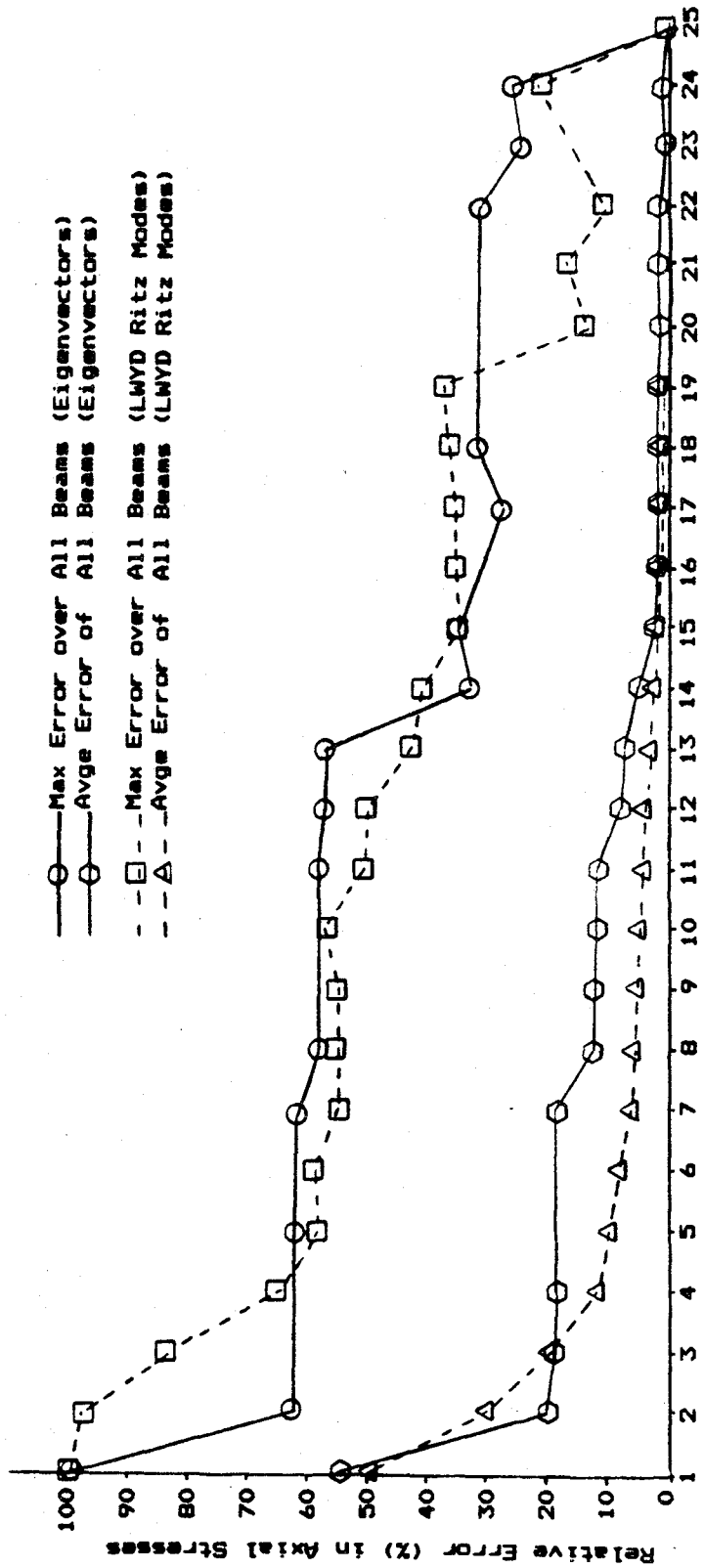

Fig. 5.15 Axial Stress Convergence (Asymmetric Model)

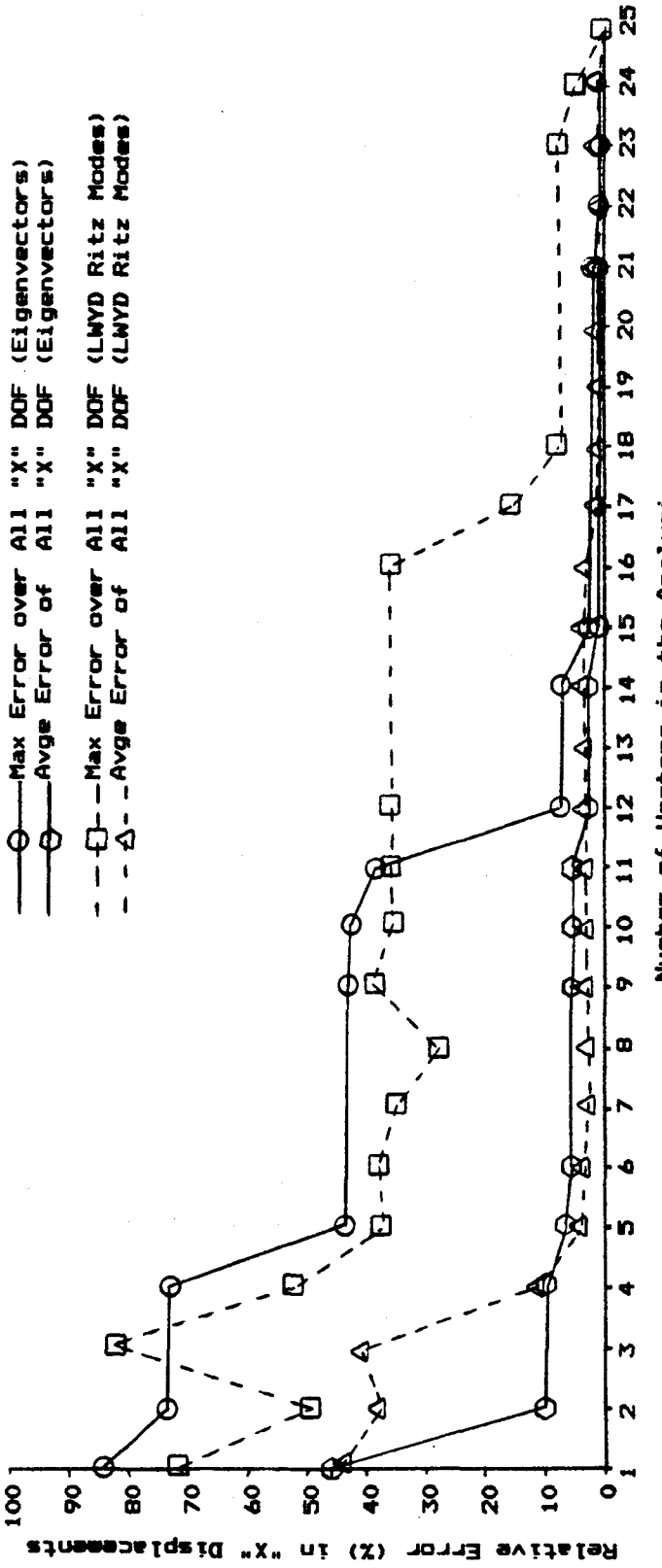

Fig. 5.16 Displacement Convergence in "X" Direction (Symmetric Model)

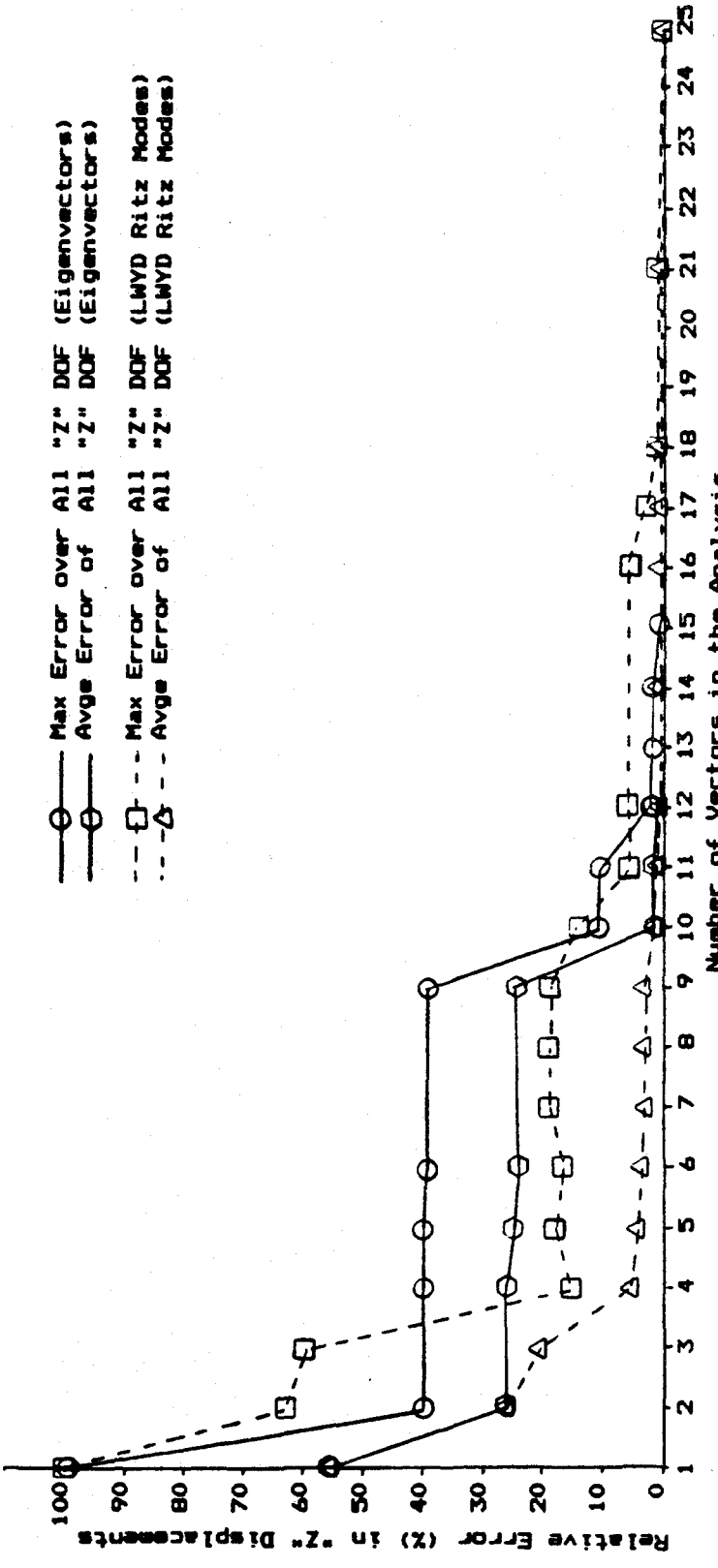

Fig. 5.17 Displacement Convergence in "Z" Direction (Symmetric Model)

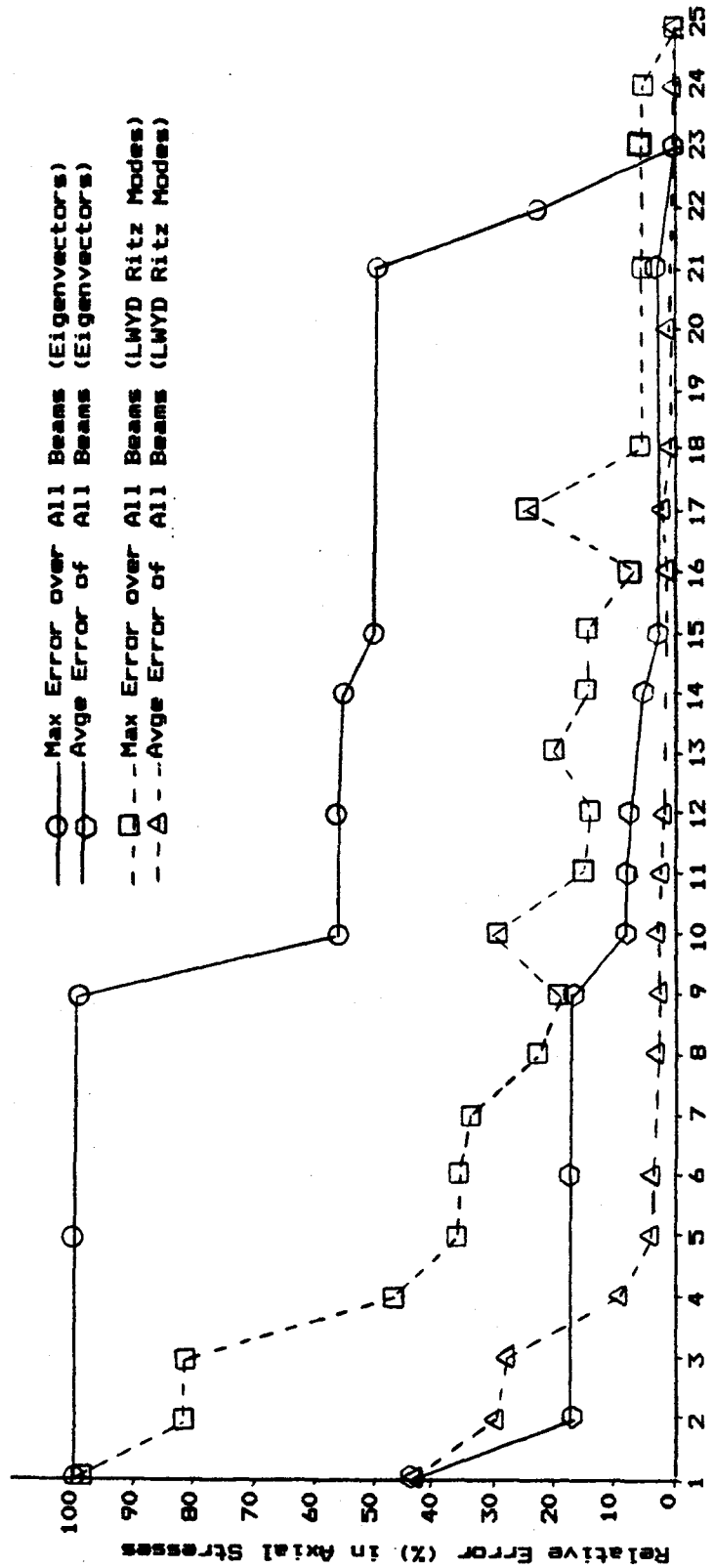

Fig. 5.18 Axial Stress Convergence (Symmetric Model)

To compare the rate of convergence of each solution procedure the following two criteria were used to define a "converged" solution;

- the first criterion requires that the displacements and stresses be in average within 10% of the corresponding master solution,

- the second criterion was more severe and requires that the displacements and stresses be in average within 5% of the corresponding master solution.

The number of vectors required for convergence under these two criteria for each analysis are presented in table 5.7. It was generally found that for either criterion the LWYD Ritz solutions achieved convergence with only half the number of vectors required by the eigensolutions. This was mainly due to the better "Z" loading representation of the first LWYD Ritz vectors compared to the eigenvectors.

To establish a correlation between the error norms measuring the dynamic load representation presented in chapter 3 and the convergence of displacements and stresses the percent error in these response quantities were plotted against the error norm based on the summation of the represented force and the Euclidean norm, e^*; a sample of these results is presented in fig 5.19. The following rule of thumb was then established, a loading representation of at least 90% (95%) in all the directions for either of the error norms is sufficient to obtained an average error of 10% (5%) in the response quantity of interest. To avoid potential instability problems it is also suggested that if there is a sharp increase in loading representation from the addition of a single vector, say greater than 5% when the error norms are already in the 85% range, two or three additional vectors should be added to the basis to smooth out its contribution to the modal summation. The numbers of vectors required for

TABLE 5.7

Number of Vectors for Convergence of the Spectral Analyses

1- "Exact" solutions are defined from the response obtained after an overall loading representation of 98% was achieved

"Exact" Master Solutions (displacements or stresses)

Analysis	# of vectors	% Modal Mass (XYZ)	Error norm e*
LWYD Sym.	25	(97 97 100)	98
Eigen. Sym.	25	(98 98 96)	98
LWYD Asym.	25	(99 99 99)	98
Eigen. Asym.	25	(99 99 96)	98

2- Convergence criterion no.1: Response quantities are in average within 10% of the corresponding Master solution

nc : Number of required vectors for solution convergence

neig : Number of LWYD Ritz vectors out of "nc" that can be considered "exact" eigenvectors from error norms ϵ_j or $^{e}e_j$

Displacements (direction "X" or "Z")

Analysis	nc	neig	% Modal Mass (XYZ)	Error norm e*
LWYD Sym.	4	(1)	(91 92 90)	91
Eigen. Sym.	10		(92 92 96)	94
LWYD Asym.	4	(2)	(91 91 76)	83
Eigen. Asym.	8		(92 92 53)	74

Axial Stresses

Analysis	nc	neig	% Modal Mass (XYZ)	Error norm e*
LWYD Sym.	4	(1)	(91 92 90)	91
Eigen. Sym.	10		(92 92 96)	94
LWYD Asym.	5	(3)	(92 92 89)	91
Eigen. Asym.	12		(94 94 81)	84

TABLE 5.7 (CONTINUED)

Number of Vectors for Convergence of the Spectral Analyses

3- Convergence criterion no.2: Response quantities are in average within 5% of the corresponding master solution

nc : Number of required vectors for solution convergence

neig : Number of LWYD Ritz vectors out of "nc" that can be considered "exact" eigenvectors from error norms ϵ_j or $^{*}e_j$

Displacements (direction "X" or "Z")

Analysis		nc	neig	% Modal Mass (XYZ)	Error norm e*
LWYD	Sym.	5	(2)	(94 94 93)	94
Eigen.	Sym.	10		(92 92 96)	94
LWYD	Asym.	8	(3)	(95 94 89)	91
Eigen.	Asym.	12		(94 94 81)	84

Axial Stresses

Analysis		nc	neig	% Modal Mass (XYZ)	Error norm e*
LWYD	Sym.	5	(2)	(94 94 93)	94
Eigen.	sym.	14		(96 96 96)	96
LWYD	Asym.	8	(3)	(94 94 89)	91
Eigen.	Asym.	14		(94 96 91)	91

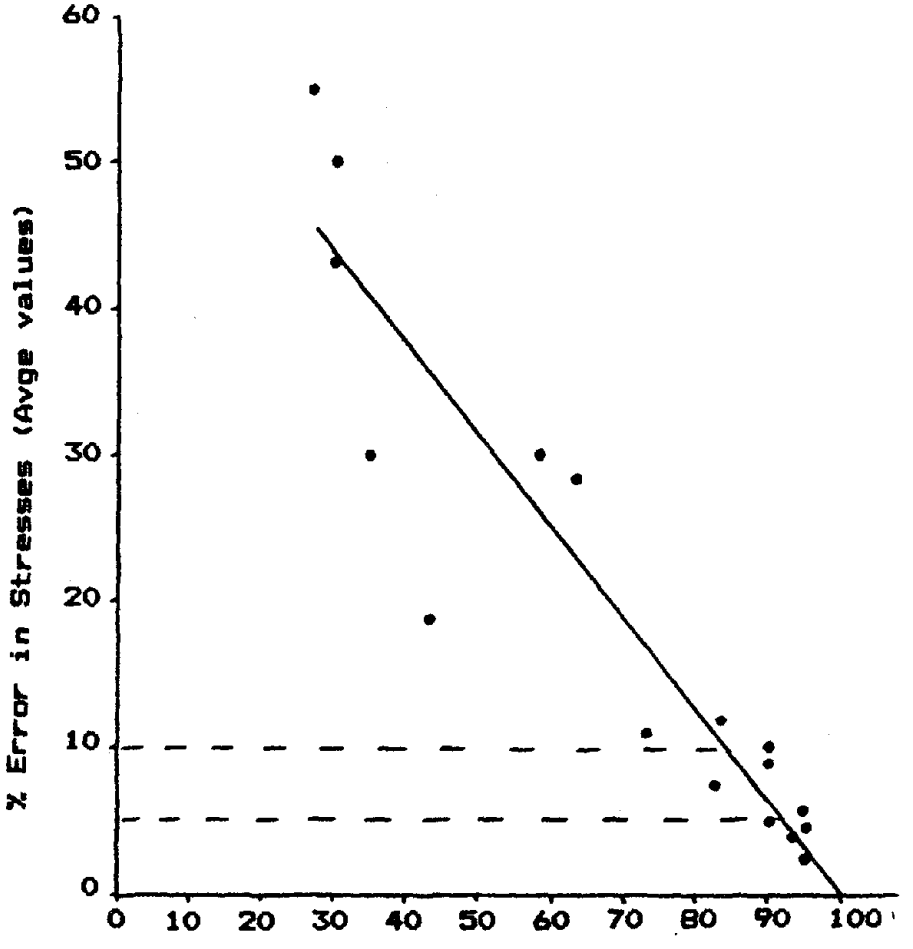

Fig. 5.19 Correlation Between Loading Error Norm and Error Stress Response

satisfactory solutions convergence were compared to the numbers of vectors required to achieved these specific values of loading representation. The results are presented in table 5.8. The rule of thumb proved to be satisfactory in all cases.

5.5.4 Conclusions from Computer Results Analysis

This section presents a summary of the main conclusions drawn from the analysis of the computer results of the two models used to study the solution characteristics of the LWYD Ritz solutions and the eigensolutions. The main conclusions were that,

- the generation of WYD Ritz vectors was approximately 7 to 9 times more efficient than shifted subspace iteration to form a vector basis to be used for the transformation of the dynamic equilibrium equations to a fixed number of generalized coordinates,

- the WYD Ritz reduction technique can be applied sucessfully to seismic analysis using the three dimensional earthquake response spectra method; the most reliable solution strategy was obtained from transformation vectors obtained from the LWYD Ritz algorithm using no static residual,

- LWYD Ritz solutions spanned a longer period range than eigensolutions for the same number of generalized coordinates retained in the analysis,

- the spatial error estimates based on the summation of the represented loading (corresponding to the effective modal mass for these examples) and the Euclidean norm of the error force vector provided satisfactory results to monitor loading representation as a function of the number of generalized coordinates retained in the analysis. For a

TABLE 5.8

Number of Vectors for Displacement and Stress Convergence
Vs
Number of Vectors for Good Loading Representation

nc : number of required vectors for solution convergence

neig : number of LWYD Ritz vectors out of "nc" that can be considered as "exact" eigenvectors from error norm $^{e}e_j$

1- Convergence criterion no.1: Response quantities (displacements or stresses) are in average within 10% of the corresponding master solution

n 90 e_j : number of vectors required to obtain 90% of the total load acting in direction "X","Y" or "Z" based on the error norm summing the represented forces (90% Modal mass for these examples)

n 90 e^*_j: number of vectors required to obtain 90% of the total load acting in directions "X", "Y" or "Z" based on the Euclidean norm of the error force vector (e^*_x, e^*_y or e^*_z)

n 90 e^* : number of vectors required to obtain an overall loading representation of 90% based on the single Euclidean error norm index e^*

Analysis		nc	neig	n 90 e_j	n 90 e^*_j	n 90 e^*
LWYD	Sym.	4	(1)	4	5	4
Eigen.	Sym.	10		10	10	10
LWYD	Asym.	5	(3)	10	13	5
Eigen.	Asym.	12		14	17	14

2- Convergence criterion no.2: Response quantities (displacements or stresses) are in average within 5% of the corresponding master solution

n 95 e_j : same definition as in (1) except 95% loading representation must be achieved

n 95 e^*_j: same definition as in (1) except 95% loading representation must be achieved

n 95 e^* : same definition as in (1) except 95% loading representation must be achieved

Analysis		nc	neig	n 95 e_j	n 95 e^*_j	n 95 e^*
LWYD	Sym.	5	(2)	10	7	7
Eigen.	Sym.	14		15	15	14
LWYD	Asym.	8	(3)	15	20	14
Eigen.	Asym.	14		18	23	22

given number of vectors the overall loading representation obtained from LWYD Ritz bases was almost always superior to the representation of corresponding eigenbases,

- better loading representation of the LWYD Ritz bases was primarily due to early appearance of relatively stiff vertical axial deformation modes. The better vertical ("Z") representation of the LWYD Ritz bases was due to the use of the spatial distribution of the dynamic load to initiate the vector calculation sequence forcing significant deformations in the "Z" direction in the first vectors,

- reduced LWYD Ritz systems considering more than 5 generalized coordinates have their first few (2 or 3) vectors close to exact eigenvectors. This number keeps increasing as the number of retained Ritz coordinates becomes larger,

- satisfactory convergence characteristics were obtained by considering LWYD Ritz systems for which the same number of generalized coordinates was used for coordinate transformation and CQC summation. It is thus unnecessary, for the type of analysis under study, to artificially increase the number of Ritz coordinates to obtain closer approximation to a larger number of exact eigenvectors,

- LWYD Ritz solutions proved to be satisfactory for systems having closely spaced modes (symmetric),

- for structural systems that do not have a simple eigenspectrum, reduced LWYD Ritz system working from the formal transformation $[X]^T[K][X] = [K]^*$ are able to provide a higher resolution of a given LWYD Ritz pair than if the tridiagonal matrix $[T_r]$ is used directly,

- in three dimensional earthquake analysis using the

response spectra method, LWYD Ritz solutions requires fewer vectors than exact eigensolutions to obtain displacements and stress convergence (approximately one half for these examples),

- for earthquake loading, a representation of 90% (or 95%) expressed by either of the error norms was able to ensure that the response quantities were in average within 10% (or 5%) of their "exact" values. To avoid potential instability problem no single vector contribution to the loading representation in a LWYD Ritz solution should be greater than 5% when the error norms are in the 85% range or above. If this is the case two or three vectors should be added to the LWYD solution to reach convergence,

- a cut off criterion in the vector generation process using the error norms to achieve 90% to 95% loading representation, under the above restriction, should provide an adequate number of vectors to obtain satisfactory convergence of LWYD Ritz solutions.

It can thus be concluded that for seismic analyses using the response spectra method, LWYD Ritz solutions have definite avantages over exact eigensolutions in terms of a much reduced numerical effort to generate the transformation vectors and improved convergence rate of the resulting bases in terms of the response quantities of interest. The WYD Ritz reduction method thus provides a suitable numerical technique to allow inexpensive reanalysis to evaluate design modifications by keeping computer costs down and decreasing the time for a typical calculation cycle.

CHAPTER 6

Generalization of the WYD Ritz Reduction Method to Arbitrary Loadings

Commonly time varying loadings such as wind, waves, and earthquakes which act on engineering structures are specified in the form of discrete time series. One classification of dynamic response problems depends on how the elements of the force vector $\{F(s,t)\}$ vary with time. The following categories can be recognized:

- zero or no loading (free vibration)
- harmonic
- periodic
- aperiodic or transient
- random

In its present form, the WYD Ritz reduction method is restricted to dynamic loads which can be defined as the product of one spatial load vector and one time function according to equation [1.10]. An important case of this category is the earthquake problem. The components of the load vector due to an earthquake motion acting along one of the structural axes have all the same time variation given by the prescribed base accelerogram.

The most general form of dynamic loading can be expressed as :

$$\{F(s,t)\} = \sum_{i=1}^{k} \{f_i(s)\}\, g_i(t) \qquad [6.1]$$

where $\{f_i(s)\}$ represents the ith spatial distribution pattern and $g_i(t)$ the ith time variation function. It is obvious that the method of Ritz vector generation can be extended to this type of loading by generating several sets of vectors starting with different load patterns $\{f_i(s)\}$. However, this

approach will be relatively inefficient and a better method will be to extend the load dependent Ritz algorithms to a recurrence sequence which uses blocks of vectors corresponding initially to the multiload patterns.

6.1 Block Ritz Algorithms

6.1.1 Description of Block Ritz Algorithms

A block version of the Ritz algorithm is presented in fig. 6.1 as a direct extension of the original WYD algorithm given in fig. 1.1. It is also possible to develop a block LWYD Ritz formulation as shown in fig. 6.2 and both algorithms can be implemented to take advantage of the tridiagonal form of the reduced system as shown in fig. 6.3 and 6.4, in such a case the resulting reduced matrix [T] becomes block tridiagonal.

The block Ritz algorithms replace each Ritz vectors, $\{X_i\}$, by an n x k orthonormal matrix $[X]_i$. The orthogonalization of the current block $[\bar{X}]_i$ is done in two steps. First, block $[\bar{X}]_i$ is [M]-orthogonalized against previous blocks $[X]_j$ by using a process similar to the Gram-Schmidt method. Second, the resulting purified vector block $[\tilde{X}]_i$ is [M]-orthonormalized by a suitable numerical technique.

The block Gram-Schmidt process will be subjected to the same instability problems that were reported for the case of the single vector method. A selective reorthogonalization procedure should thus be implemented. The orthogonality check corresponding to equation [4.7] should ensure that,

$$\| ([X]^T_j \, [M] \, [\tilde{X}]^{(m+1)}_i \|_\infty < TOL \quad \text{for } 1<j<i-1 \qquad [6.2]$$

where the infinite norm of a matrix [A] of order n is defined as,

Fig. 6.1 Block WYD Ritz Algorithm
(extension of original formulation)

1. Given Mass, Stiffness Matrices $[M]$, $[K]$, and Linearly Independent Multispatial Load vectors Distribution $[F]$

$[M]$ $n \times n$
$[K]$ $n \times n$
$[F]$ $n \times k$

where n is the number of equations in the system
k is the number of vectors in a block

2. Triangularized Stiffness Matrix:

$$[K] = [L]^T [D] [L] \qquad n \times n \text{ system}$$

3. Form First Block of Vectors $[X]_1$

(a) solve for block $[\bar{X}]_1$

$$[K] [\bar{X}]_1 = [F]$$

(b) $[M]$-orthonormalize $[\bar{X}]_1$

$$[V] = [\bar{X}]^T_1 [M] [\bar{X}]_1$$
$$[V] = [N] [\Lambda] [N]^T \qquad \text{with } [N]^T [N] = [I]$$
$$[X]_1 = [\bar{X}]_1 [N] [\Lambda]^{-1/2}$$

4. Solve for Additional Block of Vectors: i=2,...,p

(a) solve for new block $[\bar{X}]_i$

$$[K] [\bar{X}]_i = [M] [X]_{i-1}$$

(b) $[M]$-orthogonalize block $[\bar{X}]_i$ against previous blocks

$$[\tilde{X}]_i = [\bar{X}]_i - \sum_{j=1}^{i-1} [X]_j ([X]^T_j [M] [\bar{X}]_i)$$

(c) $[M]$-orthonormalize block $[\tilde{X}]_i$

$$[V]_i = [\tilde{X}]^T_i [M] [\tilde{X}]_i$$
$$[V]_i = [N] [\Lambda] [N]^T \qquad \text{with } [N]^T [N] = [I]$$
$$[X]_i = [\tilde{X}]_i [N] [\Lambda]^{-1/2}$$

5. Orthogonalization of Ritz Vectors with Respect to Stiffness Matrix (optional):

(a) Solve the r x r eigenvalue problem (r = p * k),

$$[K]^* [Z] = [M]^* [Z] [\bar{w}^2]$$

where
$$[K]^* = [X]^T [K] [X]$$
$$[M]^* = [X]^T [M] [X] = [I]$$
$\bar{w}$ = approximate frequencies

(b) Compute final orthogonal Ritz vectors

$$[^*X] = [X] [Z]$$

Fig. 6.2 Block LWYD Ritz Algorithm

1. Given Mass, Stiffness Matrices [M], [K], and Linearly Independent Multispatial Load Vector Distribution [F]

$[M]$ $n \times n$
$[K]$ $n \times n$
$[F]$ $n \times k$

where n is the number of equations in the system
k is the number of vectors in a block

2. Triangularized Stiffness Matrix:

$[K] = [L]^T [D] [L]$ n x n system

3. Solve for Initial Static Block $[\bar{U}]_o$

(a) solve for block $[\bar{U}]_o$

$[K] [\bar{U}]_o = [F]$

(b) [M]-orthonormalize $[\bar{U}]_o$

$[V] = [\bar{U}]^T_o [M] [\bar{U}]^T_o$
$[V] = [N] [\Lambda] [N]^T$ with $[N]^T [N] = [I]$
$[U]_o = [\bar{U}]_o [N] [\Lambda]^{-1/2}$

4. Solve for First Block of Vectors

(a) solve for block $[X^*]_1$

$[K] [X^*]_1 = [M] [U]_o$

(b) [M]-orthonormalize $[X^*]_1$

$[V] = [X^*]^T_1 [M] [X^*]_1$
$[V] = [N] [\Lambda] [N]^T$ with $[N]^T [N] = [I]$
$[X]_1 = [X^*]_1 [N] [\Lambda]^{-1/2}$

(c) Update Static Block $[U]_o$

$[C_u]_1 = [X]^T_1 [M] [U]_o$
$[U]_1 = [U]_o - [X]_1 [C_u]_1$

5. Solve for Additional Blocks of vectors i=2,...,p-1

(a) solve for new block $[X^*]_i$

$[K] [X^*]_i = [M] [U]_{i-1}$

(b) [M]-orthogonalize block $[X^*]_i$ against previous blocks

$$[X^{**}]_i = [X^*]_i - \sum_{j=1}^{i-1} [X]_j \, ([X]_j^T \, [M] \, [X^*]_i)$$

(c) [M]-orthonormalize block $[X^{**}]_i$

$$[V]_i = [X^{**}]_i^T \, [M] \, [X^{**}]_i$$
$$[V]_i = [N] \, [\Lambda] \, [N]^T \qquad \text{with } [N]^T \, [N] = [I]$$
$$[X]_i = [X^{**}]_i \, [N] \, [\Lambda]^{-1/2}$$

(d) Update Static Block $[U]_{i-1}$

$$[C_u]_i = [X]_i^T \, [M] \, [U]_{i-1}$$
$$[U]_i = [U]_{i-1} - [X]_i \, [C_u]_i$$

6. Add Block Residual $[U]_{p-1}$ as Static Correction $[X]_p$ (optional)

(a) [M] orthogonalize $[U]_{p-1}$ (by precaution)

$$[\tilde{U}]_{p-1} = [U]_{p-1} - \sum_{j=1}^{i-1} [X]_j \, ([X]_j^T \, [M] \, [U]_{p-1})$$

(b) [M]-orthonormalize $[\tilde{U}]_{p-1}$

$$[V]_p = [\tilde{U}]_{p-1}^T \, [M] \, [\tilde{U}]_{p-1}$$
$$[V]_p = [N]^T \, [\Lambda] \, [N] \qquad \text{with } [N]^T \, [N] = [I]$$
$$[X]_p = [\tilde{U}]_{p-1} \, [N] \, [\Lambda]^{-1/2}$$

7. Orthogonalization of Ritz Vectors with Respect to Stiffness Matrix (optional):

(a) Solve the r x r eigenvalue problem (r = p * k)

$$[K]^* \, [Z] = [M]^* \, [Z] \, [\bar{w}^2]$$

where
$$[K]^* = [X]^T \, [K] \, [X]$$
$$[M]^* = [X]^T \, [M] \, [X] = [I]$$
$\bar{w}$ = approximate frequencies

(b) Compute final orthogonal Ritz vectors

$$[^oX] = [X] \, [Z]$$

Fig. 6.3 Tridiagonal Block WYD Ritz Algorithm
(extension of original formulation)

1. Given Mass, Stiffness Matrices [M], [K], and Linearly Independent Multispatial Load vectors Distribution [F]

$[M]$ $n \times n$
$[K]$ $n \times n$
$[F]$ $n \times k$

where n is the number of equations in the system
k is the number of vectors in a block

2. Triangularized Stiffness Matrix:

$$[K] = [L]^T [D] [L] \qquad n \times n \text{ system}$$

3. Form First Block of Vectors $[\bar{X}]_1$

(a) solve for block $[X]_1$

$$[K] [\bar{X}]_1 = [F]$$

(b) [M]-orthonormalize $[\bar{X}]_1$

$$[V] = [\bar{X}]^T_1 [M] [\bar{X}]_1$$
$$[V] = [N] [\Lambda] [N]^T \qquad \text{with } [N]^T [N] = [I]$$
$$[X]_1 = [\bar{X}]_1 [N] [\Lambda]^{-1/2}$$

4. Solve for Additional Block of Vectors: i=2,...,p

(a) solve for new block $[\bar{X}]_i$

$$[K] [\bar{X}]_i = [M] [X]_{i-1}$$

(b) form diagonal block $[A]_{i-1}$ of [T]

$$[A]_{i-1} = [X]^T_{i-1} [M] [\bar{X}]_i$$

(c) [M]-orthogonalize block $[\bar{X}]_i$ against previous blocks

$$[\tilde{X}]_i = [\bar{X}]_i - \sum_{j=1}^{i-1} [X]_j ([X]^T_j [M] [\bar{X}]_i)$$

(d) [M]-orthonormalize block $[\tilde{X}]_i$

$$[V]_i = [\tilde{X}]^T_i [M] [\tilde{X}]_i$$
$$[V]_i = [N] [\Lambda] [N]^T \qquad \text{with } [N]^T [N] = [I]$$
$$[X]_i = [\tilde{X}]_i [N] [\Lambda]^{-1/2}$$

(e) form off-diagonal block $[B]_i$ of [T]

$$[B]_i = [N] [\Lambda]^{1/2}$$

5. Orthogonalization of Ritz Vectors with Respect to Stiffness Matrix (optional):

(a) construct symmetric block tridiagonal matrix [T] of order r x r (r = p * k)

$$[T] = \begin{bmatrix} [A]_1 & [B]_2 & [O] & [O] & \cdots & [O] \\ [B]_2 & [A]_2 & [B]_3 & [O] & \cdots & [O] \\ [O] & [B]_3 & [A]_3 & [B]_4 & [O] & [O] \\ \vdots & \vdots & \vdots & & & \vdots \\ [O] & \vdots & & [B]_{p-1} & [A]_{p-1} & [B]_p \\ [O] & \vdots & \vdots & & [B]_p & [A]_p \end{bmatrix}$$

(b) calculate eigenvalues and eigenvectors of [T]

$$[T]\,[Z] = [Z]\,[\lambda]$$

(c) calculate approximate eigenvalues of original system

$$[\bar{w}^2] = [1/\lambda]$$

(d) Compute final orthogonal Ritz vectors

$$[^{o}X] = [X]\,[Z]$$

Fig. 6.4 Tridiagonal Block LWYD Ritz Algorithm

1. Given Mass, Stiffness Matrices [M], [K], and Linearly Independent Multispatial Load Vector Distribution [F]

$[M]$ n x n
$[K]$ n x n
$[F]$ n x k

where n is the number of equations in the system
k is the number of vectors in a block

2. Triangularized Stiffness Matrix:

$$[K] = [L]^T [D] [L] \qquad n \times n \text{ system}$$

3. Solve for Initial Static Block $[U]_o$

(a) solve for block $[U]_o$

$$[K] [U]_o = [F]$$

(b) [M]-orthonormalize $[U]_o$

$$[V] = [U]^T_o [M] [U]_o$$
$$[V] = [N] [\Lambda] [N]^T \qquad \text{with } [N]^T [N] = [I]$$
$$[U]_o = [U]_o [N] [\Lambda]^{-1/2}$$

4. Solve for First Block of Vectors

(a) solve for block $[X^*]_1$

$$[K] [X^*]_1 = [M] [U]_o$$

(b) [M]-orthonormalize $[X^*]_1$

$$[V] = [X^*]^T_1 [M] [X^*]_1$$
$$[V] = [N] [\Lambda] [N]^T \qquad \text{with } [N]^T [N] = [I]$$
$$[X]_1 = [X^*]_1 [N] [\Lambda]^{-1/2}$$

(c) Update Static Block $[U]_o$

$$[C_u]_1 = [X]^T_1 [M] [U]_o$$
$$[U]_1 = [U]_o - [X]_1 [C_u]_1$$

5. Solve for Additional Blocks of vectors i=2,...,p-1

(a) solve for new block $[X^*]_i$

$$[K] [X^*]_i = [M] [U]_{i-1}$$

(b) form diagonal block of [T]

$$[A]_{i-1} = -([X]^T_{i-1} [M] ([X^*]_i - [X^*]_{i-1}) [C_u]^{-1}_{i-1})$$

(c) [M]-orthogonalize block $[X^*]_i$ against previous blocks

$$[X^{**}]_i = [X^*]_i - \sum_{j=1}^{i-1} [X]_j \, ([X]^T_j \, [M] \, [X^*]_i)$$

(d) [M]-orthonormalize block $[X^{**}]_i$

$$[\bar{X}^{**}]_i = -[X^{**}]_i \, [C_u]^{-1}_{i-1}$$
$$[V]_i = [\bar{X}^{**}]^T_i \, [M] \, [\bar{X}^{**}]_i$$
$$[V]_i = [N] \, [\Lambda] \, [N]^T \qquad \text{with } [N]^T \, [N] = [I]$$
$$[X]_i = [\bar{X}^{**}]_i \, [N] \, [\Lambda]^{-1/2}$$

(e) calculate off-diagonal block

$$[B]_i = [N] \, [\Lambda]^{1/2} \, [C_u]^{-1}_{i-1}$$

(f) Update Static Block $[U]_{i-1}$

$$[C_u]_i = [X]^T_i \, [M] \, [U]_{i-1}$$
$$[U]_i = [U]_{i-1} - [X]_i \, [C_u]_i$$

(f) calculate off-diagonal block

$$[B]_i = [N] \, [\Lambda]^{1/2} \, [C_u]^{-1}_{i-1}$$

6. Add Block Residual $[U]_{p-1}$ as Static Correction $[X]_p$ (optional)

(a) [M] orthogonalize $[U]_{p-1}$ (by precaution)

$$[\tilde{U}]_{p-1} = [U]_{p-1} - \sum_{j=1}^{i-1} [X]_j \, ([X]^T_j \, [M] \, [U]_{p-1})$$

(b) [M]-orthonormalize $[\tilde{U}]_{p-1}$

$$[V]_p = [\tilde{U}]^T_{p-1} \, [M] \, [\tilde{U}]_{p-1}$$
$$[V]_p = [N]^T \, [\Lambda] \, [N] \qquad \text{with } [N]^T \, [N] = [I]$$
$$[X]_p = [\tilde{U}]_{p-1} \, [N] \, [\Lambda]^{-1/2}$$

(c) complete diagonal of [T]

$$[K] \, [X]_{p+1} = [M] \, [X]_p \qquad \text{solve for } [X]_{p+1}$$
$$[A]_p = [X]^T_p \, [M] \, [X]_{p+1}$$

(d) complete off-diagonal of [T]

$$[B]_p = [X]^T_{p-1} \, [M] \, [X]_{p+1}$$

7. Orthogonalization of Ritz Vectors with Respect to Stiffness Matrix (optional):

(a) construct symmetric block tridiagonal matrix [T] of order r x r (r = p * k)

$$[T] = \begin{bmatrix} [A]_1 & [B]_2 & [O] & [O] & \cdots & \cdots & [O] \\ [B]_2 & [A]_2 & [B]_3 & [O] & \cdots & \cdots & [O] \\ [O] & [B]_3 & [A]_3 & [B]_4 & [O] & \cdots & [O] \\ \vdots & \vdots & \vdots & & & & \vdots \\ [O] & \vdots & & [B]_{p-1} & [A]_{p-1} & [B]_p & \\ [O] & \vdots & \vdots & & [B]_p & [A]_p & \end{bmatrix}$$

(b) calculate eigenvalues and eigenvectors of [T]

$$[T]\,[Z] = [Z]\,[\lambda]$$

(c) calculate approximate eigenvalues of original system

$$[\bar{w}^2] = [1/\lambda]$$

(d) Compute final orthogonal Ritz vectors

$$[^{o}X] = [X]\,[Z]$$

$$\|[A]\|_\infty = \max_i \sum_{j=1}^{n} |a_{i,j}| \qquad [6.3]$$

All other observations presented in chapter 4 for the single vector iteration method are still valid for the block method and will not be repeated here.

The selection of the numerical method to [M]-orthonormalize the purified block $[\tilde{X}]_i$ gives room for some freedom of choice. In order to be able to implement the method by taking advantage of the block tridiagonal form of the reduced system the off-diagonal matrix $[B]_i$ should satisfy

$$[B]_i\ [B]^T_i = [\tilde{X}]^T_i\ [M]\ [\tilde{X}]_i = [V]_i \qquad [6.4]$$

The formulation for $[B]_i$ is therefore directly related to the method used to [M]-orthonormalize the individual vectors of the purified block $[\tilde{X}]_i$. The following alternatives can be used to satisfy equation [6.4];

- reverse Cholesky factorization of $[V]_i$ such that $[B]_i$ is an upper triangular matrix, the [M]-orthonormal vectors $[X]_i$ will then be given by

$$[X]_i = [\tilde{X}]_i\ [B]^{-T}_i \qquad [6.5]$$

- QR factorization of $[\tilde{X}]_i$ such that,

$$[\tilde{X}]_i = [X]_i\ [B]^T_i \qquad [6.6]$$

with

$$[X]^T_i\ [M]\ [X]_i = [I] \qquad [6.7]$$

where $[B]^T_i$ is a lower triangular matrix. The [M]-orthonormal vectors $[X]_i$ will be given by equation [6.5],

- spectral decomposition of $[V]_i$ such that,

$$[V]_i = [N]\ [\Lambda]\ [N]^T \qquad [6.8]$$

with

$$[N]^T\ [N] = [I] \qquad [6.9]$$

the [M]-orthonormal vectors $[X]_i$ are then obtained from

$$[X]_i = [X]_i\ [N]\ [\Lambda]^{-1/2} \qquad [6.10]$$

and the $[B]_i$ matrix is given by

$$[B]_i = [N]\ [\Lambda]^{1/2} \qquad [6.11]$$

Each method has some advantages and inconveniences. If the reverse Cholesky factorization or the QR factorization are used, the blocks $[B]^T_i$ should be included as the upper diagonal elements of the [T] matrix. On account of the triangular form of $[B]_i$, [T] will be of band form with semi-bandwidth of k+1 rather than block tridiagonal. However, these methods require a special factorization subroutine that should overcome the instability of the Gram-Schmidt method. A simpler and more accurate approach as suggested in the block Ritz algorithms presented in fig. 6.1 to 6.4 is to use the spectral decomposition of the matrix $[V]_i$. The eigensolution of the problem

$$[V]\ [N] = [N]\ [\Lambda] \qquad [6.12]$$

can be obtained from the same subroutine that is needed to solve for the eigenvalues and eigenvectors of the reduced system. A minor disadvantage of this procedure is that if the implementation is carried out taking advantage of the block tridiagonal form of the reduced system then the topology of [T] will remain block tridiagonal with a semi-bandwidth of 2k.

6.1.2 Spatial Error Estimates for Multiload Representation

The spatial error norms developed for a single loading vector representation can easily be extended to a multiload representation. Block Ritz vectors should be generated until all the specified loading distributions are adequately represented by the basis. As soon as a new block

of vectors $[X]_i$ has been calculated the error norms should be evaluated considering successively each loading distribution and each vector of the new block. For earthquake analysis the error norm based on the summation of the represented forces (e_x, e_y, e_z) or the error norm based on the Euclidean norm (e^*_x, e^*_y, e^*_z) of the error force vector can be used. For more general form of loadings, it is recommended that the Euclidean error norm be used due to its superior convergence characteristics for arbitrary loadings.

6.1.3 Relationship Between Block Ritz Solutions and Exact Eigensolutions

If the block Ritz algorithm is implemented without taking advantage of the block tridiagonal form of the reduced system the error norm $^{e}e_j$ described by equation [3.46] can be used directly to get an appreciation for the accuracy in which the block Ritz vectors satisfy the free vibration problem $[K][\Phi] = [M][\Phi][\omega^2]$.

If the implementation is done by taking advantage of the block tridiagonal form of the reduced system then an error bound to evaluate the relationship between the eigensolution of the reduced system and the original system can easily be established as an extension of equation [3.47] developed for single vector algorithm. The block version of the error bound will be given by

$$| (\tilde{\omega}^2_j)/(\omega^2_j) - 1 | \leqslant \eta_j/\lambda_j \qquad [6.13]$$

where

$$\eta_j = |[B]_{p+1}[P]_k\{Z_j\}|_2 \qquad [6.14]$$

and $[B]_{p+1}$ is the k x k off-diagonal block calculated in the last step of the algorithm

$[P]_k = [\ [O]\ [I]\ ]$

$[P]_k$ is a k x r projection matrix to obtain the

last k components of vector $\{Z_j\}$. The size of matrix [I] is thus equal to k x k.

$\{Z_j\}$ is the jth eigenvector of [T] normalized such that $\{Z_j\}^T \{Z_j\} = 1$.

λ_j is the jth eigenvalue of the reduced block tridiagonal system.

6.2 Starting Spatial Vectors for Block Algorithm

In complex structural systems, the selection of the initial deformation vectors, the starting static deflected shapes, should be supplemented by an automated linear independency criterion to reduce the number of repetitive load patterns to a minimum and to favor the generation of an orthogonal vector basis.

A basic requirements of the block Ritz formulation is that the starting static deformation patterns selected to initiate the algorithm be linearly independent. In order to satisfy this requirements and to identify, out of the complete loading sequence, the spatial distributions that will be most important to the structural response a loading correlation matrix, $[C]^L$ can be established. A typical entry will be given by

$$c^L_{i,j} = \frac{\{f_i(s)\} \cdot \{f_j(s)\}}{\|\{f_i(s)\}\|_2 \, \|\{f_j(s)\}\|_2} \qquad [6.15]$$

the value of $c^L_{i,j}$ corresponds to the cosine of the angle between vectors $\{f_i(s)\}$ and $\{f_j(s)\}$ and will vary between 0 and 1. A value of 1 will indicate the the loading distributions are linearly dependent, a value of 0 will indicate that the loading distributions are orthogonal, intermediate values can be interpreted as the degree of linear independence relating a given pair of loading distributions $\{f_i(s)\}$, $\{f_j(s)\}$.

It should be observed that the correlation of the static deflected shapes $\{U_i(s)\}$, $\{U_j(s)\}$ obtained from the loading distributions will generally be higher than the loading correlation due to structural coupling. The selection of the starting static deformation patterns should therefore be done in two steps. First the loading correlation matrix is calculated and the loading patterns are chosen such that no loading pairs have a strong correlation coefficient (say greater than 0.8). Second the static deflected shapes corresponding to the selected load patterns are calculated. The correlation matrix of the mass weighted deflected shapes is then evaluated from

$$c^{U}_{ij} = \frac{\{U_i(s)\} \cdot \{[M]\{U_j(s)\}}{|\{U_i(s)\}|_2 \; |[M]\{U_j(s)|_2} \qquad [6.16]$$

the initial deformation patterns are selected such that no static deflection pair having a strong correlation is included in the starting block because the algorithm will not be able to maintain the orthogonality of the iteration vectors. This procedure thus provides a rational method to choose the deformation patterns that will be important to the structural response.

Finally while using the block Ritz algorithm there are two parameters that will influence the final results. The first one is k the number of vectors that are iterated simultaneously and the other one is p the number of steps used by the algorithm. The final dimension of the reduced problem will be r = k x p. In any practical analysis the maximum dimension of the reduced problem will be limited by some computer restrictions. If k is made fairly large then the number of steps, p, available to reach the error norm criterion will be small and may lead to a poorer approximation of the dynamic effects of the inertial characteristics, therefore the number of initial loading patterns should be kept small.

6.3 Numerical Applications of Block Ritz Reduction Method

To illustrate the performance of the block Ritz method this section will present numerical results obtained from three specific examples.

6.3.1 Responses to Independent Dynamic Loading Distributions

In the first example it is assumed that the response of the simple offshore platform of chapter 4, modelled as a shear beam system as shown in fig. 4.4, needs to be obtained for the wave and earthquake loadings separately but that a single vector basis is to be used in the response calculations. The block LWYD Ritz algorithm was used to calculate the vector basis using the spatial distribution of the earthquake and wave loads to initiate the recurrence relationship. The following correlation coefficients were calculated;

- spatial loading distribution : 0.106
- static deflected shape : 0.993
- [M] weighted static deflected shape : 0.657

The representation of the dynamic load achieved by the block Ritz basis is shown in fig. 6.5. It is observed that the representation of a uniformly distributed loading such as earthquake loads is very close to the representation obtained from single vector iteration. In the case of wave loading modelled by a concentrated load, more block Ritz vectors were required to achieve the same representation as obtained from the single vector iteration algorithm.

The responses to wave and earthquake loads were then computed from Ritz bases calculated with and without static residual, with the same convergence criterion that was used for the single vector iteration algorithm, a maximum error of 1% allowed in beam shear forces. The results are summarized

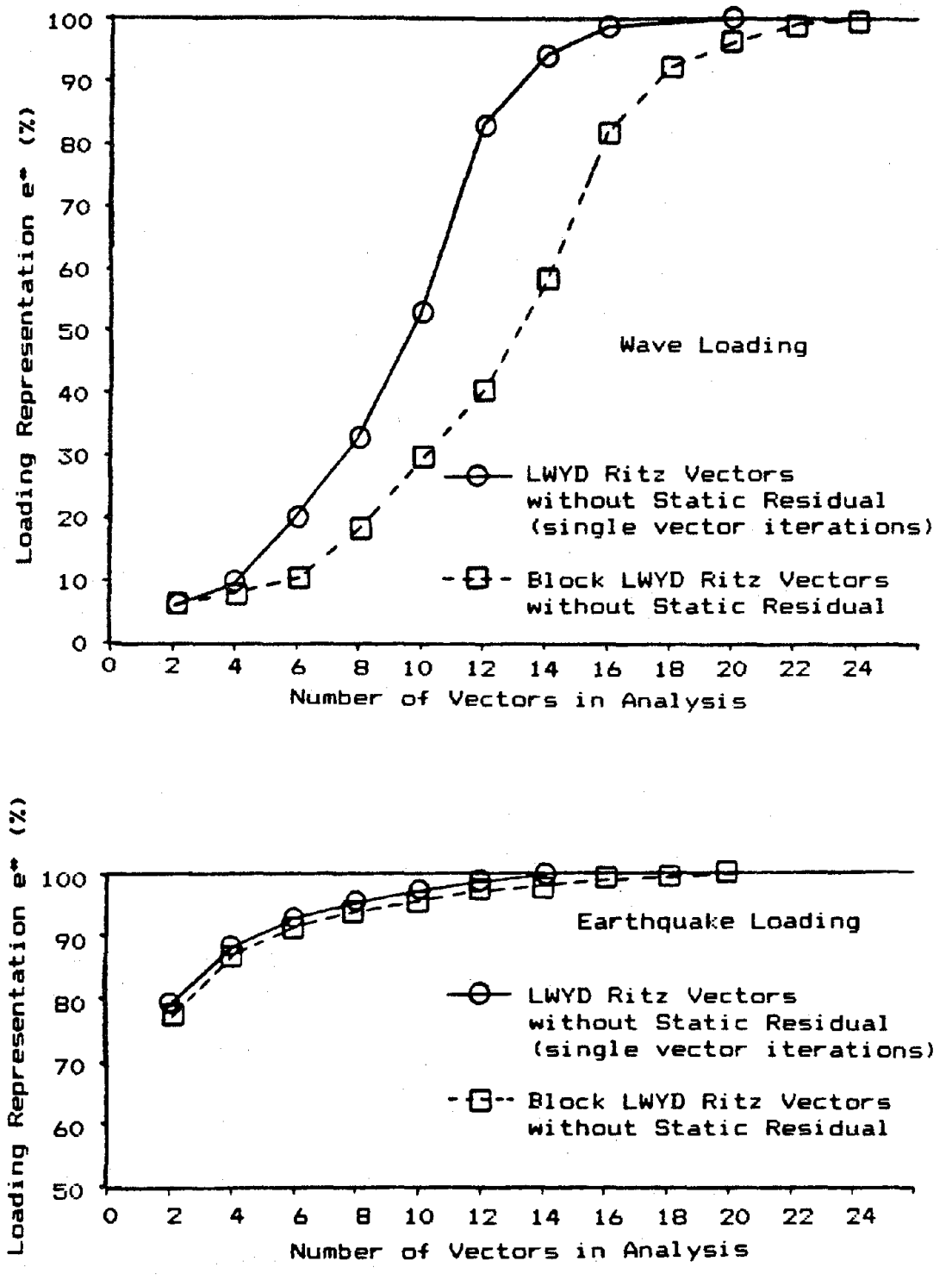

Fig. 6.5 Representation of Dynamic Loads from Block Ritz Bases (Example no. 1)

in table 6.1 and a graphical representation of the wave load response is given in fig. 6.6. It is observed that the block LWYD Ritz algorithm requires slightly more vectors than the single vector iteration method to achieve convergence. The effect of static residual was beneficial to both response calculations. If a correction for higher modes effects is to be included in the analysis it was found slightly advantageous, in terms of the number of requested vectors, to use the block LWYD Ritz algorithm without static residual and add to the modal summation the modal acceleration terms calculated from the loading for which the response was requested.

It was observed that when exact eigensolutions are used, the account of higher modes effects by the application of static correction terms in the form of equation [3.42] or of modal acceleration terms in the form of equation [3.43] is equivalent. If these modal summation procedures are to be used along with the WYD Ritz reduction method without static residual it was found that modal acceleration provides much better results than static correction.

It can thus be concluded that independent dynamic response analyses can be obtained from a single vector basis generated simultaneously from the multiload pattern distributions. The number of vectors required for convergence will be smaller as compared to the calculation of different vector bases obtained from individual loading distributions.

6.3.2 Three Dimensional Earthquake Analysis

The second example is related to the three dimensional earthquake analysis of the jacket platform presented in chapter 5 (see fig. 5.1). The analysis was carried out using the response spectra method as before but the vector basis was formed by the block LWYD Ritz algorithm using

TABLE 6.1

Convergence of Block Ritz Bases for Independent Dynamic Response Analysis

I. Wave load

Analysis	Number of vector for convergence
- Block Ritz without static residual	16
- Single vector iteration without static residual	12
- Block Ritz with static residual	4
- Block Ritz without static residual + modal acc.	2
- Single vector iteration with static residual	3

II. Earthquake load

Analysis	Number of vector for convergence
- Block Ritz without static residual	16
- Single vector iteration without static residual	12
- Block Ritz with static residual	14
- Block Ritz without static residual + modal acc.	12
- Single vector iteration with static residual	10

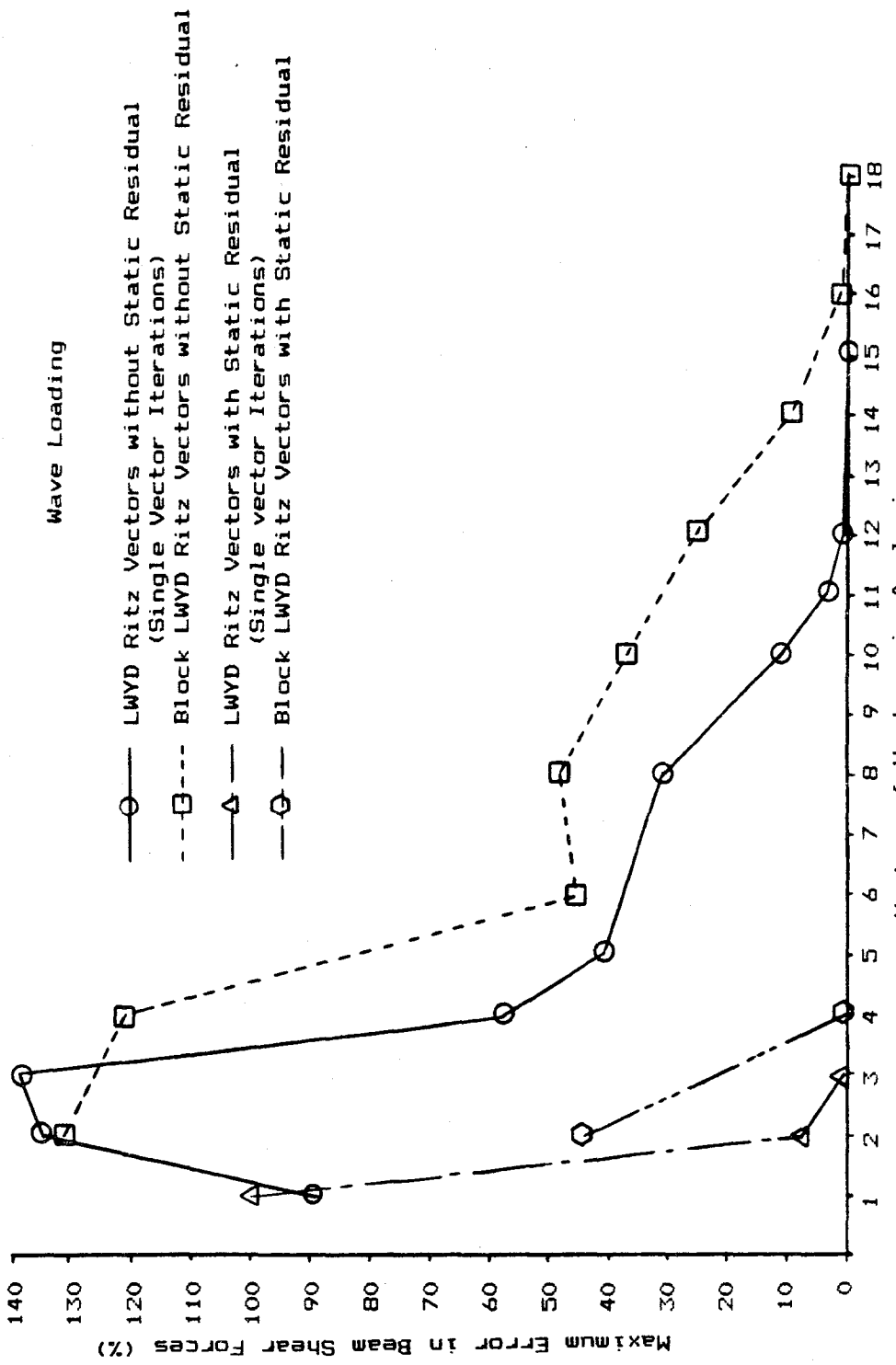

Fig. 6.6 Maximum Error in Beam Shear Forces Vs Number of Vectors in Analysis (wave loading)

$$[F(s)] = [\ [M]\{r_x\},\ [M]\{r_y\},\ [M]\{r_z\}\ ] \qquad [6.16]$$

as initial loading distribution to initiate the reccurence relationship. The analysis was carried out for the symmetric and asymmetric model. The application using the symmetric model represents an ideal situation for the block algorithm because the loading as well as the corresponding static deflected shapes are perfectly uncorrelated since the geometric axes "X", "Y" and "Z" are also principal structural axes.

The representation of the dynamic load achieved by the block Ritz basis is shown, for the symmetric model, in fig. 6.7. It can be observed that the block Ritz algorithm produced results that are equivalent or slightly superior to the single vector iteration procedure.

It was then verified that the structural response using block Ritz vectors, with at least 98% loading representation, was in average within 1% of the exact eigensolution or the results of single WYD Ritz iteration. The rate of convergence of the block Ritz solution was also compared with the rate of convergence of the single vector iteration procedure according to the method outlined in section 5.4.4. These results are shown in fig. 6.8. It was found that after the first few vectors were included in the basis the rate of convergence of average values were nearly identical. The rate of convergence of maximum error values was faster for displacements calculated from the block Ritz solution, however maximum error values of stresses did converge more rapidly from the single vector iteration procedure. The rule of thumb of 90% (95%) loading representation corresponding to an average error of 10(%) (5%) in the response quantity of interest was always respected.

The relationship between the block Ritz solution and the exact eigensolution is shown in fig. 6.9. It was found

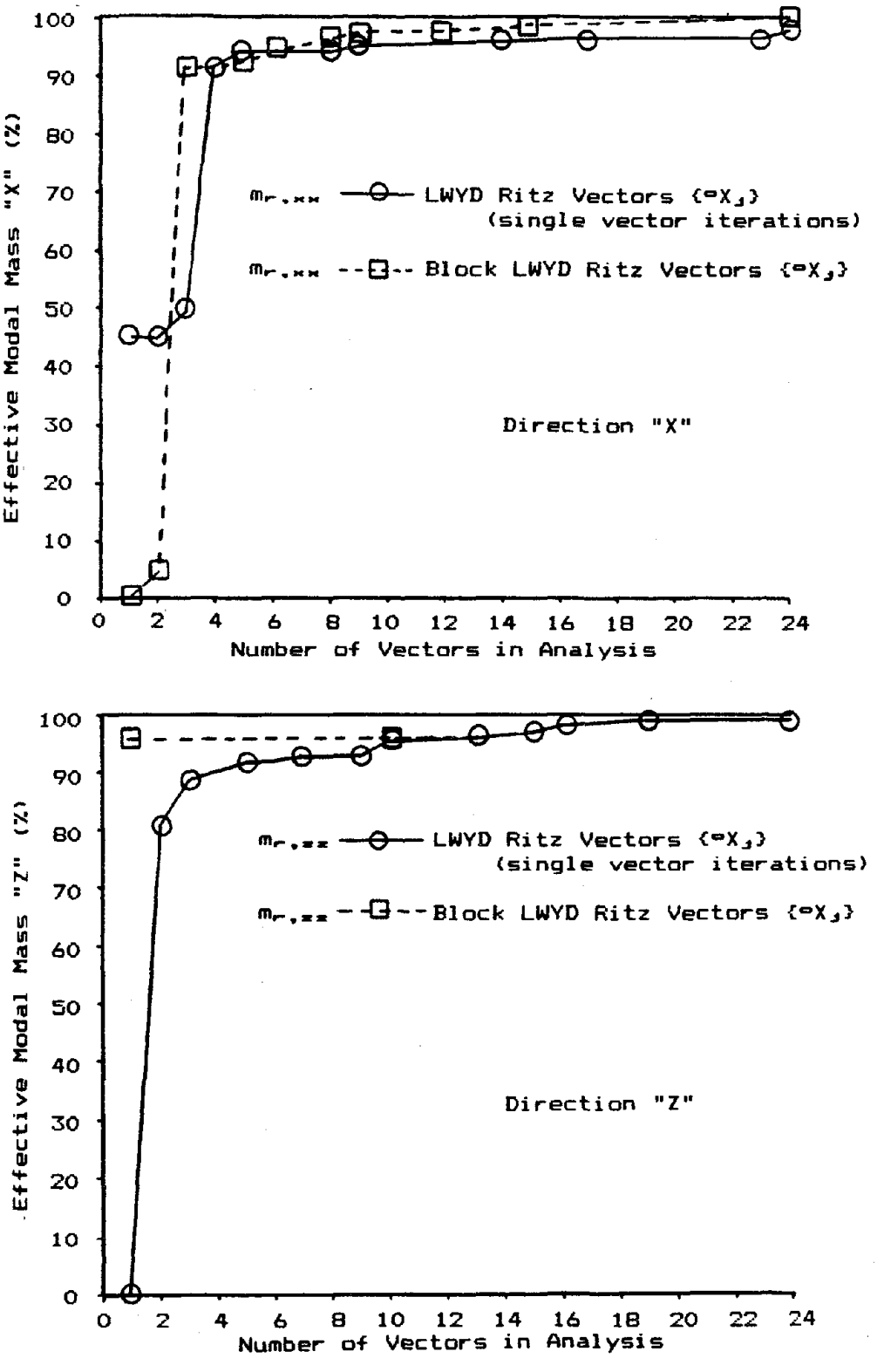

Fig. 6.7 Representation of Dynamic Loads by Block Ritz Bases (Example 2)

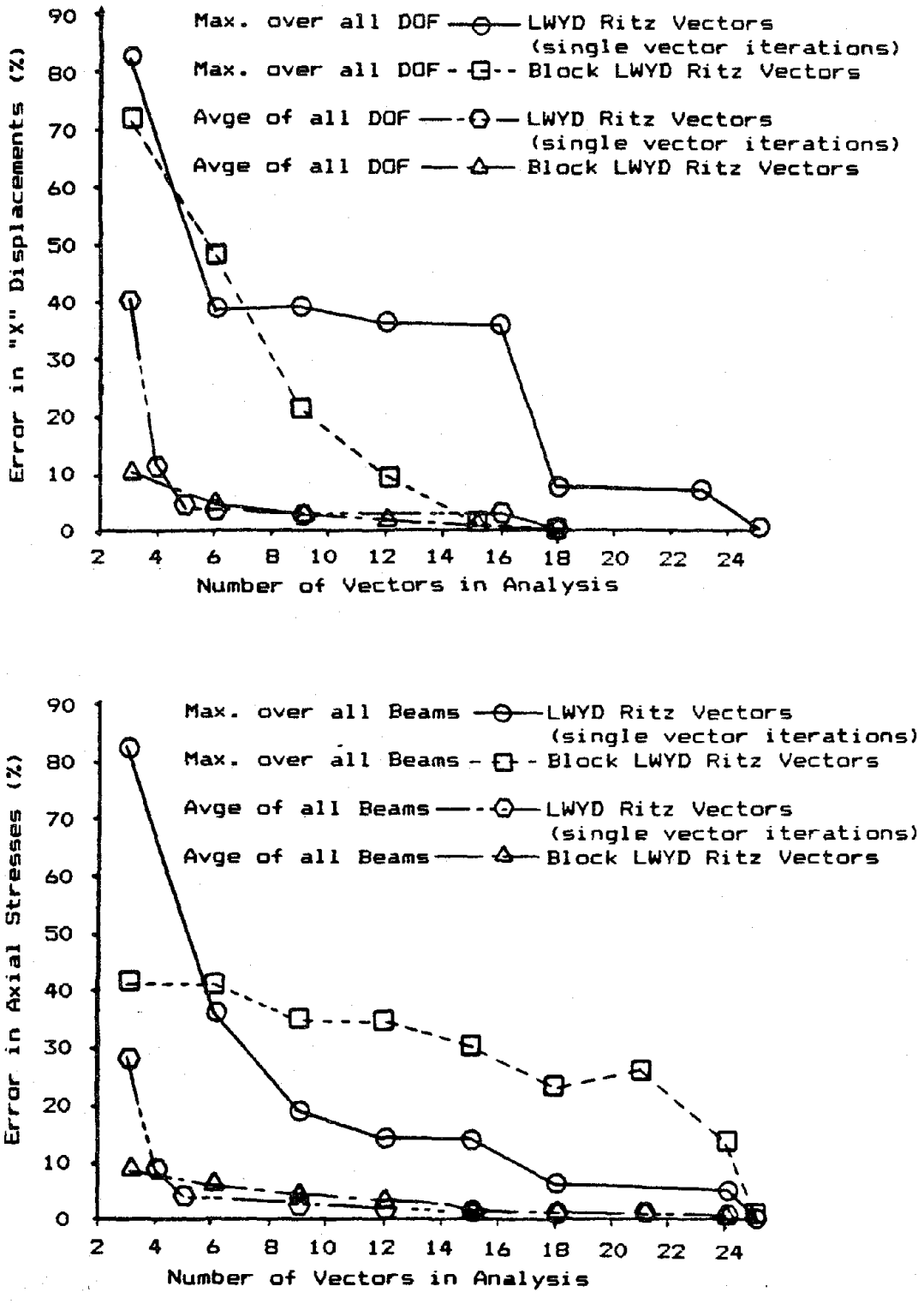

Fig. 6.8 Rate of Convergence of Block Ritz Solution
(Example no.2 3D Earthquake Analysis)

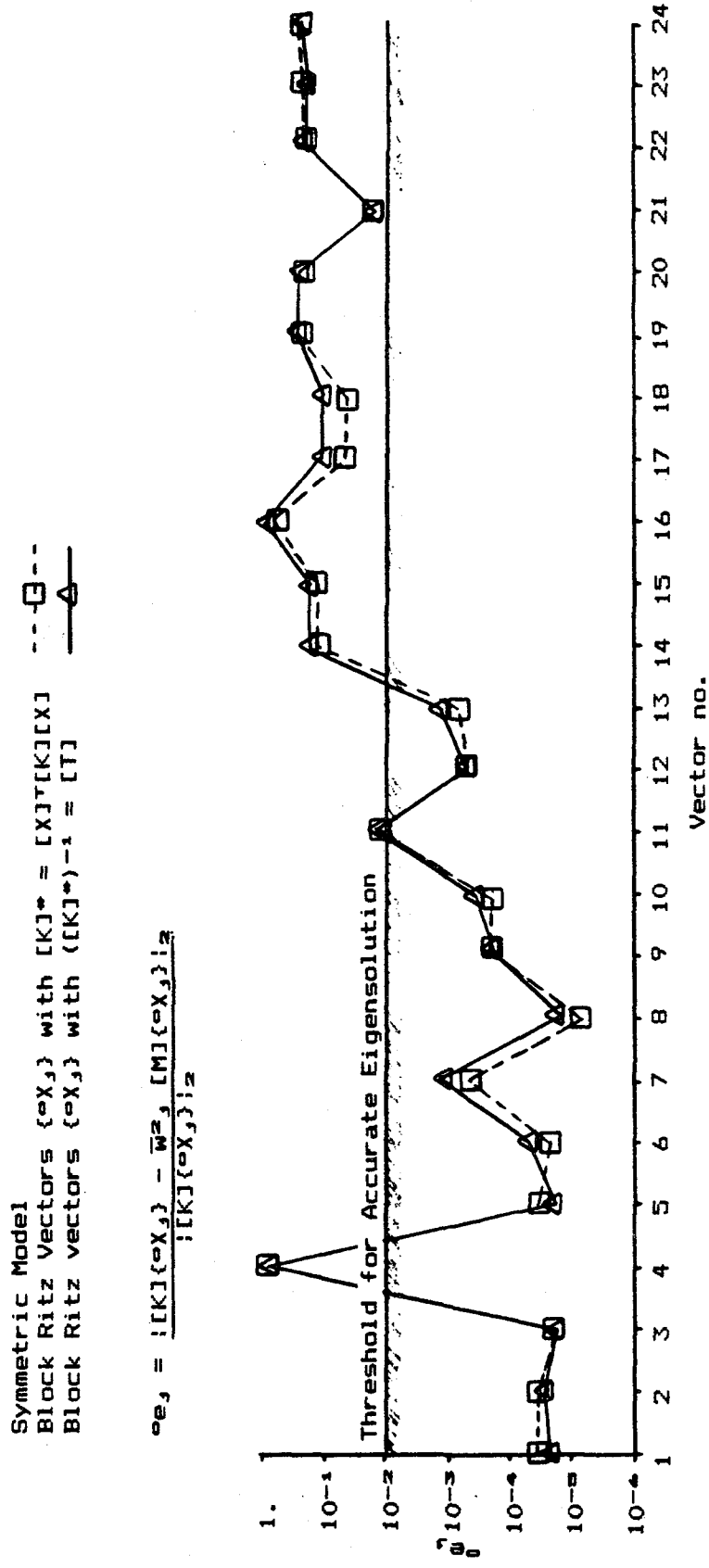

Fig. 6.9 Accuracy of Block Ritz Pairs as the Solution of the Free Vibration Problem (Example 2, 3D Earthquake Analysis)

that with the block Ritz solution considering 27 generalized coordinates only 3 block Ritz pairs located at the beginning of the eigenspectrum can be considered exact eigenpairs as compared to 12 Ritz pairs from the single vector iteration procedure. This is due to the fact that the block algorithm performs less steps to obtain the same number of vectors. On the other hand the vector resolution obtained from the eigen-solution of $[K]^*[Z] = [\bar{w}^2][M]^*[Z]$ and the reduced block tridiagonal system $[T][Z] = [\lambda][Z]$ is now nearly identical even for the symmetric model where there are repeated eigenvalues. This is due to the fact that multiple eigenvalues are now found simultaneously (up to block size k) rather than sequentially with improved convergence characteristics.

For the asymmetric model the following correlation coefficients were obtained;

- spatial loading distribution : uncorrelated

- static deflected shape : $\{U_1\}\{U_2\} = 0.003$
  $\{U_1\}\{U_3\} = 0.237$
  $\{U_2\}\{U_3\} = 0.131$

- [M] weighted static deflected shape : $\{U_1\}\{U_2\} = 0.132$
  $\{U_1\}\{U_3\} = 0.277$
  $\{U_2\}\{U_3\} = 0.156$

showing a weak correlation of the static deflected shapes through structural coupling. The detailed analysis of the structural response substantiated the observations obtained for the symmetric model.

It can thus be concluded that for three dimensional earthquake analysis using the response spectra method the block Ritz algorithm and the single vector iteration algorithm, as applied in chapter 5, will produce results of

comparable accuracy. One advantage of the block Ritz method is that the matrix [K] and [M] need to be accessed less frequently which might be important to limit I/O operations if [K] and [M] are stored in block form on low speed storage.

6.3.3 Multiload Pattern Analysis

The third example is related to the study of structural systems where the spatial distribution of the load is a function of time. The response to wave loading of the simple offshore platform shown in fig. 6.10 was evaluated for that purpose. The platform is modeled as a space frame with 48 dynamic DOF. A diagonal mass matrix including rotatory inertia was calculated from the procedure outlined by Hinton et al. (6.4) and Surana (6.11). The mass matrix included contributions from the mass of the material of the structural elements, including contained fluid, the added mass and the mass of the deck.

A lumped description of wave forces was used for the analysis. This treatment involves lumping the areas and volume of individual structural members into areas and volumes at the nodes of the structure and calculating the horizontal wave forces acting on these assumed concentrated bodies. The linear (Airy) wave theory was used to determine the water motion to be considered in the wave force calculations. A detailed description of the procedure has been given by Dawson in reference 6.2.

The final form of the load acting on a typical node "i" of the structure will be given by

$$f_i(s,t) = f_i(s) * \sin(-w_L t + A) \qquad [6.17]$$

where $f_i(s)$ is a constant coefficient
w_L is the specified wave frequency
t is the time

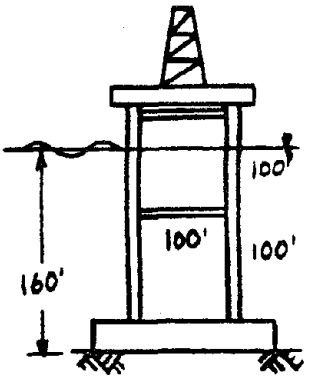

Flexible Steel Offshore Structure

4 Faces of Structure are Identical

Vertical Members D = 4' t = 1.5"
Horizontal Members D = 2' t = 0.5"
E = 29000 Ksi
Water Depth = 160'
Wave Height = 40'
Wave Period = 9 sec (W_L = 0.6981 rad/sec)
Deck Weight = 2000 Kips (Asymmetric)

Mathematical Model

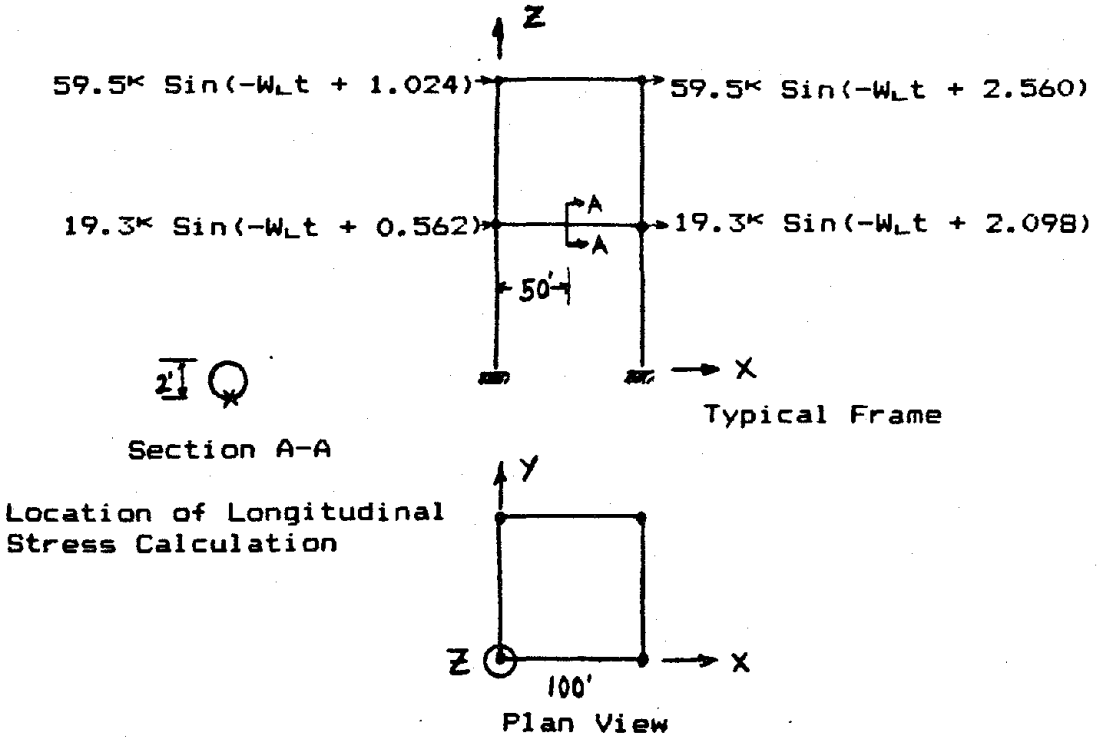

Fig. 6.10 Flexible Offshore Structure (Example no. 3)

A is an angle reflecting the difference in phase between the inertial and drag loading components of the water wave acting on a single node as well as the spatial location of the nodes with respect to the position of the wave crest.

The wave used in the calculation had a height of 40 ft and a period of 9 sec (w_L = 0.6981 rad/sec) and was assumed to act in the structural "X" direction. The total base shear as well as typical load patterns obtained from these calculations are shown in fig 6.11. It is observed that the loading is periodic (with a period of 9 sec) but that the spatial distribution of the load is continuously changing within this period.

The loading was discretized using a time increment of 0.5 sec and the loading correlation matrix was calculated. Three load patterns were identified as important to the structural response. The correlation of the corresponding deflected shape was evaluated and two deformation patterns (using t=7 sec and t=9 sec) were retained for the block Ritz analysis. A summary of these calculations is presented in table 6.2.

The representation of the specified loading patterns was then evaluated from the Euclidean norm of the error force vector for different vector bases comparing block Ritz solutions to the exact eigensolution and single vector Ritz solutions. The single vector *LWYD* Ritz algorithm used the spatial distribution at time t=9 sec, causing maximum base shear, to initiate the recurrence relationship. A summary of the results is showm in fig. 6.12. It can be observed that all the Ritz solutions were able to achieve a good representation of the simple load distribution specified at time t=9 sec with relatively few vectors. However, only the block Ritz solution was able to achieve simultaneously a good representation of the dynamic load at t=7 sec. In fact the

TABLE 6.2

Correlation Analysis for Multiload Pattern Analysis

Loading Correlation (sperscripts correspond to specific time t)

	f^{7}	f^{8}	f^{9}
f^{7}	1.000	0.755	0.168
f^{8}	0.755	1.000	0.773
f^{9}	0.168	0.773	1.000

Correlation of static deflected shapes

	U^{7}	U^{8}	U^{9}
U^{7}	1.000	0.755	0.168
U^{8}	0.755	1.000	0.773
U^{9}	0.168	0.773	1.000

Correlation of mass weighted static deflected shapes

	U^{7}	U^{8}	U^{9}
U^{7}	1.000	0.445	0.447
U^{8}	0.445	1.000	0.829
U^{9}	0.447	0.829	1.000

Selected time to specified starting deformation pattern are t=7 sec and t=9 sec

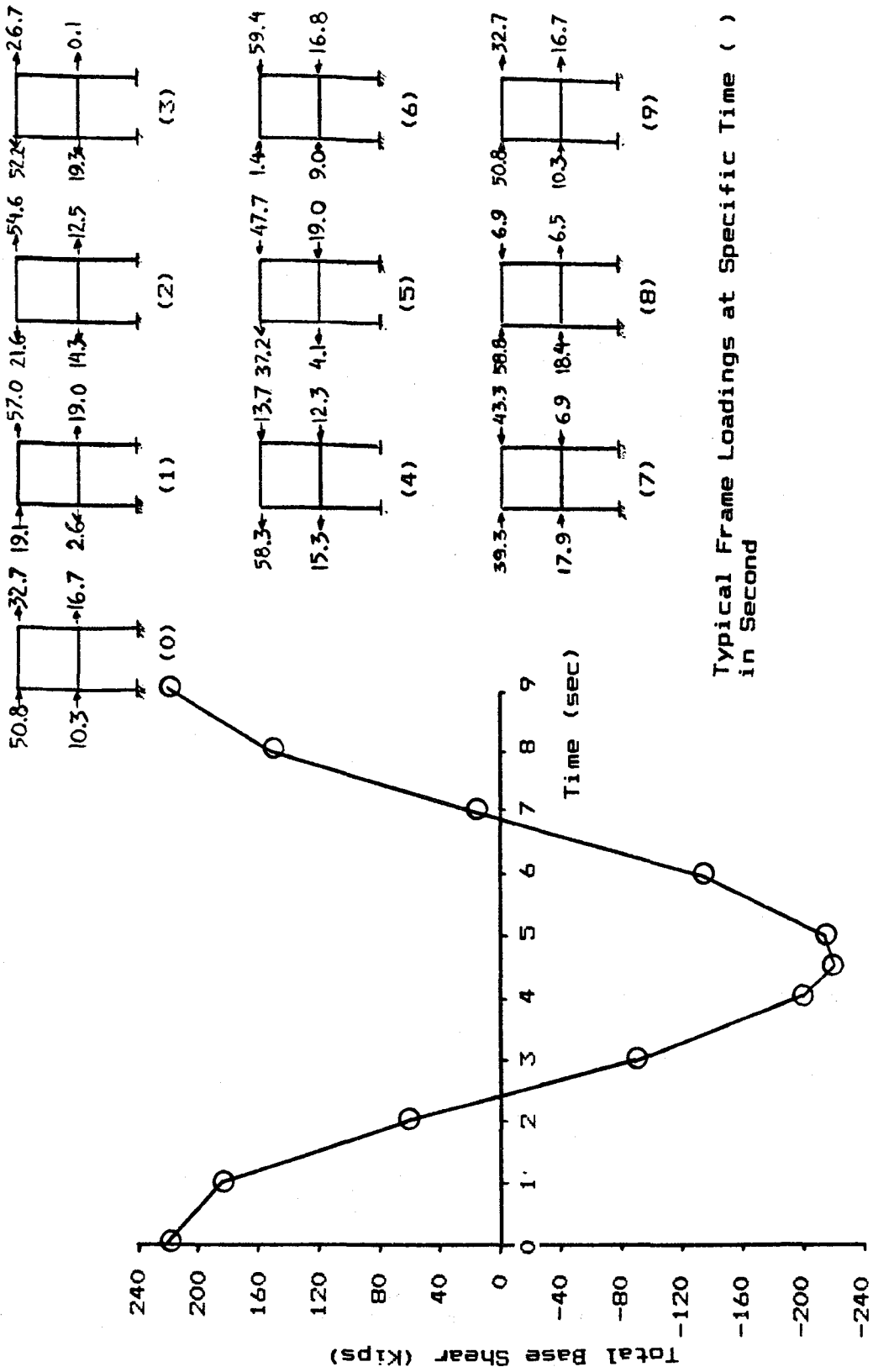

Fig. 6.11 Wave Loading Characteristics (Example no. 3)

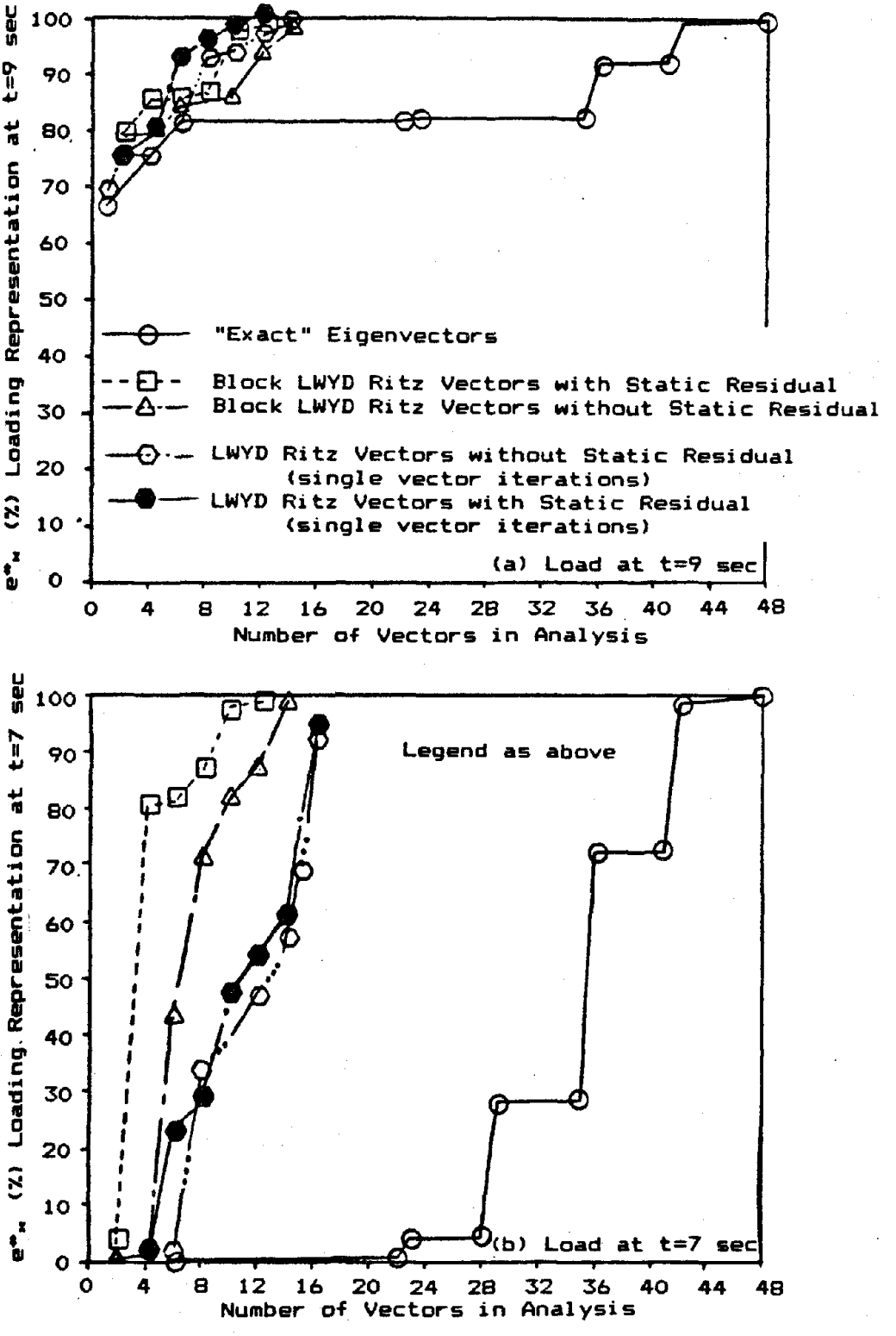

Fig. 6.12 Representation of Dynamic Load from Block Ritz Bases (Example no. 3)

spectral content of the starting vector of the single WYD Ritz method (using t=9 sec) was exhausted before a complete representation (say 98%) of the load at t=7 sec could be obtained. The eigensolution required many more vectors than any Ritz solution to obtain a good loading representation, reflecting once again the importance of higher modes to represent concentrated loads.

The fundamental period of vibration was found to be close to 10 sec. The periods of the first few modes are shown in table 6.3. By comparing the frequency content of the loading to the structural frequencies it can be anticipated that after the first few modes are included in the summation the concept of static correction to approximate higher modes effects will be very effective.

The steady state structural response was calculated by direct vector superposition. By assuming appropriate trigonometric identities it was possible to obtain a closed form solution for the displacements. For these calculations it was assumed that the damping in each generalized coordinate can be taken as 8% of the critical damping of the first Ritz or eigenmode. The exact solution was obtained by considering a complete exact eigenbasis of 48 vectors. The convergence of displacements was fairly rapid for any vector basis and is not worth reporting. The convergence of a typical response quantity such as the total longitudinal fiber stress at the bottom chord of the horizontal bracing member was calculated. The location of the section for stress calculation (see fig. 6.10) was chosen near the midlength inflection point such that the response is dominated by axial stresses. The stress response was then calculated from different vector bases for various number of vector retained in the analysis. A sample of these computations is shown in fig. 6.13 where 6 vectors were included in the summation and a comparison with exact results was also established.

TABLE 6.3

Natural Periods of Vibration of

Flexible Steel Offshore Platform

	Exact Eigenanalysis		Block Ritz Analysis*	
	period(sec)	freq(rad/sec)	period(sec)	freq(rad/sec)
1-	10.343	0.607	10.339	0.608
2-	10.294	0.610	7.559	0.831
3-	7.509	0.837	5.907	1.064
4-	5.894	1.066	1.298	4.839
5-	1.301	4.830	0.673	9.333
6-	1.298	4.838	0.182	34.504

Note : * 6 vectors included in Block Ritz analysis (2 static and 4 dynamic)

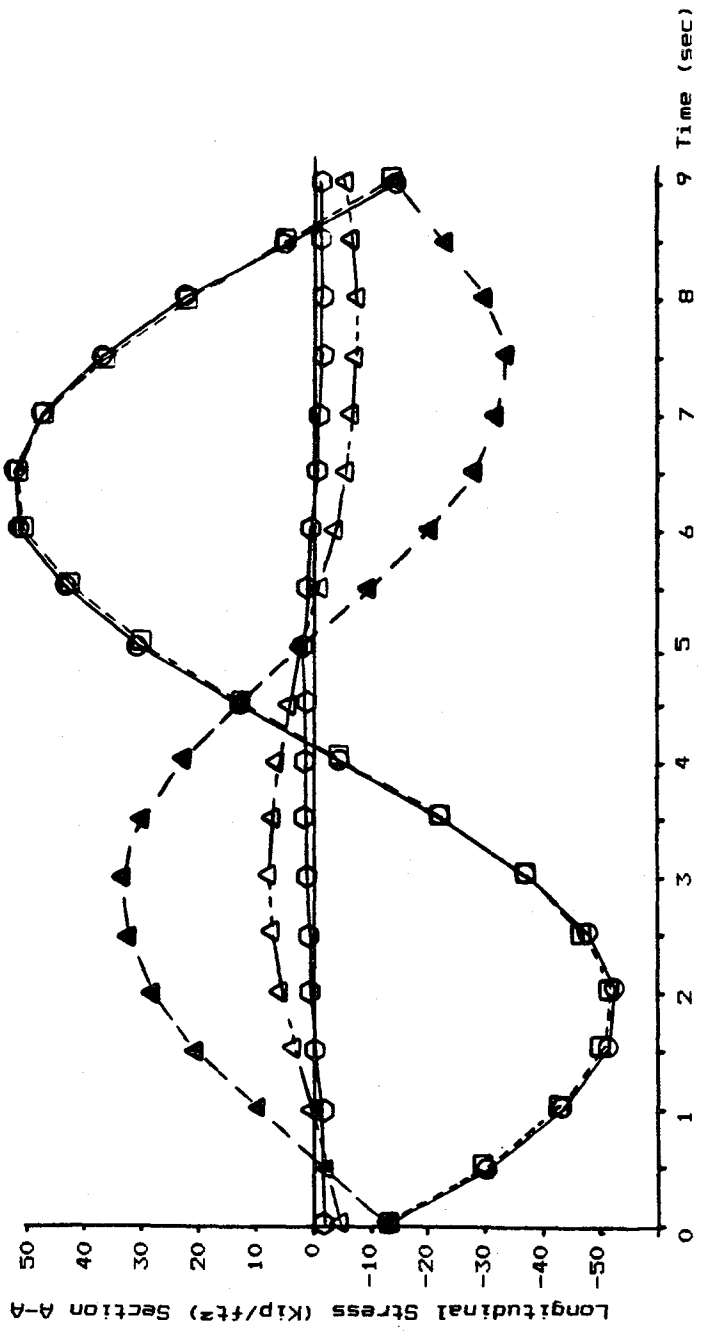

Fig. 6.13 Convergence of Stress Response for Block Ritz Analysis
(Example no. 3)

The results using 6 eigenvectors supplemented by modal acceleration virtually coincided with the exact solution. The block Ritz solution using 2 static and 4 dynamic vectors was also almost identical to the exact solution. It should be noted that formal application of the static correction concept is very simple for loading that can be written as the product of a spatial distribution and a single time variation parameter. In this case only the magnitude but not the spatial distribution of the loads varies with time such that the pseudo-static displacement correction vector has only to be solved once, an appropriate scaling factor is then applied at each time step to obtained the required correction effect. For more general loading, such as the wave loads used in this analysis, this procedure becomes much more involved since a new pseudo-static solution has to be calculated at each time step since the spatial distribution vary with time.

The results obtained from the WYD Ritz method using single vector iteration with static residual were completely erroneous except at time t=0, 4.5 and 9 sec where they were almost exact. As expected these are the times when the spatial distribution of the loading coincide with the loading chosen to initiate the single vector iteration algorithm. The solution using 6 exact eigenvectors is also completely false as expected from the poor loading representation achieved by the first few exact eigenvectors.

It can thus be concluded that this example, although very simplified, clearly illustrates the advantage of a block Ritz solution over the alternative vector superposition method for loadings that are function of space and time. The block Ritz method was able to provide very good results in an economical way as no extra terms need to be added to the usual modal summation procedure.

CHAPTER 7

Use of the WYD Ritz Reduction Method for Multilevel Substructure Analysis

The concept of dividing a structure into parts to carry out an analysis may be advantageous in several applications:

- analysis of large FEM systems that have too many DOF to be handle by the computer in a single analysis,

- analysis of systems that have repetitive components,

- interaction studies when the behavior of different media can be separated such as soil/structure or fluid/structure problems,

- subdivision of large systems between groups of analysts that can work more independently,

- parametric studies and optimization of specific sections of complex systems,

- analysis of structure with localized nonlinearities reducing the size of the nonlinear problem by treating the linear and nonlinear sections as substructures.

In dynamic analysis, the substructuring concept is related to the idea of reducing the number of DOF of the structural system while retaining a high accuracy in the dynamic response. The reduction is not done globally but at the substructure level and compatibility of displacements and forces at the substructure interface generates the global set of equations representing an approximate mathematical model of the complete structure. The static condensation procedure, the Guyan reduction method (7.7) and the component mode

synthesis, which forms the basic tools of dynamic substructure analysis, can be understood as Ritz analysis. Variations in the methods are related to the choice of the Ritz basis vectors.

The critical point in the reduction of any dynamic problem is to find an adequate representation of the work done by the internal loads of each substructure. The internal loads in a substructure may arise from elastic forces when an external load is directly applied on a structural components, or from inertia, damping and elastic forces developed during the dynamic structural response. Typically internal inertia and damping forces are not known before the final solution is known. The classical approach to dynamic substructuring is therefore to describe the internal motion of each substructure by a linear combination of substructure modes with the implicit assumptions that these modes satisfy a certain substructure eigenvalue problem. To enforce compatibility between substructures, constraint or attachment modes are used; these are displacement patterns corresponding to successive unit displacements or forces applied at each boundary DOF.

Three basic variants of the method have been developed depending on whether the modes of each substructure are obtained with its interface held fixed (7.5, 7.12), free (7.4) or loaded (7.2, 7.6). Since it is not possible to define a unique eigenvalue problem for a given substructure and because none of these methods can yield exact results for the actual structure using a truncated set of exact mode shapes, the significance of using exact substructure mode shapes can be seriously questioned. The suggestion for improvements should therefore be directed toward two basic questions;

- how to select a set of substructure modes,

- how to enforce geometric compatibility at substructure boundaries.

It should be recognized that the substructure synthesis method is in fact a Rayleigh Ritz method for an intermediate structure for which Ritz vectors can be used to reduce the original model. In this chapter it will be shown that dynamic substructuring methods can be greatly improved if LWYD Ritz vectors are used in the basic transformation equations. First, specific considerations concerning the application of the WYD Ritz reduction method to substructures that do not develop internal inertia or damping forces will be presented. Secondly, a component mode synthesis type of formulation, using LWYD Ritz vectors to represent the internal substructure behavior for substructures that develop inertia and damping forces, will be developed. Finally a new method to generate exactly the LWYD Ritz basis of the complete structure from basic substructure data will be introduced as the Dynamic Ritz Condensation (DRC) algorithm.

7.1 Static Condensation

Static condensation is used to reduce the total number of DOF of a substructure by eliminating the internal DOF. The term "static condensation" is chosen because a static equilibrium constraint is used to express the eliminated DOF in terms of the boundary DOF that will be retained in the assembly of the substructures.

To establish the equations used in static condensation, we partition the basic static equilibrium equations of a substructure into the internal DOF "i" to be eliminated and the boundary DOF "b" to be retained:

$$[K]\,[U] = \{F\} \qquad [7.1]$$

$$\begin{bmatrix} K_{ii} & K_{ib} \\ K_{bi} & K_{bb} \end{bmatrix} \begin{bmatrix} U_{ii} \\ U_{bb} \end{bmatrix} = \begin{bmatrix} F_{ii} \\ F_{bb} \end{bmatrix} \qquad [7.2]$$

using the first matrix equation of equation [7.2] to solve for $\{U_{ii}\}$, we get:

$$\{U_{ii}\} = [K_{ii}]^{-1} \left(\{F_{ii}\} - [K_{ib}]\{U_{bb}\}\right) \qquad [7.3]$$

The internal substructure displacements are thus obtained by superposition of two components, a local analysis to known substructure loads given by $[K_{ii}]^{-1}\{F_{ii}\}$ and the effect of boundary displacements given by $-[K_{ii}]^{-1}[K_{ib}]\{U_{bb}\}$. Substituing [7.3] in the second equation of [7.2], we get:

$$\left([K_{bb}] - [K_{bi}][K_{ii}]^{-1}[K_{ib}]\right)\{U_{bb}\} = \left(\{F_{bb}\} - [K_{bi}][K_{ii}]^{-1}\{F_{ii}\}\right) \qquad [7.4]$$

This can be written as:

$$[\bar{K}_{bb}]\{U_{bb}\} = \{\bar{F}_{bb}\} \qquad [7.5]$$

where $[\bar{K}_{bb}]$ and $[\bar{F}_{bb}]$ are the reduced stiffness and loading.

The same results can be obtained by applying the transformation matrix:

$$[V] = \begin{bmatrix} -K_{ii}^{-1}K_{ib} \\ I \end{bmatrix} \equiv \begin{bmatrix} T_i \\ I \end{bmatrix} \qquad [7.6]$$

where [I] is the identity matrix, to the original stiffness and loading matrices:

$$[\bar{K}_{bb}] = [V]^T [K] [V] \qquad [7.7]$$
$$\{\bar{F}_{bb}\} = [V]^T \{F\}$$

This constitutes a Ritz analysis in which the DOF $\{U_{bb}\}$ are the Ritz coordinates and the columns of [V] are the assumed displacement patterns or the Ritz vectors.

It should be noted that static condensation is in

fact Gauss elimination on the DOF $\{U_{ii}\}$ and that when applied to a static problem, there is no approximation in the procedure. For static structural analysis, substructuring computations can be divided into three phases:

- Generation of basic substructures

- Reduction and assembly of substructure matrices (forward and global pass)

- Local analysis of individual substructures (backward pass)

To reduce the size of the dynamic system, one alternative is to apply the transformation matrix [V] of equation [7.6] to the dynamic equilibrium equation:

$$[M]\{\ddot{U}\} + [C]\{\dot{U}\} + [K]\{U\} = \{F(s,t)\} \qquad [7.8]$$

according to the procedure of equation [1.8].

But the transformation matrix [V] is based on static equilibrium and does not account for dynamic shape inertia effects. If no inertia forces are associated with a DOF, it can be eliminated by static condensation and does not need further consideration in the dynamic analysis. If masses are associated with DOF to be eliminated, the static transformation constitutes a standard Rayleigh-Ritz reduction but there is only limited rational justification for the choice of the Ritz vectors obtained from the static condensation procedure. It should be noted that this particular choice of Ritz basis vectors is also known as Guyan reduction.

7.2 Substructure with Massless Degrees of Freedom

Structural systems that possess massless DOF are frequently encountered in practice and the formal application of the static condensation procedure can be avoided by

working directly with the singular mass matrix in the vector generation algorithm. The final results will theoretically be the same but there are however some special considerations that must be addressed.

If a structural system possesses massless DOF the space spanned by the dynamic problem, as defined by the characteristics of matrix [M], becomes a subspace of the static problem as defined by the characteristics of the [K] matrix. If an exact eigensolution is used the resulting eigenproblem will be defective; that is, it has fewer than n eigenvectors for an n DOF system. It is therefore possible that some vectors such as deflected shapes or the initial loading distribution can not be made up of a linear combination of all eigenvectors of the specified mathematical model. In such a case, the exact eigensolution will therefore be unable to yield an accurate solution spanning the entire space of the static problem. If however the WYD Ritz reduction method is used, the addition of a static residual term to the basis will provide a means to supplement the dynamic solution by a vector spanning the entire problem space and will thus be able to yield more accurate results.

A simple numerical example is used here to illustrate that point. The mass matrix of the offshore platform idealized as a 40 DOF shear beam model according to fig. 4.4 was modified by removing masses at three DOF below the mass representing the deck as shown in fig. 7.1. The "exact" mathematical response of the discrete model subjected to wave loading applied at a massless DOF was obtained from the procedure outlined in section 4.3.2.

The response was then calculated by vector superposition using a complete set of 37 eigenvectors, eigenvectors supplemented by static correction and LWYD Ritz vectors. The results in terms of displacements of the top DOF are shown in fig. 7.1. It can be observed that a full

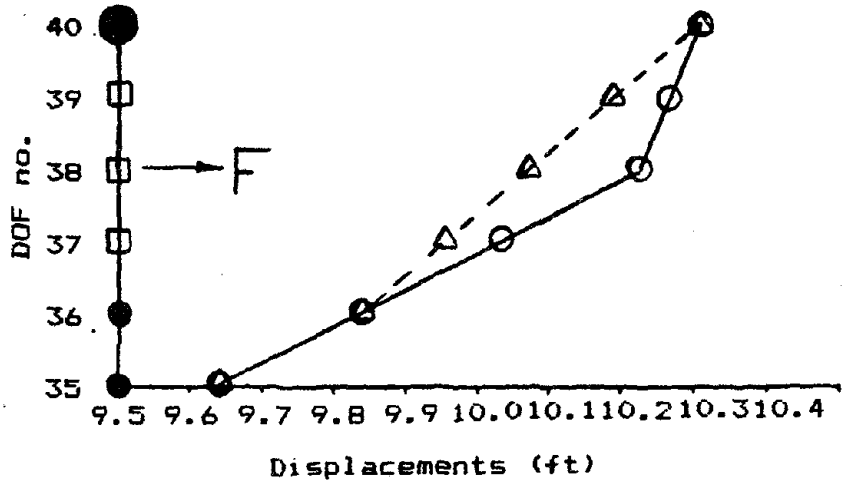

● DOF with Mass
□ Massless DOF

○ "Exact" Solution
3 LWYD Ritz Vectors with Static Residual
2 Eigenvectors + Static Correction or Modal Acceleration

△ Solution from Complete Eigenbasis of 37 Eigenvectors

Fig. 7.1 Analysis of Structural System
with Singular Mass Matrix

eigenbasis is only able to provide a linear variation between mass DOF no. 36 and mass DOF no. 40 and therefore missed the local shape deformation in the vicinity of the load. On the other hand, the solution using LWYD Ritz vectors with static residual and the eigensolution supplemented by static correction were able to yield "exact" results.

This simple example clearly illustrate the advantage of the WYD Ritz reduction method when dealing with problems where local "static" responses are significant. There are however two specific problems that need to be considered when applying directly the WYD Ritz reduction method to problems that have singular mass matrices. The first problem is related to the choice of the starting vector and the second to spatial error norm calculations.

7.2.1 Starting vector

If the problem size is designated by n and s is the rank of matrix [M], then there are (n-s) spurious eigensolutions corresponding to multiple infinite eigenvalues. If the WYD Ritz method is applied directly from the original algorithm the starting vector, given by $[K]^{-1}\{f\}$, can not be made up of a linear combination of Ritz vectors of the original problem, that is $[K]^{-1}\{f\}$ is not in the space spanned by the [M]-orthonormal Ritz vectors basis and possesses components belonging to the subspace associated with $w^2_i = \infty$. As the algorithm proceeds these components will grow since their magnitude can not be fixed by the [M] orthonormality condition and they can potentially cause numerical difficulties. To eliminate this problem the starting vector should have a null projection on the set of eigenvectors associated with $w^2_i = \infty$. To ensure that the initial vector be contained in the original problem space the starting vector should be multiplied by [M] or by $[K]^{-1}[M]$ before its [M]-normalization. The problem with this approach when applied to the original WYD Ritz algorithm is that the

benefit of the static vector contribution to the response of massless DOF is lost and that the WYD Ritz solution will suffer from the same deficiency exhibited by the eigen-solution as illustrated by the numerical example of fig. 7.1.

The LWYD Ritz vector algorithm on the other hand is well suited to the application with singular mass matrices since the initial static vector $\{U_o\}$ is multiplied by the mass matrix before entering the recurrence relationship thus avoiding the growth of components belonging to the subspace of infinite eigenvalues. The static residual, if added to the basis, will however possess significant components belonging to the subspace of infinite eigenvalues and there will be a high frequency associated with this vector as given by the reduced eigenproblem $[K]^*[Z] = [M]^*[Z][\bar{w}^2]$ or $[T][Z] = [Z][\lambda]$.

7.2.2 Spatial Error Norm Calculations

If the applied loading has no components belonging to the subspace of infinite eigenvalues, that is no dynamic loads are applied at massless DOF, the error norm to monitor the degree of loading representation achieved by a truncated LWYD Ritz basis, as defined in chapter 3, can be applied directly without any problem. It should be noted that this condition will always be satisfied for earthquake loading.

On the other hand, in the case of forced vibration if the dynamic load has components assigned at massless DOF, the spatial error norms (which implicitly assumed that the loading distribution can be represented by a complete set of [M]-orthonormal LWYD Ritz vectors) will fail to provide a measure of the representation of these components by a truncated LWYD Ritz basis. In such a case, one can either formally apply the static condensation transformation to the dynamic loading and monitor the representation of the resulting virtual work equivalent or use the error norm based

on the magnitude of the static residual.

For this application the error norm based on the magnitude of the static residual (see section 4.2.1) should be written as

$$(|[M]\{U_1\}|_2 \;/\; |[M]\{U_o\}|_2) < tol \qquad [7.9]$$

since the magnitude of $\{U_1\}$ components is based on an [M]-orthonormality condition. The initial static vector $\{U_o\}$ will span the complete problem space, and the error norm defined in equation [7.9] will ensure a good representation of dynamic subspace components excited by the loading. When a good representation of dynamic components is ensured the solution can be supplemented by the static residual. If the benefit of static correction can be ascertained from frequency considerations prior to the analysis then a good response can be obtained with only a few vectors even if the error norm given by equation [7.9] is still relatively large. An example of the use of this error norm for the 40 DOF shear beam model with singular mass matrix is given in fig. 7.2.

It is shown that the error norm which monitors the magnitude of the static residual components lying in the subspace of the mass matrix, as defined by equation [7.9], exhibit a logarithmic type of decrement until its value reaches the order of the numerical roundoff of the computer. The error norm measuring the magnitude of all static residual components (including those of massless DOF) reaches a constant value after the calculation of a few vectors. This is due to the fact that the magnitude of components of massless DOF of the initial static vector $\{U_o\}$ are not reduced by the application of the mass orthogonality condition used to update the static residual as the algorithm proceeds. As the components lying in the subspace of the mass matrix are reduced the unreduced components of massless DOF start to dominate the ratio $|\{U_1\}|_2/|\{U_o\}|_2$ which stabilize to a near constant value. This value is therefore

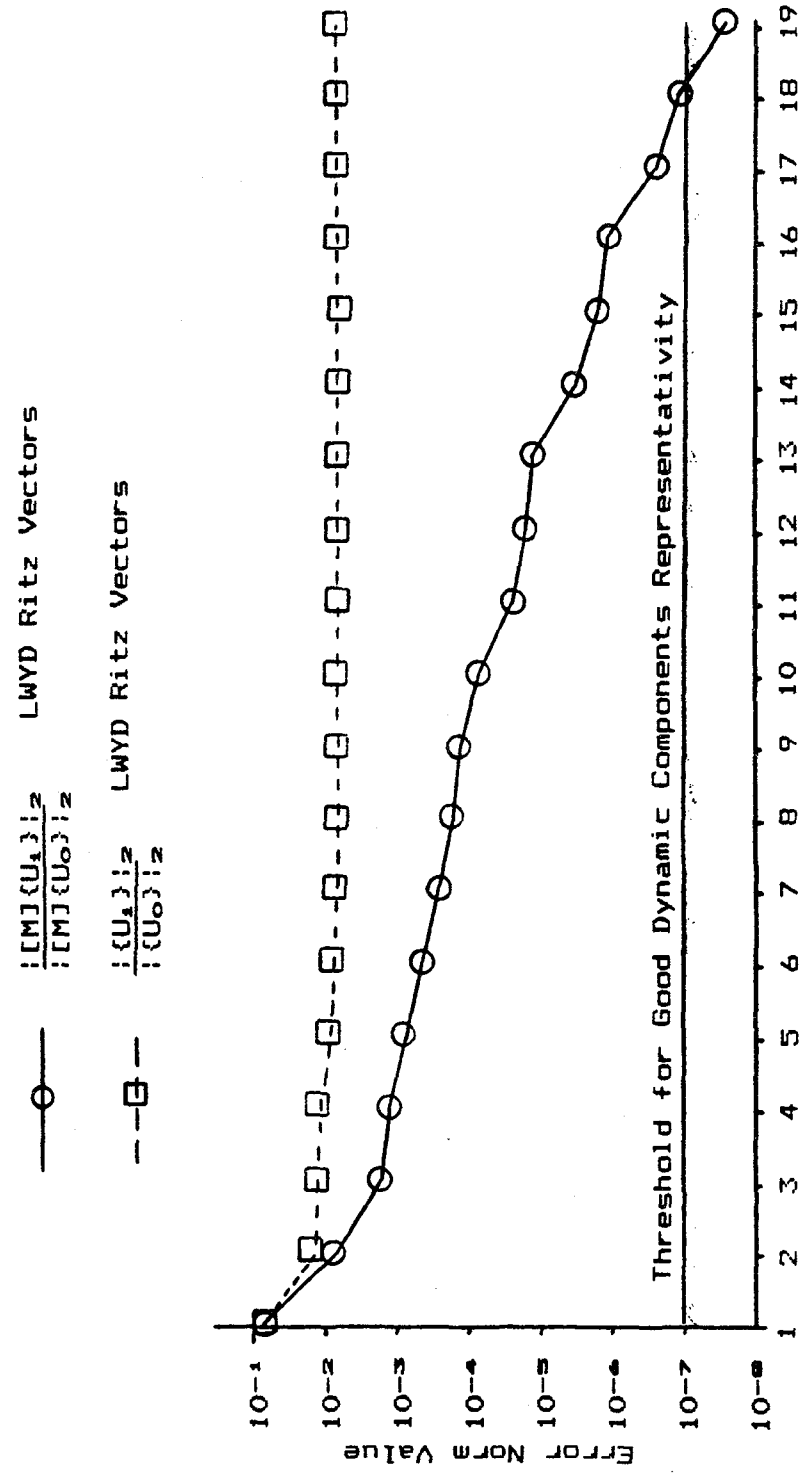

Fig. 7.2 Spatial Error Norm Calculations for Model with Singular Mass Matrix (see fig. 7.1)

not indicative of the representation of dynamic subspace components achieved by the basis.

7.3 Substructuring in Dynamic Analysis

In order to obtain a better set of reduced coordinates than those obtained from Guyan reduction, it is necessary to account for the inertia and damping forces of the substructures in a rational way. The internal dynamic behavior may, in many cases, be represented by a relatively few generalized coordinates representing the lowest vibration shapes of the structure. The effectiveness of this type of reduction depends on the nature of the loading acting on the structure as discussed previously.

The mass, stiffness, damping, and load matrices of each substructure can be partitioned according to:

$$\begin{bmatrix} M_{ii} & M_{ib} \\ M_{bi} & M_{bb} \end{bmatrix} \quad \begin{bmatrix} C_{ii} & C_{ib} \\ C_{bi} & C_{bb} \end{bmatrix} \quad \begin{bmatrix} K_{ii} & K_{ib} \\ K_{bi} & K_{bb} \end{bmatrix} \quad \begin{bmatrix} F_{ii} \\ F_{bb} \end{bmatrix} \qquad [7.10]$$

where "i" represents the interior coordinate and "b" the boundary or juncture coordinates.

The physical coordinates {U} may be represented in terms of component generalized coordinates {Y} by the coordinate transformation:

$$\{U\} = [\Psi]\ \{Y\} \qquad [7.11]$$

where $[\Psi]$ represents a matrix of preselected component modes. In the proposed application the following two types of Ritz modes will be considered: the LWYD Ritz vectors to represent the internal dynamic behavior of the substructures, and the constraint modes to connect the substructures.

7.3.1 Ritz Vector Calculation

The Ritz vectors calculated at the substructure level will be easily obtained by restraining the interface coordinates and using the LWYD Ritz vector algorithm. This approach will be consistent with the fixed interface normal modes method used in classical mode synthesis formulation which was shown by Curnier (7.6) to be the best technique for designs controlled by low frequency modes. The use of LWYD Ritz vectors instead of exact eigenvectors will provide a significant improvement to the procedure by reducing the numerical effort and generating accurate load dependent vectors.

In forced vibration analysis it might happen that only one or a few substructures are directly subjected to applied dynamic loads. In such a case, the spatial load distribution assigned to each substructure should be used to obtain the corresponding LWYD Ritz vectors. To obtain an accurate structural response in all substructures LWYD Ritz vectors should also be included for substructures that are not externally loaded. In fact the first LWYD Ritz vector should satisfy the fixed boundary conditions and somehow reflects the effects of the load in adjacent substructures as if the analysis was performed on the complete system treated as a single entity.

If the dynamic model was first validated by a static analysis, as it should always be, then the best choice will be to initiate the LWYD Ritz algorithm for the unloaded substructures from fictitious inertia loadings obtained from

$$\{f_{ii}\} = [M_{ii}]\ \{U_{ii}\}^{s} \qquad [7.12]$$

where $[M_{ii}]$ is a specified substructure mass matrix and $\{U_{ii}\}^{s}$ is the static deflected shape obtained from a static substructure analysis of the system subjected to the spatial distribution of dynamic loads. In the absence of information

on the static deformation shape $\{U_{ii}\}^*$ a uniform displacement field might be used. It should be noted that if no substructure LWYD Ritz vectors are used the transformed equations will be identical to those obtained from the Guyan reduction technique.

The spatial error norms can be computed at the substructure level to ensure an adequate representation of the specified substructure loading. The error in the final structural response of the complete system will in general be small if there is a good representation of the loading in each substructure, however since there is no interaction between the substructures at this stage of the calculation there is still an uncertainty related to the synthesis of errors that can not easily be quantified.

7.3.2 Constraint modes:

The physical coordinates $\{U\}$ may be partitioned into a set $\{U_{bb}\}$ relative to which constraint modes are to be defined; let $\{U_{ii}\}$ be the complement of $\{U_{bb}\}$. A constraint mode is defined by imposing a unit displacement on one physical coordinate of the $\{U_{bb}\}$ set and zero displacement on the remaining $\{U_{bb}\}$ coordinates while the $\{U_{ii}\}$ set is free. Thus the set of constraint modes will be defined as:

$$\begin{bmatrix} K_{ii} & K_{ib} \\ K_{bi} & K_{bb} \end{bmatrix} \begin{bmatrix} \psi_{ib} \\ I_{bb} \end{bmatrix} = \begin{bmatrix} 0_{ib} \\ R_{bb} \end{bmatrix} \qquad [7.13]$$

where $[R_{bb}]$ is the set of reactions at the $\{U_{bb}\}$ coordinates. From the top equation of [7.13], we get:

$$\psi_{ib} = -[K_{ii}]^{-1}\,[K_{ib}] \qquad [7.14]$$

The constraint mode matrix is thus:

$$\begin{bmatrix} \psi_{ib} \\ I_{bb} \end{bmatrix} = \begin{bmatrix} -K_{ii}^{-1} K_{ib} \\ I_{bb} \end{bmatrix} = \begin{bmatrix} T_i \\ I \end{bmatrix} \qquad [7.15]$$

This matrix corresponds to the static condensation transformation matrix of equation [7.6] presented in section 7.1.

7.3.3 System Synthesis at the First Level

The generalized coordinates employed in the component mode synthesis method can be identified as the boundary DOF needed for interconnection, $\{U_{bb}\}$, and interior DOF, $\{Y_i\}$, to represent the internal dynamic behavior. Thus, the displacements $\{U_{ii}\}$ can be expressed as:

$$\{U_{ii}\} = [X_i]\{Y_i\} + [T_i]\{U_{bb}\} \qquad [7.16]$$

for each component. This equation can be written in partitioned form as:

$$\begin{bmatrix} U_{ii} \\ U_{bb} \end{bmatrix} = \begin{bmatrix} X_i & T_i \\ 0 & I \end{bmatrix} \begin{bmatrix} Y_i \\ U_{bb} \end{bmatrix} \qquad [7.17]$$

where $\{U_{ii}\}$ are the internal DOF for the substructure
$\{U_{bb}\}$ are the boundary DOF needed for interconnection
$\{Y_i\}$ are the generalized Ritz coordinates for the substructure corresponding to Ritz vectors $[X_i]$
$[T_i]$ is the static condensation transformation, $-[K_{ii}]^{-1}[K_{ib}]$, obtained by back substitution of $[K_{ii}][T_i] = -[K_{ib}]$
$[I]$ is the identity matrix.

Equation [7.17] represents a coordinates transformation that can be used to reduce the dynamic equilibrium equations of each substructure according to:

$$[\bar{K}] = [A]^T [K] [A]$$
$$[\bar{M}] = [A]^T [M] [A] \qquad [7.18]$$

$$[\bar{C}] = [A]^T [C] [A]$$
$$\{\bar{F}\} = [A]^T \{F\}$$

where [A] is the displacement transformation from Ritz coordinates and retained DOF to component DOF according to equation [7.17].

If the retained system coordinates are ordered as:

$$\begin{bmatrix} Y_1 \\ Y_2 \\ . \\ . \\ . \\ U_{bb} \end{bmatrix} \qquad [7.19]$$

for substructures 1,2,..., the assembly of reduced substructures matrices can be done directly and will yield the global stiffness, mass, damping and load matrices shown in table 7.1 at the first substructure level.

7.3.4 Higher Substructure Levels

After the reduced mass and stiffness matrices of each substructure have been obtained they can be coupled together to form the next level of substructuring. If the number of boundary DOF $\{U_{bb}\}$ is very large, they may be reduced at the next substructure level considering some of them as internal unknowns. The procedure for reduction of each substructuring level is similar to that followed at the first level.

The repetition of this process will lead to the formation of a reduced set of coupled equations corresponding to the complete structural system. The reduced coupled set of equations may be integrated numerically by using a step-by-step algorithm or may be uncoupled using eigenvectors. Displacements and stresses are then obtained from equations

TABLE 7.1

Global System Matrices at First Substructure Level

Stiffness : $[K]_a$

$$\begin{bmatrix} X_1^T K_{11} X_1 & 0 & .. & 0 \\ 0 & X_2^T K_{22} X_2 & .. & 0 \\ .. & .. & .. & .. \\ .. & .. & .. & .. \\ .. & .. & .. & .. \\ 0 & 0 & 0 & K_{bb} + \sum_{i=1}^{i=n} K_{ib} T_i \end{bmatrix}$$

Mass : $[M]_a$

$$\begin{bmatrix} I & 0 & .. & .. & X_1^T M_{11} T_1 + X_1^T M_{1b} \\ 0 & I & .. & .. & X_2^T M_{22} T_2 + X_2^T M_{2b} \\ .. & .. & .. & .. & .. \\ .. & .. & .. & .. & .. \\ .. & .. & .. & .. & .. \\ \text{Sym} & & & M_{bb} + \sum_{i=1}^{i=n} (T_i^T M_{ii} T_i + T_i^T M_{ib} + M_{bi} T_i) \end{bmatrix}$$

Damping : $[C]_a$

$$\begin{bmatrix} X_1^T C_{11} X_1 & 0 & .. & X_1^T C_{11} T_1 + X_1^T C_{1b} \\ 0 & X_2^T C_{22} X_2 & .. & X_2^T C_{22} T_2 + X_2^T C_{2b} \\ .. & .. & .. & .. \\ .. & .. & .. & .. \\ .. & .. & .. & .. \\ \text{Sym} & & C_{bb} + \sum_{i=1}^{i=n} (T_i^T C_{ii} T_i + T_i^T C_{ib} + C_{bi} T_i) \end{bmatrix}$$

Loading : $\{F\}_a$

$$\begin{bmatrix} X_1^T F_1 \\ X_2^T F_2 \\ .. \\ .. \\ .. \\ F_{bb} + \sum_{i=1}^{i=n} T_i^T F_i \end{bmatrix}$$

Where C, F, I, K, M, T, X are appropriate vectors or matrices

of the form given by eq. [7.16].

In practical design applications, it is often interesting to know approximately the stresses at critical section locations when the final set of equations is assembled and solved before the backward pass required to evaluate the internal displacements and stresses in each substructure is done. Although, it is a requirement that all nodes interfacing two substructures be declared boundary nodes of the substructures for continuity purposes, boundary nodes can also be declared within a substructure for nodes not lying on a physical boundary. These fictitious boundary nodes can be linked at the global resolution level, the final substructure level, by "gauge" elements consisting of beams being only able to carry unidirectional loads. The area of the "gauges" should be selected to be of unit value, such that stresses can be obtained directly from the force calculation. The addition of these elements, at the global level, can significantly speed up the results interpretation phase of the analysis. Gauge elements should be used only in critical locations since an abusive repetition of this idea will increase significantly the number of boundary nodes and the cost of the solution.

7.4 Dynamic Ritz Condensation Algorithm

If one considers the interconnection of components it should be recognized that it is almost impossible to simply formulate a substructure LWYD Ritz system that will reflect exactly the effect of the rest of the substructures. The effects of adjoining substructures are only accounted for in the synthesis process by mean of constraint equations enforcing compatibility at the boundary DOF.

The LWYD Ritz vectors are generated from a recurrence relationship that uses a static solution to a fictitious inertial loading. It is therefore appropriate to think about

the generation of LWYD Ritz vectors using a static substructuring method. In fact from the coordinate transformation equation, it is shown that static substructuring is a subset of dynamic substructuring. The local inertia effects can be captured by an iterative procedure where the inertial load from internal DOF of each substructure will be condensed to boundary DOF at each step of the LWYD Ritz algorithm. The generation of global LWYD Ritz vectors using static substructuring data will be able to take account of the effect of adjoining substructures exactly. This method will be introduced as the Dynamic Ritz Condensation (DRC) algorithm.

The three important type of matrix computations that need to be performed to calculate LWYD Ritz vectors are:

- the mass-vector product of the form

$$\{Y\} = [M]\ \{U_{i-1}\} \qquad [7.20]$$

- the solution of a linear system of equations of the form

$$[K]\ \{X^*_i\} = \{Y\} \qquad [7.21]$$

- the quadratic transformation of the form

$$[K]^* = [X]^T\ [K]\ [X] \qquad [7.22]$$

These computations can be performed with substructure matrices rather than complete system matrices so that there is no need to generate and store the stiffness and mass matrice of the entire structure. Consider first the mass-vector product defined by equation [7.20]. The mass matrix [M] is formed by adding the contribution of each finite element such that we may write [7.20] as

$$\{Y\} = \left(\sum_{i=1}^{l} [a_i]^T [m_i] [a]_i\right) \{U_{i-1}\} \qquad [7.23]$$

where l is the number of finite elements

$[m_i]$ is the mass matrix of the ith element expressed in global coordinates

$[a_i]$ is a Boolean transformation matrix taking the contribution from $[m_i]$ to the final matrix [M].

It should be noted that for each element the matrix $([a_i]^T[m_i][a_i])$ is therefore an n x n matrix. Equation [7.23] can be rewritten as

$$\{Y\} = \sum_{i=1}^{l} \{ [a_i]^T [m_i] [a_i] \{U_{i-1}\} \} \qquad [7.24]$$

such that {Y} may be calculated without ever forming and storing the complete system matrix [M]. In practical computer operations the multiplication of matrices are never performed, instead an identification array is used to express the connectivity of the elements and the contribution of each element is added directly to assemble system matrices. The identification array can be used to perform the computation of equation [7.24] by considering the final position of each entry of $[m_i]$ in [M] such that the formal application of the $[a_i]$ matrix is never required.

The same approach can be implemented to assemble substructure matrices $[M_{ii}]$. The calculation with equation [7.24] basically implies the generation of the mass matrix [M] for each mass-vector product which will be relatively inefficient since this computation has to be repeated many time at each step of the LWYD algorithm. It will be more appropriate, if possible, to establish the system mass matrix, [M], only once and store it either in core or on low speed storage for use in all mass-vector product computations. This become a trivial operation if [M] is a lumped diagonal matrix.

The calculation of $\{X^*_i\}$ from equation [7.21] can be performed using only substructure stiffness matrices. Equation [7.21] can be interpreted as an equilibrium equation corresponding to the static response of the system to a pseudo-load vector $\{Y\}$ which can be solved using static substructuring concepts as explained in section 7.1. The boundary stiffness matrix $[\overline{K}_{bb}]$ will be assemble and decomposed only once. Each step of the LWYD Ritz algorithm will require the reduction of substructure components of the $\{Y\}$ vector to form the effective boundary load vector $\{\overline{F}_{bb}\}$, the solution of $[\overline{K}_{bb}]\ \{X^*_{i\,(bb)}\} = \{\overline{F}_{bb}\}$, the expansion to compute $\{X^*_{i\,(ii)}\}$ and assembly to obtain the complete $\{X^*_i\}$ vector.

Once the Ritz basis has been calculated we need to establish the reduced set of equilibrium equations expressed in WYD Ritz coordinates or in Lanczos coordinates. If advantage is taken of the tridiagonal form of the reduced system, there will be no need to compute the transformation $[X]^T[K][X]$ and the procedure will be most efficient. If the computation of $[X]^T[K][X]$ is required, the product $[K][X]=[E]$ can first be evaluated by the same procedure outlined for the mass-vector product substituting $[k_i]$ an elementary stiffness matrix for $[m_i]$ in equation [7.24]. The product $[X]^T[E]$ can then be calculated directly or by using matrix partitioning keeping in mind that the rules used in the calculation with partitioned matrices follow from the definition of matrix addition, substraction and multiplication as if submatrices were ordinary matrix elements. The Dynamic Ritz Condensation algorithm can thus be summarized as follow :

- generate partitioned substructures stiffness, mass and load matrices,

- assemble and store complete system mass matrix [M],

- calculate static substructure transformation matrix $[T_i]$,

- transform substructure stiffness matrices, assemble global $[K]_o$ matrix, triangularized $[K]_o$,

- solve for initial static vector by static substructuring,

    - reduce loads,
    - solve global set of equations,
    - backsubstitute for complete vector,

- compute Ritz basis from the LWYD Ritz vector algorithm, the only modifications are in the solution for new vectors at each step of the algorithm by the

    - reduction of pseudo-load vector $[M]\{U_{i-1}\}$,
    - solution of boundary Ritz displacements,
    - expansion and assembly of complete vectors.

The relative efficiency of the DRC algorithm compared to classical dynamic substructuring using synthesis of LWYD Ritz vectors, as developed in section 7.3, will be discussed in the next section dealing with a specific numerical example.

7.5 Application of Dynamic Substructuring using LWYD Ritz Vectors

In order to test the proposed dynamic substructuring algorithms the 40 DOF shear beam model with complete diagonal mass matrix presented in section 4.3.2 was divided into four substructures, SSA, SSB, SSC and SSD as shown in fig. 7.3. Four boundary displacements were retained for the analysis. The structural response to concentrated wave loading applied in SSD was first calculated by the method of component mode systhesis adding generalized coordinate one by one only in SSD. The following vector shapes were used:

- "exact" eigenvectors,
- "exact" eigenvectors + static correction,

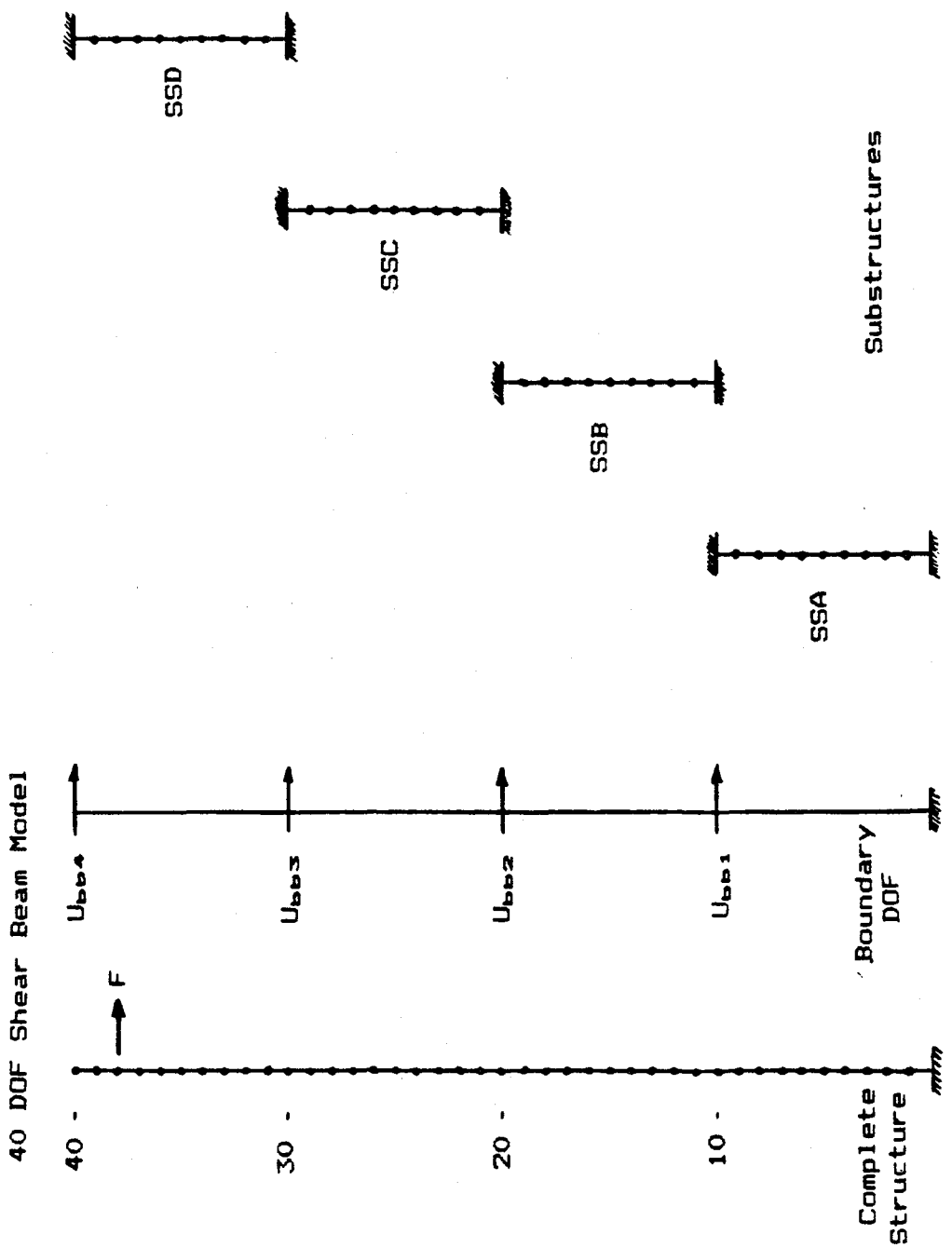

Fig. 7.3 Mathematical Model for Dynamic Substructuring Applications
(see fig. 4.4 for material and geometric properties)

- LWYD Ritz vectors with static residual obtained from the specified loading distribution.

It is interesting to note that static correction terms can be added to the solution using "exact" eigenvectors on a local basis to improve the results obtained from modal truncation. The expression used to calculate $\{U_{ii}\}$ by this approach was

$$\{U_{ii}\} = [K_{ii}]^{-1}(\{f_{ii}\} - \{f_{r,ii}\}) + [\emptyset]\{Y_i\} + [T_i]\{U_{bb}\} \quad [7.25]$$

where $\{f_{r,ii}\} = [M][\emptyset][\emptyset]^T\{f_{ii}\}$

and $[\emptyset]$ is a truncated set of exact mode shapes of the substructure obtained with fixed boudaries.

The periods of the first few approximate modes of vibration obtained from any vector basis were close to the exact natural periods of vibration. The structural response in terms of maximum error in SSD beam shear forces is shown in fig. 7.4. If a maximum error of 1% is used to define a fully converged solution, the use of exact eigenvectors to capture the internal behavior of SSD required a full basis of 9 eigenvectors while 5 eigenvectors supplemented by static correction or 4 LWYD Ritz vectors with static residual were sufficient to obtain the same results. It should be observed that the response in SSA, SSB and SSC can be considered almost independent of the number of generalized coordinates retained to capture the internal behavior of SSD. A constant maximum error of 9% was obtained in SSC from any vector basis.

In order to obtain convergence in SSA, SSB, and SSC generalized coordinates were added to capture their internal behavior. The following vector bases were used:

- "exact" eigenvectors,
- LWYD Ritz vectors obtained from $\{f_{ii}\} = [M_{ii}]\{U_{ii}\}^*$ as initial loading distribution, with $\{U_{ii}\}^*$ taken to be

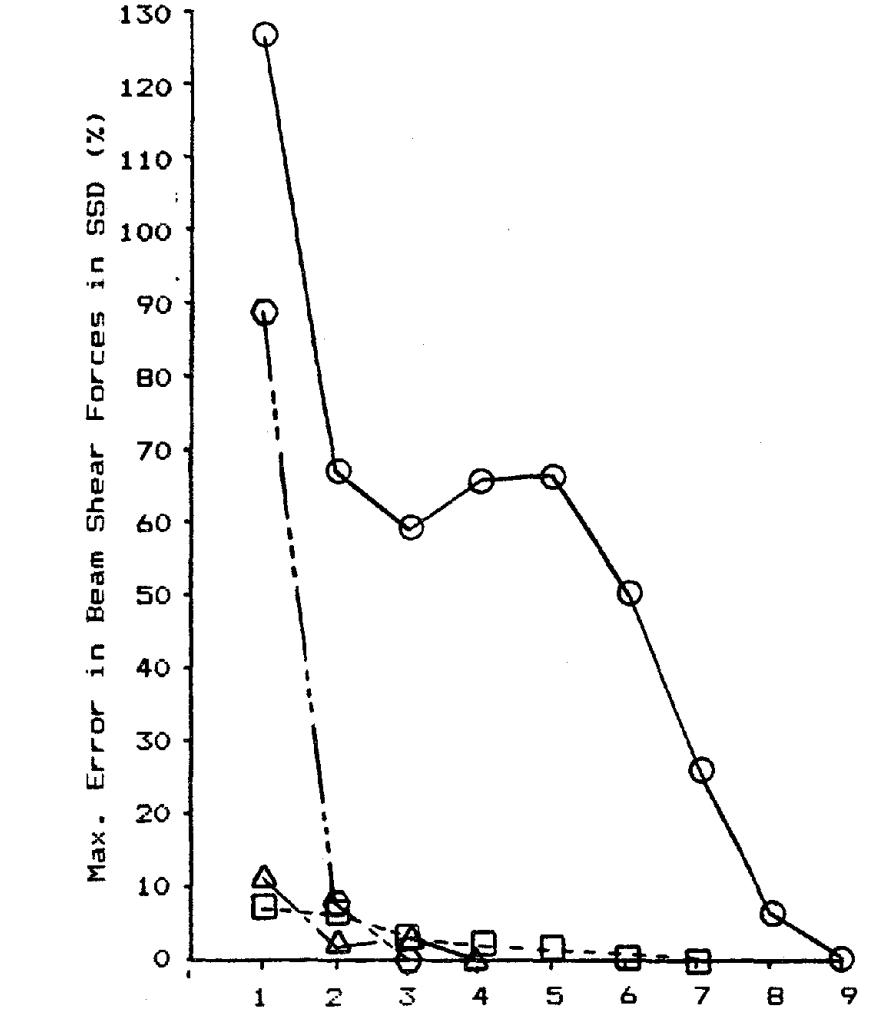

"Exact" Eigenvectors (SSD only)
"Exact" Eigenvectors + Static Correction (SSD only)
LWYD Ritz Vectors with static Residual (SSD only)
DRC Algorithm (exact LWYD Ritz basis of complete system)

Fig. 7.4 Convergence Characteristics of Various Dynamic Substructuring Methods

uniform displacements and displacements obtained from a full static substructure analysis to the applied SSD loading distribution.

It was found that the addition of 1 generalized coordinate in each substructure was sufficient to obtained convergence from any basis, the most accurate results being obtained from LWYD Ritz vectors generated from fictitious loading corresponding to static displacements analysis. In summary, the total number of DOF (boundary and internal) that had to be uncoupled in the eigensolution of the global matrix system for steady state response calculations, to obtain shear force convergence in all substructures, was the following:

- "exact" eigenvectors : 16
- "exact" eigenvectors + static correction : 12
- LWYD Ritz vectors : 11

showing that the most efficient vector basis for synthesis computations is obtained from LWYD Ritz vectors.

The results obtained from the DRC algorithm corresponding to the response obtained from an exact LWYD Ritz basis of the complete system, are also reported in fig. 7.4 for comparison purposes. Only 3 LWYD Ritz vectors were necessary by this approach such that the size of the reduced eigenproblem was of order 3. If one considers the number of numerical operations required for convergence by the WYD Ritz synthesis method and the DRC algorithm it was found, for this particular example, that the opreation counts are roughly equivalent for the formation of the global matrix system, $[K]_a[Z] = [M]_a[Z][\bar{w}^2]$ (11 x 11) or the reduced WYD Ritz system, $[K]^*[Z] = [M]^*[Z][\bar{w}^2]$ (3 x 3). The difference in the two methods comes from the topology of the global or reduced system of equations that must be uncoupled using eigenvectors.

The eigenproblem generated by the WYD Ritz synthesis method is larger than the eigenproblem obtained from the DRC algorithm, moreover, there is mass coupling terms in the $[M]_s$ matrix such that a numerical algorithm adapted to the solution of the generalized eigenproblem must be used. On the other hand, the eigenproblem obtained from the DRC algorithm is already cast in the standard form since $[M]^*$ corresponds to the identity matrix from orthonormality conditions. For this example, the solution using the DRC algorithm was thus found to be more efficient than the WYD Ritz synthesis method. It is anticipated that if accurate results are required in all substructures, the DRC algorithm will be able to maintain a numerical advantage over the WYD Ritz synthesis method for a wide range of applications by generating reduced WYD Ritz systems that require fewer generalized DOF for convergence.

CHAPTER 8

Nonlinear Dynamic Analysis by Direct Superposition of Ritz Vectors

The increasing importance of nonlinear analysis is due to the need for the structural engineer to develop realistic modelling and accurate analysis of critical structural components. The most important factors in the efficiency of dynamic calculations are generally associated with the solution procedure employed. The selection of an appropriate solution technique can bring an analysis to an economic possibility and technical feasibility without making compromises in the modelling to the point of rendering questionable any results obtained.

For certain classes of problems, the use of direct superposition of Ritz vectors for nonlinear dynamic analysis can present an advantageous solution strategy as compared to the classical step-by-step integration of the fully coupled system of nonlinear equations. This chapter presents various solution strategies to apply the WYD Ritz reduction method to globally and locally nonlinear dynamic problems.

8.1 Source and Extent of Nonlinear Behavior

The major sources of nonlinearity in a structural system can be classified as follows:

1- Geometric nonlinearity: This type of nonlinearity arises through nonlinearity in the strain-displacement relations and through the need to formulate equilibrium conditions in the deformed configuration.

2- Material nonlinearity: This type of nonlinearity arises through nonlinearity in the stress-strain or member-force

deformation relationships.

3- Force nonlinearity: This type of nonlinearity occurs when the forces are a function of the displacements of the system. Examples are hydrodynamic loadings on offshore platforms, or pressure loadings on thin membranes.

After the type and severity of nonlinearities affecting the behavior of a particular system have been identified, an important aspect in the choice of the solution scheme is to evaluate the extent to which such nonlinear behavior can be expected. In many practical problems complete general nonlinear analysis capabilities are not required when the structure may exhibit nonlinearities in only one or a few local regions while the rest of the system remains linear elastic. Efficient numerical solution procedures can be developed if advantage is taken of the prior knowledge of the nonlinear localizations. A summary of the possible solution techniques for nonlinear dynamic problems will next be presented. The extension of these techniques to the use of substructuring for local nonlinearities will be discussed in section 8.4.

8.2 Solution Techniques for Nonlinear Dynamic Analysis

Solution techniques can be classified according to the manner in which they attempt to solve the equations of motion written in the form:

$$[M]\{\ddot{U}\} + [C_{NL}]\{\dot{U}\} + [K_{NL}]\{U\} = \{F_{NL}\} \qquad [8.1]$$

where:

$[M]$ is the consistent or lumped mass matrix usually taken as a constant in time and independent of displacement parameters,

$[C_{NL}]$ is the nonlinear damping matrix dependent upon

velocities and displacements,

$[K_{NL}]$ is the nonlinear stiffness matrix dependent upon displacements,

$\{F_{NL}\}$ is the applied force vector that can depend upon displacements.

The most obvious division of the solution techniques is based upon whether the approach seeks to use direct integration techniques or vector superposition methods to solve equation [8.1]. In both cases, the solution procedure is based on an incremental step-by-step solution of the governing equations of motion.

The solution requires that for each time step, the incremental dynamic equilibrium equations be established and then solved using equilibrium iterations. This can be interpreted as the solution of an equivalent nonlinear static problem at every time step. Integration procedures for solving equation [8.1], can be based on either the tangent stiffness method or the pseudo-force approach. The evaluation and decomposition of the tangent stiffness matrix (to speed up the convergence of the equilibrium iterations) at each time step is a costly procedure. Depending on the problem considered, a new tangent stiffness matrix need not to be calculated in each time step. In many analyses, the original stiffness matrix can be employed throughout the complete response calculation and all nonlinearities can be taken fully into account in the evaluation of pseudo-forces on the right hand side of the equations of motion.

Let:

$$[C_{NL}] = [C_L] + [C_N]$$

and

$$[K_{NL}] = [K_L] + [K_N] \qquad [8.2]$$

where $[C_L]$ and $[K_L]$ are the damping and stiffness matrices representing the reference state of the structure. $[C_N]$ and $[K_N]$ are the damping and stiffness matrices dependent on velocities and displacements. If equations [8.2] are substituted in equation [8.1], we get:

$$[M]\{\ddot{U}\} + [C_L]\{\dot{U}\} + [K_L]\{U\} = \{F_{NL}\} - \{F_N\} \qquad [8.3]$$

where the pseudo-force vector is defined by:

$$\{F_N\} = [C_N]\{\dot{U}\} + [K_N]\{U\} \qquad [8.4]$$

If the nonlinear properties are restricted to a small portion of the structure, the matrices $[C_N]$ and $[K_N]$ will be sparse and the cost of pseudo-forces evaluation will be small if computations are performed at the element level.

8.2.1 Direct Integration Methods

A lot of different procedures are currently available for direct step-by-step integration of the fully coupled equations of motion. The critical parameter in the use of these techniques is generally the largest value of the time step which can be used to provide sufficiently accurate results. The ultimate comparison standard for any method is therefore the total cost per satisfactory analysis.

Various explicit and implicit integration operators have been used in structural dynamic calculations. The eigenmode of the complete finite element assemblage with the shortest period is usually critical to fix the time step for an accurate and stable application of explicit integration operators. The unconditional stability of many single step implicit schemes (as applied in linear analysis) has favored their use for practical nonlinear analysis. The time step of implicit operators is selected only from consideration of the required accuracy of solution. Implicit schemes are

characterized by the dependence of the displacement vector $\{U_{j+1}\}$ at the end of the time step upon the loads, damping and stiffness matrices evaluated at the end of the j+1 step. This requires either iterative calculations at each time step or an aproximation procedure using some type of extrapolation. Implicit formulations leads to simultaneous equations relations where the coefficient matrix is a combination of the mass, stiffness, and damping matrices.

The most popular schemes are:

- the Newmark Beta method,
- the Houbolt method,
- the Wilson θ method (unconditionally stable for linear problem for $\theta > 1.37$).

A detailed presentation of the application of these methods to the incremental form of the equilibrium equation in nonlinear dynamics can be found in references 1.2 and 3.2. Computer implementation of incremental integration with corrective equilibrium iterations algorithm at each time step have been summarized by Bathe and Cimento in reference 8.2. A review of the recent developments in direct time integration methods for nonlinear structural dynamics has been reported by Fellipa and Park in reference 8.7.

8.2.2 Vector Superposition Methods

The integration procedure mathematically corresponds to simultaneous integration of all modes using the same time step. The possible use of vector superposition in nonlinear analysis should not be surprising since only a change of basis to a more effective system of equations is performed. Although, at a first glance, modal methods in nonlinear problems appears to violate the well known fact that superposition principle are not applicable to nonlinear systems, Nickell (8.14) suggested the use of the principle of

"local modal superposition". This principle states that small harmonic motions may be super-imposed upon large static motions and that small forced motions may be represented in terms of the nonlinear (tangent stiffness) frequency spectrum.

Vector superposition methods can be more efficient than direct step-by-step integration of the unreduced coupled system in two different ways. If the coordinate transformation completely uncouples the equations of motion, time integration may be performed with more precise methods than the unconditionally stable methods used in direct time integration. The time step required by vector superposition will also be generally greater than that required by the direct method. The time steps may also be subdivided to consider separately the integration of higher modes of the reduced system. If the time steps required by the direct integration and the vector superposition solution are the same, the vector superposition approach can still be more economical if the amount of computations for the application of the coordinate transformation and solution of the reduced system is smaller than solving the complete set of equations directly. This will be true if the number of required transformation vectors, r, is much less than, n, the order of the original system. The larger the structural system the more likely that this will be the case. Moreover, approximate eigensolutions of the reduced system of equations will provide knowledge of the spectrum of frequencies for the dominating modes throughout the nonlinear response.

The effectiveness of vector superposition techniques in nonlinear dynamic problems depends on:

- The number of basis vectors required to accurately simulate the response. This is a function of the frequency content and spatial distribution of the loading versus the vibrational characteristics of the system.

- The frequency of updating or recalculating the basis vectors which is a function of the rate of change of these vectors with time.

- The efficiency in the algorithm used to calculate the initial deformation vectors and updating them.

It should be noted that the actual (instantaneous) frequencies of the system are continuously changing during the nonlinear response. If the system stiffens during the response history, the frequencies become larger and the number of selected vectors based on a linear analysis will probably be conservative. However, in analysis of softening structure (elasto-plastic conditions), the number of generalized displacements may have to be larger than in linear analysis.

8.3 Selection of Transformation Vectors for Superposition Methods

In a first approach, the change of basis could be performed at each time step using the exact mode shapes corresponding to time t. Such a procedure would require the solution of the generalized eigenproblem:

$$ {}^{t}[K]\ {}^{t}[\Phi] = [M]\ {}^{t}[\Phi]\ {}^{t}[\omega^2] \qquad [8.5] $$

where the superscript "t" indicates that the stiffness matrix, mode shapes and frequencies correspond to the instantaneous configuration at time t. It is questionable if such a scheme would be effective due to the large numerical effort involved.

Nickell (8.14) presented an algorithm using subspace iteration to extract only the lowest modes from the generalized eigenvalue problem that represents the initial state of the structure. An iterative procedure based on a

first order perturbation theory of the eigenvalue problem was then used to update the vector basis as nonlinearities were felt. For the one dimensional problems considered by Nickell, about 10% more computer time was required in using modal technique as compared to direct methods. It was expected that this economic penalty might be eliminated when models with significantly larger bandwidths were to be analysed.

More recently, Idelsohn and Cardona (8.11) presented a reduction procedure based on a vector basis selection using tangent eigenmodes together with some modal derivatives that indicate the way in which the spectrum is changing. The calculation of the derivatives, which are not evaluated in a standard finite element code, is performed by special subroutines at the level of element computations. The calculation of modal derivatives requires the the same amount of computations as the evaluation of an internal force vector and associated displacements. An implicit integration operator, used along with error estimates and an efficient equilibrium iteration algorithm, was able to provide economical solutions for the nonlinear problems reported.

For mildly nonlinear problems with localized nonlinearities, the use of modal techniques in conjunction with the pseudo-force method seems promising. This is because a single set of modes (based on linear analysis) can be used throughout the analysis. Only the residual forces due to nonlinearities need to be transformed in each time step. This approach was suggested by Bathe and Gracewski (8.3). It should be noted that although the reduced stiffness, damping and mass matrices are diagonal (Rayleigh dumping assumed) the reduced system is coupled by the nonlinear force vectors, so a direct time integration must be employed. In a number of simple nonlinear structural dynamic problems, modal methods were found to be competitive with direct integration operators (see ref. 8.3, 8.8, 8.13, 8.16,

8.19). However, it should be noted that experienced analysts are required if the technique, in its present form, is to be efficiently used since the choice of the number of modes retained greatly affects both the accuracy and cost of the analysis.

It is believed that the use of the LWYD vectors can improve the effectiveness of the modal methods in nonlinear dynamics since it provides a more economical way to generate a vector basis to transform the equations of the system. Moreover, the WYD Ritz method usually converges with fewer vectors than if exact eigenvectors are used leading to further computational advantages. In fact, Idelsohn and Cardona (8.12) extended the procedure developed in reference 8.11 to use Ritz vectors calculated from the original algorithm proposed by Wilson, Yuan and Dickens (1.17) to treat geometrically nonlinear dynamic problems. Comparisons made with computations performed using exact tangent modes and their derivatives have shown that the basis obtained from the WYD Ritz method (including some derivatives) was easier to generate and gave results of equal or better accuracy than if exact eigenmodes (and associated derivatives) were used. Alternate solution strategies to apply the WYD Ritz method to globally nonlinear problems will next be presented.

8.4 Solution Strategies for Globally Nonlinear Systems

Whenever the basis vectors are no longer representative of the dynamic behavior, the equilibrium iteration procedure will fail to converge and a change of basis should be performed. The current set of vectors can be modified and vectors can also be deleted or added to the basis.

A first approach to modify the LWYD vector basis is to recalculate new vectors, based on the tangent stiffness at each step of the time integration. Even if the cost of generating LWYD vectors is much smaller than calculating

exact eigenvectors, this technique still remain expensive since a complete factorization of the tangent stiffness matrix will be required at each step. If the nonlinearities are not too severe a better way will be to modified the current vector basis to take into account the nonlinearities without factorization of the tangent stiffness matrix. For that purpose the application of the following perturbation technique is suggested

$$
\begin{aligned}
&{}^{t}[X]^{T}\ {}^{dt}[DK]\ {}^{t}[X] = {}^{dt}[DK]^{*} \\
&{}^{t}[K]^{*} + {}^{dt}[DK]^{*} = {}^{t+dt}[K]^{*} \qquad [8.6] \\
&{}^{t+dt}[K]^{*}\ {}^{t+dt}[Z] = [M]^{*}\ {}^{t+dt}[Z]\ {}^{t+dt}[w^{2}] \\
&{}^{t+dt}[X] = {}^{t}[X]\ {}^{t+dt}[Z]
\end{aligned}
$$

where ${}^{t}[X]$ is the current LWYD Ritz basis at time t,

${}^{t}[K]^{*}$ is the current reduced stiffness,

${}^{dt}[DK]$ is the modifications to the ${}^{t}[K]$ matrix due to the nonlinearities,

${}^{t+dt}[X]$ is the updated LWYD Ritz basis at time t+dt.

For each basis update a solution of the reduced eigenproblem will therefore be required.

If new vectors need to be added to the basis, the triangularized stiffness matrix can be updated directly after a certain number of time steps to generate these vectors. An algorithm proposed by Benett (8.4) has been adapted for this purpose by Argyris and Roy (8.1) to structural mechanics problems. The break even point for complete matrix triangularization was established when the number of modified DOF do not exceed 35% of the semibandwidth of the stiffness matrix.

If the modified DOF are concentrated in the highest numbered equations, the application of the modified Cholesky algorithm proposed by Row et al. (8.18) will be most efficient to reformulate the triangularized stiffness matrix.

Iterative equation solvers can also be used as an inner loop of the Newton's method to solve the linearized system of equations at each time step. Classical Lanczos vectors have been used in a conjugate gradient algorithm for that purpose. The procedure was developed by Nour-Omid (8.15) for the solution of static nonlinear problems. The same approach can be extended to nonlinear dynamic problems using LWYD vectors to possibly improve the convergence characteristics of this technique.

8.5 Solution Stategy for Locally Nonlinear Systems

Many types of structures exhibiting local nonlinear behavior can be identified. Some examples are elastic structures mounted on yielding supports to protect them against earthquake motions or offshore platforms supported by soil conditions that offer nonlinear response. Additional examples are given by structures that are designed to permit uplift in response to earthquake excitation or in structures with joints that may open or close during loading. The determination of the possible regions of nonlinearity at the beginning of the analysis is a key factor since it permits the use of substructuring procedures as discussed in chapter 7, to reduce the size of the nonlinear problem to a minimum.

Our attention will now be restricted to structural systems where a small number of members experience nonlinear material behavior since this represents one of the most important and common type of nonlinearity occuring in practical dynamic analysis. The basic idea of the proposed method will be to use LWYD Ritz vectors to reduce the elastic region of the structure to a small number of generalized

coordinates. The DOF associated with the nonlinear behavior will be retained in the modelling. A step-by-step nonlinear analysis will then be conducted on a relatively small system in which only the stiffness of the nonlinear elements will need to be considered at each time step.

8.5.1 Substructuring for Local Nonlinearities

Clough and Wilson (1.6) have presented a review of the applications of the substructuring concept to the dynamic response analysis of structures having localized nonlinearities. One of the proposed algorithm used exact substructure eigenvectors to reduce the elastic region of the system to a small number of generalized coordinates, $\{Y_{LL}\}$, using the transformation matrix

$$\begin{bmatrix} U_{LL} \\ U_{NN} \end{bmatrix} = \begin{bmatrix} \emptyset_{LL} & -K_{LL}^{-1} K_{LN} \\ 0 & I \end{bmatrix} \begin{bmatrix} Y_{LL} \\ U_{NN} \end{bmatrix} \qquad [8.7]$$

where $[\emptyset_{LL}]$ are substructure eigenvectors obtained with restrained nonlinear DOF and the subscripts "L" and "N" correspond to the linear and nonlinear DOF respectively. Equation [8.7] is used to reduce the partitioned system matrices according to the procedure presented in section 7.3.3, with the understanding that the linear DOF correspond to internal DOF "i" and the nonlinear DOF to boundary DOF "b".

It was showm in chapter 7 that transformations of the form described by equation [8.7] will be more efficient if LWYD Ritz vectors are used instead of exact eigenvectors. There is however one problem with this formulation, that is the LWYD Ritz vectors calculated for the reduction of the linear portion of the structure will not represent the effects of the loading applied to the nonlinear DOF since these are assumed fixed during the vectors computation. If it is supposed that LWYD Ritz vectors of the complete system can be obtained directly (or using the DRC algorithm) the

following modifications should eliminate this problem. The LWYD Ritz vectors of the complete reference system without any restraints of the nonlinear DOF are initially computed and partitioned according to

$$\begin{bmatrix} {}^{C}X_{LL} \\ {}^{C}X_{NN} \end{bmatrix} \qquad [8.8]$$

where the superscript "C" is used as a reminder that the vectors were calculated from complete system matrices. the transformation matrix of equation [8.7] can be rewritten as

$$\begin{bmatrix} U_{LL} \\ U_{NN} \end{bmatrix} = \begin{bmatrix} {}^{C}X_{LL} + K_{LL}^{-1}\, K_{LN}\, {}^{C}X_{NN} & -K_{LL}^{-1}\, K_{LN} & Y_{LL} \\ 0 & I & U_{NN} \end{bmatrix} \qquad [8.9]$$

where the term $[K_{LL}]^{-1}[K_{LN}]\{{}^{C}X_{NN}\}$ is used to modify the linear portion of the vector basis for nonzero Ritz displacements, $\{{}^{C}X_{NN}\}$, corresponding to nonlinear DOF. By this approach the LWYD Ritz vectors are generated from the complete system matrices such that the spatial error norms, as presented in chapter 3, can be applied without any synthesis approximation.

8.5.2 Solution Algorithm

The complete solution algorithm using substructuring for locally nonlinear systems is divided into two phases,

- the reduction of the number of DOF describing the linear part of the structure,

- the nonlinear step-by-step solution of the reduced system of equations considering changes in the nonlinear elements.

A summary of the procedure is presented in table 8.1. The important feature of this solution method is that any changes in the stiffness of nonlinear elements will not affect the representation of the linear portion of the structure leading

TABLE 8.1

Solution Procedure for Locally Nonlinear System

(Adapted from Clough and Wilson (1.6))

I. Initial Calculations

A. Establish and Partition System Matrices (linear)
("N" refers to expected location of nonlinear DOF)

$$[K] \qquad [C] \qquad [M] \qquad \{F\}$$

$$\begin{bmatrix} K_{LL} & K_{LN} \\ K_{NL} & K_{NN} \end{bmatrix} \quad \begin{bmatrix} C_{LL} & C_{LN} \\ C_{NL} & C_{NN} \end{bmatrix} \quad \begin{bmatrix} M_{LL} & M_{LN} \\ M_{NL} & M_{NN} \end{bmatrix} \quad \begin{bmatrix} F_{L} \\ F_{N} \end{bmatrix}$$

B. Compute and partition linear LWYD Ritz vectors of the complete system with expected nonlinear DOF unrestrained

$$\begin{bmatrix} {}^{c}X_{LL} \\ {}^{c}X_{NN} \end{bmatrix}$$

C. Form Coordinate Transformation and Reduce System Matrices

$$\begin{bmatrix} U_{LL} \\ U_{NN} \end{bmatrix} = \begin{bmatrix} {}^{c}X_{LL} + K_{LL}^{-1} K_{LN} {}^{c}X_{NN} & -K_{LL}^{-1} K_{LN} \\ 0 & I \end{bmatrix} \begin{bmatrix} Y_{LL} \\ U_{NN} \end{bmatrix}$$

or $\{U\} = [A] \{U\}^{R}$

$$[K]^{R} = [A]^{T}[K][A] \qquad [C]^{R} = [A]^{T}[C][A] \qquad [M]^{R} = [A]^{T}[M][A]$$

II. Step-by-step solution at t = dt, 2dt, ...jdt

A. Form incremental stiffness for nonlinear elements $[K_{NN_j}]$

B. Form incremental load vector

$$\{DF\}^{R} = [A]^{T} \{DF\}$$

C. Form reduced incremental equations

$$[M]^{R} \{DU_j\}^{R} + [C]^{R} \{DU_j\}^{R} + ([K]^{R} + [K_{NN_j}]) \{DU_j\}^{R} = \{DF\}^{R}$$

D. Solve for $\{DU_j\}^{R}$ and $\{U_j\}^{R}$ by step-by-step method

E. Return to step II A.

to an efficient algorithm. Moreover, if the expected location of the nonlinearities is to be modified, the original set of Ritz shapes, $\{^{c}X\}$, needs only to be partitioned differently such that the generation of a new Ritz basis is avoided.

CHAPTER 9

Conclusion

9.1 Summary

This report has presented theoretical formulations and computational procedures that will be most efficient for the dynamic analysis of large structural systems. The numerical techniques are essentially based on the direct superposition of a special class of Ritz vectors generated from the spatial distribution of the dynamic load. The method first introduced by Wilson, Yuan and Dickens (1.17) as an economic alternative to classical mode superposition, recognized the special nature of structural dynamic problems mainly that a dynamic analysis can be interpreted as a static analysis which takes into account inertia forces.

The report first established a formal mathematical framework for the WYD Ritz reduction method by showing that the algorithm used to produce WYD Ritz vectors is similar to the method used to produce Lanczos vectors. Error norms to measure the representation of the spatial distribution of the dynamic load achieved by a truncated WYD Ritz basis and to establish a relationship between WYD Ritz solutions and exact eigensolutions were developed. Computational variants to generate load dependent vector bases for dynamic analyses were then studied. One of the proposed formulations, the LWYD algorithm, was shown to be more stable than the original WYD algorithm and allows a better control of the static correction effects included in the method.

Theoretical developments and computational procedures to apply the proposed Ritz reduction method to three dimensional earthquake response spectra analysis, to analysis of systems subjected to multispatial dynamic load distributions, to multilevel substructure analysis and to

nonlinear dynamic problems were presented. Solution algorithms related to linear systems were evaluated by numerical applications on simple structural models to validate the techniques for industrial applications.

9.2 Conclusions

The main conclusions of this study can be summarized as follows :

- the convergence characteristics of the WYD Ritz reduction method follow very closely the convergence characteristics of exact eigensolutions supplemented by static correction or modal acceleration to approximate the contribution of higher modes not retained in the usual modal summation,

- the WYD Ritz reduction method includes the benefit of static correction directly in the vector basis used to transform the equations of motion. This was shown to be very effective as new pseudo-static solutions do not need to be calculated at each time step even when the spatial distribution of the load varies with time,

- accurate structural responses were obtained from Ritz bases that were able to achieve a good representation of the specified dynamic loads (from 90% to 100% as defined by the proposed spatial error norms) and that produced retained structural frequencies, from the contribution of dynamic vectors, that spanned adequately the frequency range of the applied loading,

- the solution of the reduced eigenproblem in Ritz coordinates, applied to convergent Ritz bases that included static residual components, indicated that mass and stiffness orthogonal Ritz shapes were generally good approximations to exact eigenvectors up to the frequency range of the applied loading,

- load dependent Ritz bases that completely uncouple the equations of motion can be constructed at a cost of approximately one seventh of that required to obtain exact eigenvectors, with much improved convergence characteristics,

- a further 20% reduction in computer execution time is possible for linear systems if advantage is taken of the similarity between the algorithm used to generate load dependent Ritz vectors and Lanczos vectors to cast directly the reduced Ritz system in tridiagonal form,

- dynamic response analyses based on the tridiagonal form of the reduced system were found to exhibit poorer resolution than solutions based on the application of the formal transformation $[X]^T[K][X]$ for structural systems that possess repeated eigenvalues,

- an algorithm to ensure that the Ritz vectors maintain global orthogonality as they are generated is essential in order to apply the method to large structural systems,

- the load dependent Ritz reduction method, using either single vector iterations or simultaneous vector iteration, was shown to be effective in reducing the numerical effort and improving the convergence characteristics of three dimensional earthquake analysis by the response spectra method,

- a block form of the load dependent Ritz reduction method can effectively be used in transient dynamic analysis where the loads are specified by a relatively small number(say from 1 to 10) of dynamic load distributions,

- the method can be advantageously applied to multilevel dynamic substructure analysis by producing a better convergence rate of a component mode synthesis type of

formulation or by using substructuring concepts directly in the recurrence relationship used to calculate the Ritz basis of the complete system without any synthesis approximation,

- the method has the potential to be extended to treat nonlinear dynamic problems more effectively than if exact eigenvectors are used in coordinate reduction procedures,

- the proposed Ritz reduction algorithms can easily be implemented on micro-computers providing an efficient mean of analysis for medium size structures.

9.3 Suggestions for Future Research and Development

9.3.1 Linear Systems

The proposed algorithms will benefit from numerical experimentation in an industrial environment where the variety of structural dynamic problems to be analyzed should provide complementary information on the actual performance of the WYD Ritz reduction method when applied to more complex problems than those presented in this report.

One specific area suggested for future development is to extend the load dependent Ritz reduction method to generate directly complex Ritz shapes for the analysis of non-proportionally damped systems. A recent study by Traill-Nash (9.4) proposed that the use of complex eigenvectors with the modal acceleration type of summation could possibly be one of the most effective procedures to analyze non-classically damped systems. Complex Ritz vectors can be substituted to replace complex eigenvectors to further improve the efficiency of this approach. A numerical technique to calculate complex eigenvectors from a matrix iteration formulation similar to the one used for undamped systems has been presented by Hurty and Rubinstein (9.2).

This algorithm can potentially be extended to compute complex Ritz shapes directly.

9.3.2 Nonlinear Systems

When dealing with nonlinear problems no solution procedure can be universally applied to all analyses. The lack of uniformity in the selection of a solution procedure can be attributed to varying levels of priority assigned to factors affecting the choice of the technique such as

- type and extent of expected nonlinear behavior,
- degree of nonlinearity,
- desired level of accuracy,
- problem size,
- computational economy,
- user interaction and experience required.

A careful evaluation of the influence of these factors, as reflected by practical implementation strategies, on the convergence characteristics of the theoretical solution procedures presented in chapter 8 will be essential to apply successfully these methods to solve nonlinear dynamic probelms. The identification and quantification of critical formulation parameters from actual numerical experimentation will be required to determine the range of applicability of the proposed solution algorithms and validate the techniques for practical use.

Finally, in developing solution algorithms for nonlinear systems it should always be remembered that current numerical solution capabilities are usually in advance of the knowledge of fundamental material behavior. This is particularly true for dynamic problems where there is a need for more information on material properties under transient conditions.

9.4 Final Remarks

As the need for methods of analysis with better performance is felt by industry, it is believed that analytical trends in the near future will be to recognize that the specific nature of structural dynamic problems can be exploited to formulate efficient reduction procedures which will depart from the traditional the eigensolution as the sole criterion to accept a basis for dynamic response calculations. In fact, the paper presented by Wilson et al. (1.17) has already started to generate great interest in the literature as more and more analysts recognize the advantages of the approach (see ref. 1.14, 3.3, 8.12, 9.1).

This report contributed to this process by clearly showing that solution procedures based on the direct superposition of load dependent Ritz vectors can be developed as complete analytical tools being able to improve the convergence characteristics and numerical efficiency of any classical dynamic analysis techniques that are currently using eigenvectors as bases for response computations.

REFERENCES

The following abbreviations are used in the citations:

AIAAJ: Journal of the American Institute of Aeronautics and Astronautics.

CompSt: Computers and Structures, An International Journal.

EEStDy: International Journal of Earthquake Engineering and Structural Dynamics.

IJNME: International Journal of Numerical Methods in Engineering.

JStDiv: Journal of the Structural division, Proceedings of ASCE.

ShViDi: The Shock and Vibration digest, The Shock and Vibration Information center, Naval Research Laboratory, Washington D.C.

CMAME: Computer Methods in Applied Mechanics and Engineering.

EngSt: Engineering Structures.

AdvEngSoft: Advanced Engineering Software.

Chapter 1 Introduction

1.1 Almroth, B.O., Stern, P., Brogan, F.A., "Automatic Choice of Global Shape Functions in Structural Analysis", AIAAJ, Vol. 16, No.5, pp 525-528, 1978.

1.2 Bathe, K.J., "Finite Element Procedure in Engineering Analysis", Printice Hall, 1982.

1.3 Bayo, E., Wilson, E.L., "Numerical Techniques for the Evaluation of Soil-Structure Interaction Effects in the Time Domain", Report No. EERC 83-04, Earthquake Engineering Research Center, University of California, Berkeley, February 1983.

1.4 Bayo, E., Wilson, E.L., "Use of Ritz Vectors in Wave Propagation and Foundation Response", EEStDy, Vol. 12, 1984.

1.5 Chowdhury, P.C., "An Alternative to Normal Mode Method", CompSt, Vol. 5, p 315, 1975.

1.6 Clough, R.W., and Wilson, E.L., "Dynamic Analysis of Large Structural Systems with Local Nonlinearities", CMAME, Vol. 17/18, pp 107-129, 1979.

1.7 Craig, R.R., "Structural Dynamics an Introduction to Computer Methods", John Wiley & Sons, 1981.

1.8 Crandall, S.H., "Engineering Analysis", Mc Graw Hill, 1956.

1.9 Glowinski, R., Rodin, E.Y., Zienkeiwicz, O.C., "Energy Methods in Finite Element Analysis", John Wiley & Sons, 1979.

1.10 Idelsohn, S.R., Cardona, A., "Reduction Methods and Explicit Time Integration in Structural Dynamics", AdvEngSoft, Vol. 6, No. 1, pp 36-44, 1984.

1.11 Jennings, A., "Eigenvalue Methods and the Analysis of Stuctural Vibrations", Sparse Matrix and their Uses, Edited by Iain S. Duff, Academic Press, 1981.

1.12 Noor, A.K., "Recent Advances in Reduction Methods for Nonlinear Problems", CompSt, Vol. 13, pp 31-44, 1981.

1.13 Noor, A.K., Peters, J.M., "Reduced Basis Techniques for Nonlinear Analysis of Structures", AIAAJ, Vol. 18, No. 4, pp 455-461, 1980.

1.14 Nour-Omid, B., Clough, R.W., "Dynamic Analysis of Structures Using Lanczos Coordinates", EEStDy, Vol. 12, No. 4, pp 565-577,1984.

1.15 Ruiming, D., Wilson, E.L, "An Effective Modified Ritz Vector Direct Superposition Method", 8th International Conference on Structural Mechanics in Reactor Technology, 1985.

1.16 Wilson, E.L., "New Approaches for the Dynamic Analysis of Large Structural Systems", Report No. EERC 84-04, Earthquake Engineering Research Center, University of California, Berkeley, June 1982.

1.17 Wilson, E.L., Yuan, M.W., Dickens, J.M., "Dynamic Analysis by Direct Superposition of Ritz Vectors", EEStDy, Vol. 10, pp 813-821, 1982.

1.18 Wilson, E.L., "A New Method of Dynamic Analysis for Linear and Nonlinear Systems", Finite Elements Analysis and Design, vol.1, pp 21-23,1985.

Chapter 2 Relationship Between the WYD Ritz Algorithm and the Lanczos Method

2.1 ADINA Engineering Inc., "The ADINA System - Version 1981", ADINA Engineering Inc., Watertown, 1981.

2.2 Bathe, K.J., Ramaswamy, S., "An Accelerated Subspace Iteration Method", CMAME, vol.23, pp 313-331, 1980.

2.3 Bathe, K.J., Wilson, E.L., Peterson, F.E. "SAP-IV A Structural Program for Static and Dynamic Response of Linear Systems", Report no.EERC 73-11, University of California, Berkeley, April 1974.

2.4 Caughey, T.K., O'Kelly, M.J.E, "Classical Normal Modes in Damped Dynamic Systems", Journal of Applied Mechanics, pp 583- 588, Sept. 1965.

2.5 Caughey, T.K., "Classical Normal Modes in Damped Linear Dynamic Systems", Journal of Applied Mechanics, pp 269-271, June 1960.

2.6 Clough, R.W., Mojtahedi, S., "Earthquake Response Analysis Considering Non-Proportional Damping", EEStDy, vol.4, pp 489- 496, 1976.

2.7 Ericsson, T., Ruhe, A., "The Spectral transformation Lanczos Method for the Numerical Solution of Large Sparse Generalized Symmetric Eigenproblem", Mathematics of Computation, vol.35, no.152, pp 1251-1268, Oct. 1980.

2.8 Hilbit, Karlsson & Sorensen Inc. ABAQUS " Theory Manual ", Hilbit, Karlsson & Sorensen Inc., Providence, 1981.

2.9 Lanczos, C., "An Iteration Method for the Solution of the Eigenvalue Problem of Linear Differential And Integral Operators", J.Res.Nat.Bar.Standard, Vol. 45, pp 255-282, 1950.

2.10 Newman, M., Flanagan, F.P., "Eigenvalue Extraction in NASTRAN by Tridiagonal Reduction (FEER) Method", Report No. NASA CR-2731, Washington DC, August, 1976.

2.11 Newman, M., Pipano, A., "Fast Modal Extraction in Nastran Via the FEER Computer Program", Report No. NASA TMX-2893, Langley Research Center, Hampton, Virginia, Sept. 1973.

2.12 Ojalvo, I.V., "ALARM a Highly Efficient Eigenvalue Extraction Routine for Very Large Matrices". NASA Scientific and Technical publication 1970.

2.13 Parlett, B.N., Scott D.S., "The Lanczos Algorithm with Selective Orthogonalization", Mathematics of Computation, vol.33, no.145 pp 217-238, January 1979.

2.14 Parlett, B.N., "The Symmetric Eigenvalue Problem", Prentice Hall, 1980.

2.15 Ramaswamy, S., "On the Effectiveness of the Lanczos Method for the Solution of Large Eigenvalue Problem", Journal of Sound and Vibration vol.73, no.3, pp 405-418, 1980.

2.16 Singh, P., "Seismic Response by the SRSS for Non-Proportional Damping", Journal of Eng. Mech. Division, ASCE, vol.106, no.EM6 pp 1405-1419, Dec 1980.

2.17 Wilson, E.L., Itoh, T., "An Eigensolution Strategy for Large Systems", CompSt, vol.16, no.1-4, pp 259-265, 1983.

Chapter 3 Development of Error Estimates for the WYD Ritz Reduction Method

3.1 American Petroleum Institute, "API Recommended Practice for Planning Designing and Constructing Fixed Offshore Platforms", Washington, DC, Jan. 1980.

3.2 Clough, R.W., Penzien, J.P., "Dynamics of Structures", Mc Graw Hill, 1975.

3.3 Cornwell, R.E., Craig, R.R., Johnson, C.P., "On the Application of the Mode-Acceleration Method to Structural Engineerng Problems", EEStDy, Vol 11, pp 679-688, 1983.

3.4 Hansteen, O.E., Bell, K., "On the Accuracy of Mode Superposition Analysis in Structural Dynamics", EEStDy, Vol. 7, No. 5, pp 405-411, 1979.

3.5 Maddox, N.R., "On the Number of Modes Necessary for Accurate Response and Resulting Forces in Dynamic Analysis", Journal of Applied Mechanics, ASMC, pp 516-517, June 1975.

3.6 Leger, P., "A Study Proposal on the Use of Ritz Vectors in Structural Dynamics", Graduate Student Report, Dept. of Civil Eng., SESM, University of California Berkeley, Sept. 84.

3.7 Paige, C.C, "Computational Variants of the Lanczos Method for the Eigenproblem", J. Inst. Maths Applics, vol 10., pp 373-381, 1972.

3.8 Salmonte, A.J., "Consideration on the Residual Contribution in Modal Analysis", EEStDy, Vol. 10, pp 295-304, 1982.

3.9 Singh, P., Mehta, K.B, "Seismic Design Response by Alternative SRSS Rule", EEStDy, vol.11, pp 771-783, 1983.

Chapter 4 A New Algorithm for Ritz Vectors Generation

4.1 Bowdler, H.B., Martin, R.S., et al. "The QR and QL Algorithm for Symmetric Matrices", Numer. Math., vol. 11, pp 293-306, 1968

4.2 Chowdhury, P.C., "The Truncated Lanczos Algorithm for Partial Solution of the Symmetric EigenProblem", CompSt, Vol. 6, No. 6, pp 439-446, 1976.

4.3 Cullum, J., Willoughly, R.A., "Computing Eigenvalues of Very Large Symmetric Matrix - An Implementation of a Lanczos Algorithm with No Reorthogonalization", Journal of Computational Physics, Vol. 44, pp 329-358, 1981.

4.4 Edwards, J.T., et al. "Use of the Lanczos Method for Finding Complete Sets of Eigenvalues of Large Sparse Symmetric Matrices", J. Inst. Maths Applics, vol. 23, pp 277-283, 1979.

4.5 EISPACK Guide, "Matrix Eigensystem Routines - Lecture Notes in Computer Sciences 16", B.T. Smith et al. 2nd ed., Springer Verlag, New-York, 1976.

4.6 Golub, G.H., Van Loan, C.F.,"Matrix Computations", The John Hopkins University Press, 1983.

4.7 Gregory, R.T., "Results Using Lanczos Method for Finding Eigenvalues of Arbitrary Matrices", J.Soc.Ind. and Appl Math, Vol. 6, pp 182-188, 1958.

4.8 Hoit, I.M. "New Computer Programming Technique for Structural Engineering", Ph.D Dissertation, University of California, Berkeley, 1983.

4.9 Jennings, A., "Eigenvalue Method for Vibration Analysis", ShViDi, Vol. 12, No. 2, pp 3-16, 1980.

4.10 Jennings, A., "Eigenvalue Methods for Vibration Analysis II", ShViDi, Vol. 10, No. 3, pp 25-33, 1981.

4.11 Ojalvo, I.V, Newman, M., "Vibration Modes of Large Structures by Automatic Matrix Reduction Method", AIAAJ Journal, Vol. 8, No. 7, pp 1234-1239, July 1970.

4.12 Paige, C.C, "Practical Use of the Symmetric Lanczos Process with Reorthogonalization", BIT, vol. 10, pp 183-195, 1970.

4.13 Paige, C.C, "Accuracy and Effectiveness of the Lanczos Algorithm for the Symmetric Eigenproblem", Linear Algebra and its Applications, vol. 34, pp 235-258, 1980.

4.14 Parlett, B.N, Reid, J.K., "Tracking the Progress of the Lanczos Algorithm for Large Symmetric Eigenproblem", IMA Journal of Numerical Analysis, vol. 1, pp135-155, 1981.

4.15 Simon, H.D., "The Lanczos Algorithm for Solving Symmetric Linear Systems", Technical Report PAM-74, Center for Pure and Applied Mathematics, University of California, Berkeley, CA, 1982.

4.16 Wilson, E.L., "CAL - A computer Analysis Language for Teaching Structural Analysis", CompSt, Vol. 10, pp 127-132, 1979.

4.17 Wilson, E.L., "A Computer Adaptive Language for the development of Structural Analysis Programs", CompSt, 1984.

4.18 Wilson, E.L., "The SAP-80 Series of Structural Analysis Programs for CP/M-80 Microcomputer Systems", Structural Analysis Programs Inc., El Cerrito, California.

Chapter 5 Application of the WYD Ritz Reduction Method in Earthquake Engineering

5.1 Anagnostopoulos, S.A., "Dynamic Response of Offshore Platforms to Extreme Waves Including Fluid Structure Interaction", EngSt, vol.4, pp 179-185, July 1982.

5.2 Anagnostopoulos, S.A., "Wave and Earthquake Response of Offshore Structures: Evaluation of Modal Solutions", JStDiv, Vol. 108, No. St 10, pp 2175-2191, October 1982.

5.3 Arnold, R.R., Citerley, R.L., Chargin, M., Galant, D., "Application of Ritz Vectors for Dynamic Analysis of Large Structures", CompSt, Vol. 21, No.5, pp. 901-908, 1985.

5.4 Bathe, K.J., Wilson, E.L., "Numerical Methods in Finite Element Analysis", Prentice-Hall inc.,1976.

5.5 Det Norske Veritas, "Rules for the Design Construction and Inspection of Offshore Structures - Appendix G Dynamic Analysis", April 1980.

5.6 Ferrante, A.J., Valenzuela, E.C., Ellwanger, G.B., "An Integrated Computational Procedure for the Analysis of Offshore Structures Supported by Piles", AdvEngSoft, Vol. 2, No. 4, pp 169-173, 1980.

5.7 Vughts, J.H., Hines, M.I., "Modal Superposition vs Direct Solution Techniques in the Dynamic Analysis of Offshore Structures", International Conference on Behavior of Offshore Structures, Paper 49, 1979.

5.8 Wilson, E.L., Der Kiureghian, A., Bayo, E.P., "A Replacement for the SRSS Methos in Seismic Analysis", EEStDy, Vol. 9, pp 187-194, 1981.

Chapter 6 Generalization of the WYD Ritz Reduction Method to Arbitrary Loadings

6.1 Appa, K., Smith, G.C.C., Hughes, J.T., "Rational Reduction of Large Scale Eigenvalue Problems", AIAAJ, Vol. 10, No.7, pp 964-965, 1972.

6.2 Dawson, T.H., "Offshore Structural Engineering", Prentice Hall, Englewood Cliffs, N.J., 1983.

6.3 Golub, G.H., Underwood, R., "The Block Lanczos Method for Computing Eigenvalues", in Mathematical Software III, edited by J. Rice, Academic Press, New-York, pp 364-377, 1977.

6.4 Hinton, E., Rock, T., Zeinkiewicz, O.C, "A note on Mass Lumping and Related Processes in the Finite element Method", EEStDy, Vol. 4, No. 3, pp. 245-249, 1976.

6.5 Jennings, A., "Solution of Sparse Eigenvalue Problems", in Sparsity and its Applications, edited by D.J., Evans, Cambridge University Press, 1985.

6.6 Matthies, H.G., "A Subspace Lanczos Method for the Generalized Symmetric Eigenproblem", CompSt, vol. 21, no. 1/2, pp 319-325, 1985.

6.7 Matthies, H.G., "Computable Error Bounds for the Generalized Symmetric Eigenproblem", Communications in Applied Numerical Methods, vol. 1, pp 33-38, 1985.

6.8 Nour-Omid, B., Clough, R.W., "Block Lanczos Method for Dynamic Analysis of Structures", EEStDy, vol. 13, pp 271-275, 1985.

6.9 Ojalvo, I.U., "Proper Use of Lanczos Vectors for Large Eigenvalue Problems", ComptSt, vol. 20, no. 1-3, pp 115-120, 1985.

6.10 Ruhe, A., "Implementation Aspects of Band Lanczos Algorithm for Computation of Eigenvalues of Large Sparse Symmetric Matrices", Mathematics of Computation vol. 33, no. 146, pp 680-687, April 1979.

6.11 Scott, D.S., "The Lanczos Algorithm", in Sparse Matrix and their Uses, edited by I.S., Duff, Academic Press, 1981.

6.12 Surana, K.S., "Lumped Mass Matrices With Non-Zero Inertia for General Shell and Axisymmetric Shell Elements", IJNME, Vol. 12, No. 11, pp. 1635-1650, 1978.

Chapter 7 Use of the WYD Ritz Reduction Method for Multilevel Substructure Analysis

7.1 Arora, J.S., Nguyen, D.T., "Eigensolution for Large Structural System with Substructures", IJNME, Vol. 15, pp 333-341, 1980.

7.2 Benfield, W., Hruda, R., " Vibration Analysis of Structure by Component Mode Substitution", AIAAJ, vol.9, pp 1255-1261, 1971.

7.3 Craig, R.R., "Methods of Component Mode Synthesis", ShViDi, vol. 9, pp 3-10, 1977.

7.4 Craig R.R., Chang, C.J., "Free Interface Method of Substructure Coupling for Dynamic Analysis", AIAAJ, Vol. 14, No. 11, pp 1633-1635, 1976.

7.5 Craig, R.R., Bampton, M., "Coupling Substructure for Dynamic Analysis", AIAAJ, Vol. 6, No. 7, pp 1313-1319, 1968.

7.6 Curnier, A., " On Three Modal Synthesis Variants", Journal of Sound and Vibration, vol.90, no.4, pp 527-540, 1983.

7.7 Guyan, R.J., "Reduction of Stiffness and Mass Matrices", AIAAJ, Vol. 3, No. 2, p 380, 1965.

7.8 Hale, A.L., Meirovitch L., " A General Procedure for Improving Substructure representation in Dynamic Synthesis", Journal of Sound and Vibration, vol.84, no.2, pp 269-287, 1982.

7.9 Hintz, R.M., "Analytical Methods in Component Modal Synthesis", ALIAAJ, Vol. 13, pp 1007-1016, 1975.

7.10 Holze, H.G., Borin, A.P., "Free Vibration Analysis Using Substructuring", JStDiv, Vol. 101, No. ST12, December 1975.

7.11 Hurty, W.C., "Dynamic Analysis of Structural System Using Component Modes", AIAAJ, Vol. 3, NO. 4, pp 678-685, 1965.

7.12 Hurty, W.C., Collins, J.D., Hart, G.C., " Dynamic Analysis of Large Structures by Modal Synthesis Techniques", CompSt, vol.1, pp 553-563, 1971.

7.13 Kaufman, S., Hall, D.B., "Reduction of Mass and Loading Matrices", AIAAJ, Vol. 6, No. 3, pp 550, March 1968.

7.14 Kuhar, E., Stahle, V.C.,"Dynamic Transformation Methods for Modal Synthesis", AIAAJ, Vol. 12, No. 5, pp 672-679.

7.15 Leung, A.Y.T., "An Accurate Method of Dynamic Condensation in Stuctural Analysis", IJNME, Vol. 12, pp 1705-1715, 1978.

7.16 Martin, K.F., Ghlaim, K.H., "On the Solution of Approximated Systems When Using Reduced Component Modes", EESTDy, Vol. 12, pp 417-426, 1984.

7.17 Meirovitch, L., Hale, A.L., " A General Dynamic Synthesis for Structure with Discrete Substructure", Journal of Sound and Vibration, vol.85, no.4, pp 445-457, 1982.

7.18 Noor, A.K., Hussein, K., Fulton, R.,"Substructuring Techniques Status and Projections", CompSt, Vol. 8, pp 621-632, 1978.

Chapter 8 Nonlinear Dynamic Analysis by Direct Superposition of Ritz Vectors

8.1 Argyris, J.H., Roy, J.R., "General Treatment of Structural Modifications", JStDiv, vol. 98, no. ST2, pp 465-492, February 1972.

8.2 Bathe, K.J., Cimento, A.P., "Some Practical Procedures for the Solution of Nonlinear Finite Element Equations", CMAME, vol. 22, pp 59-85, 1980.

8.3 Bathe, K.J., Gracewsky, S., "On Nonlinear Dynamic Analysis Using Mode Superposition and Substructuring", CompSt, Vol. 13, pp 699-707, 1981.

8.4 Bennett, J.M., "Triangular Factors of Modified Matrices", Numerische Mathematik, vol. 7, pp 217-221, 1965.

8.5 Chen, S.H., Liu, Y.L., Huang, D.P., "A Matrix Perturbation of Vibration Modal Analysis", 2nd International Conference on Modal Analysis, 1984.

8.6 Dickens, J.M., Wilson, E.L., "Numerical Methods for Dynamic Substructure Analysis", Report UCB/EERC 80-20, University of California, Berkeley, June 1980.

8.7 Felippa, C.A., Park, K.C., "Direct Time Integration Methods in Nonlinear Structural Dynamics", CMAMA, Vol. 17/18, pp 277-318, 1979.

8.8 Ferrarite, A.J., Valenzuela, E.C., Ellwanger, G.B., "An Integrated Computational Procedure for the Analysis of Offshore Structures Supported by Piles", AdvEngSoft, vol. 2, no.4, pp 169-173, 1980.

8.9 Hirai, I., Kashiwaki, M., "Derivatives of Eigenvectors of Locally Modified Structures", IJNME, vol. 11, pp 1769-1773, 1977.

8.10 Huckelbridge, A.A., Ferincz, R.M., "Comparative Seismic Analysis of a Framed Tube with Localized and General Nonlinearity", EEStDy, Vol. 11, pp 167-177, 1983.

8.11 Idelsohn, S.R., Cardona, A., "A Reduction Method for Nonlinear Structural Dynamics", CMAME, vol. 49,pp 253-279, 1985.

8.12 Idelsohn, S.R., Cardona, A.,"A Load Dependent Basis for Reduced Nonlinear Structural Dynamics", CompSt, vol. 20, no. 1-3, pp 203-210, 1985.

8.13 Morris, F.N., "The Use of Modal Superposition in Nonlinear Dynamics", CompSt, Vol. 7, pp 65-72, 1977.

8.14 Nickell, R.E., "Nonlinear Dynamics by Mode Superposition", CMAME, Vol. 7, pp 107-129, 1976.

8.15 Nour-Omid, B., "A Newton-Lanczos Method for Solution of Nonlinear Finite Element Equations", Ph.D Dissertation, University of California, Berkeley, 1981.

8.16 Remsith, S.N., "Nonlinear Static and Dynamic Analysis of Framed Structures", CompSt, Vol. 10, pp 879-897, 1979.

8.17 Row, D.G., Powell, G.H., "A Substructure Technique for Nonlinear Static and Dynamic Analysis", Report EERC 78-15, University of California, Berkeley, 1978.

8.18 Row, D.G., Powell, G.H., Mondkar, D.P," Solution of Progressively Changing Equilibrium Equations for Nonlinear Structures", CompSt, vol. 7, pp 659-665, 1977.

8.19 Shah, V.N., Bohm, G.J., Nahovandi, A.N., "Modal Superposition Method for Computationally Economical Nonlinear Structural Analysis", Journal of Pressure Vessel Technology (ASME), Vol. 101, No. 2, pp 131-141, 1979.

8.20 Takamura, K., "On a Direct Eigenvalue Analysis for Locally Modified Structures", IJNME, vol. 6, pp 441-456, 1973.

8.20 Tillerson, J.R., "Selecting Solution Procedure for Nonlinear Structural Dynamics", ShViDi, Vol. 7, No. 4, pp 2-13, 1975.

Chapter 9 Conclusion

9.1 Arnold, R.R., Citerley, R.L., Chagrin, M., Galant, D., "Application of Ritz Vectors for Dynamic Analysis of Large Structures", CompSt, vol. 21, no.3, pp 461-467, 1985.

9.2 Hurty, W.C., Rubinstein, M.F., "Dynamics of Structures", Prentice-Hall inc., 1964.

9.3 Owen, D.R.J., Hinton, E., "Finite Elements in Plasticity", Pineridge Press Limited, Swansea U.K., 1980.

9.4 Traill-Nash, R.W., "Modal Methods in the Dynamics of Systems with Non-Classical Damping", EEStDy, vol. 9, pp 153-169, 1981.

EARTHQUAKE ENGINEERING RESEARCH CENTER REPORTS

NOTE: Numbers in parentheses are Accession Numbers assigned by the National Technical Information Service; these are followed by a price code. Copies of the reports may be ordered from the National Technical Information Service, 5285 Port Royal Road, Springfield, Virginia, 22161. Accession Numbers should be quoted on orders for reports (PB --- ---) and remittance must accompany each order. Reports without this information were not available at time of printing. The complete list of EERC reports (from EERC 67-1) is available upon request from the Earthquake Engineering Research Center, University of California, Berkeley, 47th Street and Hoffman Boulevard, Richmond, California 94804.

UCB/EERC-79/01 "Hysteretic Behavior of Lightweight Reinforced Concrete Beam-Column Subassemblages," by B. Forzani, E.P. Popov and V.V. Bertero - April 1979(PB 298 267)A06

UCB/EERC-79/02 "The Development of a Mathematical Model to Predict the Flexural Response of Reinforced Concrete Beams to Cyclic Loads, Using System Identification," by J. Stanton & H. McNiven - Jan. 1979(PB 295 875)A10

UCB/EERC-79/03 "Linear and Nonlinear Earthquake Response of Simple Torsionally Coupled Systems," by C.L. Kan and A.K. Chopra - Feb. 1979(PB 298 262)A06

UCB/EERC-79/04 "A Mathematical Model of Masonry for Predicting its Linear Seismic Response Characteristics," by Y. Mengi and H.D. McNiven - Feb. 1979(PB 298 266)A06

UCB/EERC-79/05 "Mechanical Behavior of Lightweight Concrete Confined by Different Types of Lateral Reinforcement," by M.A. Manrique, V.V. Bertero and E.P. Popov - May 1979(PB 301 114)A06

UCB/EERC-79/06 "Static Tilt Tests of a Tall Cylindrical Liquid Storage Tank," by R.W. Clough and A. Niwa - Feb. 1979 (PB 301 167)A06

UCB/EERC-79/07 "The Design of Steel Energy Absorbing Restrainers and Their Incorporation into Nuclear Power Plants for Enhanced Safety: Volume 1 - Summary Report," by P.N. Spencer, V.F. Zackay, and E.R. Parker - Feb. 1979(UCB/EERC-79/07)A09

UCB/EERC-79/08 "The Design of Steel Energy Absorbing Restrainers and Their Incorporation into Nuclear Power Plants for Enhanced Safety: Volume 2 - The Development of Analyses for Reactor System Piping,""Simple Systems" by M.C. Lee, J. Penzien, A.K. Chopra and K, Suzuki "Complex Systems" by G.H. Powell, E.L. Wilson, R.W. Clough and D.G. Row - Feb. 1979(UCB/EERC-79/08)A10

UCB/EERC-79/09 "The Design of Steel Energy Absorbing Restrainers and Their Incorporation into Nuclear Power Plants for Enhanced Safety: Volume 3 - Evaluation of Commercial Steels," by W.S. Owen, R.M.N. Pelloux, R.O. Ritchie, M. Faral, T. Ohhashi, J. Toplosky, S.J. Hartman, V.F. Zackay and E.R. Parker - Feb. 1979(UCB/EERC-79/09)A04

UCB/EERC-79/10 "The Design of Steel Energy Absorbing Restrainers and Their Incorporation into Nuclear Power Plants for Enhanced Safety: Volume 4 - A Review of Energy-Absorbing Devices," by J.M. Kelly and M.S. Skinner - Feb. 1979(UCB/EERC-79/10)A04

UCB/EERC-79/11 "Conservatism In Summation Rules for Closely Spaced Modes," by J.M. Kelly and J.L. Sackman - May 1979(PB 301 328)A03

UCB/EERC-79/12 "Cyclic Loading Tests of Masonry Single Piers; Volume 3 - Height to Width Ratio of 0.5," by P.A. Hidalgo, R.L. Mayes, H.D. McNiven and R.W. Clough - May 1979(PB 301 321)A08

UCB/EERC-79/13 "Cyclic Behavior of Dense Course-Grained Materials in Relation to the Seismic Stability of Dams," by N.G. Banerjee, H.B. Seed and C.K. Chan - June 1979(PB 301 373)A13

UCB/EERC-79/14 "Seismic Behavior of Reinforced Concrete Interior Beam-Column Subassemblages," by S. Viwathanatepa, E.P. Popov and V.V. Bertero - June 1979(PB 301 326)A10

UCB/EERC-79/15 "Optimal Design of Localized Nonlinear Systems with Dual Performance Criteria Under Earthquake Excitations," by M.A. Bhatti - July 1979(PB 80 167 109)A06

UCB/EERC-79/16 "OPTDYN - A General Purpose Optimization Program for Problems with or without Dynamic Constraints," by M.A. Bhatti, E. Polak and K.S. Pister - July 1979(PB 80 167 091)A05

UCB/EERC-79/17 "ANSR-II, Analysis of Nonlinear Structural Response, Users Manual," by D.P. Mondkar and G.H. Powell July 1979(PB 80 113 301)A05

UCB/EERC-79/18 "Soil Structure Interaction in Different Seismic Environments," A. Gomez-Masso, J. Lysmer, J.-C. Chen and H.B. Seed - August 1979(PB 80 101 520)A04

UCB/EERC-79/19 "ARMA Models for Earthquake Ground Motions," by M.K. Chang, J.W. Kwiatkowski, R.F. Nau, R.M. Oliver and K.S. Pister - July 1979(PB 301 166)A05

UCB/EERC-79/20 "Hysteretic Behavior of Reinforced Concrete Structural Walls," by J.M. Vallenas, V.V. Bertero and E.P. Popov - August 1979(PB 80 165 905)A12

UCB/EERC-79/21 "Studies on High-Frequency Vibrations of Buildings - 1: The Column Effect," by J. Lubliner - August 1979 (PB 80 158 553)A03

UCB/EERC-79/22 "Effects of Generalized Loadings on Bond Reinforcing Bars Embedded in Confined Concrete Blocks," by S. Viwathanatepa, E.P. Popov and V.V. Bertero - August 1979(PB 81 124 018)A14

UCB/EERC-79/23 "Shaking Table Study of Single-Story Masonry Houses, Volume 1: Test Structures 1 and 2," by P. Gülkan, R.L. Mayes and R.W. Clough - Sept. 1979 (HUD-000 1763)A12

UCB/EERC-79/24 "Shaking Table Study of Single-Story Masonry Houses, Volume 2: Test Structures 3 and 4," by P. Gülkan, R.L. Mayes and R.W. Clough - Sept. 1979 (HUD-000 1836)A12

UCB/EERC-79/25 "Shaking Table Study of Single-Story Masonry Houses, Volume 3: Summary, Conclusions and Recommendations," by R.W. Clough, R.L. Mayes and P. Gülkan - Sept. 1979 (HUD-000 1837)A06

UCB/EERC-79/26 "Recommendations for a U.S.-Japan Cooperative Research Program Utilizing Large-Scale Testing Facilities," by U.S.-Japan Planning Group - Sept. 1979(PB 301 407)A06

UCB/EERC-79/27 "Earthquake-Induced Liquefaction Near Lake Amatitlan, Guatemala," by H.B. Seed, I. Arango, C.K. Chan, A. Gomez-Masso and R. Grant de Ascoli - Sept. 1979(NUREG-CR1341)A03

UCB/EERC-79/28 "Infill Panels: Their Influence on Seismic Response of Buildings," by J.W. Axley and V.V. Bertero Sept. 1979(PB 80 163 371)A10

UCB/EERC-79/29 "3D Truss Bar Element (Type 1) for the ANSR-II Program," by D.P. Mondkar and G.H. Powell - Nov. 1979 (PB 80 169 709)A02

UCB/EERC-79/30 "2D Beam-Column Element (Type 5 - Parallel Element Theory) for the ANSR-II Program," by D.G. Row, G.H. Powell and D.P. Mondkar - Dec. 1979(PB 80 167 224)A03

UCB/EERC-79/31 "3D Beam-Column Element (Type 2 - Parallel Element Theory) for the ANSR-II Program," by A. Riahi, G.H. Powell and D.P. Mondkar - Dec. 1979(PB 80 167 216)A03

UCB/EERC-79/32 "On Response of Structures to Stationary Excitation," by A. Der Kiureghian - Dec. 1979(PB 80166 929)A03

UCB/EERC-79/33 "Undisturbed Sampling and Cyclic Load Testing of Sands," by S. Singh, H.B. Seed and C.K. Chan Dec. 1979(ADA 087 298)A07

UCB/EERC-79/34 "Interaction Effects of Simultaneous Torsional and Compressional Cyclic Loading of Sand," by P.M. Griffin and W.N. Houston - Dec. 1979(ADA 092 352)A15

UCB/EERC-80/01 "Earthquake Response of Concrete Gravity Dams Including Hydrodynamic and Foundation Interaction Effects," by A.K. Chopra, P. Chakrabarti and S. Gupta - Jan. 1980(AD-A087297)A10

UCB/EERC-80/02 "Rocking Response of Rigid Blocks to Earthquakes," by C.S. Yim, A.K. Chopra and J. Penzien - Jan. 1980 (PB80 166 002)A04

UCB/EERC-80/03 "Optimum Inelastic Design of Seismic-Resistant Reinforced Concrete Frame Structures," by S.W. Zagajeski and V.V. Bertero - Jan. 1980(PB80 164 635)A06

UCB/EERC-80/04 "Effects of Amount and Arrangement of Wall-Panel Reinforcement on Hysteretic Behavior of Reinforced Concrete Walls," by R. Iliya and V.V. Bertero - Feb. 1980(PB81 122 525)A09

UCB/EERC-80/05 "Shaking Table Research on Concrete Dam Models," by A. Niwa and R.W. Clough - Sept. 1980(PB81 122 368)A06

UCB/EERC-80/06 "The Design of Steel Energy-Absorbing Restrainers and their Incorporation into Nuclear Power Plants for Enhanced Safety (Vol 1A): Piping with Energy Absorbing Restrainers: Parameter Study on Small Systems," by G.H. Powell, C. Oughourlian and J. Simons - June 1980

UCB/EERC-80/07 "Inelastic Torsional Response of Structures Subjected to Earthquake Ground Motions," by Y. Yamazaki April 1980(PB81 122 327)A08

UCB/EERC-80/08 "Study of X-Braced Steel Frame Structures Under Earthquake Simulation," by Y. Ghanaat - April 1980 (PB81 122 335)A11

UCB/EERC-80/09 "Hybrid Modelling of Soil-Structure Interaction," by S. Gupta, T.W. Lin, J. Penzien and C.S. Yeh May 1980(PB81 122 319)A07

UCB/EERC-80/10 "General Applicability of a Nonlinear Model of a One Story Steel Frame," by B.I. Sveinsson and H.D. McNiven - May 1980(PB81 124 877)A06

UCB/EERC-80/11 "A Green-Function Method for Wave Interaction with a Submerged Body," by W. Kioka - April 1980 (PB81 122 269)A07

UCB/EERC-80/12 "Hydrodynamic Pressure and Added Mass for Axisymmetric Bodies," by F. Nilrat - May 1980(PB81 122 343)A08

UCB/EERC-80/13 "Treatment of Non-Linear Drag Forces Acting on Offshore Platforms," by B.V. Dao and J. Penzien May 1980(PB81 153 413)A07

UCB/EERC-80/14 "2D Plane/Axisymmetric Solid Element (Type 3 - Elastic or Elastic-Perfectly Plastic) for the ANSR-II Program," by D.P. Mondkar and G.H. Powell - July 1980(PB81 122 350)A03

UCB/EERC-80/15 "A Response Spectrum Method for Random Vibrations," by A. Der Kiureghian - June 1980(PB81 122 301)A03

UCB/EERC-80/16 "Cyclic Inelastic Buckling of Tubular Steel Braces," by V.A. Zayas, E.P. Popov and S.A. Mahin June 1980(PB81 124 885)A10

UCB/EERC-80/17 "Dynamic Response of Simple Arch Dams Including Hydrodynamic Interaction," by C.S. Porter and A.K. Chopra - July 1980(PB81 124 000)A13

UCB/EERC-80/18 "Experimental Testing of a Friction Damped Aseismic Base Isolation System with Fail-Safe Characteristics," by J.M. Kelly, K.E. Beucke and M.S. Skinner - July 1980(PB81 148 595)A04

UCB/EERC-80/19 "The Design of Steel Energy-Absorbing Restrainers and their Incorporation into Nuclear Power Plants for Enhanced Safety (Vol 1B): Stochastic Seismic Analyses of Nuclear Power Plant Structures and Piping Systems Subjected to Multiple Support Excitations," by M.C. Lee and J. Penzien - June 1980

UCB/EERC-80/20 "The Design of Steel Energy-Absorbing Restrainers and their Incorporation into Nuclear Power Plants for Enhanced Safety (Vol 1C): Numerical Method for Dynamic Substructure Analysis," by J.M. Dickens and E.L. Wilson - June 1980

UCB/EERC-80/21 "The Design of Steel Energy-Absorbing Restrainers and their Incorporation into Nuclear Power Plants for Enhanced Safety (Vol 2): Development and Testing of Restraints for Nuclear Piping Systems," by J.M. Kelly and M.S. Skinner - June 1980

UCB/EERC-80/22 "3D Solid Element (Type 4-Elastic or Elastic-Perfectly-Plastic) for the ANSR-II Program," by D.P. Mondkar and G.H. Powell - July 1980(PB81 123 242)A03

UCB/EERC-80/23 "Gap-Friction Element (Type 5) for the ANSR-II Program," by D.P. Mondkar and G.H. Powell - July 1980 (PB81 122 285)A03

UCB/EERC-80/24 "U-Bar Restraint Element (Type 11) for the ANSR-II Program," by C. Oughourlian and G.H. Powell July 1980(PB81 122 293)A03

UCB/EERC-80/25 "Testing of a Natural Rubber Base Isolation System by an Explosively Simulated Earthquake," by J.M. Kelly - August 1980(PB81 201 360)A04

UCB/EERC-80/26 "Input Identification from Structural Vibrational Response," by Y. Hu - August 1980(PB81 152 308)A05

UCB/EERC-80/27 "Cyclic Inelastic Behavior of Steel Offshore Structures," by V.A. Zayas, S.A. Mahin and E.P. Popov August 1980(PB81 196 180)A15

UCB/EERC-80/28 "Shaking Table Testing of a Reinforced Concrete Frame with Biaxial Response," by M.G. Oliva October 1980(PB81 154 304)A10

UCB/EERC-80/29 "Dynamic Properties of a Twelve-Story Prefabricated Panel Building," by J.G. Bouwkamp, J.P. Kollegger and R.M. Stephen - October 1980(PB82 117 128)A06

UCB/EERC-80/30 "Dynamic Properties of an Eight-Story Prefabricated Panel Building," by J.G. Bouwkamp, J.P. Kollegger and R.M. Stephen - October 1980(PB81 200 313)A05

UCB/EERC-80/31 "Predictive Dynamic Response of Panel Type Structures Under Earthquakes," by J.P. Kollegger and J.G. Bouwkamp - October 1980(PB81 152 316)A04

UCB/EERC-80/32 "The Design of Steel Energy-Absorbing Restrainers and their Incorporation into Nuclear Power Plants for Enhanced Safety (Vol 3): Testing of Commercial Steels in Low-Cycle Torsional Fatigue," by P. Spencer, E.R. Parker, E. Jongewaard and M. Drory

UCB/EERC-80/33 "The Design of Steel Energy-Absorbing Restrainers and their Incorporation into Nuclear Power Plants for Enhanced Safety (Vol 4): Shaking Table Tests of Piping Systems with Energy-Absorbing Restrainers," by S.F. Stiemer and W.G. Godden - Sept. 1980

UCB/EERC-80/34 "The Design of Steel Energy-Absorbing Restrainers and their Incorporation into Nuclear Power Plants for Enhanced Safety (Vol 5): Summary Report," by P. Spencer

UCB/EERC-80/35 "Experimental Testing of an Energy-Absorbing Base Isolation System," by J.M. Kelly, M.S. Skinner and K.E. Beucke - October 1980(PB81 154 072)A04

UCB/EERC-80/36 "Simulating and Analyzing Artificial Non-Stationary Earthquake Ground Motions," by R.F. Nau, R.M. Oliver and K.S. Pister - October 1980(PB81 153 397)A04

UCB/EERC-80/37 "Earthquake Engineering at Berkeley - 1980," - Sept. 1980(PB81 205 874)A09

UCB/EERC-80/38 "Inelastic Seismic Analysis of Large Panel Buildings," by V. Schricker and G.H. Powell - Sept. 1980 (PB81 154 338)A13

UCB/EERC-80/39 "Dynamic Response of Embankment, Concrete-Gravity and Arch Dams Including Hydrodynamic Interaction," by J.F. Hall and A.K. Chopra - October 1980(PB81 152 324)A11

UCB/EERC-80/40 "Inelastic Buckling of Steel Struts Under Cyclic Load Reversal," by R.G. Black, W.A. Wenger and E.P. Popov - October 1980(PB81 154 312)A08

UCB/EERC-80/41 "Influence of Site Characteristics on Building Damage During the October 3, 1974 Lima Earthquake," by P. Repetto, I. Arango and H.B. Seed - Sept. 1980(PB81 161 739)A05

UCB/EERC-80/42 "Evaluation of a Shaking Table Test Program on Response Behavior of a Two Story Reinforced Concrete Frame," by J.M. Blondet, R.W. Clough and S.A. Mahin

UCB/EERC-80/43 "Modelling of Soil-Structure Interaction by Finite and Infinite Elements," by F. Medina - December 1980(PB81 229 270)A04

UCB/EERC-81/01 "Control of Seismic Response of Piping Systems and Other Structures by Base Isolation," edited by J.M. Kelly - January 1981 (PB81 200 735)A05

UCB/EERC-81/02 "OPTNSR - An Interactive Software System for Optimal Design of Statically and Dynamically Loaded Structures with Nonlinear Response," by M.A. Bhatti, V. Ciampi and K.S. Pister - January 1981 (PB81 218 851)A09

UCB/EERC-81/03 "Analysis of Local Variations in Free Field Seismic Ground Motions," by J.-C. Chen, J. Lysmer and H.B. Seed - January 1981 (AD-A099508)A13

UCB/EERC-81/04 "Inelastic Structural Modeling of Braced Offshore Platforms for Seismic Loading," by V.A. Zayas, P.-S.B. Shing, S.A. Mahin and E.P. Popov - January 1981(PB82 138 777)A07

UCB/EERC-81/05 "Dynamic Response of Light Equipment in Structures," by A. Der Kiureghian, J.L. Sackman and B. Nour-Omid - April 1981 (PB81 218 497)A04

UCB/EERC-81/06 "Preliminary Experimental Investigation of a Broad Base Liquid Storage Tank," by J.G. Bouwkamp, J.P. Kollegger and R.M. Stephen - May 1981(PB82 140 385)A03

UCB/EERC-81/07 "The Seismic Resistant Design of Reinforced Concrete Coupled Structural Walls," by A.E. Aktan and V.V. Bertero - June 1981(PB82 113 358)A11

UCB/EERC-81/08 "The Undrained Shearing Resistance of Cohesive Soils at Large Deformations," by M.R. Pyles and H.B. Seed - August 1981

UCB/EERC-81/09 "Experimental Behavior of a Spatial Piping System with Steel Energy Absorbers Subjected to a Simulated Differential Seismic Input," by S.F. Stiemer, W.G. Godden and J.M. Kelly - July 1981

UCB/EERC-81/10 "Evaluation of Seismic Design Provisions for Masonry in the United States," by B.I. Sveinsson, R.L. Mayes and H.D. McNiven - August 1981 (PB82 166 075)A08

UCB/EERC-81/11 "Two-Dimensional Hybrid Modelling of Soil-Structure Interaction," by T.-J. Tzong, S. Gupta and J. Penzien - August 1981(PB82 142 118)A04

UCB/EERC-81/12 "Studies on Effects of Infills in Seismic Resistant R/C Construction," by S. Brokken and V.V. Bertero - September 1981 (PB82 166 190)A09

UCB/EERC-81/13 "Linear Models to Predict the Nonlinear Seismic Behavior of a One-Story Steel Frame," by H. Valdimarsson, A.H. Shah and H.D. McNiven - September 1981(PB82 138 793)A07

UCB/EERC-81/14 "TLUSH: A Computer Program for the Three-Dimensional Dynamic Analysis of Earth Dams," by T. Kagawa, L.H. Mejia, H.B. Seed and J. Lysmer - September 1981(PB82 139 940)A06

UCB/EERC-81/15 "Three Dimensional Dynamic Response Analysis of Earth Dams," by L.H. Mejia and H.B. Seed - September 1981 (PB82 137 274)A12

UCB/EERC-81/16 "Experimental Study of Lead and Elastomeric Dampers for Base Isolation Systems," by J.M. Kelly and S.B. Hodder - October 1981 (PB82 166 182)A05

UCB/EERC-81/17 "The Influence of Base Isolation on the Seismic Response of Light Secondary Equipment," by J.M. Kelly - April 1981 (PB82 255 266)A04

UCB/EERC-81/18 "Studies on Evaluation of Shaking Table Response Analysis Procedures," by J. Marcial Blondet - November 1981 (PB82 197 278)A10

UCB/EERC-81/19 "DELIGHT.STRUCT: A Computer-Aided Design Environment for Structural Engineering," by R.J. Balling, K.S. Pister and E. Polak - December 1981 (PB82 218 496)A07

UCB/EERC-81/20 "Optimal Design of Seismic-Resistant Planar Steel Frames," by R.J. Balling, V. Ciampi, K.S. Pister and E. Polak - December 1981 (PB82 220 179)A07

UCB/EERC-82/01 "Dynamic Behavior of Ground for Seismic Analysis of Lifeline Systems," by T. Sato and A. Der Kiureghian - January 1982 (PB82 218 926)A05

UCB/EERC-82/02 "Shaking Table Tests of a Tubular Steel Frame Model," by Y. Ghanaat and R. W. Clough - January 1982 (PB82 220 161)A07

UCB/EERC-82/03 "Behavior of a Piping System under Seismic Excitation: Experimental Investigations of a Spatial Piping System supported by Mechanical Shock Arrestors and Steel Energy Absorbing Devices under Seismic Excitation," by S. Schneider, H.-M. Lee and W. G. Godden - May 1982 (PB83 172 544)A09

UCB/EERC-82/04 "New Approaches for the Dynamic Analysis of Large Structural Systems," by E. L. Wilson - June 1982 (PB83 148 080)A05

UCB/EERC-82/05 "Model Study of Effects of Damage on the Vibration Properties of Steel Offshore Platforms," by F. Shahrivar and J. G. Bouwkamp - June 1982 (PB83 148 742)A10

UCB/EERC-82/06 "States of the Art and Practice in the Optimum Seismic Design and Analytical Response Prediction of R/C Frame-Wall Structures," by A. E. Aktan and V. V. Bertero - July 1982 (PB83 147 736)A05

UCB/EERC-82/07 "Further Study of the Earthquake Response of a Broad Cylindrical Liquid-Storage Tank Model," by G. C. Manos and R. W. Clough - July 1982 (PB83 147 744)A11

UCB/EERC-82/08 "An Evaluation of the Design and Analytical Seismic Response of a Seven Story Reinforced Concrete Frame - Wall Structure," by F. A. Charney and V. V. Bertero - July 1982(PB83 157 628)A09

UCB/EERC-82/09 "Fluid-Structure Interactions: Added Mass Computations for Incompressible Fluid," by J. S.-H. Kuo - August 1982 (PB83 156 281)A07

UCB/EERC-82/10 "Joint-Opening Nonlinear Mechanism: Interface Smeared Crack Model," by J. S.-H. Kuo - August 1982 (PB83 149 195)A05

UCB/EERC-82/11 "Dynamic Response Analysis of Techi Dam," by R. W. Clough, R. M. Stephen and J. S.-H. Kuo - August 1982 (PB83 147 496)A06

UCB/EERC-82/12 "Prediction of the Seismic Responses of R/C Frame-Coupled Wall Structures," by A. E. Aktan, V. V. Bertero and M. Piazza - August 1982 (PB83 149 203)A09

UCB/EERC-82/13 "Preliminary Report on the SMART 1 Strong Motion Array in Taiwan," by B. A. Bolt, C. H. Loh, J. Penzien, Y. B. Tsai and Y. T. Yeh - August 1982 (PB83 159 400)A10

UCB/EERC-82/14 "Shaking-Table Studies of an Eccentrically X-Braced Steel Structure," by M. S. Yang - September 1982 (PB83 260 778)A12

UCB/EERC-82/15 "The Performance of Stairways in Earthquakes," by C. Roha, J. W. Axley and V. V. Bertero - September 1982 (PB83 157 693)A07

UCB/EERC-82/16 "The Behavior of Submerged Multiple Bodies in Earthquakes," by W.-G. Liao - Sept. 1982 (PB83 158 709)A07

UCB/EERC-82/17 "Effects of Concrete Types and Loading Conditions on Local Bond-Slip Relationships," by A. D. Cowell, E. P. Popov and V. V. Bertero - September 1982 (PB83 153 577)A04

UCB/EERC-82/18 "Mechanical Behavior of Shear Wall Vertical Boundary Members: An Experimental Investigation," by M. T. Wagner and V. V. Bertero - October 1982 (PB83 159 764)A05

UCB/EERC-82/19 "Experimental Studies of Multi-support Seismic Loading on Piping Systems," by J. M. Kelly and A. D. Cowell - November 1982

UCB/EERC-82/20 "Generalized Plastic Hinge Concepts for 3D Beam-Column Elements," by P. F.-S. Chen and G. H. Powell - November 1982 (PB83 247 981)A13

UCB/EERC-82/21 "ANSR-III: General Purpose Computer Program for Nonlinear Structural Analysis," by C. V. Oughourlian and G. H. Powell - November 1982 (PB83 251 330)A12

UCB/EERC-82/22 "Solution Strategies for Statically Loaded Nonlinear Structures," by J. W. Simons and G. H. Powell - November 1982 (PB83 197 970)A06

UCB/EERC-82/23 "Analytical Model of Deformed Bar Anchorages under Generalized Excitations," by V. Ciampi, R. Eligehausen, V. V. Bertero and E. P. Popov - November 1982 (PB83 169 532)A06

UCB/EERC-82/24 "A Mathematical Model for the Response of Masonry Walls to Dynamic Excitations," by H. Sucuoğlu, Y. Mengi and H. D. McNiven - November 1982 (PB83 169 011)A07

UCB/EERC-82/25 "Earthquake Response Considerations of Broad Liquid Storage Tanks," by F. J. Cambra - November 1982 (PB83 251 215)A09

UCB/EERC-82/26 "Computational Models for Cyclic Plasticity, Rate Dependence and Creep," by B. Mosaddad and G. H. Powell - November 1982 (PB83 245 829)A08

UCB/EERC-82/27 "Inelastic Analysis of Piping and Tubular Structures," by M. Mahasuverachai and G. H. Powell - November 1982 (PB83 249 987)A07

UCB/EERC-83/01 "The Economic Feasibility of Seismic Rehabilitation of Buildings by Base Isolation," by J. M. Kelly - January 1983 (PB83 197 988)A05

UCB/EERC-83/02 "Seismic Moment Connections for Moment-Resisting Steel Frames," by E. P. Popov - January 1983 (PB83 195 412)A04

UCB/EERC-83/03 "Design of Links and Beam-to-Column Connections for Eccentrically Braced Steel Frames," by E. P. Popov and J. O. Malley - January 1983 (PB83 194 811)A04

UCB/EERC-83/04 "Numerical Techniques for the Evaluation of Soil-Structure Interaction Effects in the Time Domain," by E. Bayo and E. L. Wilson - February 1983 (PB83 245 605)A09

UCB/EERC-83/05 "A Transducer for Measuring the Internal Forces in the Columns of a Frame-Wall Reinforced Concrete Structure," by R. Sause and V. V. Bertero - May 1983 (PB84 119 494)A06

UCB/EERC-83/06 "Dynamic Interactions between Floating Ice and Offshore Structures," by P. Croteau - May 1983 (PB84 119 486)A16

UCB/EERC-83/07 "Dynamic Analysis of Multiply Tuned and Arbitrarily Supported Secondary Systems," by T. Igusa and A. Der Kiureghian - June 1983 (PB84 118 272)A11

UCB/EERC-83/08 "A Laboratory Study of Submerged Multi-body Systems in Earthquakes," by G. R. Ansari - June 1983 (PB83 261 842)A17

UCB/EERC-83/09 "Effects of Transient Foundation Uplift on Earthquake Response of Structures," by C.-S. Yim and A. K. Chopra - June 1983 (PB83 261 396)A07

UCB/EERC-83/10 "Optimal Design of Friction-Braced Frames under Seismic Loading," by M. A. Austin and K. S. Pister - June 1983 (PB84 119 288)A06

UCB/EERC-83/11 "Shaking Table Study of Single-Story Masonry Houses: Dynamic Performance under Three Component Seismic Input and Recommendations," by G. C. Manos, R. W. Clough and R. L. Mayes - June 1983

UCB/EERC-83/12 "Experimental Error Propagation in Pseudodynamic Testing," by P. B. Shing and S. A. Mahin - June 1983 (PB84 119 270)A09

UCB/EERC-83/13 "Experimental and Analytical Predictions of the Mechanical Characteristics of a 1/5-scale Model of a 7-story R/C Frame-Wall Building Structure," by A. E. Aktan, V. V. Bertero, A. A. Chowdhury and T. Nagashima - August 1983 (PB84 119 213)A07

UCB/EERC-83/14 "Shaking Table Tests of Large-Panel Precast Concrete Building System Assemblages," by M. G. Oliva and R. W. Clough - August 1983

UCB/EERC-83/15 "Seismic Behavior of Active Beam Links in Eccentrically Braced Frames," by K. D. Hjelmstad and E. P. Popov - July 1983 (PB84 119 676)A09

UCB/EERC-83/16 "System Identification of Structures with Joint Rotation," by J. S. Dimsdale and H. D. McNiven - July 1983

UCB/EERC-83/17 "Construction of Inelastic Response Spectra for Single-Degree-of-Freedom Systems," by S. Mahin and J. Lin - July 1983

UCB/EERC-83/18 "Interactive Computer Analysis Methods for Predicting the Inelastic Cyclic Behaviour of Structural Sections," by S. Kaba and S. Mahin - July 1983 (PB84 192 012) A06

UCB/EERC-83/19 "Effects of Bond Deterioration on Hysteretic Behavior of Reinforced Concrete Joints," by F.C. Filippou, E.P. Popov and V.V. Bertero - August 1983 (PB84 192 020) A10

UCB/EERC-83/20 "Analytical and Experimental Correlation of Large-Panel Precast Building System Performance," by M.G. Oliva, R.W. Clough, M. Velkov, P. Gavrilovic and J. Petrovski - November 1983

UCB/EERC-83/21 "Mechanical Characteristics of Materials Used in a 1/5 Scale Model of a 7-Story Reinforced Concrete Test Structure," by V.V. Bertero, A.E. Aktan, H.G. Harris and A.A. Chowdhury - September 1983 (PB84 193 697) A05

UCB/EERC-83/22 "Hybrid Modelling of Soil-Structure Interaction in Layered Media," by T.-J. Tzong and J. Penzien - October 1983 (PB84 192 178) A08

UCB/EERC-83/23 "Local Bond Stress-Slip Relationships of Deformed Bars under Generalized Excitations," by R. Eligehausen, E.P. Popov and V.V. Bertero - October 1983 (PB84 192 848) A09

UCB/EERC-83/24 "Design Considerations for Shear Links in Eccentrically Braced Frames," by J.O. Malley and E.P. Popov - November 1983 (PB84 192 186) A07

UCB/EERC-84/01 "Pseudodynamic Test Method for Seismic Performance Evaluation: Theory and Implementation," by P.-S. B. Shing and S. A. Mahin - January 1984 (PB84 190 644) A08

UCB/EERC-84/02 "Dynamic Response Behavior of Xiang Hong Dian Dam," by R.W. Clough, K.-T. Chang, H.-Q. Chen, R.M. Stephen, G.-L. Wang, and Y. Ghanaat - April 1984

UCB/EERC-84/03 "Refined Modelling of Reinforced Concrete Columns for Seismic Analysis," by S.A. Kaba and S.A. Mahin - April, 1984

UCB/EERC-84/04 "A New Floor Response Spectrum Method for Seismic Analysis of Multiply Supported Secondary Systems," by A. Asfura and A. Der Kiureghian - June 1984

UCB/EERC-84/05 "Earthquake Simulation Tests and Associated Studies of a 1/5th-scale Model of a 7-Story R/C Frame-Wall Test Structure," by V.V. Bertero, A.E. Aktan, F.A. Charney and R. Sause - June 1984

UCB/EERC-84/06 "R/C Structural Walls: Seismic Design for Shear," by A.E. Aktan and V.V. Bertero

UCB/EERC-84/07 "Behavior of Interior and Exterior Flat-Plate Connections subjected to Inelastic Load Reversals," by H.L. Zee and J.P. Moehle

UCB/EERC-84/08 "Experimental Study of the Seismic Behavior of a two-story Flat-Plate Structure," by J.W. Diebold and J.P. Moehle

UCB/EERC-84/09 "Phenomenological Modeling of Steel Braces under Cyclic Loading," by K. Ikeda, S.A. Mahin and S.N. Dermitzakis - May 1984

UCB/EERC-84/10 "Earthquake Analysis and Response of Concrete Gravity Dams," by G. Fenves and A.K. Chopra - August 1984

UCB/EERC-84/11 "EAGD-84: A Computer Program for Earthquake Analysis of Concrete Gravity Dams," by G. Fenves and A.K. Chopra - August 1984

UCB/EERC-84/12 "A Refined Physical Theory Model for Predicting the Seismic Behavior of Braced Steel Frames," by K. Ikeda and S.A. Mahin - July 1984

UCB/EERC-84/13 "Earthquake Engineering Research at Berkeley - 1984" - August 1984

UCB/EERC-84/14 "Moduli and Damping Factors for Dynamic Analyses of Cohesionless Soils," by H.B. Seed, R.T. Wong, I.M. Idriss and K. Tokimatsu - September 1984

UCB/EERC-84/15 "The Influence of SPT Procedures in Soil Liquefaction Resistance Evaluations," by H. B. Seed, K. Tokimatsu, L. F. Harder and R. M. Chung - October 1984

UCB/EERC-84/16 "Simplified Procedures for the Evaluation of Settlements in Sands Due to Earthquake Shaking," by K. Tokimatsu and H. B. Seed - October 1984

UCB/EERC-84/17 "Evaluation and Improvement of Energy Absorption Characteristics of Bridges under Seismic Conditions," by R. A. Imbsen and J. Penzien - November 1984

UCB/EERC-84/18 "Structure-Foundation Interactions under Dynamic Loads," by W. D. Liu and J. Penzien - November 1984

UCB/EERC-84/19 "Seismic Modelling of Deep Foundations," by C.-H. Chen and J. Penzien - November 1984

UCB/EERC-84/20 "Dynamic Response Behavior of Quan Shui Dam," by R. W. Clough, K.-T. Chang, H.-Q. Chen, R. M. Stephen, Y. Ghanaat and J.-H. Qi - November 1984

UCB/EERC-85/01 "Simplified Methods of Analysis for Earthquake Resistant Design of Buildings," by E.F. Cruz and A.K. Chopra - Feb. 1985 (PB86 112299/AS) A12

UCB/EERC-85/02 "Estimation of Seismic Wave Coherency and Rupture Velocity using the SMART 1 Strong-Motion Array Recordings," by N.A. Abrahamson - March 1985

UCB/EERC-85/03 "Dynamic Properties of a Thirty Story Condominium Tower Building," by R.M. Stephen, E.L. Wilson and N. Stander - April 1985 (PB86 118965/AS) A06

UCB/EERC-85/04 "Development of Substructuring Techniques for On-Line Computer Controlled Seismic Performance Testing," by S. Dermitzakis and S. Mahin - February 1985 (PB86 132941/AS) A08

UCB/EERC-85/05 "A Simple Model for Reinforcing Bar Anchorages under Cyclic Excitations," by F.C. Filippou - March 1985 (PB86 112919/AS) A05

UCB/EERC-85/06 "Racking Behavior of Wood-Framed Gypsum Panels under Dynamic Load," by M.G. Oliva - June 1985

UCB/EERC-85/07 "Earthquake Analysis and Response of Concrete Arch Dams," by K.-L. Fok and A.K. Chopra - June 1985 (PB86 139672/AS) A10

UCB/EERC-85/08 "Effect of Inelastic Behavior on the Analysis and Design of Earthquake Resistant Structures," by J.P. Lin and S.A. Mahin - June 1985 (PB86 135340/AS) A08

UCB/EERC-85/09 "Earthquake Simulator Testing of Base Isolated Bridge Deck Superstructures," by J.M. Kelly and I.G. Buckle

UCB/EERC-85/10 "Simplified Analysis for Earthquake Resistant Design of Concrete Gravity Dams," by G. Fenves and A.K. Chopra - September 1985

UCB/EERC-85/11 "Dynamic Interaction Effects in Arch Dams," by R.W. Clough, K.-T. Chang, H.-Q. Chen and Y. Ghanaat - October 1985 (PB86 135027/AS) A05

UCB/EERC-85/12 "Dynamic Response of Long Valley Dam in the Mammoth Lake Earthquake Series of May 25-27, 1980," by S. Lai and H.B. Seed - November 1985 (PB86 142304/AS) A05

UCB/EERC-85/13 "A Methodology for Computer-Aided Design of Earthquake-Resistant Steel Structures," by M.A. Austin, K.S. Pister and S.A. Mahin - December 1985 (PB86 159480/AS) A10

UCB/EERC-85/14 "Response of Tension-Leg Platforms to Vertical Seismic Excitations," by G.-S. Liou, J. Penzien and R.W. Yeung - December 1985

UCB/EERC-85/15 "Cyclic Loading Tests of Masonry Single Piers: Volume 4 - Additional Tests with Height to Width Ratio of 1," by H. Sucuoglu, H.D. McNiven and B. Sveinsson - December 1985

UCB/EERC-85/16 "An Experimental Program for Studying the Dynamic Response of a Steel Frame with a Variety of Infill Partitions," by B. Yanev and H.D. McNiven - December 1985

UCB/EERC-86/01 "A Study of Seismically Resistant Eccentrically Braced Steel Frame Systems," by K. Kasai and E.P. Popov - January 1986

UCB/EERC-86/02 "Design Problems in Soil Liquefaction," by H.B. Seed - February 1986

UCB/EERC-86/03 "Lessons Learned from Recent Earthquakes and Research, and Implications for Earthquake Resistant Design of Building Structures in the United States," by V.V. Bertero - March 1986

UCB/EERC-86/04 "The Use of Load Dependent Vectors for Dynamic and Earthquake Analyses," by P. Léger, E.L. Wilson and R.W. Clough - March 1986

UCB/EERC-86/05 "Alternative Designs and Tests of Beam-to-Column Web Seismic Moment Connections," by K.-C. Tsai and E.P. Popov - April 1986